DEFINING THE ROLE OF POLYPHOSPHATE IN THE BACTERIAL STRESS RESPONSE

By: Kanchi Baijal

A thesis submitted to the
University of Ottawa, Faculty of Medicine
In partial fulfillment of requirements for the
Doctorate in Philosophy Degree in Cellular and Molecular Medicine

Department of Cellular and Molecular Medicine
Faculty of Medicine
University of Ottawa

AUTHORIZATIONS

Manuscripts used as chapters in the thesis:

Manuscript #1 – Chapter 2

Baijal, K., Abramchuk, I., Herrera, C. M., Mah, T. F., Trent, M. S., Lavallée-Adam, M., & Downey, M. (2024). Polyphosphate kinase regulates LPS structure and polymyxin resistance during starvation in *E. coli*. *PLoS biology*, *22*(3), e3002558. https://doi.org/10.1371/journal.pbio.3002558

Manuscript #2 – Chapter 3

Baijal, K., Kore, B., Abramchuk, I., Denoncourt, A., Han, S., Simms, A., Dagenais, A., Long, A.R., Rudner, A.D., Lavallée-Adam, M., Gray, M.J., and Downey, D. (2025) Identification of polyphosphate-binding proteins in *E. coli* uncovers targets involved in translation control and ribosome biogenesis. Submitted to *mBio*: Out for review.

Manuscript #3 – Appendix A

Baijal, K., & Downey, M. (2021). The promises of lysine polyphosphorylation as a regulatory modification in mammals are tempered by conceptual and technical challenges. *BioEssays: News and Reviews in Molecular, Cellular and Developmental Biology*, *43*(7), e2100058. https://doi.org/10.1002/bies.202100058

Manuscripts not used as chapters in thesis:

Manuscript #4
Parts of this review have been reproduced or adapted for use in the general introduction (Chapter 1) and discussion (Chapter 4) sections of the thesis.

*Co-first authors
*McCarthy, L., ***Baijal, K.**, & Downey, M. (2024) A framework for understanding and investigating polyphosphate-protein interactions. *Biochemical Society Transactions*, 21:BST20240678. https://doi.org/10.1042/BST20240678

Manuscript #5
Parts of this commentary have been reproduced or adapted for use in the general introduction (Chapter 1) and discussion (Chapter 4) sections of the thesis.

Baijal, K., & Downey, M. (2021). Targeting polyphosphate kinases in the fight against *Pseudomonas aeruginosa*. *mBio*, *12*(4), e0147721. https://doi.org/10.1128/mBio.01477-21

Manuscript #6 – Not included in thesis

Bondy-Chorney, E., Abramchuk, I., Nasser, R., Holinier, C., Denoncourt, A., **Baijal, K.**, McCarthy, L., Khacho, M., Lavallée-Adam, M., & Downey, M. (2020). A broad response to intracellular long-chain polyphosphate in human cells. *Cell reports*, *33*(4), 108318. https://doi.org/10.1016/j.celrep.2020.108318

ABSTRACT

Polyphosphates (polyP) are chains of phosphate residues that are joined together by high energy bonds. In bacteria, the role of polyP is implicated in the stress response. By comparison of wildtype (WT) to *ppk* mutant (Δ*ppk*) *E. coli,* the role of polyP has been tied to processes aimed to help bacteria adapt to stress. However, the underlying PPK-dependent pathways involved in promoting these processes remain unclear.

To identify the broader role of polyP during bacterial stress, I conducted proteomics analysis of *E. coli* exposed to nutrient deprivation. I found 92 proteins significantly differentially expressed between wild-type and Δ*ppk* mutant cells. Wild-type cells were enriched for proteins related to amino acid biosynthesis and transport, while Δ*ppk* mutants were enriched for proteins related to translation and ribosome biogenesis, suggesting that without PPK, cells remain inappropriately primed for growth even in the absence of the required building blocks. Furthermore, from the dataset I followed up on Arn and EptA proteins which are downregulated in Δ*ppk* mutants compared to WT controls, because they play a role in lipid A modifications linked to polymyxin resistance. I provided evidence that mis-regulation in Δ*ppk* cells stems from a failure to induce the BasRS two-component system and showed that loss of *ppk* restores polymyxin sensitivity in resistant strains. Furthermore, I confirmed PPK-dependent regulation of the Bas-Arn circuit in uropathogenic *E. coli.*

To better understand how polyphosphate (polyP) regulates protein function, I performed a screen to identify polyP-binding proteins in *E. coli*. This led to the discovery of 7 novel targets linked to ribosome biogenesis and translation control. For two of these targets—YihI and the ribonuclease Rnr—I mapped the interaction sites to non-PASK sequences within each protein and identified critical lysine residues involved in binding. Deletion of *ppk* resulted in reduced

expression of Rnr, an exoribonuclease known to degrade mRNA and rRNA under stress and participate in trans-translation. In contrast, deleting *rnr* alleviated the slow growth phenotype observed in *ppk* mutants grown on MOPS minimal media. These phenotypic changes seem to depend on the polyP-binding region of Rnr, yet are independent of polyP binding itself, suggesting a complex interaction between PPK and Rnr in *E. coli*. Overall, this work expands our understanding of polyP-binding proteins in *E. coli*.

Together, these works emphasize the pathways by which polyP and PPK promote bacterial adaptation and survival. Further, they uncover PPK and polyP-binding proteins as novel targets to manipulate bacterial fitness.

TABLE OF CONTENTS

List of Tables by Chapter
Only the tables included in this thesis are listed here. See list of tables in the respective chapter for links to all tables included in the published manuscript.

Chapter 1 – Introduction
No tables presented.

Chapter 2 – Manuscript #1
Title: Polyphosphate kinase regulates LPS structure and polymyxin resistance during starvation in *E. coli*.

Chapter 3 – Manuscript #2
*Title***:** Identification of polyphosphate-binding proteins in *E. coli* uncovers targets involved in translation control and ribosome biogenesis.

Chapter 4 – Discussion
No tables presented.

Chapter 5 – Appendix
Review: Problems and Paradigms
Title: The promises of lysine polyphosphorylation as a regulatory modification in mammals are tempered by conceptual and technical challenges.

List of Figures by Chapter

Chapter 1 – Introduction

Chapter 2 – Manuscript #1
Title: Polyphosphate kinase regulates LPS structure and polymyxin resistance during starvation in *E. coli*.

Chapter 3 – Manuscript #2
Title: Identification of polyphosphate-binding proteins in *E. coli* uncovers targets involved in translation control and ribosome biogenesis.

Chapter 4 – Discussion
No figures presented.

Chapter 5 – Appendix A
Review: Problems and Paradigms
Title: The promises of lysine polyphosphorylation as a regulatory modification in mammals are tempered by conceptual and technical challenges.

List of Abbreviations

ADP	Adenosine diphosphate
ALP	Alkaline phosphatase
ALS	Amyotrophic later sclerosis
ATP	Adenosine triphosphate
BPS	Bathophenanthrolinedisulfonic acid
CSD	Cold shock domain
D-A	Aspartic acid to alanine mutation
D-N	Aspartic acid to asparagine mutation
D/E/S/K	Aspartic acid/glutamic acid/serine/lysine
*Dd*PPK	*Dictyostelium discoidieum PPK*
DNA	Deoxyribonucleic acid
E-L	Glutamic acid to leucine mutation
E-Q	Glutamic acid to glutamine mutation
*Ec*PPK	*Escherichia coli* PPK enzyme
FDR	False discovery rate
FL	Full-length (referring to a protein)
FRT	Flp recognition target
GO	Gene ontology
GSEA	Gene set enrichment analysis
GST	Glutathione S-transferase
HRP	Horseradish peroxidase
K-R	Lysine to arginine mutation
K_2HPO_4	Potassium phosphate
L-Ara4N	4-amino-4-deoxy-L-arabinose
LB	Luria-Bertani broth
LDH	lactic acid dehydrogenase
LPS	Lipopolysaccharide
MDR	Multidrug resistance
MOPS	3-(N-morpholino) propane-sulfonic acid
MS	Mass spectrometry
ND	Nuclease domain
p130	Polyphosphate chains with modal size of 130 phosphate units
p700	Polyphosphate chains with modal size of 700 phosphate units
PASK	Polyacidic serine and lysine
PCR	Polymerase chain reaction
pEtN	Phosphoethanolamine

Pi	Phosphate monomers
PolyHis	Histidine repeats
PolyLys	Lysine repeats
PolyP	polyphosphate
PPBD	Polyphosphate binding domain
ppGpp	Guanosine-5′,3′-tetraphosphate
PPK	Polyphosphate kinase
pppGpp	Guanosine-5′,3′-pentaphosphate
PPX	Exopolyphosphatase
PTM	Post-translational modification
qPCR	Quantitative polymerase chain reaction
RNA	Ribonucleic acid
S-A	Serine to alanine mutation
*Sc*Ppx1	*Saccharomyces cerevisiae* Ppx1 enzyme
SPA	Sequential peptide affinity
TAP	Tandem affinity purification
TCA	Trichloro-acetic acid
TEAB	Tetraethylammonium bicarbonate
UPEC	Uropathogenic *E. coli*
VTC	Vacuolar transport chaperone
VWF	Van Willebrand factor

Acknowledgements

I would like to express my deepest gratitude to all those who have supported me throughout this journey.

First and foremost, I am incredibly grateful to my supervisor, Dr. Michael Downey, for his unwavering support, mentorship, and guidance. I would also like to thank Dr. Adam Rudner for his mentorship, and my collaborators, lab members, and students who have all contributed to my growth, both personally and professionally.

To my partner, soon to be Dr. Liam McCarthy, and our dog Yana, I cannot thank you both enough for your constant support.

Finally, I owe an immense debt of gratitude to my parents, Jessie and Rupam Baijal. Your unconditional support, love, and patience over the many, many years have been the foundation upon which I built this achievement. I am forever grateful for everything you have done for me.

CHAPTER 1 – INTRODUCTION

Statement of rights and permissions

(1) *McCarthy, L., ***Baijal, K.**, & Downey, M. (2024) A framework for understanding and investigating polyphosphate-protein interactions. *Biochemical Society Transactions*, 21:BST20240678. https://doi.org/10.1042/BST20240678.
*Co-first authors

The following sections of this chapter concerning polyP regulation (1.2 to 1.4) and polyP-protein binding (1.8 to 1.10) were either reproduced or adapted from the review article listed above (2024), of which I am a first co-author.

Sections: 1.2 to 1.4., 1.8., 1.9. and 1.10. (including sections 1.10.1 to 1.10.5), Figures 5 and 6.

Note, in section 1.3. the explanation about PPK conservation in *D. discoidieum.*is new, and section 1.8. has been significantly adapted from the review to fit the flow of my introduction.

(2) **Baijal, K.**, & Downey, M. (2021). Targeting polyphosphate kinases in the fight against *Pseudomonas aeruginosa*. *mBio*, 12(4), e0147721. https://doi.org/10.1128/mBio.01477-21.

The last section in this chapter discussing PPK inhibitors (1.12) is reproduced and slightly adapted from the commentary listed above (2021), of which I am a first author.

Sections: 1.12.

1.1. Polyphosphates are ubiquitous molecules

Inorganic phosphates can be assembled into negatively charged and energy rich linear chains called polyphosphates (hereafter polyP) (**Figure 1**) (1). Recent years have seen a surge of interest in polyP biology based in part on discoveries highlighting tantalizing links to human disease from SARS-CoV-2 (2) to amyotrophic lateral sclerosis (ALS) (3). While connections to human health are exciting, it is noteworthy that the fundamentals of polyP metabolism are perhaps best understood in microorganisms.

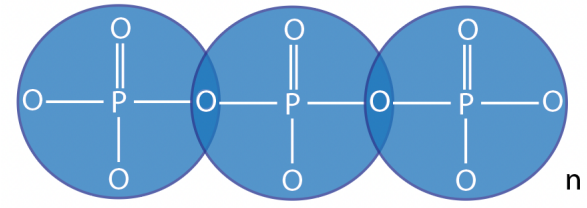

Figure 1. Polyphosphate (polyP) are chains of phosphate residues. PolyP chains are joined together by high energy phosphoanhydride bonds and can be 3-1000s of phosphates in length.

In fact, polyP was first observed in the 19th century, when it was misidentified as a form of nucleic acid (4). It was not until the mid-20th century that polyP was accurately characterized by Wiame (5). In the 1970s, biochemist Arthur Kornberg advanced our understanding of polyP by revealing its essential role in bacteria (6–10). Despite these significant breakthroughs, much remains to be discovered about the diverse and critical functions of polyP, particularly in modulating cellular processes in bacteria.

1.2. Mechanisms of polyP synthesis and degradation in bacteria

In bacteria, polyP synthesis is achieved by the action of polyphosphate kinase (PPK) enzymes, which transfer the gamma phosphate of ATP to growing polyP chains. While *Escherichia coli* have just one PPK enzyme (**Figure 2A**) (7), other bacteria have both PPK1 and PPK2 (11). These

enzymes have unique properties, but in some cases function redundantly to regulate polyP dynamics (12). Bacterial polyP accumulation is countered by the action of the PPX exopolyphosphatase enzyme (**Figure 2A**), which degrades polyP beginning at the end of the chain to release monomers of inorganic phosphate (13). While most bacteria possess only one *ppx* gene, some bacteria such as *Mycobacterium tuberculosis* and *Corynebacterium glutamicum* express PPX1 and PPX2 proteins, both of which have exopolyphosphatase activity (14,15).

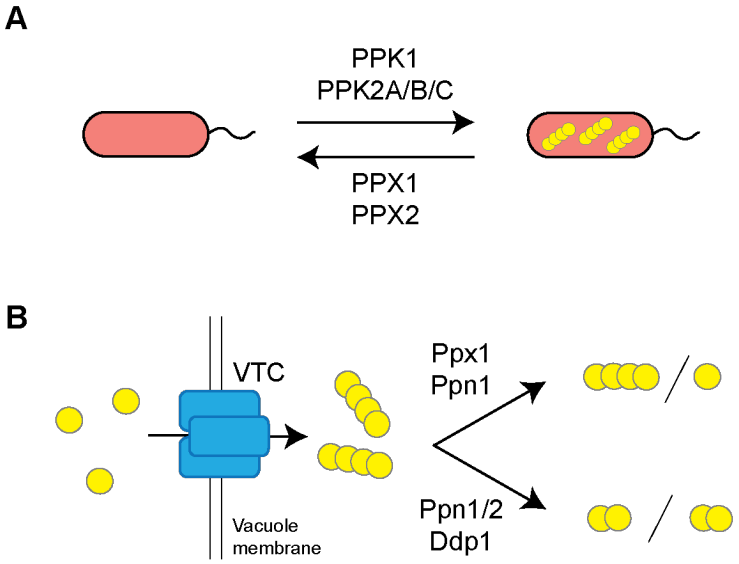

Figure 2. PolyP synthesis and degradation enzymes in bacteria and yeast. A) In bacteria polyP is synthesized by the polyphosphate kinase (PPK) family of enzymes and degraded by exopolyphosphatases (PPX). B) In yeast, polyP is made by the VTC complex that synthesizes polyP and translocates it into the vacuolar lumen for storage. In yeast, polyP is degraded by endopolyphosphatases that cleave polyP chains internally or exopolyphosphatases that cleave the terminal phosphate. Yeast Ddp1 is a homolog of the mammalian NUDT3 polyphosphatases.

1.3. Bacterial PPK and PPX enzymes are not highly conserved in eukaryotes

In some lower eukaryotes, such as the social amoeba *Dictyostelium discoidieum* (16) and the unicellular red alga *Cyanidioschyzon merolae* (17), the PPK enzyme is conserved and may have been acquired by horizontal gene transfer. In particular, the *D. discoidieum* PPK (*Dd*PPK) enzyme shares 30% identity and 51% sequence similarity with *E. coli* PPK (*Ec*PPK). In contrast to the

long chains, greater than 700 phosphate residues in length, that are synthesized by *Ec*PPK (18), *Dd*PPK makes chains that are about 300 phosphates long (16). Additionally, *Dd*PPK is implicated in regulating cytokinesis, sporulation and predation of *D. discoidieum* (16,19)

In contrast, in fungi, such as the budding yeast *Saccharomyces cerevisiae,* polyP is synthesized by the vacuolar transporter chaperone complex (VTC) which is embedded in the vacuole membrane and uses ATP as a substrate to synthesize polyP chains of 3–300 units in length (**Figure 2B**) (20). As they are synthesized, these chains are translocated into and stored within the vacuole lumen (i.e. inside the vacuole) at high concentration (>200 mM by some measurements) (21), serving in part as a reserve of inorganic phosphate that can be rapidly mobilized during starvation (22). PolyP is also found in other cellular compartments (e.g. nucleus, cytoplasm, and mitochondria), but the processes by which these pools are made, or perhaps transported to these locations, are unknown (23). Also unclear is the actual amount of polyP in these organelles, with estimates varying widely from study to study and complicated by the unintended rupture of polyP-rich vacuoles during fractionation procedures (23). In fact, the forced accumulation of polyP outside the yeast vacuole, driven by ectopic expression of *Ec*PPK, is toxic (22,24). This observation strongly suggests that there are upper limits to the amount of polyP normally permitted to accumulate in some areas of the cell.

As in bacteria, the turnover of polyP chains in yeast also depends on the action of polyphosphatase enzymes, which include both exopolyphosphatases that cleave terminal phosphates, and endopolyphosphatases that cleave chains internally (**Figure 2B**) (25). We can think of these enzymes as analogous to exo- and endo-nucleases that act on nucleic acid (RNA or DNA) substrates (26). Some of these polyphosphatases are vacuolar (Ppn1, Ppn2, and possibly Pho8), and function to modulate overall chain length or to degrade polyP chains into free inorganic

phosphate during phosphate starvation (20,27–29). The Ppx1 and Ddp1 polyphosphatases are found predominately in the cytoplasm (27). In contrast with the vacuolar enzymes, the function of these proteins in overall polyP homeostasis is unclear (27). We speculate that they function to titrate the level of minor populations of cytoplasmic polyP in response to environmental changes.

1.4. The mechanisms of polyP synthesis and degradation remain elusive in humans

In mammalian cells, there are lower levels of polyP (typically in the range of 25–120 μM) and the enzymes involved in its metabolism are poorly understood (30). The F_oF_1 mitochondrial ATPase has been suggested to synthesize polyP (31), but its contribution to total cellular levels of polyP remains unclear (32). Several mammalian proteins have been proposed as polyphosphatases (27), with the best evidence for *in vivo* function resting with NUDT3 (a homolog of yeast Ddp1 (**Figure 2B**), which may be particularly important for the regulation of the DNA damage response during oxidative stress (33).

1.5. PolyP is a stress associated metabolite in bacteria

In bacteria, polyP accumulation is considered a 'hallmark' of the stress response (34). This is because there is no detectable polyP present in several bacterial species, such as *E. coli* and *Pseudomonas aeruginosa*, during nutrient rich conditions of growth. However, when these bacteria are exposed to stress conditions, they rapidly accumulate large amounts (20-50 mM) of long-chain polyP (>700 phosphate residues in length) (23,34).

In *E. coli*, some polyP-inducing stressors include nutrient limitation, osmotic stress and oxidative stress (23,35–37). It is thought that through overlapping signalling cascades polyP

accumulation is regulated (35). However, the details of how these pathways are coordinated remain unclear.

In general, a careful balance between stress induced activation of the Pho regulon, RpoS sigma-factor and other transcription factors plays a key role in polyP accumulation (34,38,39). The Pho regulon can be activated by the PhoBR two-component system which consists of PhoR, the sensor histidine kinase that responds to conditions of low phosphate, and PhoB, the response regulator which is a transcription factor (40). Disruption of this system by mutating the *phoB* gene leads to a significant reduction of polyP in cells (34,41). This likely stems from misregulation of pathways required for phosphate uptake. In contrast, mutants lacking PhoU, an inhibitor of the Pho regulon (40), constitutively accumulate polyP (42). The high and low affinity phosphate transport systems, PstA and PitA, that have interplay with PhoBR and PhoU, may also contribute to stress-induced polyP accumulation (43–47). Other two-component systems that have yet to be tested may also play a role. Alternatively, RpoS activation may be bi-directional as mutation of *rpoS* results in the loss of polyP accumulation during nitrogen starvation (35). Conversely, polyP itself has been shown to stimulate an increase in RpoS levels (48,49). Other transcription factors including NtrC, DksA, and RpoN have also been shown to impact polyP levels in *E. coli* (39,50).

Additionally, activation of pathways that result in polyP accumulation may be stress specific. For example, during nutrient starvation activation may occur through stringent response regulators RelA and SpoT (35), while during nitrogen limitation it happens through the nitrogen response transcription factor NtrC (35). Alternatively, during salt stress activation may occur via the membrane bound osmoregulator EnvZ (35). Lastly, as mentioned above there is vast overlap between signalling cascades that result in polyP accumulation and there remains the possibility of additional regulators that have yet to be identified.

1.6. Mechanisms of PPK activation

Despite what is known about stressors that activate pathways resulting in polyP accumulation, very little is known about the molecular events that result in PPK activation. This is in part complicated by the fact that there is no evidence for transcriptional regulation of the *ppk-ppx* operon upon exposure to polyP inducing conditions such as a nutrient limitation (41) and hypochlorous acid stress (51).

For several reasons (highlighted by Gray (39)) polyP accumulation was thought to be countered by the exopolyphosphatase PPX during conditions of no stress. In this theory, the alarmones guanosine-5′,3′-tetraphosphate (ppGpp) and guanosine-5′,3′-pentaphosphate (pppGpp) (collectively referred to as (p)ppGpp), produced upon exposure to stress, were thought to regulate polyP accumulation by inhibiting PPX mediated degradation of it (52). However, polyP accumulation is still stress-dependent in Δ*ppx* mutants and, compared to wild-type cells, polyP levels do not increase significantly in Δ*ppx* mutants during stress, suggesting that the mechanism of regulation does not depend solely on PPX (39). In 2019 Gray (39) disproved this model by showing that loss of polyP in cells mutated for (p)ppGpp synthesis (Δ*relA* Δ*spot* double mutants) stems from accumulation of suppressor mutations that alter the activity of RNA polymerase-binding transcription factors such as *rpoB3449* (deletion of alanine 532).

Moreover, activation of PPK may stem from its stoichiometric organization. Active PPK harboring polyP synthesis activity exists as a dimer (53–55) while other conformations of PPK (monomer, trimer and tetramer) possess a different subset of functions. For example, as a dimer PPK has polyP, ATP and GTP synthesis activity, while as a trimer and tetramer PPK is thought to be involved in the synthesis of guanosine tetraphosphate (ppppGp) (54). In contrast, tetramer and dimer conformations can promote autophosphorylation of PPK, the initial step of polyP synthesis

(56), in the presence of 5 μM and 1 mM ATP, respectively (54). In fact, when residues between dimer and tetramer interfaces are mutated (55) or poly-histidine tags are added to PPK (55), its activity is altered. This is shown by Rudat *et al.* (41) who identified PPK mutants (denoted as PPK*) with an elevated level of polyP synthesis activity, both *in vitro* and *in vivo.*

Intriguingly, expression of *Ec*PPK in mammalian HEK293T cells (57) and yeast (24) results in polyP accumulation and PPK* mutations overcome stress-dependent activation of PPK (41). Together, hinting at multiple mechanisms of PPK regulation and the possibility of condition specific small molecule/protein regulators of PPK in *E. coli*.

1.7. PolyP drives bacterial stress adaptation and virulence

To date, Kornberg and others have demonstrated that PPK enzymes have roles in virulence (58), motility (8), biofilm formation (36,59), and the response to cellular stress across diverse species of bacteria (**Figure 3**) (23,36,37,60). Compared to wild-type bacteria, *ppk* mutants (Δ*ppk*) that cannot produce polyP, are more sensitive to iron stress (37), oxidative stress (36), antibiotics (61) and have slower growth during nutrient starvation (**Figure 3**) (60).

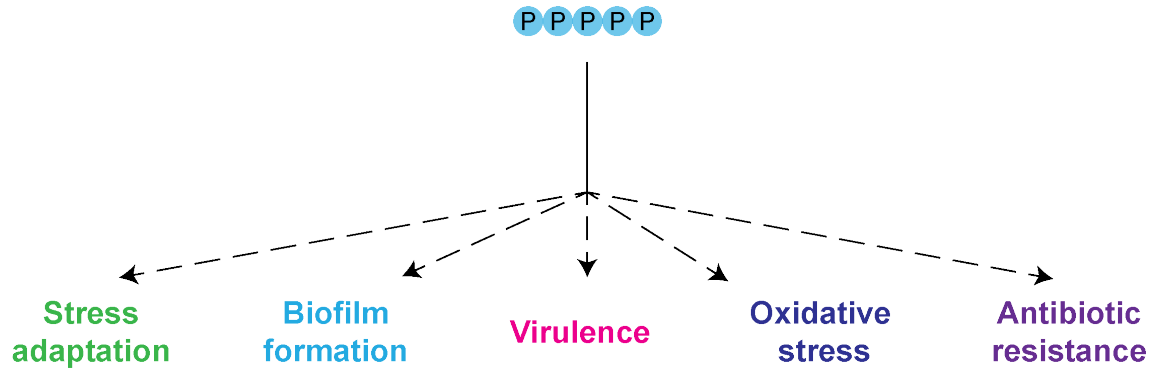

Figure 3. PolyP regulates a variety of 'pro-survival' processes in bacteria. PolyP promotes bacterial survival through a variety of mechanisms leading to phenotypic outcomes (stress adaptation, biofilm formation, virulence, oxidative stress resistance and antibiotic resistance). However, the underlying pathways leading to these outcomes, as well as the direct versus indirect effects of polyP, have not yet been characterized

Some of these functions of polyP stem from its ability to chelate positively charged cations (62,63). For example, in *E. coli*, polyP reduces iron toxicity that is caused by cisplatin treatment (37). This mechanism of iron chelation by polyP is thought to inhibit the interaction between iron and peroxide, thereby preventing the production of free hydroxyl radicals generated by the Fenton reaction (37). Alternatively, polyP can also chelate ions that are needed for bacterial survival, such as magnesium which is depleted by the expression of PPK* (41). Similarly, polyP bound to the exterior of *Staphylococcus aureus* cells plays a bactericidal role by chelating calcium and magnesium ions that are required for cell wall integrity (64). This is supported by the idea that polyP released by *P. aeruginosa* cells co-cultured with *S. aureus* plays a role in killing of *S. aureus* (65). In addition to compromising the cell wall of *S. aureus* directly, it is proposed that this effect is mediated indirectly by polyP-dependent production of pyocyanin, a potent oxidative stress stimulator, by *P. aeruginosa* (12,65). This *ppk* dependent production of pyocyanin and pyoverdine has also previously been shown to contribute to *P. aeruginosa* virulence in *Caenorhabditis elegans* infection models (12).

Moreover, biofilms are thought to protect bacteria from antibiotic treatments (61) and in *P. aeruginosa* (12,59) and *E. coli* (66) have been shown to be produced in a *ppk*-dependent manner. Surprisingly, both biofilm-grown wild-type and Δ*ppk* mutant extraintestinal pathogenic *E. coli* are similarly tolerant to antibiotics compared to planktonic Δ*ppk* mutants that are significantly more sensitive to treatment relative to their wild-type counterparts (61). This seems at odds with what is expected and may require further investigation to determine the mechanisms of resistance at play.

Finally, during nutrient starvation polyP itself can serve as a source of phosphate. In *E. coli* it can also modulate the degradation of proteins to liberate amino acids needed to adapt to

starvation (60,67). Additionally, it can modulate DNA replication (68) and cell division processes (69), which may in part contribute to how bacterial cells coordinate growth during stress.

1.8. PolyP can bind to proteins

The broad roles of polyP in bacteria raise one important question: how does such a simple molecule impart its diverse functions at a molecular level? We don't expect there to be a single answer to this question. In addition to ion chelation, another interesting possibility was proposed by Azevedo *et al.* (70), who in 2015 provided gel-based evidence that polyP chains could be covalently linked to lysine residues within two yeast proteins, Nsr1 and Top1, in a non-enzymatic reaction. Mutations that abrogate so called 'polyphosphorylation' (denoting a post-translational modification) also altered protein subcellular localization and resulted in changes to Top1's topoisomerase activity *in vitro* (70). For both proteins, polyphosphorylation occurred in polyacidic serine- and lysine-rich (abbreviated as PASK) motifs (70).

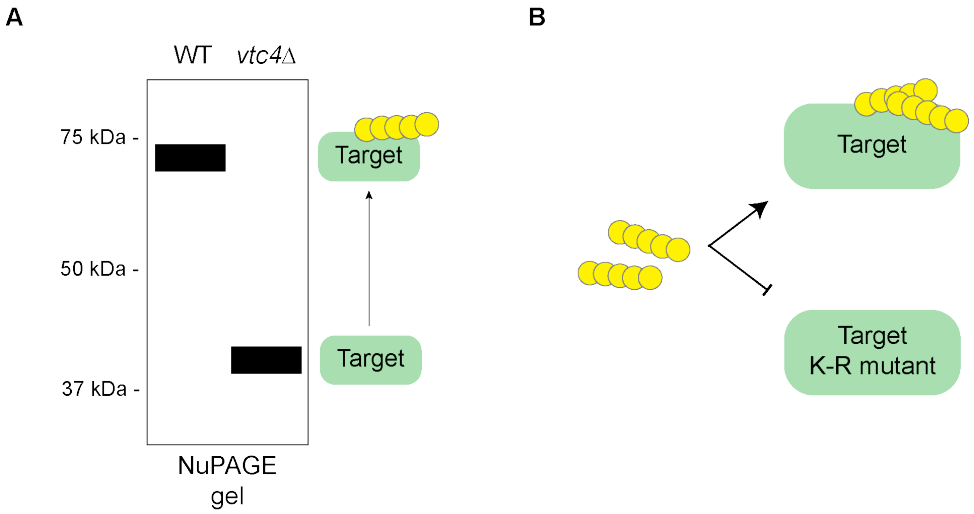

Figure 4. Basis for identifying polyP-binding proteins using NuPAGE. A) Characteristic NuPAGE gel 'shift' of polyP-binding proteins that migrate to a higher molecular weight in the presence of polyP (WT; wild-type), compared to in the absence of it (*vtc4*Δ). **B)** PolyP-binding proteins is lost when PASK lysine (K) residues, involved in polyP-binding, are mutated to arginine (R).

The evidence for covalent attachment of polyP to proteins rested in large part on the intriguing observation that Top1 and Nsr1 isolated from wild-type cells display a dramatic decrease in electrophoretic mobility, relative to proteins isolated from polyP-deficient *vtc4Δ* mutants, when analyzed on Bis-Tris polyacrylamide gels (NuPAGE) (**Figure 4A**) (70). The 'polyP shift' persisted when extracts were generated under harsh denaturing conditions (e.g. urea or SDS) (70), usually assumed to disrupt non-covalent interactions. The idea of covalent versus non-covalent attachment was further supported by Azevedo *et al.* (71), who used a protein microarray to screen for polyP-binding proteins in humans. They confirmed six targets that fit previously established criteria for polyphosphorylation, namely a polyP-dependent shift on NuPAGE gels (71). In addition, they identified five proteins that did not undergo polyP shifts on NuPAGE gels but still seemed to interact with polyP as judged by mobility shift on native PAGE or by chromatography (71), suggesting alternative modes of polyP-binding.

However, this was disproved by Neville *et al.* when the salt and pH sensitivity of polyP interaction with polyLysine (polyLys) (72) and polyHistidine (polyHis) (73) repeat proteins suggested non-covalent binding — despite the fact that the interaction slowed migration on NuPAGE gels. The studies called into question the use of NuPAGE gels to discern covalent versus non-covalent interactions and prompted a re-analysis of the biochemical characteristics of lysine polyphosphorylation. Neville *et al.* (72) showed that the NuPAGE shift for lysine polyphosphorylation targets was lost when reactions carried out on beads were subsequently washed with high salt or high pH buffers. Importantly, these salt and pH sensitivities were confirmed in separate experiments using size exclusion chromatography (72). Together, these results challenged the assertion that polyphosphorylation is covalent, since we expect covalent modifications to be resistant to these conditions.

1.9. A unified nomenclature for polyP-protein interactions

With these new findings, we now consider the evidence for covalent attachment of polyP to proteins to be lacking. Of course, we cannot say for certain that covalent attachment of polyP to lysine or other amino acids never happens. For example, it is possible that polyP interaction with some targets is covalent *in vivo*. While there is currently no evidence to support this, the term polyphosphorylation — with -ylation almost exclusively denoting a PTM — seems somewhat confusing. As do the terms 'polyP modification' (74). The introduction of new language seems largely unnecessary when the terms 'polyP binding' and 'polyP-binding proteins' suffice.

1.10. Outcomes of polyP-protein binding

It appears that polyP-binding proteins are not exactly rare. To date, at least 100 targets have been validated across prokaryotic and eukaryotic species (see review (75) for a comprehensive list), with additional candidates identified via large scale analyses. PolyP-binding proteins include PASK (76–78), polyHis (72), and polyLys (72) containing proteins, as well as those that interact with polyP via a collection of positive charges concentrated on (or across) a target's surface (79) (**Figure 5**).

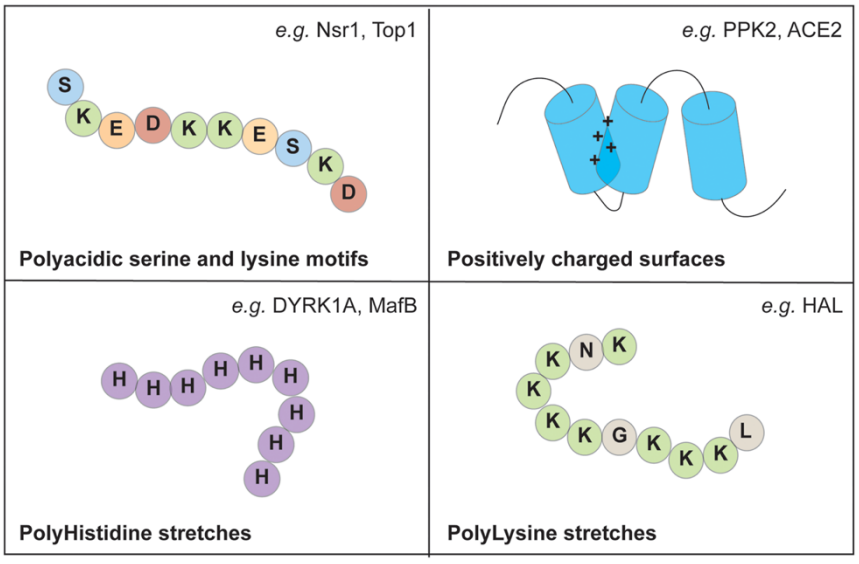

Figure 5. PolyP-protein binding sequences and regions. A) PolyP can bind to PASK (polyacidic serine- and lysine-rich), polyHistidine and polyLysine stretches, or positively charged surfaces of proteins. Examples of polyP-binding proteins fitting each category are provided and will be discussed in detail below.

As the mechanisms of regulation are unlikely to be species exclusive, below I provide examples in both prokaryotic and eukaryotic species to gain a broad understanding of the key molecular outcomes of polyP-protein interactions. Additionally, for now, I consider these outcomes independent of the proposed mode of binding (i.e. covalent versus varied types of non-covalent interactions), but it is not impossible that distinct interactions could preferentially lead to certain fates. Importantly, outcomes are not necessarily mutually exclusive, and polyP's impact on a given target could certainly be context specific. A summary is presented in **Figure 6**.

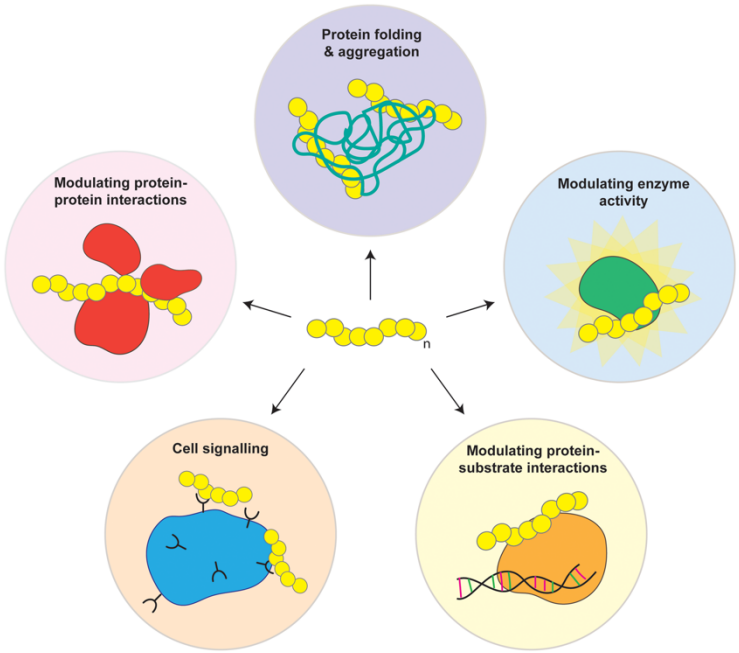

Figure 6. Outcomes of polyP-protein binding. PolyP binding to proteins can disrupt or promote protein-protein interactions or protein-substrate interactions. PolyP binding can also stabilize partially unfolded proteins or play a role in promoting protein aggregation. Additionally, polyP-protein binding events can modulate the enzymatic activity of proteins or contribute to the regulation of signalling pathways within cells. Overall, polyP has wide-reaching roles in the regulation of protein function and activity through direct binding.

1.10.1. Protein chaperone

PolyP performs a chaperone-like role in stabilizing intermediate structures of 'client' proteins including citrate synthase (36), luciferase (36), and lactate dehydrogenase (LDH) (80) when these proteins are partially unfolded. Size exclusion chromatography experiments conducted with LDH suggest that polyP behaves analogous to a protein chaperone, that binds the partially unfolded protein, to promote the formation of intermediate stabilizing structures composed of soluble beta-sheets (80). Additionally, in the case of LDH, intermediate structures formed in the presence of polyP could be refolded by actual protein chaperones upon removal of the thermal stressor that was initially used to unfold it (80,81). How the activities of polyP and protein chaperones are co-ordinated during refolding is deserving of further investigation. This type of protein stabilization may have physiological relevance during conditions of heat or oxidative stress (36,80). As noted previously, the mammalian NUDT3 polyphosphatase is proposed to regulate polyP levels during oxidative stress (33), and we wonder if changes in the folding of nuclear proteins could explain increases in H2AX phosphorylation, a marker of DNA damage, in NUDT3 depleted cells (33). On the other hand, polyP has been shown to bind amyloidogenic proteins that have a propensity to aggregate, oligomerize, and nucleate (82). For these proteins, polyP binding results in a different fate. It accelerates the aggregation and nucleation of these proteins, causing them to form compact, insoluble structures (82). An example is the fibrillation of the *E. coli* CsgA protein (66). Here, polyP plays a role in stabilization of the protein to promote biofilm formation (66). Other proteins that are structurally reorganized by polyP include those involved in the progression of neurodegenerative Alzheimer's and Parkinson's diseases such as $A\beta_{1–40/42}$, Tau, β_2-microglobulin, and alpha-synuclein proteins (66,83,84). Interestingly, fibrillation of proteins can happen in the absence of polyP, at a slower rate, presumably resulting in less compact fibrils that are cytotoxic

and contribute to faster disease progression (66). Work in neuronal cell lines and *C. elegans* neurodegenerative models suggests that polyP-stabilized alpha-synuclein fibrils are less cytotoxic and more susceptible to proteolytic degradation compared with their unstabilized counterparts (66). Two key residues (K43 and K45) within a lysine-rich region of alpha-synuclein may be critical for polyP binding (85). An open question is whether polyP can stabilize fibrils as they come apart and act as a chaperone to modulate their refolding. Understanding the residues or regions of proteins that interact to promote aggregate formation will help better predict the outcome of polyP binding to partially unfolded proteins and how it could play a role in reversing protein aggregation.

1.10.2. Modulation of protein-protein interactions

Beyond its role in modulating protein folding, polyP can impact target interactions with other proteins.

1.10.2.1. Promoting interactions

One of the earliest descriptions of a polyP-binding protein was made by Kuroda *et al.* (67), who showed that polyP binding facilitates degradation of target proteins by the Lon protease in *E. coli*. In this scenario, polyP is suggested to bind both Lon and the target, serving as a molecular adaptor. This was first proposed to play a role in the targeting of Lon to ribosomal subunits and nucleoid proteins, during starvation, as part of a broader response that allows cells to adapt to the lack of nutrients (67,86,87). Subsequent work found that this mechanism also contributes to the arrest of DNA replication initiation in *E. coli* by regulating the pool of replication initiator protein, DnaA, when bound to ADP (88). An interesting proposal by Ropelewska *et al.* (68) is that most substrates degraded by Lon in a polyP- dependent manner also bind polyP themselves. As another example, two-hybrid assays suggest that polyP binding promotes the formation of a heterodimer complex

between the *Francisella tularensis* transcription factors MglA and SspA (89). However, it is unclear if disruption of this complex in *ppk-ppx* mutant strains is due to the direct loss of polyP or a downstream effect of the mutations themselves (89).

The effect of polyP may be particularly impactful when it binds to multiple proteins functioning in the same pathway. PolyP's role in the blood coagulation contact pathway is an excellent example. PolyP binds to diverse coagulation factor proteins (FV (90), FXI (91), FXII (92), and thrombin (93)) and plays a role in activating them either directly, or indirectly by accelerating the rate of their interactions. We speculate that polyP may play a similar role in bridging transient interactions in other cases where it interacts with multiple proteins in close proximity. For example, we previously identified many polyP interacting proteins that localize to the nucleolus (77), and theorize that transient interactions mediated by polyP may be important for ribosome biogenesis.

1.10.2.2. Disrupting interactions

In addition to promoting interactions, polyP can also disrupt or prevent interactions between two or more proteins. For example, polyP competes with FVIII to bind von Willebrand Factor (VWF) (94), and instead promotes VWF interaction with glycoprotein Ib (95). This mechanism plays a role in increasing VWF binding to platelets, which is required for platelet activation and aggregation (94,95). PolyP has also been reported to disrupt the interaction between PASK-containing Nsr1 and Top1, *in vitro* (70). Whether polyP impacts interaction of these proteins *in vivo* is not clear, but it is tempting to speculate that this mechanism serves to regulate localization of both proteins to the nucleolus, which is more pronounced in *vtc4*Δ mutant cells that cannot make polyP (70). Notably, similar polyP-induced changes in localization have been observed for the mammalian kinase DYRK1A (73), which has wide-reaching roles in neurogenesis (96), cell

proliferation (97,98), and cell homeostasis (99). Specifically, in the presence of excess polyP synthesized by ectopically expressed bacterial PPK, DYRK1A failed to form nuclear speckles (73). We surmise that this effect and other changes in localization ultimately stem from changes to protein-protein interactions. For example, occlusion of a nuclear localization signal (which often contains lysine residues (100)) by polyP binding could alter a protein's subcellular distribution.

1.10.3. Modulation of cell signalling

Notably, polyP also directly interacts with cell surface receptors to initiate intracellular signaling events. While these receptors are also proteins, this function of polyP is deserving of special attention since the source of polyP is extracellular (e.g. from microorganisms (58), damaged cells (3), or dense granules of platelets (101)). For instance, polyP binding to RAGE and possibly P2Y1 receptors of endothelial cells leads to the activation of pathways like mTORC2 signaling (102) and inflammatory responses involving H4 and HMGB1, which also bind polyP with high affinity (103). Additionally, the predicted binding of polyP to P2Y1 is thought to activate calcium signaling and release of internal polyP stores by astrocytes (104). Intriguingly, released polyP can also act as a neurotransmitter to influence activation of neighboring cells and their uptake of polyP (104). Conversely, polyP can also block receptor binding sites for other ligands. For example, polyP binding to the ACE2 receptor is thought to block the binding of the SARS-CoV-2 Spike protein, thereby preventing viral entry (2,105). In these examples, polyP is proposed to act at the cell surface. However, it is also plausible that polyP may actually enter the cell during receptor internalization (2). For example, via ACE2 internalization, bound polyP could enter the cell and potentially serve as an intracellular signaling molecule or perform one or more of the functions listed above.

1.10.4. Regulation of enzymatic activity

PolyP binding may also inhibit the enzymatic activity of proteins. For example, *in vitro* assays show that in the presence of polyP, Top1 loses the ability to relax supercoiled DNA (70). Similarly, polyP inhibited the *in vitro* kinase activity of DYRK1A (73). PolyP also inhibits the catalytic activity of HAL, a histidase from *Trypanosoma cruzi* proposed to interact with polyP, via its lysine-rich intrinsically disordered region (106). Of note, it is unclear how the ability of polyP to chelate ions contributes to *in vitro* enzymatic assays and this is deserving of additional consideration in future work. Conversely, polyP could promote enzyme activation. We note that Wang *et al.* (107) demonstrated that polyP stimulates the kinase activity of mTOR, the master regulator of cellular homeostasis, in a concentration-dependent manner *in vitro*. *In vivo*, ectopic expression of the yeast exopolyphosphatase Ppx1 reduced phosphorylation of mTOR target PHAS-1 and reduced cell viability (107). Given this evidence, it would be important to establish if mTOR regulation occurs via direct binding to polyP.

1.10.5. Modulation of protein-nucleic acid interactions and protein-lipid interactions

PolyP binding can modulate the affinity of targets for other molecules besides proteins. For instance, polyP has been shown to compete with DNA for binding to the mammalian transcription factor MafB, which is unable to bind DNA when polyP-bound (73). However, it is also possible for polyP to alter the RNA or DNA binding specificity of target proteins. This activity of polyP has been shown for the *E. coli* DNA- and RNA-binding protein Hfq (108), and a similar effect is proposed for the sigma factor σ80 of *Heliobacter pylori* (109). Here we speculate that polyP binding stimulates changes in protein conformation or cofactor interactions that alter target binding specificity. In another example, polyP-stabilized lipopolysaccharide micelles bind to the TLR4

receptor of macrophages more readily than in the absence of polyP (110). However, in this case, it is unclear if polyP directly interacts with TLR4 receptors or if its role is more indirect.

1.11. The role of bacterial polyP in human infection

Beyond stress adaptation, bacterial polyP plays a significant role in virulence and pathogenesis (**Figure 3**). For example, the mortality rate of mice dropped from 94% to 7% when infected with wild-type versus Δ*ppk* mutant pathogenic *P. aeruginosa* strains, respectively (111). Similarly, compared to infection with wild-type uropathogenic *E. coli*, infection with Δ*ppk* mutants resulted in a lower bacterial load within the mouse peritoneum and increased the survival of mice (from 38% for wild-type compared to 75% for Δ*ppk* mutants) (58). Additionally, the PPK status of bacteria may play a role in antibiotic resistance. Uropathogenic *E. coli* lacking the *ppk* gene are less able to form antibiotic-resistant persister cells compared to their wild-type counterparts (112).

But in general, how does polyP promote bacterial survival and virulence during infection? In the simplest scenario, in addition to stress adaptation, polyP facilitates the production of virulence factors (example: biofilm and siderophores) (12,59,112). In the absence of the polyP synthetase, PPK, bacteria have a reduced ability to produce biofilm and siderophores pyocyanin and pyoverdine (12,66). However, the impact of polyP may extend beyond the bacterial cell itself. Exciting work by Roewe *et al.* (58) and others suggests that long-chain polyP released from pathogenic *E. coli* during infection reprograms the immune response of host macrophages (58,113,114). They propose that externally applied polyP shifts macrophage polarization from M1 to M2, a state associated with tissue repair and anti-inflammatory responses rather than pathogen clearance which is required to fight infection (58,115).

Physiologically, this may occur when bacterial polyP is released from cells that are lysed

by the host immune system (**Figure 7A**). Alternatively, some bacteria such as *M. smegmatis* and *M. tuberculosis* accumulate extracellular polyP which potentiates their survival in macrophages and *D. discoideum* (**Figure 7B**) (116). PolyP can also enter cells upon internalization of polyP bound-receptors (**Figure 7C**) (2). Intriguingly, these effects might be specific to long-chain bacterial polyP in contrast to shorter chains that are produce by human cells (117). For example, Brandt *et al.* (118) propose that short chain polyP (of 45 and 75 phosphates in length), reflective of that found in platelets (101), complexes with platelet factor 4 (PF4) to promote its binding to the bacterial surface and facilitate bacterial clearance by polymorphonuclear leukocytes. Therefore, in addition to promoting virulence and adaptation, bacterial polyP may modify the host immune system to its advantage.

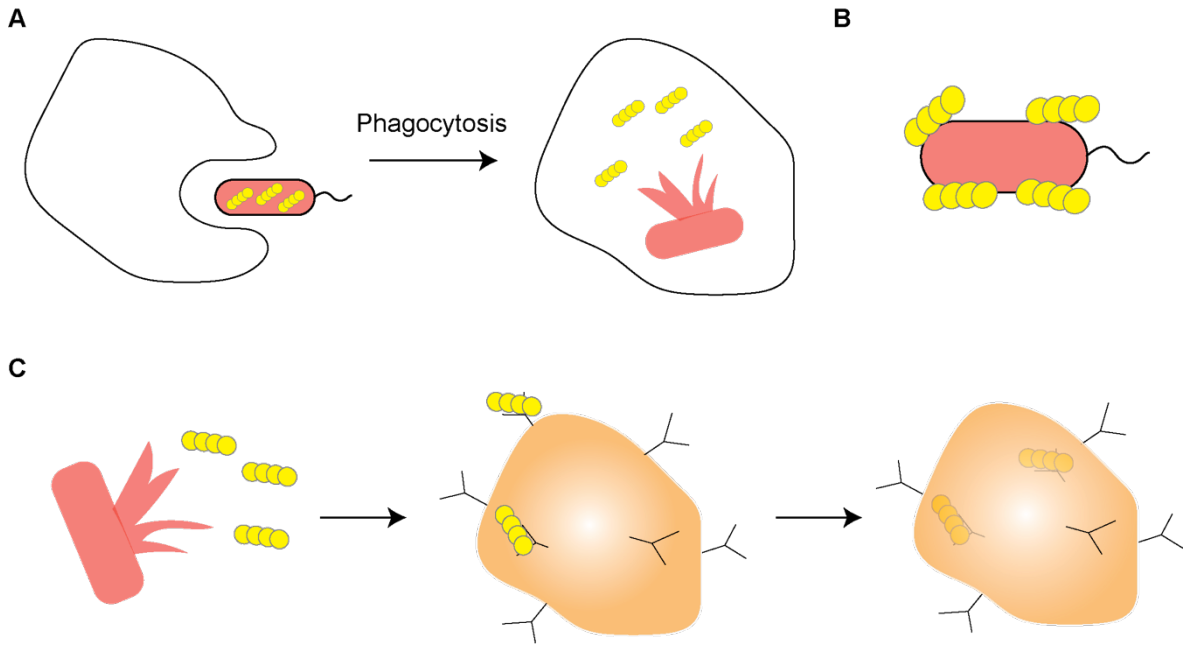

Figure 7. Mechanisms by which bacterial polyP may encounter human cells and proteins during infection. A) During phagocytosis by macrophages or other immune cells polyP may be released from bacterial that are lysed. **B**) PolyP may also accumulate on the exterior of bacterial cells during infection and interact with host-cell surfaces. This population can also be internalized by human cells via the mechanisms described in A and C. **C)** PolyP can enter cells upon endocytosis of polyP-bound receptors.

1.12. Targeting polyP synthesis as a novel strategy for antimicrobial therapy

There are multiple reasons to target polyP synthesis and accumulation as an alternative antimicrobial therapy or to sensitize bacteria to harsh conditions. First, polyP promotes bacterial virulence and facilitates the cells' ability to cope to environmental changes, such as those that occur during infection (e.g. stomach acid, changes in pH, temperature fluctuations). Second, higher eukaryotes lack PPK homologs making it a highly specific target for bacterial cells.

Previous efforts in this area have shown promise. An array of *in silico* molecular modelling and candidate-based approaches have been used to identify a few PPK inhibitors, some with 50% inhibitory concentration (IC_{50}) values in the lower micromolar (10 μM) range (see a review by Bowlin and Gray (119) for an excellent summary of these). Importantly, many recently described inhibitors show phenotypes that we would expect, based on our knowledge of PPK activities, to mirror the phenotypes of Δ*ppk* mutant bacteria. Of particular interest is the drug mesalamine. While exhibiting modest inhibition of *E. coli* PPK *in vitro*, mesalamine treatment at 100 μM decreased stress-induced polyP accumulation by ~2-fold in uropathogenic *E. coli*, *Vibrio cholerae*, and *P. aeruginosa* (112). Additionally, gallein, a commercially available fluorescent compound and G-protein antagonist has been shown to inhibit PPK1, PPK2A, PPK2B and, to a lesser extent, PPK2C classes of enzymes in *P. aeruginosa* (12).

Both mesalamine and gallein may have applications in the clinic. Like *ppk* mutants, there is a marked reduction of uropathogenic *E. coli* antibiotic-resistant persister cell formation in the caecal content of mice treated with mesalamine compared to untreated controls (112). Moreover, in addition to attenuating polyP production, biofilm production and bacterial motility, *P. aeruginosa* infection of *C. elegans* was reduced after gallein treatment, with no apparent effect on the host (12). This is thought to stem from the finding that cells lacking PPK enzymes or treated

with gallein have decreased levels of secreted siderophores (virulence factors) called pyoverdine and pyocyanin (12), which give *P. aeruginosa* cultures their distinctive green color (120).

1.13. Open questions in the field of bacterial polyP biology

In conclusion, polyP plays a vital role in bacterial survival, stress adaptation and virulence. Bacteria unable to produce polyP exhibit reduced growth under stress, a diminished ability to infect hosts, and decreased resistance to the bactericidal effects of antibiotics. As a result, PPK, the enzyme responsible for polyP production, is emerging as a promising target for alternative antimicrobial strategies. However, the precise mechanisms by which polyP supports bacterial stress adaptation and virulence remain poorly understood.

A significant gap in current research is a comprehensive understanding of the various pathways regulated by PPK and how these pathways work together to promote stress adaptation. Another area of inquiry is how polyP mechanistically influences protein activity within these signaling pathways.

1.14. Description of rationales and hypothesis

In this thesis, I present two manuscripts that address these open questions and expand on our current understanding of the roles of polyP during stress in *E. coli*. The first manuscript explores pathways that are regulated by polyP during nutrient starvation, while the second manuscript identifies proteins that may be targets of polyP binding during stress. Together, these works contribute to the field of bacterial polyP and emphasize how its regulation can be targeted for antimicrobial therapy.

1.14.1. Objective 1: Investigate pathways regulated by polyP during stress in *E. coli*

1.14.1.1. Rationale

It is certain that polyP plays a role in bacterial stress adaptation and virulence, and that PPK makes an attractive target for antimicrobial therapy. Additionally, there has been some effort made to understand how polyP mediates these pro-survival roles in bacteria. However, a broader understanding of the molecular pathways impacted by PPK activity and polyP accumulation remain poorly characterized. This question must be addressed before the potential of PPK as an antimicrobial target can be realized. Therefore, in this work, I use a mass spectrometry approach to identify pathways that are differentially regulated by PPK and subsequently, polyP. I further provide validation for the role of PPK in resistance to antimicrobial peptides.

1.14.1.2. Hypothesis

I hypothesize that PPK or polyP directly or indirectly regulate protein expression changes during nutrient starvation. To address this, I aim to use label-free mass spectrometry to identify novel proteins and pathways that are differentially regulated by PPK during nutrient starvation. Secondly, I aim to follow up on specific pathways to determine the impact of PPK or polyP on their regulation.

1.14.2. Objective 2: Determine the scope of polyP-protein binding in *E. coli*

1.14.2.1. Rationale

There is a strong link between polyP and PPK during the bacterial stress response. However, it remains largely unclear how polyP mechanistically regulates protein activity to promote stress adaptation in bacteria. In some cases, polyP is thought to interact directly with target proteins to modulate their activity. To date, our group and others have identified several yeast and mammalian proteins that bind polyP. However, despite the increasing list of targets, a thorough search for polyP-binding proteins in bacteria has yet to be conducted. Additionally, bacteria are the ideal model organism to study the function of polyP-protein binding as it overcomes the challenges posed in other species. For instance, the enzymes responsible for polyP synthesis and degradation are well-characterized. Also, there is a regulatory switch between conditions where polyP accumulates and is known to play a role. Additionally, unlike eukaryotic cells, polyP is not compartmentalized apart from its target proteins – offering the ideal system to examine the *in vivo* function of polyP-protein interactions.

1.14.2.2. Hypothesis

I hypothesize that polyP-protein binding plays a role in regulating the activity of proteins during stress in bacteria. To address this, I aim to conduct a screen to identify bacterial polyP-binding proteins. Secondly, I aim to determine the mechanism by which polyP-binding impacts the function of select proteins.

1.15. References

1. Kornberg A, Rao NN, Ault-Riché D. Inorganic polyphosphate: A molecule of many functions. Vol. 68, Annual Review of Biochemistry. 1999. p. 89–125.
2. Ferrucci V, Kong DY, Asadzadeh F, Marrone L, Boccia A, Siciliano R, et al. Long-chain polyphosphates impair SARS-CoV-2 infection and replication. Sci Signal. 2021;14(690):1–19.
3. Arredondo C, Cefaliello C, Dyrda A, Jury N, Martinez P, Díaz I, et al. Excessive release of inorganic polyphosphate by ALS/FTD astrocytes causes non-cell-autonomous toxicity to motoneurons. Neuron. 2022;110(10):1656-1670.e12.
4. Artur M. Orientierende untersuchungen über verbreitung. Morphologie, und chemie des volutins. Bot Zeit. 1904;62:113–152.
5. Wiame JM. Étude D'Une Substance Polyphosphorée, Basophile Et Métachromatique Chez Les Levures. BBA - Biochimica et Biophysica Acta. 1947;1(C):234–55.
6. Kornberg A. Inorganic polyphosphate: Toward making a forgotten polymer unforgettable. Vol. 177, Journal of Bacteriology. 1995. p. 491–6.
7. Akiyama M, Crooke E, Kornberg A. The polyphosphate kinase gene of Escherichia coli. Isolation and sequence of the ppk gene and membrane location of the protein. Journal of Biological Chemistry. 1992;267(31):22556–61.
8. Rashid MH, Rao NN, Kornberg A. Inorganic polyphosphate is required for motility of bacterial pathogens. J Bacteriol. 2000;182(1):225–7.
9. Rao NN, Gómez-García MR, Kornberg A. Inorganic polyphosphate: Essential for growth and survival. Annu Rev Biochem. 2009;78:605–47.
10. Kim KS, Rao NN, Fraley CD, Kornberg A. Inorganic polyphosphate is essential for long-term survival and virulence factors in Shigella and Salmonella spp. Proc Natl Acad Sci U S A. 2002;99(11):7675–80.
11. Zhang H, Ishige K, Kornberg A. A polyphosphate kinase (PPK2) widely conserved in bacteria. Proc Natl Acad Sci U S A. 2002;99(26):16678–83.
12. Neville N, Roberge N, Ji X, Stephen P, Lu JL, Jia Z. A Dual-Specificity Inhibitor Targets Polyphosphate Kinase 1 and 2 Enzymes To Attenuate Virulence of Pseudomonas aeruginosa. mBio. 2021;12(3):1–15.
13. Akiyama, M., Crooke, E. , Kornberg A. An exopolyphosphatase of Escherichia coli. The enzyme and its ppx gene in a polyphosphate operon. J Biochem. 1993;(1):633–9.
14. Lindner SN, Knebel S, Wesseling H, Schoberth SM, Wendisch VF. Exopolyphosphatases PPX1 and PPX2 from Corynebacterium glutamicum. Appl Environ Microbiol. 2009;75(10):3161–70.
15. Chuang YM, Bandyopadhyay N, Rifat D, Rubin H, Bader JS, Karakousis PC. Deficiency of the novel exopolyphosphatase Rv1026/PPX2 leads to metabolic downshift and altered cell wall permeability in Mycobacterium tuberculosis. mBio. 2015;6(2):1–15.
16. Zhang H, Gómez-García MR, Shi X, Rao NN, Kornberg A. Polyphosphate kinase 1, a conserved bacterial enzyme, in a eukaryote, Dictyostelium discoideum, with a role in cytokinesis. Proc Natl Acad Sci U S A. 2007;104(42):16486–91.
17. Yagisawa F, Fujiwara T, Yamashita S, Hirooka S, Tamashiro K, Izumi J, et al. A fusion protein of polyphosphate kinase 1 (PPK1) and a Nudix hydrolase is involved in inorganic polyphosphate accumulation in the unicellular red alga Cyanidioschyzon merolae. Plant Mol Biol. 2025;115(1).

18. Tzeng CM, Kornberg A. The multiple activities of polyphosphate kinase of Escherichia coli and their subunit structure determined by radiation target analysis. Journal of Biological Chemistry. 2000;275(6):3977–83.
19. Zhang H, Gómez-García MR, Brown MRW, Kornberg A. Inorganic polyphosphate in Dictyostelium discoideum: Influence on development, sporulation, and predation. Proc Natl Acad Sci U S A. 2005;102(8):2731–5.
20. Gerasimaitė, R., Mayer A. Ppn2, a novel Zn2+-dependent polyphosphatase in the acidocalcisome-like yeast vacuole. J Cell Sci. 2017;130(9):1625–36.
21. Auesukaree C, Homma T, Tochio H, Shirakawa M, Kaneko Y, Harashima S. Intracellular Phosphate Serves as a Signal for the Regulation of the PHO Pathway in Saccharomyces cerevisiae. Journal of Biological Chemistry. 2004;279(17):17289–94.
22. Gerasimaite, R., Sharma, S., Desfougeres, Y., Schmidt, A. and Mayer A. Coupled synthesis and translocation restrains polyphosphate to acidocalcisome-like vacuoles and prevents its toxicity. J Cell Sci. 2014;127(23):5093–5104.
23. Denoncourt A, Downey M. Model systems for studying polyphosphate biology: a focus on microorganisms. Vol. 67, Current Genetics. 2021. p. 331–46.
24. McCarthy L, Abramchuk I, Wafy G, Denoncourt A, Lavallée-Adam M, Downey M. Ddp1 Cooperates with Ppx1 to Counter a Stress Response Initiated by Nonvacuolar Polyphosphate. mBio. 2022;13(4):1–19.
25. Gerasimaite R, Mayer A. Enzymes of yeast polyphosphate metabolism: Structure, enzymology and biological roles. Biochem Soc Trans. 2016;44:234–9.
26. Yang W. Nucleases: diversity of structure, function and mechanism. Q Rev Biophys. 2011;44(1):1–93.
27. McCarthy L, Downey M. The emerging landscape of eukaryotic polyphosphatases. FEBS Lett. 2023;597(11):1447–61.
28. Sethuraman A, Rao NN, Kornberg A. The endopolyphosphatase gene: Essential in Saccharomyces cerevisiae. Proc Natl Acad Sci U S A. 2001;98(15):8542–7.
29. Kizawa K, Aono T, Ohtomo R. PHO8 gene coding alkaline phosphatase of Saccharomyces cerevisiae is involved in polyphosphate metabolism. Journal of General and Applied Microbiology. 2016;62(6):297–302.
30. Desfougères Y, Saiardi A, Azevedo C. Inorganic polyphosphate in mammals: Where's Wally? Biochem Soc Trans. 2020;48(1):95–101.
31. Baev, A.Y., Angelova, P.R. and Abramov AY. Inorganic polyphosphate is produced and hydrolyzed in F0F1-ATP synthase of mammalian mitochondria. Biochemistry. 2020;477(8):1515–24.
32. Baijal K, Downey M. The promises of lysine polyphosphorylation as a regulatory modification in mammals are tempered by conceptual and technical challenges. BioEssays. 2021;43(7).
33. Saiardi A, La B, Bru S. Polyphosphate degradation by Nudt3-Zn 2 + mediates oxidative stress response. Cell Rep. 2021;37(7):110004.
34. Rao NN, Liu S, Kornberg A. Inorganic polyphosphate in Escherichia coli: The phosphate regulon and the stringent response. J Bacteriol. 1998;180(8):2186–93.
35. Ault-Riché D, Fraley CD, Tzeng CM, Kornberg A. Novel assay reveals multiple pathways regulating stress-induced accumulations of inorganic polyphosphate in Escherichia coli. J Bacteriol. 1998;180(7):1841–7.
36. Gray MJ, Wholey WY, Wagner NO, Cremers CM, Mueller-Schickert A, Hock NT, et al.

Polyphosphate Is a Primordial Chaperone. Mol Cell. 2014;53(5):689–99.
37. Beaufay F, Quarles E, Franz A, Katamanin O, Wholey WY, Jakob U. Polyphosphate functions in vivo as an iron chelator and fenton reaction inhibitor. mBio. 2020;11(4):1–14.
38. Battesti, A., Majdalani, N., Gottesman S. The RpoS-Mediated General Stress Response in Escherichia coli*. Annu Rev Microbiol. 2011;65:189–213.
39. Gray MJ. Inorganic polyphosphate accumulation in Escherichia coli is regulated by DksA but not by (p)ppGpp. J Bacteriol. 2019;201(9).
40. Santos-Beneit F. The Pho regulon: a huge regulatory network in bacteria. Front Microbiol. 2015;6:402.
41. Rudat AK, Pokhrel A, Green TJ, Gray MJ. Mutations in Escherichia coli polyphosphate kinase that lead to dramatically increased in vivo polyphosphate levels. J Bacteriol. 2018;200(6).
42. Morohoshi T, Maruo T, Shirai Y, Kato J, Ikeda T, Takiguchi N, et al. Accumulation of inorganic polyphosphate in phoU mutants of Escherichia coli and Synechocystis sp. strain PCC6803. Appl Environ Microbiol. 2002;68(8):4107–10.
43. JD. K. Regulation of intracellular toxic metals and other cations by hydrolysis of polyphosphate. Ann N Y Acad Sci. 1997;829:242–9.
44. Grillo-Puertas M, Schurig-Briccio LA, Rodríguez-Montelongo L, Rintoul MR RVA. Copper tolerance mediated by polyphosphate degradation and low-affinity inorganic phosphate transport system in Escherichia coli. BMC Microbiol. 2014;14:72.
45. Lubin EA, Henry JT, Fiebig A, Crosson S LMT. Identification of the PhoB Regulon and Role of PhoU in the Phosphate Starvation Response of Caulobacter crescentus. J Bacteriol. 2015;198(1):187–200.
46. Harris RM, Webb DC, Howitt SM CGB. Characterization of PitA and PitB from Escherichia coli. J Bacteriol. 2001;183(17):5008–14.
47. Gardner SG, Johns KD, Tanner R MWR. The PhoU protein from Escherichia coli interacts with PhoR, PstB, and metals to form a phosphate-signaling complex at the membrane. J Bacteriol. 2014;196(9):1741–52.
48. Shiba T, Tsutsumi K, Yano H, Ihara Y, Kameda A, Tanaka K, et al. Inorganic polyphosphate and the induction of rpoS expression. Proc Natl Acad Sci U S A. 1997;94(21):11210–5.
49. Mandel MJ, Silhavy TJ. Starvation for different nutrients in Escherichia coli results in differential modulation of RpoS levels and stability. J Bacteriol. 2005;187(2):434–42.
50. Bowlin MQ, Long AR, Huffines JT GMJ. The role of nitrogen-responsive regulators in controlling inorganic polyphosphate synthesis in Escherichia coli. Microbiology (reading). 2022;168(4):001185.
51. Wang S, Deng K, Zaremba S, Deng X, Lin C, Wang Q, et al. Transcriptomic response of Escherichia coli O157:H7 to oxidative stress. Appl Environ Microbiol. 2009;75(19):6110–23.
52. Kuroda A, Murphy H, Cashel M, Kornberg A. Guanosine tetra- and pentaphosphate promote accumulation of inorganic polyphosphate in Escherichia coli. Journal of Biological Chemistry. 1997;272(34):21240–3.
53. Zhu Y, Huang W, Lee SSK, Xu W. Crystal structure of a polyphosphate kinase and its implications for polyphosphate synthesis. EMBO Rep. 2005;6(7):681–7.
54. Tzeng CM, Kornberg A. The multiple activities of polyphosphate kinase of Escherichia coli and their subunit structure determined by radiation target analysis. Journal of Biological Chemistry. 2000;275(6):3977–83.

55. Bowlin MQ, Lieber AD, Long AR, Gray MJ. C-terminal Poly-histidine Tags Alter Escherichia coli Polyphosphate Kinase Activity and Susceptibility to Inhibition. J Mol Biol. 2024;436(16).
56. Kyunghye, A., Kornberg A. Polyphosphate Kinase from Escherichia coli. Purification and demonstration of a phosphoenzyme intermediate. Biochemistry. 1990;265(20):11734–9.
57. Bondy-Chorney E, Abramchuk I, Nasser R, Holinier C, Denoncourt A, Baijal K, et al. A Broad Response to Intracellular Long-Chain Polyphosphate in Human Cells. Cell Rep. 2020;33(4).
58. Roewe J, Stavrides G, Strueve M, Sharma A, Marini F, Mann A, et al. Bacterial polyphosphates interfere with the innate host defense to infection. Nat Commun [Internet]. 2020;11(1):1–12. Available from: http://dx.doi.org/10.1038/s41467-020-17639-x
59. Rashid MH, Rumbaugh K, Passador L, Davies DG, Hamood AN, Iglewski BH, et al. Polyphosphate kinase is essential for biofilm development, quorum sensing, and virulence of Pseudomonas aeruginosa. Proc Natl Acad Sci U S A. 2000;97(17):9636–41.
60. Kuroda A, Tanaka S, Ikeda T, Kato J, Takiguchi N, Ohtake H. Inorganic polyphosphate kinase is required to stimulate protein degradation and for adaptation to amino acid starvation in Escherichia coli. Proc Natl Acad Sci U S A. 1999;96(25):14264–9.
61. Chen J, Su L, Wang X, Zhang T, Liu F, Chen H, et al. Polyphosphate kinase mediates antibiotic tolerance in extraintestinal pathogenic Escherichia coli PCN033. Front Microbiol. 2016;7(MAY).
62. Momeni A, Filiaggi MJ. Comprehensive study of the chelation and coacervation of alkaline earth metals in the presence of sodium polyphosphate solution. Langmuir. 2014;30(18):5256–66.
63. Keasling JD. Regulation of intracellular toxic metals and other cations by hydrolysis of polyphosphate. Ann N Y Acad Sci. 1997;829(510):242–9.
64. Lee RM, Hartman PA, Stahr HM, Olson DG, Williams FD. Antibacterial mechanism of long-chain polyphosphates in Staphylococcus aureus. J Food Prot [Internet]. 1994;57(4):289–94. Available from: https://doi.org/10.4315/0362-028X-57.4.289
65. Shah R, Narh JK, Urlaub M, Jankiewicz O, Johnson C, Livingston B, et al. Pseudomonas aeruginosa kills Staphylococcus aureus in a polyphosphate-dependent manner. mBio. 2024;9(10):1–23.
66. Cremers CM, Knoefler D, Gates S, Martin N, Dahl JU, Lempart J, Xie L, Chapman MR, Galvan V, Southworth DR JU. Polyphosphate: A Conserved Modifier of Amyloidogenic Processes. Mol Cell. 2016;63(5):768–80.
67. Kuroda A, Nomura K, Ohtomo R, Kato J, Ikeda T, Takiguchi N, et al. Role of inorganic polyphosphate in promoting ribosomal protein degradation by the Lon protease in E. coli. Science (1979). 2001;293(5530):705–8.
68. Ropelewska M, Gross MH KI. DNA and Polyphosphate in Directed Proteolysis for DNA Replication Control. Front Microbiol. 2020;11:585717.
69. Racki LR, Tocheva EI, Dieterle MG, Sullivan MC, Jensen GJ, Newman DK. Polyphosphate granule biogenesis is temporally and functionally tied to cell cycle exit during starvation in Pseudomonas aeruginosa. Proc Natl Acad Sci U S A. 2017;114(12):E2440–9.
70. Azevedo C, Livermore T, Saiardi A. Protein polyphosphorylation of lysine residues by inorganic polyphosphate. Mol Cell. 2015;58(1):71–82.
71. Azevedo C, Singh J, Steck N, Hofer A, Ruiz FA, Singh T, et al. Screening a Protein Array with Synthetic Biotinylated Inorganic Polyphosphate to Define the Human PolyP-ome.

ACS Chem Biol. 2018;13(8):1958–63.
72. Neville N, Lehotsky K, Klupt KA, Downey M, Neville N, Lehotsky K, et al. Polyphosphate attachment to lysine repeats is a non-covalent protein modification. Mol Cell. 2024;84(9):1802–10.
73. Neville N, Lehotsky K, Yang Z, Klupt KA, Denoncourt A, Downey M, et al. Modification of histidine repeat proteins by inorganic polyphosphate. Cell Rep. 2023;42(9).
74. Neville N, Lehotsky K, Jia Z. Back on the chain gang: polyphosphate modification of proteins. Trends Biochem Sci. 2024;49(9):757–60.
75. McCarthy, L., Baijal, K., Downey M. A framework for understanding and investigating polyphosphate-protein interactions. Biochem Soc Trans. 2025;21:BST20240678.
76. Azevedo C, Livermore T, Saiardi A. Protein polyphosphorylation of lysine residues by inorganic polyphosphate. Mol Cell. 2015;58(1):71–82.
77. Bentley-DeSousa A, Holinier C, Moteshareie H, Tseng YC, Kajjo S, Nwosu C, et al. A Screen for Candidate Targets of Lysine Polyphosphorylation Uncovers a Conserved Network Implicated in Ribosome Biogenesis. Cell Rep. 2018;22(13):3427–39.
78. McCarthy L, Bentley-DeSousa A, Denoncourt A, Tseng YC, Gabriel M, Downey M. Proteins required for vacuolar function are targets of lysine polyphosphorylation in yeast. FEBS Lett. 2020;594(1):21–30.
79. Parnell AE, Mordhorst S, Kemper F, Giurrandino M, Prince JP, Schwarzer NJ, et al. Substrate recognition and mechanism revealed by ligand-bound polyphosphate kinase 2 structures. Proc Natl Acad Sci U S A. 2018;115(13):3350–5.
80. Yoo NG, Dogra S, Meinen BA, Tse E, Haefliger J, Southworth DR, et al. Polyphosphate Stabilizes Protein Unfolding Intermediates as Soluble Amyloid-like Oligomers. J Mol Biol. 2018;430(21):4195–208.
81. Sasahara K, Yamaguchi K, So M GY. Polyphosphates diminish solubility of a globular protein and thereby promote amyloid aggregation. J Biol Chem. 2019;294(42):15318–29.
82. Guan J, Jakob U. The Protein Scaffolding Functions of Polyphosphate. J Mol Biol. 2024;436(14).
83. Wickramasinghe SP, Lempart J, Merens HE, Murphy J, Huettemann P, Jakob U RE. Polyphosphate Initiates Tau Aggregation through Intra- and Intermolecular Scaffolding. Biophys J. 2019;117(4):717–28.
84. Zhang CM, Yamaguchi K, So M, Sasahara K, Ito T, Yamamoto S, Narita I, Kardos J, Naiki H GY. Possible mechanisms of polyphosphate-induced amyloid fibril formation of β2-microglobulin. 2019. 116(26):12833–8.
85. Huettemann P, Mahadevan P, Lempart J, Tse E, Dehury B, Edwards BFP, Southworth DR, Sahoo BR JU. Amyloid accelerator polyphosphate fits as the mystery density in α-synuclein fibrils. PLoS Biol. 2024;22(10):e3002650.
86. Kuroda A. A polyphosphate-lon protease complex in the adaptation of Escherichia coli to amino acid starvation. Biosci Biotechnol Biochem. 2006;70(2):325–31.
87. Kuroda A, Nomura K, Takiguchi N, Kato J OH. Inorganic polyphosphate stimulates lon-mediated proteolysis of nucleoid proteins in Escherichia coli. Cell and Mol Bio. 2006;52(4):23–9.
88. Gross MH, Konieczny I. Polyphosphate induces the proteolysis of ADP-bound fraction of initiator to inhibit DNA replication initiation upon stress in Escherichia coli. Nucleic Acids Res. 2021;48(10):5457–66.
89. Wrench AP, Gardner CL, Siegel SD, Pagliai FA, Malekiha M, Gonzalez CF, et al.

MglA/SspA Complex Interactions Are Modulated by Inorganic Polyphosphate. PLoS One. 2013;8(10).
90. Choi, SH., Smith, SA., Morrissey JH. Polyphosphate accelerates factor V activation by factor XIa. Thrmb Haemost. 2015;113(3):599–604.
91. Choi SH, Smith SA, Morrissey JH. Polyphosphate is a cofactor for the activation of factor XI by thrombin. Blood. 2011;118(26):6963–70.
92. Malik RA, Zhou J, Fredenburgh JC, Truong TK, Crosby JR, Revenko AS, et al. Polyphosphate-induced thrombosis in mice is factor XII dependent and is attenuated by histidine-rich glycoprotein. Blood Adv. 2021;5(18):3540–51.
93. Mutch, NJ., Myles, T., Leung, LLK., Morrissey JH. Polyphosphate binds with high affinity to exosite II of thrombin. J Throb Haemost. 2010;8(3):548–55.
94. Montilla M, Atienza-Navarro I, García-Cozar FJ, Castro C, Rodríguez-Martorell FJ, Ruiz FA. Polyphosphate Activates von Willebrand Factor Interaction with Glycoprotein Ib in the Absence of Factor VIII In Vitro. Int J Mol Sci. 2022;23(22).
95. Montilla M, Hernández-Ruiz L, García-Cozar FJ, Alvarez-Laderas I, Rodríguez-Martorell J, Ruiz FA. Polyphosphate binds to human von Willebrand factor in vivo and modulates its interaction with glycoprotein Ib. Journal of Thrombosis and Haemostasis. 2012;10(11):2315–23.
96. Martinez De Lagran M, Benavides-Piccione R, Ballesteros-Yañez I, Calvo M, Morales M, Fillat C, et al. Dyrk1A influences neuronal morphogenesis through regulation of cytoskeletal dynamics in mammalian cortical neurons. Cerebral Cortex. 2012;22(12):2867–77.
97. Dirice E, Walpita D, Vetere A, Meier BC, Kahraman S, Hu J, et al. Inhibition of DYRK1A stimulates human β-cell proliferation. Diabetes. 2016;65(6):1660–71.
98. Rammohan M, Harris E, Bhansali RS, Zhao E, Li LS, Crispino JD. The chromosome 21 kinase DYRK1A: emerging roles in cancer biology and potential as a therapeutic target. Oncogene. 2022;41(14):2003–11.
99. Barzowska A, Pucelik B, Pustelny K, Matsuda A, Martyniak A, Maksymiuk A, et al. DYRK1A kinase inhibitors promote beta-cell survival and insulin homeostasis. Cells. 2021;10(2263).
100. Lu J, Wu T, Zhang B, Liu S, Song W, Qiao J, et al. Types of nuclear localization signals and mechanisms of protein import into the nucleus. Cell Communication and Signaling. 2021;19(1):1–10.
101. Ruiz FA, Lea CR, Oldfield E, Docampo R. Human platelet dense granules contain polyphosphate and are similar to acidocalcisomes of bacteria and unicellular eukaryotes. Journal of Biological Chemistry. 2004;279(43):44250–7.
102. Hassanian SM, Dinarvand P, Smith SA RAR. Inorganic polyphosphate elicits pro-inflammatory responses through activation of the mammalian target of rapamycin complexes 1 and 2 in vascular endothelial cells. J Throb Haemost. 2015;13(5):860–71.
103. Dinarvand P, Hassanian SM, Qureshi SH, Manithody C, Eissenberg JC, Yang L RAR. Polyphosphate amplifies proinflammatory responses of nuclear proteins through interaction with receptor for advanced glycation end products and P2Y1 purinergic receptor. Blood. 2014;123(6):935–45.
104. Holmström KM, Marina N, Baev AY, Wood NW, Gourine AV AAY. Signalling properties of inorganic polyphosphate in the mammalian brain. Nat Commun. 2013;4(1362).
105. Neufurth M, Wang X, Tolba E, Lieberwirth I, Wang S, Schröder HC MWEG. The inorganic

polymer, polyphosphate, blocks binding of SARS-CoV-2 spike protein to ACE2 receptor at physiological concentrations. Biochem Pharmacol. 2020;182(114215).
106. Mantilla BS, Azevedo C, Denny PW, Saiardi A DR. The Histidine Ammonia Lyase of Trypanosoma cruzi Is Involved in Acidocalcisome Alkalinization and Is Essential for Survival under Starvation Conditions. mBio. 2021;12(6):e0198121.
107. Wang L, Fraley CD, Faridi J, Kornberg A, Roth RA. Inorganic polyphosphate stimulates mammalian TOR, a kinase involved in the proliferation of mammary cancer cells. Proc Natl Acad Sci U S A. 2003;100(20):11249–54.
108. Beaufay F, Amemiya HM, Guan J, Basalla J, Meinen BA, Chen Z, et al. Polyphosphate drives bacterial heterochromatin formation. Sci Adv. 2021;7(52).
109. Yang ZX, Zhou YN, Yang Y JDJ. Polyphosphate binds to the principal sigma factor of RNA polymerase during starvation response in Helicobacter pylori. Mol Microbiol. 2010;77(3):618–27.
110. Ito T, Yamamoto S, Yamaguchi K, Sato M, Kaneko Y, Goto S, Goto Y NI. Inorganic polyphosphate potentiates lipopolysaccharide-induced macrophage inflammatory response. J Bio Chem. 2020;295(12):4104–4023.
111. Rashid MH, Rumbaugh K, Passador L, Davies DG, Hamood AN, Iglewski BH, et al. Polyphosphate kinase is essential for biofilm development, quorum sensing, and virulence of Pseudomonas aeruginosa. Proc Natl Acad Sci U S A. 2000;97(17):9636–41.
112. Dahl JU, Gray MJ, Bazopoulou D, Beaufay F, Lempart J, Koenigsknecht MJ, et al. The anti-inflammatory drug mesalamine targets bacterial polyphosphate accumulation. Nat Microbiol. 2017;2.
113. Suess PM, Chinea LE, Pilling D, Gomer RH. Extracellular Polyphosphate Promotes Macrophage and Fibrocyte Differentiation, Inhibits Leukocyte Proliferation, and Acts as a Chemotactic Agent for Neutrophils. The Journal of Immunology. 2019;203(2):493–9.
114. Roewe J, Walachowski S, Sharma A, Berthiaume KA, Reinhardt C, Bosmann M. Bacterial polyphosphates induce CXCL4 and synergize with complement anaphylatoxin C5a in lung injury. Front Immunol. 2022;13(November):1–13.
115. Luo M, Zhao F, Cheng H, Su M, Wang Y. Macrophage polarization: an important role in inflammatory diseases. Front Immunol. 2024;15(April):1–16.
116. Rijal R, Cadena LA, Smith MR, Carr JF, Gomer RH. Polyphosphate is an extracellular signal that can facilitate bacterial survival in eukaryotic cells. Proc Natl Acad Sci U S A. 2020;117(50):31923–34.
117. Krenzlin V, Schöche J, Walachowski S, Reinhardt C, Radsak MP, Bosmann M. Immunomodulation of neutrophil granulocyte functions by bacterial polyphosphates. Eur J Immunol. 2023;53(5):1–8.
118. Brandt S, Krauel K, Jaax M, Renné T, Helm CA, Hammerschmidt S, et al. Polyphosphates form antigenic complexes with platelet factor 4 (PF4) and enhance PF4-binding to bacteria. Thromb Haemost. 2015;114(6):1189–98.
119. Bowlin, MQ., and Gray MJ. Inorganic Polyphosphate in Host and Microbe Biology. Trends Microbiol. 2021;(Epub 2021).
120. Sadikot RT, Blackwell TS, Christman JW, Prince AS. Pathogen-host interactions in pseudomonas aeruginosa pneumonia. Am J Respir Crit Care Med. 2005;171(11):1209–23.

CHAPTER 2 – MANUSCRIPT #1

Polyphosphate kinase regulates LPS structure and polymyxin resistance during starvation in *E. coli*

Publication information:
Baijal, K., Abramchuk, I., Herrera, C. M., Mah, T. F., Trent, M. S., Lavallée-Adam, M., & Downey, M. (2024). Polyphosphate kinase regulates LPS structure and polymyxin resistance during starvation in E. coli. *PLoS biology*, *22*(3), e3002558.
https://doi.org/10.1371/journal.pbio.3002558

Author's contributions:
Conceptualization: K.B., M.D. Methodology: K.B., I.A., C.M.H. Investigation: K.B., I.A., C.M.H. Supervision: S.M.T., M.L.A., M.D. T.M. Writing – original draft: K.B., M.D. Writing – review and editing: All authors.

Contributions by figure: Fig 1 (K.B., I.A.), Fig 2 (K.B.), Fig 3 (K.B.), Fig 4 (K.B., C.M.H.), Fig S1-S6 (K.B.).

Polyphosphate kinase regulates LPS structure and polymyxin resistance during starvation in *E. coli*

Kanchi Baijal[1,2], Iryna Abramchuk[1,3#], Carmen M. Herrera[4#], Thien-Fah Mah[3,5], M. Stephen Trent[4], Mathieu Lavallée-Adam[1,3], and Michael Downey[1,2*]

1. Ottawa Institute of Systems Biology, Ottawa, Ontario, Canada.
2. Department of Cellular & Molecular Medicine, University of Ottawa, Ottawa, Ontario, Canada.
3. Department of Biochemistry, Microbiology, and Immunology, University of Ottawa, Ottawa, Ontario, Canada.
4. Department of Infectious Diseases, College of Veterinary Medicine, University of Georgia, Athens, GA, USA.
5. Centre for Infection, Immunity, and Inflammation, University of Ottawa, Ottawa, Ontario, Canada.

# Equal contribution from second authors

* Correspondence: mdowne2@uottawa.ca

2.1. Abstract

Polyphosphates (polyP) are chains of inorganic phosphates that can reach over 1000 residues in length. In *Escherichia coli*, polyP is produced by the polyP kinase (PPK) and is thought to play a protective role during the response to cellular stress. However, the molecular pathways impacted by PPK activity and polyP accumulation remain poorly characterized. In this work we used label-free mass spectrometry to study the response of bacteria that cannot produce polyP (Δ*ppk*) during starvation to identify novel pathways regulated by PPK.

In response to starvation, we found 92 proteins significantly differentially expressed between wild-type and Δ*ppk* mutant cells. Wild-type cells were enriched for proteins related to amino acid biosynthesis and transport, while Δ*ppk* mutants were enriched for proteins related to translation and ribosome biogenesis, suggesting that without PPK, cells remain inappropriately primed for growth even in the absence of the required building blocks.

From our dataset, we were particularly interested in Arn and EptA proteins, which were downregulated in Δ*ppk* mutants compared to wild-type controls, because they play a role in lipid A modifications linked to polymyxin resistance. Using western blotting, we confirm differential expression of these and related proteins in K-12 strains and a uropathogenic isolate, and provide evidence that this mis-regulation in Δ*ppk* cells stems from a failure to induce the BasRS two-component system during starvation. We also show that Δ*ppk* mutants unable to upregulate Arn and EptA expression lack the respective L-Ara4N and pEtN modifications on lipid A. In line with this observation, loss of *ppk* restores polymyxin sensitivity in resistant strains carrying a constitutively active *basR* allele.

Overall, we show a new role for PPK in lipid A modification during starvation and provide a rationale for targeting PPK to sensitize bacteria towards polymyxin treatment. We further

anticipate that our proteomics work will provide an important resource for researchers interested in the diverse pathways impacted by PPK.

2.2. Introduction

Polyphosphates (polyP) are homopolymers of inorganic phosphates joined together by high energy phosphoanhydride bonds. Although polyP is found across diverse organisms from bacteria to humans, the intracellular concentrations, and mechanisms by which it is produced vary widely (1-3). In *Escherichia coli* (*E. coli*), polyP is synthesized by the polyphosphate kinase PPK and degraded by the exopolyphosphatase PPX (1). In general, *E. coli* produce little to no detectable polyP when undergoing logarithmic growth in nutrient rich media (4). However, in response to diverse cellular stressors including oxidative stress caused by exposure to hypochlorous acid (bleach) (5), heat shock (6), and nutrient starvation (7), PPK rapidly synthesizes polyP using ATP as a co-substrate (1). This stress-induced population of polyP has been linked to protein folding and turnover (5, 6), transcriptional (8, 9) and translational control (10), and the regulation of bacterial heterochromatin (11). In some cases, polyP is thought to impart these changes by interacting directly with protein targets to modulate their activity. For example, polyP produced during nutrient downshift interacts with the Lon protease to direct its activity towards degradation of ADP-bound DnaA and ribosomal proteins (12-14). Collectively, these pathways inhibit DNA replication, while increasing the intracellular pool of amino acids to help *E. coli* adapt to changing conditions (12, 14). PolyP can also function by chelating cations, for example as an inhibitor of the Fenton reaction in which iron catalyzes the formation of reactive oxygen species (15). *E. coli* *ppk* mutants (e.g. Δ*ppk*) display increased sensitivity to cellular stress (5, 6, 16) and decreased motility (17), biofilm formation (16), and virulence (18-20). While the molecular events underlying these phenotypes are not always known, the role of PPK enzymes as regulators of survival during cell stress is conserved across the bacterial kingdom. Notably, in addition to synthesizing polyP, PPK enzymes can also use polyP as a donor substrate to catalyze the

phosphorylation of nucleoside diphosphates (21), although the degree to which these functions contribute to stress resistance is unclear.

The PPK status of pathogenic *E. coli* is an important regulator of infectivity in mouse models of infection (18, 22). It has been suggested that polyP released by *E. coli* may play an important role in the reprogramming of macrophages, and this may involve polyP interaction with host receptors on the cell membrane or entry into host cells (18). PPK has also been proposed as a novel target for various bacterial infections (16, 23). It is noteworthy that mesalamine, a drug used to treat ulcerative colitis and Crohn's disease, inhibits PPK enzymes *in vitro* and can reduce ampicillin-resistant persister cell formation of uropathogenic *E. coli* in a *ppk*-dependent manner (16). The pursuit of PPK as a valid therapeutic target demands a thorough understanding of how PPK impacts bacterial stress responses at a systems-wide level.

To better understand the role of PPK and polyP in bacterial stress responses, we used label-free proteomics to identify proteins up- or downregulated in Δ*ppk* mutant cells relative to wild-type MG1655 K-12 controls undergoing prolonged starvation, when polyP levels are high. We report that mutant Δ*ppk* cells fail to upregulate pathways required for amino acid biosynthesis and instead are enriched for processes related to ribosome biogenesis. In follow up work, we show a role for PPK in the modification of lipid A – the lipid anchor of the lipopolysaccharide (LPS) at the cell surface of Gram-negative bacteria (24). We demonstrate that during starvation, PPK is required for expression of EptA and the Arn proteins, and their respective phosphoethanolamine (pEtN) and 4-amino-4-deoxy-L-arabinose (L-Ara4N) lipid A modifications, as well as for expression of the upstream BasRS two-component system. In an antibiotic-resistant strain background, cells lacking *ppk* display increased susceptibility to the cationic antimicrobial peptide polymyxin B. Together, our work provides a novel resource for investigating molecular

functions of polyP and new insights into how PPK inhibition might be best exploited in the clinic.

2.3. Results

2.3.1. Proteomic differences between wild-type controls and Δ*ppk E. coli* upon nutrient starvation

We used label-free mass spectrometry analysis to compare proteomic differences between wild-type MG1655 K-12 and Δ*ppk* mutants following a shift from LB to MOPS minimal media (**Fig. 1A**). In the bacterial polyP field, a shift from nutrient rich to MOPS minimal media is commonly used to trigger polyP accumulation (4, 25, 26). At the 3-hour time point used for analysis, all five replicates of wild-type cells showed accumulation of polyP, whereas Δ*ppk* mutants did not (**Fig. S1**). Bioinformatics analysis of mass spectrometry data uncovered 1909 proteins total, of which 78 were significantly differentially expressed between the two conditions (FDR-adjusted *p*-value < 0.05) (**Fig. 1B, Supplementary Table 1**). In addition, 14 proteins were classified as all-or-none (detected in 0 replicates of Δ*ppk* mutant cells but detected in all 5 replicates of wild-type cells, or vice versa) (**Fig. 1C, Supplementary Table 1**). We used western blotting to confirm expression differences for 6 (ArnB, ArnC, MetE, YbdL, YeaG, OtsA) out of the 7 top hits, validating the overall high-quality of the data set (**Fig. 1D**). Only RaiA-3Flag failed to confirm in targeted western blotting experiments, showing inconsistent results between replicates.

Previous work by Varas *et al.* used mass spectrometry to compare proteomes of wild-type controls and Δ*ppk* mutants in nutrient rich LB media (27), where there is no detectable polyP accumulation (4, 28). There, the authors identified 60 proteins upregulated and 32 proteins downregulated in Δ*ppk* cells (29). The overlap between these differentially expressed proteins and

the dataset described in our work is poor (**Supplementary Table 2**). This suggests that there are vast proteomic differences between bacteria experiencing stress compared to those grown in LB media, and that there are unique roles of PPK and polyP in proteomic regulation during starvation that are uncovered by our work.

We performed Gene Ontology (GO) (30) enrichment analysis on the significantly differentially expressed and all-or-none proteins (92 total) and identified 16 enriched GO terms (FDR-adjusted *p*-value < 0.05) (**Fig. 1 E**). These included terms related to amino acid, organic acid, and small molecule biosynthesis. We next used Gene Set Enrichment Analysis (GSEA) (31) on the entire data set of 1909 proteins to look for GO terms that are differentially expressed between the wild-type cells and Δ*ppk* mutants. This analysis showed that wild-type cells were enriched for proteins related to amino acid biosynthesis and transport (**Fig. 1F**). In contrast, Δ*ppk* mutant cells were enriched for proteins broadly related to ribosome biogenesis and translation (**Fig. 1F**). We also searched our data set for key regulators of the stringent response, a stress signalling system activated by nutrient starvation and mediated by the alarmones guanosine tetraphosphate (ppGpp) and guanosine pentaphosphate (pppGpp), collectively referred to as (p)ppGpp (32). Notably, we did not observe significant differential expression of the proteins involved in (p)ppGpp synthesis such as RelA, SpoT and GppA (33), or other regulators such as DksA (34) and RplK (35) between wild-type and Δ*ppk* mutants. Regardless, these data point to a model wherein Δ*ppk* mutants fail to properly respond to starvation by remaining primed for growth while failing to activate pathways to increase the availability of amino acids and other biomolecules needed for that purpose. In line with this interpretation, polyP interacts with the Lon protease to promote degradation of ribosomal proteins including S2, L9 and L13, as well as nucleoid proteins such as HupA, HimA (IhfA) and translational elongational protein InfC (12, 36). This degradation has

been proposed to provide free amino acids to allow for targeted translation during starvation (12). In agreement with this data, we detected significant upregulation of 30S ribosomal proteins S7 and S8 in Δ*ppk* mutants compared to wild-type controls (**Fig. 1B and Supplementary Table 1**). Overall, our work demonstrates that PPK is required for a timely response to MOPS-induced starvation.

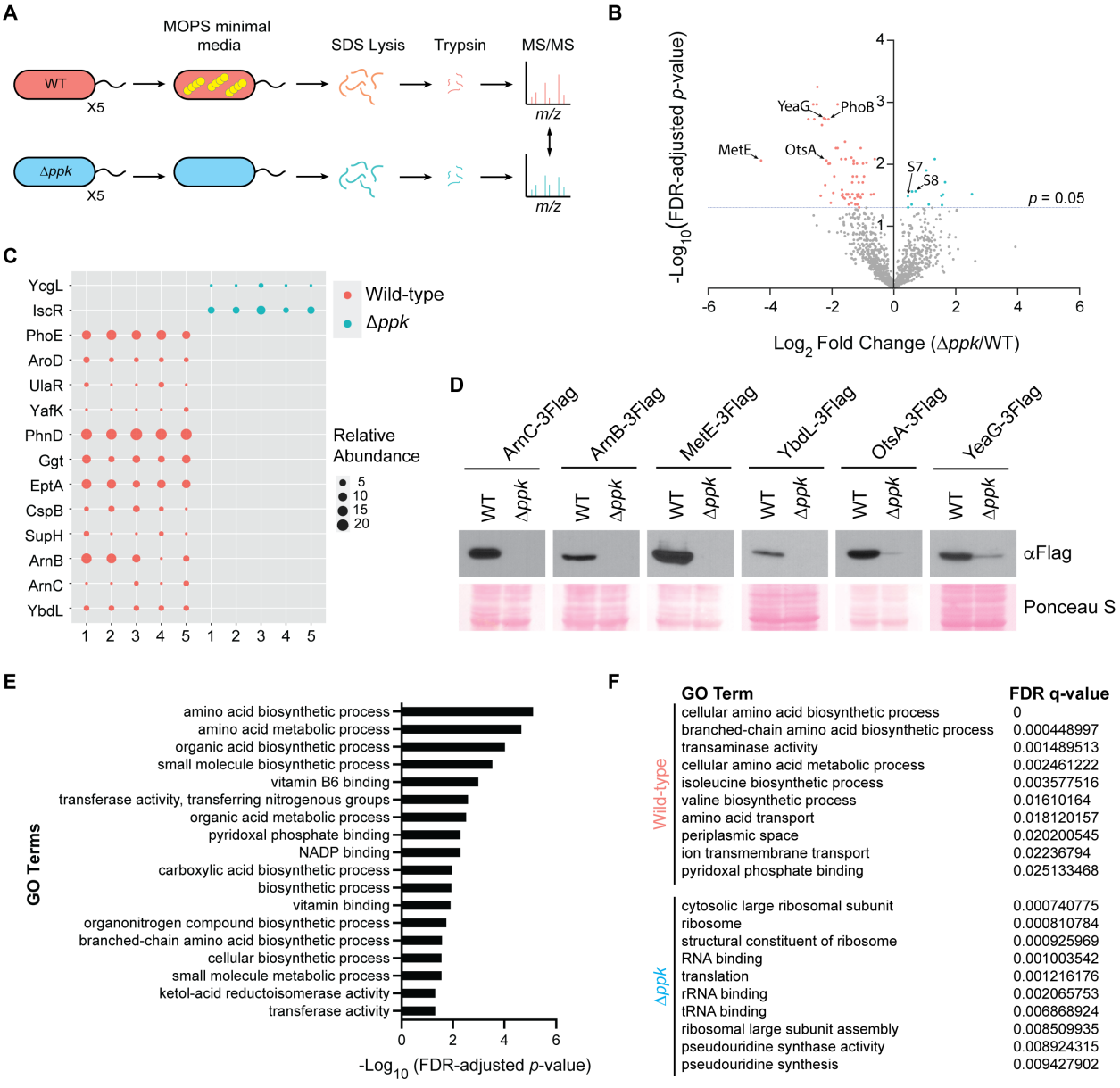

Figure 1 – Figure legend on the next page

Figure 1. Broad proteomic changes in Δ*ppk* cells during stress. A) Experimental set up for proteomics analysis. Cells were grown in LB media to mid-exponential phase before a shift into MOPS minimal media (0.1 mM K_2HPO_4, 0.4% glucose) for 3 hours to induce amino acid starvation and polyP accumulation. The experiment was conducted using n=5 biological replicates. **B)** Volcano plot of significantly differentially expressed proteins (log_2(fold-change Δ*ppk*/WT)). In red and blue are the significantly upregulated proteins (FDR-adjusted *p*-value < 0.05) in wild-type and Δ*ppk* strains, respectively. **C)** Bubble plot showing the 'all-or-none' proteins detected only in either wild-type cells or Δ*ppk* mutants. Data represent the raw protein spectral counts in 5 biological replicates from each condition. **D)** Select confirmations of mass spectrometry data. Chromosomally C-terminal 3Flag-tagged strains were grown under the same conditions used for the mass spectrometry analysis. Protein extracts were resolved using a 12% (for YbdL-3Flag) and 10% (for all other proteins) SDS-PAGE gel, transferred to PVDF membrane, and probed using an anti-Flag antibody. Images are representative of results from ≥3 experiments. **E)** GO terms that are significantly enriched among the differentially expressed and 'all-or-none proteins' identified by mass spectrometry analysis. **F**) GO terms deemed differentially expressed based on GSEA for wild-type and Δ*ppk* mutant cells. The underlying data for Figs. 1B, 1C and 1E can be found in S1_Data.

2.3.2. Lack of amino acids does not explain Δ*ppk* mutant phenotypes

We detected upregulation of many amino acid biosynthesis and binding enzymes in wild-type controls compared to Δ*ppk* mutants (33% of significantly differentially expressed proteins, **Supplementary Table 1**). We wondered if a lack of available amino acids could account for the phenotypic and proteomic differences observed in our experiments. In comparison to wild-type cells grown in MOPS media, Δ*ppk* mutants displayed decreased growth rate and maximum cell density (**Figs. 2A-C**). We found that Δ*ppk* cells also had a dramatic increase in the lag phase (**Fig. 2D**). Supplementation of MOPS media with 0.05 % amino acids improved the growth parameters of both strains, but the difference in growth rate and lag phase persisted (**Figs. 2B and 2D**). The growth rate defect conferred by *ppk* mutation persisted even with the addition of 10-fold excess amino acids (0.5 %) (**Fig. 2B**). At the protein level, addition of amino acids to MOPS media increased the expression of YbdL-3Flag, with minor increases for MetE-3Flag, YeaG-3Flag, and OtsA-3Flag in wild-type cells (**Fig. 2E**). However, in Δ*ppk* mutants, addition of amino acids failed to rescue protein expression to levels seen in untreated wild-type cells (**Fig. 2E**).

Together, these data suggest that while amino acid deficiencies may contribute to some phenotypes of Δ*ppk* mutant cells, they are unlikely to explain the broad protein dysregulation observed in our proteomics dataset. Instead, we postulate that wild-type cells respond to MOPS-induced stress more promptly than Δ*ppk* cells by modulating the expression of multiple pathways. Protein differences could stem from changes in transcription or translation, or from changes in protein stability. Investigation of these distinct pathways will uncover new insights into PPK and polyP modes of action.

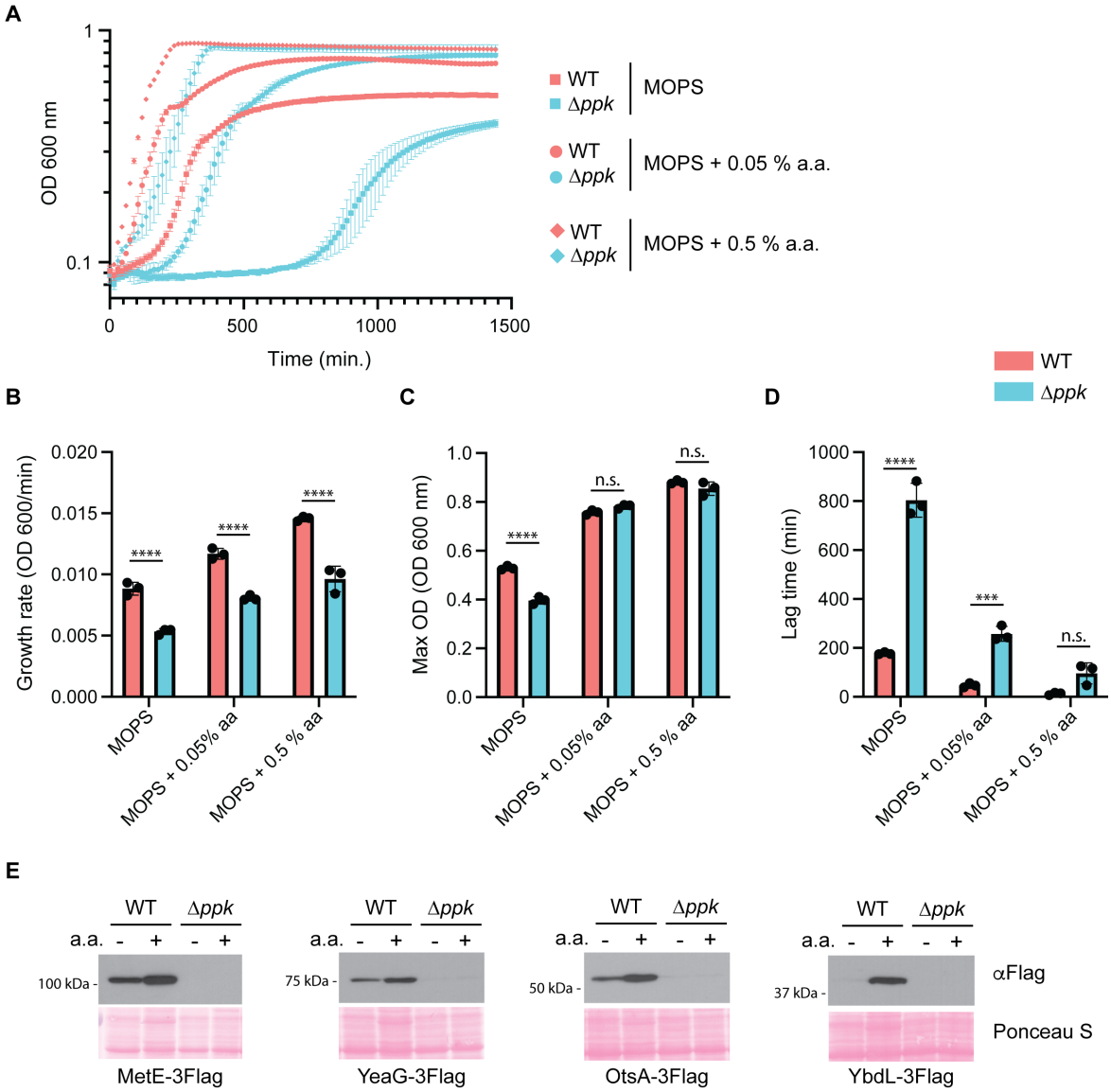

Figure 2 – Figure legend on the next page.

Figure 2. Impact of amino acid deficiencies on growth and proteome regulation in Δ*ppk* mutants. A) Growth of wild-type and Δ*ppk* mutant cells in MOPS media without and with 0.05 % or 0.5% amino acid supplementation. Cells were grown in LB to mid-exponential phase and then diluted to 0.1 OD_{600} in MOPS minimal media in the absence or presence of 0.05% or 0.5% amino acids. Growth was monitored using the BioscreenC plate reader (37 °C with shaking, wavelength 600 nm). Error bars represent standard deviation of the mean for 3 biological replicates. Error bars not shown for data points where standard deviation is smaller than size of the symbol itself. **B-D)** Impact of amino acids on wild-type and Δ*ppk* mutant growth dynamics. Growth rate (OD_{600}/min) (B), max OD_{600} (C) and lag time (min) (D) measurements of the growth curves shown in Figure 2A were calculated using GrowthRates 6.2 (Bellingham Research Institute). Mean values with standard deviation are shown. ****, $p< 0.0001$; *** $p< 0.001$, n.s., non-significant via two-way ANOVA with Tukey's post hoc analysis. The underlying data for Figs. 2A-D can be found in S2_Data. **E)** Effect of amino acid supplementation on the expression of significantly differentially expressed proteins. Cells were grown to mid-exponential phase in LB and then shifted to MOPS minimal media in the presence or absence of 0.05% amino acids for 3 hours. Protein extracts were resolved using a 12% SDS-PAGE gel, transferred to PVDF membrane, and detected using an anti-Flag antibody. Images are representative of results from ≥3 experiments.

2.3.3. PPK plays a role in regulating expression of proteins required for lipid A modification

We were intrigued by the proteins ArnB, ArnC and EptA, which were only detected in wild-type control but not in Δ*ppk* mutant samples, because they function in pathways associated with cationic antibiotic resistance (24, 37-39). The Arn proteins (ArnA, B, C and D) synthesize the donor substrate for the L-Ara4N modification, undecaprenyl-phosphate-L-Ara4N, on the cytoplasmic side of the inner membrane (38-40) **(Fig. 3A)**. The undecaprenyl substrate is then flipped across the membrane by ArnE and ArnF (41) (**Fig. 3A**). The glycosyl transferase ArnT then transfers L-Ara4N from the undecaprenyl donor to the lipid A domain of the LPS at the periplasmic face of the inner membrane (42) **(Fig. 3A)**. Like ArnT, the active site of EptA that is responsible for pEtN modification resides in the periplasm (43) **(Fig. 3A)**. Lastly, both pEtN and L-Ara4N modified lipid A are transported to the outer membrane by the LPS transport system (44). For more information on the pathway, see review by Whitfield and Trent (45).

Together, L-Ara4N and pEtN modifications decrease the net negative charge of the outer membrane and reduce the interaction with cationic antimicrobial peptides such as polymyxin (46). As we found for ArnC-3Flag and ArnB-3Flag in **Fig. 1D**, expression of EptA-3Flag was reduced in *ppk* mutants compared to wild-type controls (**Fig. 3B**). Other Arn proteins were either not detected by mass spectrometry or did not meet the stringent cut offs to allow analysis by *t*-test (i.e. **Fig. 1B**), but we used Western blotting to confirm the same trend for ArnA-3Flag and ArnT-3Flag (**Fig. 3C and 3D**). Importantly, Arn protein levels could be restored by plasmid-based expression of *ppk* from its endogenous promoter (pPPK, **Fig. S2**). In fact, cells expressing pPPK in either wild-type or Δ*ppk* mutant backgrounds had somewhat higher levels of Arn proteins compared to wild-type strains with empty vector controls (**Fig. S2**). We surmise that PPK is somewhat overexpressed in both strain backgrounds due to multiple copies of the plasmid and that Arn expression scales with total PPK levels.

Next, we asked if the switch from LB to MOPS media was triggering Arn expression. As anticipated, Arn proteins were low for both wild-type and Δ*ppk* mutants during growth in LB, and it was only during prolonged growth in MOPS that their levels increased in wild-type cells (**Fig. S3A**). This led us to check if regulation depended on the BasRS two-component system, which sits upstream of the *arnBCADTEF* operon and *eptA* gene, and responds to various stresses (**Fig. 3E**). In *E. coli,* the BasS membrane protein auto-phosphorylates in response to high concentrations of iron and zinc, and subsequently trans-phosphorylates the transcription factor BasR to promote transcription of *arnBCADTEF* and of *eptA,* which is found in the same operon as *basS* and *basR* (47-50). In parallel, the PhoPQ two-component system, activated under conditions of low magnesium promotes BasR activation via PmrD (**Fig. 3E**) (51, 52). We found that expression of both BasS-3Flag and BasR-3Flag were decreased in Δ*ppk* mutant cells, compared to wild-type

cells, during starvation (**Fig. 3F**). In contrast, we found that PhoP and PhoQ-3Flag protein levels remained largely unchanged (**Figs. S3B and S3C**), and the induction of ArnC-3Flag expression was not changed by the inclusion of excess magnesium (**Fig. S3D**). Thus, while we cannot rule out additional points of regulation, our data support a model wherein Arn and EptA expression during starvation in MOPS depends on upstream PPK and/or polyP-dependent regulation of the BasRS two-component system. Indeed, qPCR analysis demonstrated that MOPS treatment induced the transcription of Arn, BasS and BasR encoding genes in wild-type cells, and this response was defective in Δ*ppk* mutants (**Fig. 3G**). Interestingly, loss of *ppk* had a less dramatic impact on *arnB* expression than that of *arnA* and *arnC*, even though they are encoded in the same operon (**Fig. 3G**). Likewise, we did not observe a significant difference between wild-type and *ppk* mutants for *eptA* expression (**Fig. 3G**), despite its regulation at the protein level. This suggests the possibility that PPK and/or polyP exert their function at multiple levels. Importantly, differences in expression of genes within a single operon has been documented previously, and could stem from variations in transcription initiation from additional promoter elements or mRNA processing (53). Finally, there are several reports of BasR and BasS regulation by the stationary phase sigma factor RpoS (54, 55). However, we found that Δ*ppk* mutants had RpoS protein levels that were similar to those of wild-type cells during starvation in MOPS (**Fig. S3E**), suggesting additional modes of action.

To our knowledge this is the first description of *E. coli* EptA and Arn protein induction by MOPS media, and the mechanism at play is unknown. In LB media, the BasRS transcriptional circuit induces Arn expression and downstream modifications in the presence of high iron levels (>200 μM) (47, 56), but the iron concentration in MOPS is quite low (10 μM). Still, we remained curious about the role of iron based on a previous report that MOPS-induced polyP can bind iron

to inhibit the Fenton reaction, which decreases the production of reactive oxygen species (15). Consistent with a requirement for iron in BasS activation, treatment with iron chelator BPS blunted expression of Arn-3Flag proteins in wild-type cells grown in MOPS (**Fig. 3H**). However, we note that loss of *ppk* did not impact expression of Arn-3Flag proteins in LB media treated with high iron (**Fig. S3F**). Thus, while iron is important for BasRS induction in both LB and MOPS, the impact of Δ*ppk* is unique to MOPS. We reasoned that BasRS regulation by PPK could depend on polyP accumulation, which occurs in MOPS (**Fig. S1A**), but not in LB treated with iron (**Fig. S3G**). To test this idea, we analyzed Arn protein induction in Δ*phoB* mutants, which are deficient in polyP accumulation even in MOPS media (**Fig. S3H)** (4, 25). Additionally, PhoB is down-regulated in Δ*ppk* mutants compared to wild-type cells (**Fig. 1B and Supplementary Table 1**). To our surprise, Δ*phoB* cells had levels of Arn-3Flag expression comparable to wild-type controls (**Fig. 3I**), suggesting that additional PPK activities beyond polyP synthesis may contribute to the molecular phenotypes described here (see Discussion).

Figure 3 and Figure 3 – Figure legend on the following pages.

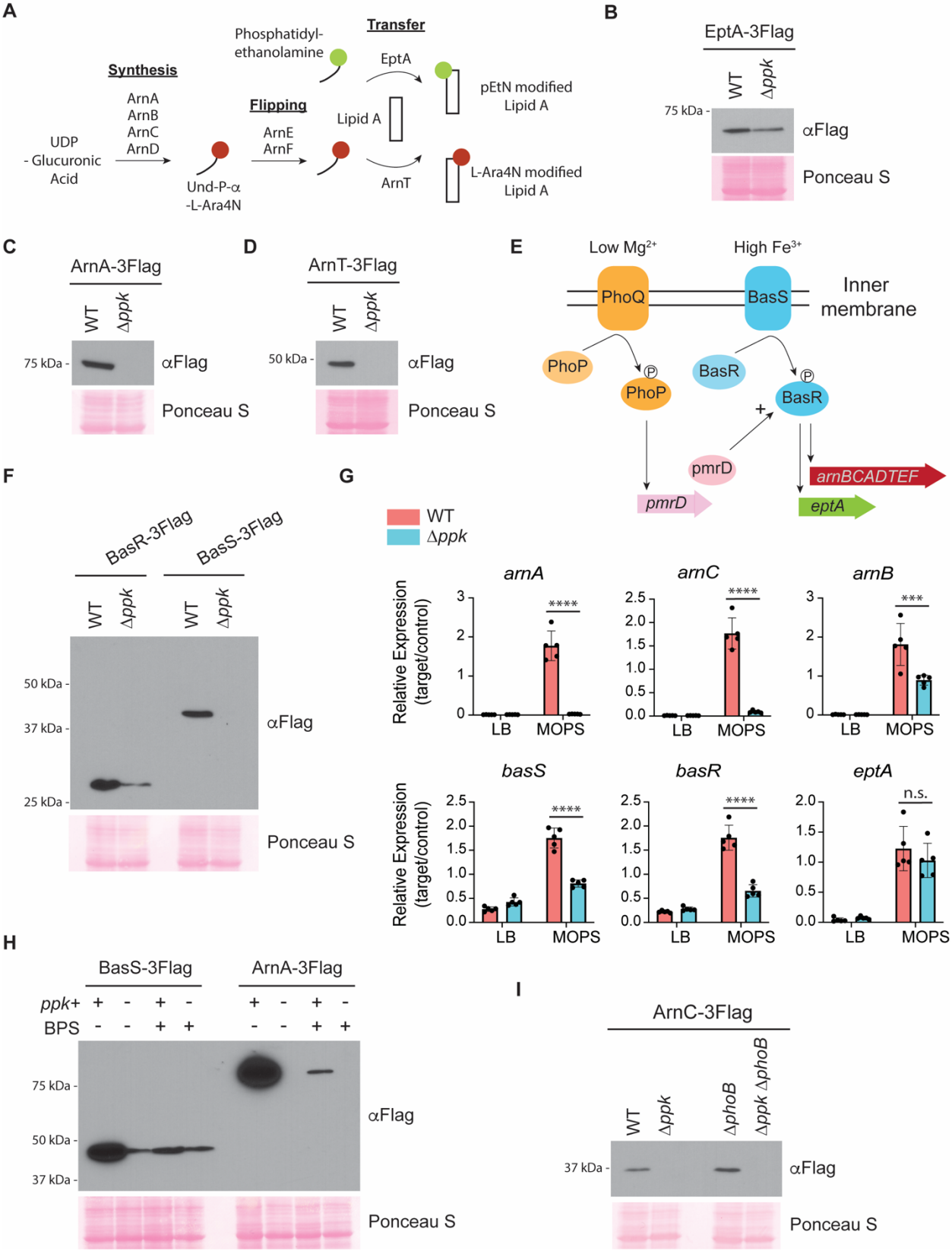

Figure 3 – Figure legend on next page

Figure 3. PPK positively regulates the BasRS transcriptional circuit during starvation. A) Schematic for Arn and EptA-catalyzed lipid A modifications in *E. coli.* ArnA, ArnB, ArnC, ArnD synthesize the donor substrate (Und-P-α-LAra4N). ArnE and ArnF flip and transport the donor substrate to ArnT. ArnT and EptA transfer their respective modifications to newly synthesized lipid A molecules. Note that pEtN and L-Ara4N are shown as single modifications, but doubly modified species containing 2 moieties (total) of pEtN and/or L-Ara4N are also possible. **B-D**) Expression of EptA-3Flag (B), ArnA-3Flag, (C) and ArnT-3Flag (D) following MOPS starvation for 3 hours. Extracted protein samples were resolved using SDS-PAGE, transferred to PVDF and detected using an anti-Flag antibody. Note that polar effects due to tagging may influence *eptA* regulation and visualized expression in both wild-type and mutant strain backgrounds. **E)** Schematic showing magnesium (Mg^{2+}) and iron (Fe^{3+}) dependent induction of *arnBCADTEF* and *eptA* transcription by the PhoPQ and BasRS two-component systems. **F)** BasS-3Flag and BasR-3Flag expression following MOPS starvation. Proteins were extracted from the indicated strains and analyzed as described above. **G)** RT-qPCR measurements of *arn*, *eptA* and *bas* genes in wild-type and Δ*ppk* mutants during growth in MOPS minimal media. RT-qPCR analysis was conducted on cells grown to mid-exponential phase in LB followed by 3 hours in MOPS minimal media. Primers and primer efficiencies used for qPCR are listed in Table S3. Mean values with standard deviation are shown. ****, $p < 0.0001$; *** $p < 0.001$, n.s., non-significant via two-way ANOVA with Tukey's post-hoc analysis. The underlying data for Fig. 3G can be found in S3_Data. **H)** Role of iron in BasS-3Flag and ArnA-3Flag expression. BPS was used to chelate iron from MOPS media, following the switch from LB. At the 3-hour timepoint, proteins were extracted and analyzed as described above. **I)** Expression of ArnC-3Flag by Δ*phoB* mutants. Following MOPS starvation, proteins were extracted from the indicated strains and analyzed as described above. Images shown are representative of results from ≥3 experiments.

2.3.4. pEtN and L-Ara4N modifications are downregulated in Δ*ppk* mutants

Next, we directly examined lipid A modifications that depend on Arn and EptA expression, namely L-Ara4N and pEtN addition. For these experiments, we used the W3110 strain (K-12) background that has been used extensively for lipid A analyses (57, 58). As a control, these strains showed PPK-dependent expression of Arn-3Flag proteins in MOPS media, similar to what we observed in the MG1655 background used for our other assays (**Fig. S4A**). A time course of protein expression showed that in wild-type cells, ArnC-3Flag was detectable after 3 hours in MOPS media and remained upregulated for the duration of the experiment (**Fig. S4B**). In contrast, ArnC-3Flag was undetectable in Δ*ppk* mutants after 6 hours in MOPS media and was only observed after overnight growth (**Fig. S4B**). Therefore, we chose 6 hours (3 hours post-Arn upregulation) as a timepoint to

measure lipid A modifications using radio-labelling and thin-layer chromatography. Indeed, compared to their wild-type counterparts, we saw that Δ*ppk* mutants were defective in the accumulation of lipid A species singly or doubly modified with pEtN and L-Ara4N modifications (**Fig. 4A**). This defect was fully rescued by introduction of the pPPK plasmid (**Fig. 4A**). Therefore, differences in levels of Arn and EptA proteins translate to changes in lipid A modification between wild-type and Δ*ppk* mutants.

2.3.5. PPK promotes polymyxin resistance

Positively charged L-Ara4N and pEtN modifications play a role in resistance to cationic antimicrobial peptides that alter membrane permeability and structure (59-61). To study the phenotypic consequences of disrupting PPK-dependent regulation of lipid A modifications, we focused on polymyxin antibiotics, used both topically to treat Gram-negative bacterial infections, and systemically as a last-resort antibiotic in the clinic (62). For these experiments, we used a polymyxin resistant strain (WD101) that carries a constitutively active *basR* allele (*basR*^{C}) resulting in lipid A that is heavily modified with L-Ara4N and pEtN (63). This strain is otherwise isogenic to W3110 (63). Importantly, compared to wild-type cells, Arn-3Flag protein expression was decreased in Δ*ppk* mutants carrying this allele as observed previously in other backgrounds (**Fig. S4A**). Using dilution assays, we confirmed that the *basR*^{C} strain is resistant to polymyxin compared to the wild-type W3110 counterparts grown on MOPS (**Fig. S4C**) and this resistance requires ArnA (**Fig. S4D**). Deletion of *ppk* decreased polymyxin resistance in the *basR*^{C} strain (**Fig. 4B and S4C**), and this effect could be reversed by introduction of the pPPK plasmid (**Fig. 4B**). These experiments demonstrate that *ppk* contributes to *basR*^{C}-mediated polymyxin resistance under starvation conditions. Finally, we were interested in testing whether the role of *ppk* in Arn

expression was conserved in pathogenic *E. coli*. For this we used a uropathogenic *E. coli* (UPEC) strain (UTI89). We found that UPEC also accumulated polyphosphate during MOPS starvation (**Fig. 4C**), and that Arn-3Flag protein expression in these strains was dependent on *ppk* (**Fig. 4D**). We speculate that targeting PPK in UPEC may serve as a strategy to sensitize cells to drug treatment following acquisition of polymyxin resistance.

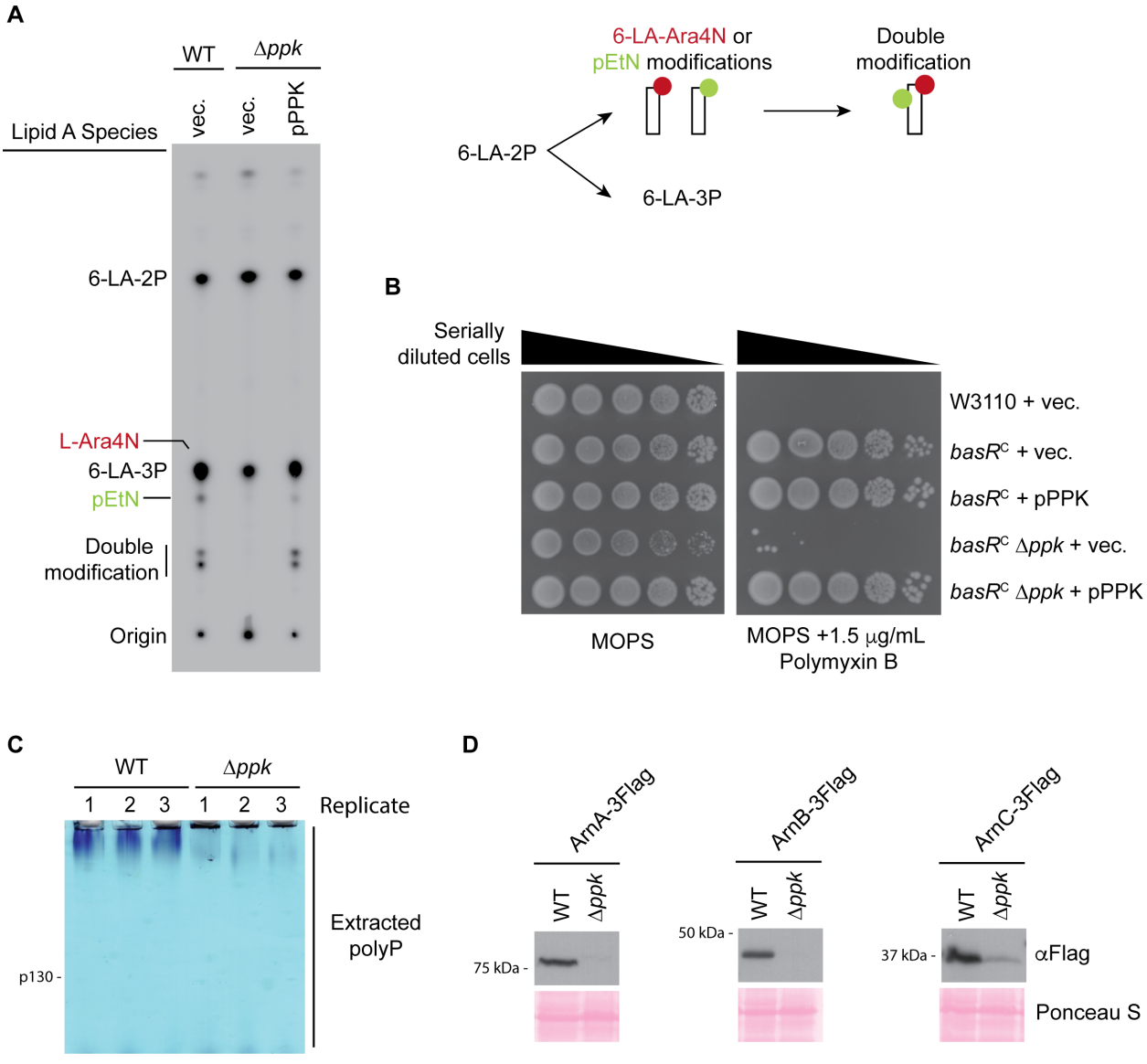

Figure 4. Consequences of LPS mis-regulation in *ppk* mutants A) Schematic of lipid A modification (right) and lipid A profiles (left) of strains mutated for or expressing *ppk*. The indicated strains were grown in LB until mid-log phase before being shifted to MOPS media

supplemented with ^{32}P for 6 hours. Lipid A was isolated as described in the Materials & Methods and analyzed via thin-layer chromatography prior to phosphorimaging. ^{32}P-labelled lipid A species are labelled on the right side of the image. During growth in LB, most of the lipid A (LA) is hexa-acylated and *bis*-phosphorylated (6-LA-2P) and ~1/3rd is modified with an additional phosphate group (6-LA-3P). Upon stimulation of BasRS, 6LA-2P is used as the substrate for EptA and ArnT to generate pEtN and L-Ara4N-modified lipid A species. Note that the singly modified 6-LA-Ara4N species is not resolved from the 6-LA-3P species. 'Doubly-modified' refers to lipid A species carrying two moieties (total) of pEtN and/or L-Ara4N. Images shown are representative of results from ≥3 biological replicates. **B)** Polymyxin growth phenotypes of Δ*ppk* mutants. The indicated strains were spotted in 10-fold serial dilutions on the indicated media and incubated at 37 °C for 2 days prior to imaging. Images shown are representative of results from ≥3 biological replicates. **C)** PolyP extracts from wild-type and Δ*ppk* mutant UPEC strains. Cells were grown in LB media to mid-exponential phase and then switched to MOPS minimal media for 3 hours. PolyP was extracted from the indicated strains and analyzed on a TBE-urea gel stained with toluidine **blue.** The migration of a chain ~130 phosphate residues in length (p130) is indicated. **D)** PPK-dependent ArnA-3Flag, ArnB-3Flag and ArnC-3Flag expression in UPEC. Cells were grown as described in C. Extracted protein samples were resolved using SDS-PAGE, transferred to PVDF, and detected using an anti-Flag antibody. Images shown are representative of results from ≥3 experiments.

2.4. Discussion

Our study is the first whole proteome analysis in *E. coli* comparing wild-type cells to Δ*ppk* mutants under conditions permissive for polyP synthesis. Our work will serve as a resource for researchers interested in how PPK and polyP control protein homeostasis, and, more broadly, how bacterial cells respond to starvation. We find that Δ*ppk* mutant cells remain poised for growth during starvation at the expense of upregulating biosynthetic pathways for nutritional building blocks such as amino acids. We further elaborate a critical role for PPK in regulating the conserved BasRS two-component system and downstream expression of proteins involved in lipid A modifications. Finally, we uncover evidence that PPK-dependent differences in lipid A modification contribute to polymyxin sensitivity. Together, our results illuminate a previously unexplored role of PPK in lipid A modification and antibiotic resistance.

The simplest interpretation of our data, illustrated in **Fig. S5**, is that PPK and/or polyP promote expression or activation of the BasS sensor protein and its cognate transcription factor

BasR. In turn, BasR acts to stimulate transcription of both itself and genes encoding the EptA and Arn proteins. In support of the idea that the BasRS-Arn circuit is regulated by polyP, as distinct from PPK, we only observed defects in Arn protein expression in MOPS media where polyP is synthesized to high levels. In LB media supplemented with iron, where polyP is absent, no differences in Arn protein expression was observed between wild-type strains and Δ*ppk* mutants. However, we note that a proposed role for polyP is complicated by the observation that Δ*phoB* strains express ArnC-3Flag protein at a level similar to wild-type cells, even though they are largely deficient in polyP accumulation. Based on this finding, it is possible that an unknown activity of PPK may underlie the molecular and cellular phenotypes described here. Alternatively, a non-zero level of polyP has been detected in Δ*phoB* strains previously (4), and this pool of polyP, or at least its cyclical synthesis and destruction, may be sufficient to drive Arn expression. In this scenario, polyP could act upstream and interact directly with BasS, BasR, or as-yet-unknown transcriptional regulators to promote transcription of the *eptA-basR-basS* operon.

The impact of PPK could also be several steps removed from the transcriptional activities occurring directly at *eptA-basR-basS*. Here, it is particularly relevant that the trigger for activation of the BasRS transcriptional program during MOPS starvation is unknown. The failure of wild-type cells to upregulate Arn expression in the presence of the iron chelator BPS suggests an iron-dependent response. However, given that induction of Arn protein expression occurs abruptly after three hours, we theorize that additional time-dependent changes are required. In media-switch experiments, we found that incubation of 'spent' MOPS media from wild-type cells that have induced ArnC-3Flag expression fails to rapidly trigger ArnC-3Flag expression in either wild-type or Δ*ppk* mutants (**Fig. S6A and B**). This observation argues against changes in media composition as the sole contributor to BasS activation in MOPS, and intracellular depletion of specific

metabolites or accumulation of by-products is likely required. Finding the trigger for BasS activation will provide important clues into unknown functions of PPK and new insights into the regulation of lipid A modifications.

Collectively, our findings underscore that the pathways regulating modification of *E. coli* LPS, and the associated changes in antibiotic resistance, are intimately coupled to nutrient availability. In the context of host infection, the validity of PPK as a target to sensitize bacteria to cationic peptides like polymyxin may depend on whether bacteria at the site of infection are exposed to conditions that activate PPK. Intriguingly, there is evidence to suggest that bacteria colonizing in the center of dense biofilms experience starvation concomitant with decreased susceptibility to antibiotics (64-66). We theorize that PPK may play an important role in this context. Notably, the immediate molecular events that activate PPK during stresses of any kind remain unclear (26, 67-69). Our work predicts that genes encoding PPK activators are also likely to play a role in polymyxin resistance.

In general, the enzymes involved in LPS modifications, including the pEtN and L-Ara4N modifications, are highly conserved across Gram-negative bacteria (59). Yet, there are important differences between some species in the details of regulation, such as in the crosstalk between two-component systems (51, 70). As such, it is imperative to test if PPK and polyP impact these modifications in other bacteria. We anticipate that comparing and contrasting the role of PPK across multiple species will help to elucidate molecular mechanisms governing antibiotic sensitivity and the acquisition of resistance.

2.5. Experimental Procedures

Bacterial strains, media, and growth

All bacterial strains and plasmids, as well as their sources, used in this work are listed in **Supplementary Table 3**. Reagents are listed in **Supplementary Table 4**.

Tagged and deletion strains were generated using lambda-red mediated site-specific recombination via the arabinose or heat shock inducible systems expressed from pKD46 (71) and pSIM6 (72) plasmids, respectively. The kanamycin deletion and C-terminal 3Flag-kanamycin tagging cassettes were amplified from pKD4 (71) and pSUB11 (73), respectively. In select cases (**Supplementary Table 3**), resistance markers were excised using FLP recombinase activity expressed from pCP20 (74). Antibiotics were added when appropriate: kanamycin (50 μg/mL), ampicillin (100 μg/mL). For recombineering genetic transformations cells were made electrocompetent and transformed using protocols described previously (75). Plasmids were also introduced into the bacteria by electroporation.

(1) Nutrient downshift

All strains were grown in LB media at 37 °C unless carrying pSIM6 and pKD46 plasmids which were grown at 30 °C. For nutrient downshift experiments overnight cultures, grown in LB media, were diluted to 0.1 OD_{600} in LB the next day and grown to mid-exponential phase (~0.6 OD_{600}). Cells were then washed twice with 1xPBS and resuspended in MOPS minimal media (Teknova™) supplemented with 0.1 mM K_2HPO_4, 0.4% glucose – this recipe was used for starvation unless otherwise indicated. Cells were grown in minimal media for 3 hours before harvesting on ice. Cell pellets were flash frozen using dry ice and stored at -80 °C.

(2) Other growth conditions

Where indicated, exponentially growing LB cultures were switched to MOPS minimal media

containing casamino acids (Bacto^{TM}) at a final concentration of 0.05% and 0.5%. Where indicated, iron in MOPS media was chelated using 0.2 mM bathophenanthrolinedisulfonic acid disodium salt hydrate (BPS). BPS was added to MOPS media at the start of the nutrient downshift. Where indicated, LB media was supplemented with 0.2 mM iron sulfate when overnight cultures were diluted to 0.1 OD_{600}. LB minus and plus iron cultures were grown to mid-exponential phase (about 1.5 hours) at 37 °C before harvesting cells. Where indicated, exponentially growing LB cultures were switched to MOPS minimal media containing 1 mM magnesium chloride or 1mM calcium chloride and grown at 37 °C for 3 hours before harvesting.

Mass spectrometry

(1) Cell growth

Five overnight cultures (n=5) were prepared for each wild-type and *ppk* strains from freshly streaked plates. The next day, overnight cultures were diluted in 100 mL LB and grown to mid-exponential phase, washed two times with 1xPBS and then switched to MOPS minimal media without amino acids for three hours as described above (*Methods: Nutrient downshift*). 60 OD_{600} and 5 OD_{600} equivalents of cell volume were harvested for mass spectrometry analysis and polyP extraction, respectively.

(2) Protein extraction and precipitation

Protein extracts were prepared by trichloro-acetic acid (TCA) precipitation. Cells pellets were thawed on ice and resuspended in 700 µL mass spectrometry-grade lysis buffer (5% SDS, 100 mM tetraethylammonium bromide (TEAB), Roche cOmplete protease inhibitor cocktail tablets). The cell suspension was lysed by sonication on ice for 30 seconds at power level 3 with 1 minute break in between, for a total of 3 times. The cell lysate was then centrifuged at 13 000 rpm, 4 °C for 15

minutes. The supernatant was transferred to a new tube and centrifuged again for 10 minutes prior to being collected.

Proteins were precipitated by adding 2.8 mL 15% TCA in acetone to the cell lysate (brings final concentration of TCA to 10%), mixing by inverting and incubating at -20 °C overnight. The next day, the samples were centrifuged at max speed, 4 °C for 10 minutes and supernatant was discarded immediately after the spin. The pellet was air dried for 30 mins, then resuspended in dissolution buffer (5% SDS, 100 mM tetraethylammonium bromide) prior to BCA quantification and lyophilization. Lyophilized samples were sent to UC Davis Proteomics Core for mass spectrometry analysis.

(3) Sample preparation

The following protocols (3-5) were provided by the UC Davis Proteomics Core with minor alterations.

Lyophilised proteins were solubilised in 50 µL of solubilization buffer, consisting of 5% SDS, 50 mM triethyl ammonium bicarbonate, pH 7.5. A Bichinoic Acid Assay was taken of all samples, and 100 µg total protein from each sample was then used to perform protein digestion via suspension-trap devices (S-Trap) (ProtiFi). Disulfide bonds were reduced with dithiothreitol and alkylated with iodoacetamide in 50mM TEAB buffer. The enzymatic digestion consisted of an addition of trypsin at 1:100 enzyme: protein (wt/wt) for 4 hours at 37 °C, followed by a boost addition of trypsin using same wt/wt ratios for overnight digestion at 37 °C. Peptides were then eluted from the S-Trap by sequential application of elution buffers of 100 mM TEAB, 0.5% formic acid, and 50% acetonitrile 0.1% formic acid. The eluted tryptic peptides were dried in a vacuum centrifuge prior to re-constitution in 0.1% trifluoroacetic acid. These were subjected to Liquid Chromatography couple to tandem Mass Spectrometry (LC-MS/MS) analysis as described below.

(4) Liquid Chromatography

Peptides were resolved on a Thermo Scientific Dionex UltiMate 3000 RSLC system using a PepMap 75 μm x 25cm C18 column with 2 μm particle size (100 Å pores), heated to 40 °C. A final volume of 5 μL was injected, corresponding to 1 μg of total peptide, and separation was performed in a total run time of 90 min with a flow rate of 200 μL/min with mobile phases A: water/0.1% formic acid, and B: 80%ACN/0.1% formic acid. Gradient elution was performed from 10% to 8% B over 3 min, from 8% to 46% B over 66 min, and from 46 to 99% B over 3 min, and after holding at 99% B for 2 min, down to 2% B in 0.5 min followed by equilibration for 15min.

(5) Mass spectrometry

The peptides were analyzed on an Orbitrap Fusion Lumos (Thermo Fisher Scientific) mass spectrometer. Spray voltage was set to 1.8 kV, RF lens level was set at 46%, ion transfer tube temperature was set to 275 °C. The mass spectrometer was operated in a data-dependent acquisition mode. A survey full scan mass spectra (from m/z 375 to 1600) was acquired in the Orbitrap at a resolution of 60,000 (at 200 m/z). The automatic gain control (AGC) target for MS1 was set as 4e5, and ion filling time was set as 50 msec. The n=15 most abundant precursor ions with charge state +2, +3 were isolated in a 3-sec cycle, isolation window width of 1.2 m/z, fragmented by using collision-induced dissociation (CID) fragmentation with 30% normalized collision energy, and detected via IonTrap, with a scan rate set to Rapid. The AGC target for MS/MS was set as 5e3 and ion filling time was set at 35 msec. The dynamic exclusion was set to 50 sec with a 10-ppm (parts per million) mass window.

Mass Spectrometry bioinformatics analysis

(1) Protein identification

Mass spectrometry RAW data were processed using the Trans-Proteomic Pipeline (TPP v5.2.0)

(76). Files from the mass spectrometry runs were converted to mzML files using the msconvert tool from ProteoWizard (77) (v3.0.22088). Comet (78) (v2018.01.04) was used to search the files against the UniProt (79) *E. coli* protein sequence database (UP000000625 downloaded 2021-08-04), along with a target-decoy strategy where all protein sequences were reversed. The database search was performed with trypsin as a digestive enzyme, allowing for up to 3 missed cleavages and considering semi-tryptic digestion. The peptide mass tolerance was set to 20 ppm. Carbamidomethylation of cysteine was set as a fixed modification, and the variable modifications considered were deamidation of asparagine and glutamine, as well as oxidation of methionine. The probability of protein identifications was evaluated with ProteinProphet (80), and proteins identified at a false discovery rate (FDR) < 1% were deemed confidently identified.

(2) Differential expression analysis

The spectral counts from confidently identified proteins were used for downstream analysis. Proteins with zero spectral counts in a given experiment were imputed a quantification value by random sampling of the lowest 20% of non-zero spectral counts in the entire dataset to account for missing values. All spectral counts were normalized by the total number of spectral counts in a given experiment. Differential expression was assessed on the normalized spectral counts using a two-tailed, two-sample Students *t*-test, assuming unequal variance. A *t*-test was performed for proteins that had at least 3 non-zero spectral counts out of 5 replicates prior to imputation in both experimental conditions, and the Benjamini-Hochberg (81) procedure was used to adjust *p*-values for multiple hypothesis testing. Proteins with an FDR-adjusted *p*-value < 0.05 were considered significantly differentially expressed. Finally, proteins that were identified in all replicates of one condition and not identified in any replicates of the other condition did not undergo a *t*-test, but

still reflect a significant expression difference. As such, these were named "all-or-none" proteins and are reported as having differential expression.

(3) Gene Ontology enrichment analysis

Ontologizer (82) (v2.0) was used to identify Gene Ontology (30) annotations that were significantly enriched in the set of differently expressed proteins (FDR-adjusted p-value < 0.05) and "all-or-none" proteins. The enrichment was performed against a background of all proteins identified with mass spectrometry (confidently identified at an FDR < 1%). The OBO ontology file and the GAF annotation file used in the analysis were downloaded from http://geneontology.org/ on 2023-02-13. The p-values were adjusted using the Benjamini-Hochberg procedure, and Gene Ontology terms that were enriched with an adjusted p-value < 0.05 were considered significantly enriched.

(4) Gene set enrichment analysis

A Gene Set Enrichment Analysis (GSEA) (31) (v4.1.0) was performed (on 2023-05-24) to identify sets of Gene Ontology terms that were enriched in the entire set of proteins (confidently identified at an FDR < 1%). Gene sets were built of Gene Ontology terms and their annotated proteins, and GSEA excluded Gene Ontology terms that annotated more than 1000 proteins or less than 3 proteins to remove general and highly specific terms. 1000 gene set permutations were used to estimate enrichment scores. The enrichment scores were normalized with the "meandiv" parameter to allow for a more accurate comparison of enrichment scores across gene sets. Gene sets with a q-value < 0.05 were considered significantly enriched.

Polyphosphate extraction

(1) Polyphosphate extraction

Cells were grown as indicated and polyP extraction was conducted as described previously (83).

For clarity, similar language is used to describe the protocol here. Five OD_{600} equivalents of pelleted cells were thawed on ice, resuspended in 400 µL of LETS buffer (100 mM LiCl, 10 mM EDTA, 10 mM Tris-HCl, 0.2% SDS) at 4 °C, then transferred to a tube containing 600 µL of room-temperature neutral phenol (pH 8) and 150 µL of RNase-free water. Tubes were vortexed for 20 seconds and 600 µL chloroform was added. Next, tubes were again vortexed for 20 seconds, and then centrifuged for 2 minutes at 13,000 g. The top 600 µL layer was transferred to a new tube containing 600 µL of chloroform before vortexing for 20 seconds and centrifuging for 2 minutes at 13,000 g. The top 400 µL layer was transferred to a new tube and treated with 2 µL of 10 mg/mL RnaseA and DnaseI, each, for 1 hour at 37 °C. Next, the mixture was transferred to prechilled tubes containing 1 mL 100% ethanol and 120 mM sodium acetate (pH 5.3) and left overnight at -20 °C to precipitate. The next day, samples were centrifuged for 20 min at 13,000 g for 20 mins at 4 °C. Supernatant was discarded and 500 µL 70% ethanol was added before centrifuging for 5 min at 13,000 g at 4 °C. Supernatant was again discarded and pellet was air dried to remove trace ethanol. The translucent polyP pellet was resuspended in 30 µL sterile water and stored at -80 °C.

(2) Gel analysis

Extracted polyP was visualized using a 15.8% TBE-urea gel (5.25 g urea, 7.9 mL 30% acrylamide, 3 mL 5xTBE, 150 µL 10% APS and 15 µL TEMED). Extracted polyP was mixed at a 1:1 ratio with loading dye (10 mM Tris-HCL pH 7, 1 mM EDTA, 30% glycerol and bromophenol blue) and 10 µL was loaded into the gel. Gels were run at 100 V for 1 hour and 45 minutes in 1xTBE as the running buffer. Three microliters of RegeneTiss polyP standards p14 (20 mM), p60 (6.5 mM) and p130 (2.5 mM) were used. The gel was stained in fixing solution containing toluidine blue (25% methanol, 5% glycerol and 0.05% toluidine blue) for 15 minutes and washed several times

with destaining solution (fixing solution without toluidine blue) before being left overnight to fully destain.

Western blotting

Cells were grown as indicated in figure legends and described in the "Bacterial strains and growth conditions" section. Cell pellets (3 OD_{600} equivalent of cells) frozen at -80 °C were thawed on ice and resuspended in 100 µL sample buffer (800 µL sample buffer 100 µL 1 M DTT, 100 µL 1.5 M Tris-HCl pH 8.8). Samples were boiled at 100 °C for 10 mins, then centrifuged at 13,000 rpm for 2 mins and the supernatant was transferred to new tubes. Only ArnT and EptA membrane protein samples were prepared without boiling to prevent protein aggregation, typical for proteins containing transmembrane domains (84). Cell pellets resuspended in 100 µL sample buffer were sonicated at power level 1 for 12 seconds, then centrifuged at 13,000 rpm for 2 mins and the supernatant was transferred to new tubes. Protein samples were loaded on the indicated % of SDS-acrylamide gel. Proteins were transferred to PVDF membrane. Membranes were blocked for 20 minutes with shaking using TBST with 5 % milk and washed 3 times for 10 minutes each with TBST after incubation with the primary and secondary antibodies. Blots were exposed to autoradiography film from Thomas Scientific. Conditions for antibody use can be found in **Supplementary Table 4.** Scanned images were opened in Photoshop. In most cases small linear brightness and contrast adjustments were made to lighten the image background. Adjustments were applied evenly across the entire image shown.

Liquid growth curves

Three biological replicates of each strain were cultured overnight in LB media. Overnights were diluted to 0.1 OD_{600} in LB and grown to mid-exponential phase (~0.6 OD_{600}). Cells (0.5 OD_{600} equivalent) were then washed twice with 1xPBS and resuspended in 50 µL of MOPS media

(1xMOPS, 0.4% glucose, 0.1 mM K_2HPO_4) without amino acids. Twenty-five microliters of the cell suspension were transferred to 1 mL of MOPS without and with 0.05% or 0.5% amino acids (final OD ~ 0.1 OD_{600}). Two hundred microliters of cells were pipetted in technical replicates of 3 and growth was monitored using the BioscreenC plate reader set at 37 °C with continuous shaking. Optical density measurements were collected at a wavelength of 600 nm every 15 mins, 5 seconds after shaking stopped, for 24 hours. For the analysis, background OD values for each condition (0%, 0.05% and 0.5% amino acids) were subtracted from each time point. See **Supplementary S2 Data** for raw data.

Growth curve analysis

Growth rate (OD_{600}/min), lag time (min) and max OD_{600} measurements were calculated per well using GrowthRates 6.2 for Macintosh OS X (85) and Bare Bones Software text editor. GrowthRates was run using the stringent algorithm with the growth rate correlation coefficient set to r >0.99. For the analysis, the input file was in Standard Format and the program automatically compensated for the background OD at each time point. See **Supplementary S2 Data** for raw data. Statistical analysis used two-way ANOVA with multiple comparisons, with correction for multiple hypothesis testing using Tukey's test (GraphPad Prism Version 9.1.2).

Reverse transcriptase quantitative PCR (RT-qPCR)

Five biological replicates of each strain were grown in LB or MOPS media for qPCR analysis. From each condition, 1 mL of cells were collected by centrifugation and immediately resuspended in 500 µL RNA*later*™ Solution for short-term storage at 4 °C. Prior to RNA extraction. RNA*later*™ Solution was removed. RNA was extracted using the GeneJET RNA Purification Kit (Thermo Scientific) following manufacturer's instructions and RNA integrity/concentration were evaluated by NanoDrop. Genomic DNA contamination was removed from RNA extracts by Dnase

treatment following the Invitrogen Ambion Dnase I (Rnase-free) protocol. Dnase was removed using phenol-chloroform extraction as described previously (86). Final RNA concentration was measured by NanoDrop. One microgram of RNA was reverse transcribed using SuperScript V VILO kit (Thermo Fisher) following manufacturer's instructions (25 °C for 10 minutes, 50 °C for 10 minutes and 85 °C for 5 minutes). The cDNA was then diluted 1/10, aliquoted into 15 µL working solutions and stored at -80 °C. We found that this dilution of cDNA was optimal to obtain Cq-values greater than 20 for our genes of interest. Quantitative PCRs were conducted in technical replicates of 3 and in a 10 µL final volume using iQ Sybr Green Supermix following manufacturer's protocol under the following conditions: 95 °C for 3 mins and 39 cycles of 95 °C for 15 seconds, 63 °C for 30 seconds and 72 °C for 30 seconds. Melt curve analysis was performed at the end of each run and standard curves using serially diluted gDNA (extracted using One-4-All Genomic DNA MiniPreps Kit (BioBasic)) were performed to assess primer efficiency. All primers and primer efficiencies are reported in **Supplementary Table 3**. Gene expression was normalized to *yqfB*, used previously under polyP inducing conditions (69), and expression changes were calculated using the $\Delta\Delta C_T$ method using Bio-Rad CFX Maestro 2.3 version 5.3.002.1030 software. Statistical analysis used two-way ANOVA with multiple comparisons, with correction for multiple hypothesis testing using Tukey's test (GraphPad Prism Version 9.1.2). See **Supplementary S3_Data** for raw data.

Polymyxin sensitivity

Indicated strains were streaked on LB or LB-kanamycin (plasmid carrying strains) plates and grown overnight at 37 °C. The next day, a single colony from each strain was resuspended in 100 µL sterile water and serially diluted 10-fold in sterile water. Five microliters of each dilution were spotted onto the indicated plates that were prepared fresh on the day of use. Plates were allowed

to dry prior to incubation at 37 °C for 2 days (for MOPS plates) before imaging. Linear brightness and contrast adjustments made in Photoshop were made evenly across the entire image shown.

Lipid analysis

Overnight cultures were diluted 1:50 in fresh LB medium. Cells were harvested at OD_{600} of 0.6 and washed with 1X PBS. Bacteria were resuspended in 1X MOPS medium supplemented with 0.4% glucose, 0.1 mM K2HPO4 and 2.5 μCi/ml ^{32}Pi. Labeled cells were grown at 37 °C and harvested after 6h. Pellets were washed with 1X PBS. ^{32}P-lipid A was extracted using mild acid hydrolysis as previously described (87). The lipid A species were then resolved by thin-layer chromatography (TLC) in a solvent system consisting of chloroform, pyridine, 88 % formic acid and water (50:50:16:5, vol/vol, respectively). The plates were exposed to a phosphor screen, and the radiolabeled lipids were visualized using an Amersham Typhoon phosphorimager system. Linear brightness and contrast adjustments were made in Photoshop to make clear the pEtN and L-Ara4N modifications. Linear adjustments were made evenly across the entire image shown.

2.6. Acknowledgements

We thank members of the Downey Lab for critical evaluation of the manuscript. We thank the UC Davis Proteomics Core, especially Dr. Gabriela Grigorean for providing method details. We would also like to thank Dr. Michael Gray for the WT and Δ*ppk* parent strains, and pPPK plasmid, and Dr. Ursula Jakob for the UPEC WT and Δ*ppk* strains. Lastly, we thank Dr. Lionello Bossi and Dr. Donald Court for the tagging and recombineering helper plasmids used in this work.

2.7. References

1. Denoncourt A, Downey M. Model systems for studying polyphosphate biology: a focus on microorganisms. Curr Genet. 2021;67(3):331-46. Epub 2021/01/10. doi: 10.1007/s00294-020-01148-x. PubMed PMID: 33420907.
2. Desfougeres Y, Saiardi A, Azevedo C. Inorganic polyphosphate in mammals: where's Wally? Biochem Soc Trans. 2020;48(1):95-101. Epub 2020/02/13. doi: 10.1042/BST20190328. PubMed PMID: 32049314.
3. Baijal K, Downey M. The promises of lysine polyphosphorylation as a regulatory modification in mammals are tempered by conceptual and technical challenges. Bioessays. 2021:e2100058. Epub 2021/05/18. doi: 10.1002/bies.202100058. PubMed PMID: 33998006.
4. Rudat AK, Pokhrel A, Green TJ, Gray MJ. Mutations in Escherichia coli Polyphosphate Kinase That Lead to Dramatically Increased In Vivo Polyphosphate Levels. J Bacteriol. 2018;200(6). Epub 2018/01/10. doi: 10.1128/JB.00697-17. PubMed PMID: 29311274; PubMed Central PMCID: PMCPMC5826030.
5. Gray MJ, Wholey WY, Wagner NO, Cremers CM, Mueller-Schickert A, Hock NT, et al. Polyphosphate is a primordial chaperone. Mol Cell. 2014;53(5):689-99. Epub 2014/02/25. doi: 10.1016/j.molcel.2014.01.012. PubMed PMID: 24560923; PubMed Central PMCID: PMCPMC3996911.
6. Yoo NG, Dogra S, Meinen BA, Tse E, Haefliger J, Southworth DR, et al. Polyphosphate Stabilizes Protein Unfolding Intermediates as Soluble Amyloid-like Oligomers. J Mol Biol. 2018;430(21):4195-208. Epub 2018/08/22. doi: 10.1016/j.jmb.2018.08.016. PubMed PMID: 30130556; PubMed Central PMCID: PMCPMC6186493.
7. Kuroda A, Tanaka S, Ikeda T, Kato J, Takiguchi N, Ohtake H. Inorganic polyphosphate kinase is required to stimulate protein degradation and for adaptation to amino acid starvation in Escherichia coli. Proc Natl Acad Sci U S A. 1999;96(25):14264-9. Epub 1999/12/10. doi: 10.1073/pnas.96.25.14264. PubMed PMID: 10588694; PubMed Central PMCID: PMCPMC24425.
8. Yang ZX, Zhou YN, Yang Y, Jin DJ. Polyphosphate binds to the principal sigma factor of RNA polymerase during starvation response in Helicobacter pylori. Mol Microbiol. 2010;77(3):618-27. Epub 2010/06/18. doi: 10.1111/j.1365-2958.2010.07233.x. PubMed PMID: 20553390; PubMed Central PMCID: PMCPMC2917625.
9. Shiba T, Tsutsumi K, Yano H, Ihara Y, Kameda A, Tanaka K, et al. Inorganic polyphosphate and the induction of rpoS expression. Proc Natl Acad Sci U S A. 1997;94(21):11210-5. Epub 1997/10/23. doi: 10.1073/pnas.94.21.11210. PubMed PMID: 9326588; PubMed Central PMCID: PMCPMC23418.
10. McInerney P, Mizutani T, Shiba T. Inorganic polyphosphate interacts with ribosomes and promotes translation fidelity in vitro and in vivo. Mol Microbiol. 2006;60(2):438-47. Epub 2006/04/01. doi: 10.1111/j.1365-2958.2006.05103.x. PubMed PMID: 16573692.
11. Beaufay F, Amemiya HM, Guan J, Basalla J, Meinen BA, Chen Z, et al. Polyphosphate drives bacterial heterochromatin formation. Sci Adv. 2021;7(52):eabk0233. Epub 2021/12/23. doi: 10.1126/sciadv.abk0233. PubMed PMID: 34936433.
12. Kuroda A, Nomura K, Ohtomo R, Kato J, Ikeda T, Takiguchi N, et al. Role of inorganic polyphosphate in promoting ribosomal protein degradation by the Lon protease in E. coli. Science. 2001;293(5530):705-8. Epub 2001/07/28. doi: 10.1126/science.1061315. PubMed PMID: 11474114.

13. Nomura K, Kato J, Takiguchi N, Ohtake H, Kuroda A. Effects of inorganic polyphosphate on the proteolytic and DNA-binding activities of Lon in Escherichia coli. J Biol Chem. 2004;279(33):34406-10. Epub 2004/06/10. doi: 10.1074/jbc.M404725200. PubMed PMID: 15187082.
14. Gross MH, Konieczny I. Polyphosphate induces the proteolysis of ADP-bound fraction of initiator to inhibit DNA replication initiation upon stress in Escherichia coli. Nucleic Acids Res. 2020;48(10):5457-66. Epub 2020/04/14. doi: 10.1093/nar/gkaa217. PubMed PMID: 32282902; PubMed Central PMCID: PMCPMC7261185.
15. Beaufay F, Quarles E, Franz A, Katamanin O, Wholey WY, Jakob U. Polyphosphate Functions In Vivo as an Iron Chelator and Fenton Reaction Inhibitor. mBio. 2020;11(4). Epub 2020/07/30. doi: 10.1128/mBio.01017-20. PubMed PMID: 32723918; PubMed Central PMCID: PMCPMC7387796.
16. Dahl JU, Gray MJ, Bazopoulou D, Beaufay F, Lempart J, Koenigsknecht MJ, et al. The anti-inflammatory drug mesalamine targets bacterial polyphosphate accumulation. Nat Microbiol. 2017;2:16267. Epub 2017/01/24. doi: 10.1038/nmicrobiol.2016.267. PubMed PMID: 28112760; PubMed Central PMCID: PMCPMC5514548.
17. Rashid MH, Rao NN, Kornberg A. Inorganic polyphosphate is required for motility of bacterial pathogens. J Bacteriol. 2000;182(1):225-7. Epub 1999/12/30. doi: 10.1128/jb.182.1.225-227.2000. PubMed PMID: 10613886; PubMed Central PMCID: PMCPMC94263.
18. Roewe J, Stavrides G, Strueve M, Sharma A, Marini F, Mann A, et al. Bacterial polyphosphates interfere with the innate host defense to infection. Nat Commun. 2020;11(1):4035. Epub 2020/08/14. doi: 10.1038/s41467-020-17639-x. PubMed PMID: 32788578; PubMed Central PMCID: PMCPMC7423913.
19. Tang-Fichaux M, Chagneau CV, Bossuet-Greif N, Nougayrede JP, Oswald E, Branchu P. The Polyphosphate Kinase of Escherichia coli Is Required for Full Production of the Genotoxin Colibactin. mSphere. 2020;5(6). Epub 2020/12/18. doi: 10.1128/mSphere.01195-20. PubMed PMID: 33328353; PubMed Central PMCID: PMCPMC7771237.
20. Chen J, Su L, Wang X, Zhang T, Liu F, Chen H, et al. Polyphosphate Kinase Mediates Antibiotic Tolerance in Extraintestinal Pathogenic Escherichia coli PCN033. Front Microbiol. 2016;7:724. Epub 2016/06/01. doi: 10.3389/fmicb.2016.00724. PubMed PMID: 27242742; PubMed Central PMCID: PMCPMC4871857.
21. Kuroda A, Kornberg A. Polyphosphate kinase as a nucleoside diphosphate kinase in Escherichia coli and Pseudomonas aeruginosa. Proc Natl Acad Sci U S A. 1997;94(2):439-42. Epub 1997/01/21. doi: 10.1073/pnas.94.2.439. PubMed PMID: 9012801; PubMed Central PMCID: PMCPMC19530.
22. Du Y, Wang X, Han Z, Hua Y, Yan K, Zhang B, et al. Polyphosphate Kinase 1 Is a Pathogenesis Determinant in Enterohemorrhagic Escherichia coli O157:H7. Front Microbiol. 2021;12:762171. Epub 2021/11/16. doi: 10.3389/fmicb.2021.762171. PubMed PMID: 34777317; PubMed Central PMCID: PMCPMC8578739.
23. Neville N, Roberge N, Ji X, Stephen P, Lu JL, Jia Z. A Dual-Specificity Inhibitor Targets Polyphosphate Kinase 1 and 2 Enzymes To Attenuate Virulence of Pseudomonas aeruginosa. mBio. 2021;12(3):e0059221. Epub 2021/06/16. doi: 10.1128/mBio.00592-21. PubMed PMID: 34126765; PubMed Central PMCID: PMCPMC8262977.
24. Raetz CR, Reynolds CM, Trent MS, Bishop RE. Lipid A modification systems in gram-negative bacteria. Annu Rev Biochem. 2007;76:295-329. Epub 2007/03/17. doi:

10.1146/annurev.biochem.76.010307.145803. PubMed PMID: 17362200; PubMed Central PMCID: PMCPMC2569861.
25. Rao NN, Liu S, Kornberg A. Inorganic polyphosphate in Escherichia coli: the phosphate regulon and the stringent response. J Bacteriol. 1998;180(8):2186-93. Epub 1998/04/29. PubMed PMID: 9555903; PubMed Central PMCID: PMCPMC107147.
26. Gray MJ. Inorganic Polyphosphate Accumulation in Escherichia coli Is Regulated by DksA but Not by (p)ppGpp. J Bacteriol. 2019;201(9). Epub 2019/02/13. doi: 10.1128/JB.00664-18. PubMed PMID: 30745375; PubMed Central PMCID: PMCPMC6456864.
27. Varas M, Valdivieso C, Mauriaca C, Ortiz-Severin J, Paradela A, Poblete-Castro I, et al. Multi-level evaluation of Escherichia coli polyphosphate related mutants using global transcriptomic, proteomic and phenomic analyses. Biochim Biophys Acta Gen Subj. 2017;1861(4):871-83. Epub 2017/01/11. doi: 10.1016/j.bbagen.2017.01.007. PubMed PMID: 28069396.
28. Ault-Riche D, Fraley CD, Tzeng CM, Kornberg A. Novel assay reveals multiple pathways regulating stress-induced accumulations of inorganic polyphosphate in Escherichia coli. J Bacteriol. 1998;180(7):1841-7. Epub 1998/04/16. PubMed PMID: 9537383; PubMed Central PMCID: PMCPMC107098.
29. Varas M, Valdivieso C, Mauriaca C, Ortiz-Severin J, Paradela A, Poblete-Castro I, et al. Datasets for transcriptomics, q-proteomics and phenotype microarrays of polyphosphate metabolism mutants from Escherichia coli. Data Brief. 2017;12:13-7. Epub 2017/04/05. doi: 10.1016/j.dib.2017.03.010. PubMed PMID: 28373998; PubMed Central PMCID: PMCPMC5367803.
30. Ashburner M, Ball CA, Blake JA, Botstein D, Butler H, Cherry JM, et al. Gene ontology: tool for the unification of biology. The Gene Ontology Consortium. Nat Genet. 2000;25(1):25-9. Epub 2000/05/10. doi: 10.1038/75556. PubMed PMID: 10802651; PubMed Central PMCID: PMCPMC3037419.
31. Subramanian A, Tamayo P, Mootha VK, Mukherjee S, Ebert BL, Gillette MA, et al. Gene set enrichment analysis: a knowledge-based approach for interpreting genome-wide expression profiles. Proc Natl Acad Sci U S A. 2005;102(43):15545-50. Epub 2005/10/04. doi: 10.1073/pnas.0506580102. PubMed PMID: 16199517; PubMed Central PMCID: PMCPMC1239896.
32. Potrykus K, Cashel M. (p)ppGpp: still magical? Annu Rev Microbiol. 2008;62:35-51. Epub 2008/05/06. doi: 10.1146/annurev.micro.62.081307.162903. PubMed PMID: 18454629.
33. Irving SE, Choudhury NR, Corrigan RM. The stringent response and physiological roles of (pp)pGpp in bacteria. Nat Rev Microbiol. 2021;19(4):256-71. Epub 2020/11/06. doi: 10.1038/s41579-020-00470-y. PubMed PMID: 33149273.
34. Parshin A, Shiver AL, Lee J, Ozerova M, Schneidman-Duhovny D, Gross CA, et al. DksA regulates RNA polymerase in Escherichia coli through a network of interactions in the secondary channel that includes Sequence Insertion 1. Proc Natl Acad Sci U S A. 2015;112(50):E6862-71. Epub 2015/11/26. doi: 10.1073/pnas.1521365112. PubMed PMID: 26604313; PubMed Central PMCID: PMCPMC4687573.
35. Yang X, Ishiguro EE. Involvement of the N terminus of ribosomal protein L11 in regulation of the RelA protein of Escherichia coli. J Bacteriol. 2001;183(22):6532-7. Epub 2001/10/24. doi: 10.1128/JB.183.22.6532-6537.2001. PubMed PMID: 11673421; PubMed Central PMCID: PMCPMC95482.

36. Kuroda A, Nomura K, Takiguchi N, Kato J, Ohtake H. Inorganic polyphosphate stimulates lon-mediated proteolysis of nucleoid proteins in Escherichia coli. Cell Mol Biol (Noisy-le-grand). 2006;52(4):23-9. Epub 2007/06/05. PubMed PMID: 17543195.
37. Lee H, Hsu FF, Turk J, Groisman EA. The PmrA-regulated pmrC gene mediates phosphoethanolamine modification of lipid A and polymyxin resistance in Salmonella enterica. J Bacteriol. 2004;186(13):4124-33. Epub 2004/06/19. doi: 10.1128/JB.186.13.4124-4133.2004. PubMed PMID: 15205413; PubMed Central PMCID: PMCPMC421605.
38. Breazeale SD, Ribeiro AA, Raetz CR. Origin of lipid A species modified with 4-amino-4-deoxy-L-arabinose in polymyxin-resistant mutants of Escherichia coli. An aminotransferase (ArnB) that generates UDP-4-deoxyl-L-arabinose. J Biol Chem. 2003;278(27):24731-9. Epub 2003/04/22. doi: 10.1074/jbc.M304043200. PubMed PMID: 12704196.
39. Breazeale SD, Ribeiro AA, McClerren AL, Raetz CR. A formyltransferase required for polymyxin resistance in Escherichia coli and the modification of lipid A with 4-Amino-4-deoxy-L-arabinose. Identification and function oF UDP-4-deoxy-4-formamido-L-arabinose. J Biol Chem. 2005;280(14):14154-67. Epub 2005/02/08. doi: 10.1074/jbc.M414265200. PubMed PMID: 15695810.
40. Gatzeva-Topalova PZ, May AP, Sousa MC. Structure and mechanism of ArnA: conformational change implies ordered dehydrogenase mechanism in key enzyme for polymyxin resistance. Structure. 2005;13(6):929-42. Epub 2005/06/09. doi: 10.1016/j.str.2005.03.018. PubMed PMID: 15939024; PubMed Central PMCID: PMCPMC2997725.
41. Yan A, Guan Z, Raetz CR. An undecaprenyl phosphate-aminoarabinose flippase required for polymyxin resistance in Escherichia coli. J Biol Chem. 2007;282(49):36077-89. Epub 2007/10/12. doi: 10.1074/jbc.M706172200. PubMed PMID: 17928292; PubMed Central PMCID: PMCPMC2613183.
42. Trent MS, Ribeiro AA, Lin S, Cotter RJ, Raetz CR. An inner membrane enzyme in Salmonella and Escherichia coli that transfers 4-amino-4-deoxy-L-arabinose to lipid A: induction on polymyxin-resistant mutants and role of a novel lipid-linked donor. J Biol Chem. 2001;276(46):43122-31. Epub 2001/09/06. doi: 10.1074/jbc.M106961200. PubMed PMID: 11535604.
43. Kim SH, Jia W, Parreira VR, Bishop RE, Gyles CL. Phosphoethanolamine substitution in the lipid A of Escherichia coli O157 : H7 and its association with PmrC. Microbiology (Reading). 2006;152(Pt 3):657-66. Epub 2006/03/04. doi: 10.1099/mic.0.28692-0. PubMed PMID: 16514146.
44. Putker F, Bos MP, Tommassen J. Transport of lipopolysaccharide to the Gram-negative bacterial cell surface. FEMS Microbiol Rev. 2015;39(6):985-1002. Epub 2015/06/04. doi: 10.1093/femsre/fuv026. PubMed PMID: 26038291.
45. Whitfield C, Trent MS. Biosynthesis and export of bacterial lipopolysaccharides. Annu Rev Biochem. 2014;83:99-128. Epub 2014/03/04. doi: 10.1146/annurev-biochem-060713-035600. PubMed PMID: 24580642.
46. Velkov T, Deris ZZ, Huang JX, Azad MA, Butler M, Sivanesan S, et al. Surface changes and polymyxin interactions with a resistant strain of Klebsiella pneumoniae. Innate Immun. 2014;20(4):350-63. Epub 2013/07/28. doi: 10.1177/1753425913493337. PubMed PMID: 23887184; PubMed Central PMCID: PMCPMC4242413.

47. Hagiwara D, Yamashino T, Mizuno T. A Genome-wide view of the Escherichia coli BasS-BasR two-component system implicated in iron-responses. Biosci Biotechnol Biochem. 2004;68(8):1758-67. Epub 2004/08/24. doi: 10.1271/bbb.68.1758. PubMed PMID: 15322361.
48. Ogasawara H, Shinohara S, Yamamoto K, Ishihama A. Novel regulation targets of the metal-response BasS-BasR two-component system of Escherichia coli. Microbiology (Reading). 2012;158(Pt 6):1482-92. Epub 2012/03/24. doi: 10.1099/mic.0.057745-0. PubMed PMID: 22442305.
49. Lee LJ, Barrett JA, Poole RK. Genome-wide transcriptional response of chemostat-cultured Escherichia coli to zinc. J Bacteriol. 2005;187(3):1124-34. Epub 2005/01/22. doi: 10.1128/JB.187.3.1124-1134.2005. PubMed PMID: 15659689; PubMed Central PMCID: PMCPMC545701.
50. Wosten MM, Kox LF, Chamnongpol S, Soncini FC, Groisman EA. A signal transduction system that responds to extracellular iron. Cell. 2000;103(1):113-25. Epub 2000/10/29. doi: 10.1016/s0092-8674(00)00092-1. PubMed PMID: 11051552.
51. Rubin EJ, Herrera CM, Crofts AA, Trent MS. PmrD is required for modifications to escherichia coli endotoxin that promote antimicrobial resistance. Antimicrob Agents Chemother. 2015;59(4):2051-61. Epub 2015/01/22. doi: 10.1128/AAC.05052-14. PubMed PMID: 25605366; PubMed Central PMCID: PMCPMC4356761.
52. Garcia Vescovi E, Soncini FC, Groisman EA. Mg2+ as an extracellular signal: environmental regulation of Salmonella virulence. Cell. 1996;84(1):165-74. Epub 1996/01/12. doi: 10.1016/s0092-8674(00)81003-x. PubMed PMID: 8548821.
53. Conway T, Creecy JP, Maddox SM, Grissom JE, Conkle TL, Shadid TM, et al. Unprecedented high-resolution view of bacterial operon architecture revealed by RNA sequencing. mBio. 2014;5(4):e01442-14. Epub 2014/07/10. doi: 10.1128/mBio.01442-14. PubMed PMID: 25006232; PubMed Central PMCID: PMCPMC4161252.
54. Liu X, Xu J, Zhu J, Du P, Sun A. Combined Transcriptome and Proteome Analysis of RpoS Regulon Reveals Its Role in Spoilage Potential of Pseudomonas fluorescens. Front Microbiol. 2019;10:94. Epub 2019/02/23. doi: 10.3389/fmicb.2019.00094. PubMed PMID: 30787912; PubMed Central PMCID: PMCPMC6372562.
55. Wong GT, Bonocora RP, Schep AN, Beeler SM, Lee Fong AJ, Shull LM, et al. Genome-Wide Transcriptional Response to Varying RpoS Levels in Escherichia coli K-12. J Bacteriol. 2017;199(7). Epub 2017/01/25. doi: 10.1128/JB.00755-16. PubMed PMID: 28115545; PubMed Central PMCID: PMCPMC5350281.
56. Herrera CM, Hankins JV, Trent MS. Activation of PmrA inhibits LpxT-dependent phosphorylation of lipid A promoting resistance to antimicrobial peptides. Mol Microbiol. 2010;76(6):1444-60. Epub 2010/04/14. doi: 10.1111/j.1365-2958.2010.07150.x. PubMed PMID: 20384697; PubMed Central PMCID: PMCPMC2904496.
57. Wang J, Ma W, Wang Z, Li Y, Wang X. Construction and characterization of an Escherichia coli mutant producing Kdo(2)-lipid A. Mar Drugs. 2014;12(3):1495-511. Epub 2014/03/19. doi: 10.3390/md12031495. PubMed PMID: 24633251; PubMed Central PMCID: PMCPMC3967223.
58. Carty SM, Sreekumar KR, Raetz CR. Effect of cold shock on lipid A biosynthesis in Escherichia coli. Induction At 12 degrees C of an acyltransferase specific for palmitoleoyl-acyl carrier protein. J Biol Chem. 1999;274(14):9677-85. Epub 1999/03/27. doi: 10.1074/jbc.274.14.9677. PubMed PMID: 10092655.

59. Moffatt JH, Harper M, Boyce JD. Mechanisms of Polymyxin Resistance. Adv Exp Med Biol. 2019;1145:55-71. Epub 2019/08/01. doi: 10.1007/978-3-030-16373-0_5. PubMed PMID: 31364071.
60. Daugelavicius R, Bakiene E, Bamford DH. Stages of polymyxin B interaction with the Escherichia coli cell envelope. Antimicrob Agents Chemother. 2000;44(11):2969-78. Epub 2000/10/19. doi: 10.1128/AAC.44.11.2969-2978.2000. PubMed PMID: 11036008; PubMed Central PMCID: PMCPMC101588.
61. Manioglu S, Modaresi SM, Ritzmann N, Thoma J, Overall SA, Harms A, et al. Antibiotic polymyxin arranges lipopolysaccharide into crystalline structures to solidify the bacterial membrane. Nat Commun. 2022;13(1):6195. Epub 2022/10/22. doi: 10.1038/s41467-022-33838-0. PubMed PMID: 36271003; PubMed Central PMCID: PMCPMC9587031.
62. Ayoub Moubareck C. Polymyxins and Bacterial Membranes: A Review of Antibacterial Activity and Mechanisms of Resistance. Membranes (Basel). 2020;10(8). Epub 2020/08/14. doi: 10.3390/membranes10080181. PubMed PMID: 32784516; PubMed Central PMCID: PMCPMC7463838.
63. Trent MS, Ribeiro AA, Doerrler WT, Lin S, Cotter RJ, Raetz CR. Accumulation of a polyisoprene-linked amino sugar in polymyxin-resistant Salmonella typhimurium and Escherichia coli: structural characterization and transfer to lipid A in the periplasm. J Biol Chem. 2001;276(46):43132-44. Epub 2001/09/06. doi: 10.1074/jbc.M106962200. PubMed PMID: 11535605.
64. Nguyen D, Joshi-Datar A, Lepine F, Bauerle E, Olakanmi O, Beer K, et al. Active starvation responses mediate antibiotic tolerance in biofilms and nutrient-limited bacteria. Science. 2011;334(6058):982-6. Epub 2011/11/19. doi: 10.1126/science.1211037. PubMed PMID: 22096200; PubMed Central PMCID: PMCPMC4046891.
65. Ito A, Taniuchi A, May T, Kawata K, Okabe S. Increased antibiotic resistance of Escherichia coli in mature biofilms. Appl Environ Microbiol. 2009;75(12):4093-100. Epub 2009/04/21. doi: 10.1128/AEM.02949-08. PubMed PMID: 19376922; PubMed Central PMCID: PMCPMC2698376.
66. Schembri MA, Kjaergaard K, Klemm P. Global gene expression in Escherichia coli biofilms. Mol Microbiol. 2003;48(1):253-67. Epub 2003/03/27. doi: 10.1046/j.1365-2958.2003.03432.x. PubMed PMID: 12657059.
67. Gray MJ. Interactions between DksA and Stress-Responsive Alternative Sigma Factors Control Inorganic Polyphosphate Accumulation in Escherichia coli. J Bacteriol. 2020;202(14). Epub 2020/04/29. doi: 10.1128/JB.00133-20. PubMed PMID: 32341074; PubMed Central PMCID: PMCPMC7317045.
68. Downey M. A Stringent Analysis of Polyphosphate Dynamics in Escherichia coli. J Bacteriol. 2019;201(9). Epub 2019/02/21. doi: 10.1128/JB.00070-19. PubMed PMID: 30782636; PubMed Central PMCID: PMCPMC6456866.
69. Bowlin MQ, Long AR, Huffines JT, Gray MJ. The role of nitrogen-responsive regulators in controlling inorganic polyphosphate synthesis in Escherichia coli. Microbiology (Reading). 2022;168(4). Epub 2022/04/29. doi: 10.1099/mic.0.001185. PubMed PMID: 35482529; PubMed Central PMCID: PMCPMC10233264.
70. Kato A, Latifi T, Groisman EA. Closing the loop: the PmrA/PmrB two-component system negatively controls expression of its posttranscriptional activator PmrD. Proc Natl Acad Sci U S A. 2003;100(8):4706-11. Epub 2003/04/05. doi: 10.1073/pnas.0836837100. PubMed PMID: 12676988; PubMed Central PMCID: PMCPMC153620.

71. Datsenko KA, Wanner BL. One-step inactivation of chromosomal genes in Escherichia coli K-12 using PCR products. Proc Natl Acad Sci U S A. 2000;97(12):6640-5. Epub 2000/06/01. doi: 10.1073/pnas.120163297. PubMed PMID: 10829079; PubMed Central PMCID: PMCPMC18686.
72. Datta S, Costantino N, Court DL. A set of recombineering plasmids for gram-negative bacteria. Gene. 2006;379:109-15. Epub 2006/06/06. doi: 10.1016/j.gene.2006.04.018. PubMed PMID: 16750601.
73. Uzzau S, Figueroa-Bossi N, Rubino S, Bossi L. Epitope tagging of chromosomal genes in Salmonella. Proc Natl Acad Sci U S A. 2001;98(26):15264-9. Epub 2001/12/14. doi: 10.1073/pnas.261348198. PubMed PMID: 11742086; PubMed Central PMCID: PMCPMC65018.
74. Cherepanov PP, Wackernagel W. Gene disruption in Escherichia coli: TcR and KmR cassettes with the option of Flp-catalyzed excision of the antibiotic-resistance determinant. Gene. 1995;158(1):9-14. Epub 1995/05/26. doi: 10.1016/0378-1119(95)00193-a. PubMed PMID: 7789817.
75. Sharan SK, Thomason LC, Kuznetsov SG, Court DL. Recombineering: a homologous recombination-based method of genetic engineering. Nat Protoc. 2009;4(2):206-23. Epub 2009/01/31. doi: 10.1038/nprot.2008.227. PubMed PMID: 19180090; PubMed Central PMCID: PMCPMC2790811.
76. Deutsch EW, Mendoza L, Shteynberg DD, Hoopmann MR, Sun Z, Eng JK, et al. Trans-Proteomic Pipeline: Robust Mass Spectrometry-Based Proteomics Data Analysis Suite. J Proteome Res. 2023;22(2):615-24. Epub 2023/01/18. doi: 10.1021/acs.jproteome.2c00624. PubMed PMID: 36648445; PubMed Central PMCID: PMCPMC10166710.
77. Chambers MC, Maclean B, Burke R, Amodei D, Ruderman DL, Neumann S, et al. A cross-platform toolkit for mass spectrometry and proteomics. Nat Biotechnol. 2012;30(10):918-20. Epub 2012/10/12. doi: 10.1038/nbt.2377. PubMed PMID: 23051804; PubMed Central PMCID: PMCPMC3471674.
78. Eng JK, Jahan TA, Hoopmann MR. Comet: an open-source MS/MS sequence database search tool. Proteomics. 2013;13(1):22-4. Epub 2012/11/14. doi: 10.1002/pmic.201200439. PubMed PMID: 23148064.
79. UniProt C. UniProt: the Universal Protein Knowledgebase in 2023. Nucleic Acids Res. 2023;51(D1):D523-D31. Epub 2022/11/22. doi: 10.1093/nar/gkac1052. PubMed PMID: 36408920; PubMed Central PMCID: PMCPMC9825514.
80. Nesvizhskii AI, Keller A, Kolker E, Aebersold R. A statistical model for identifying proteins by tandem mass spectrometry. Anal Chem. 2003;75(17):4646-58. Epub 2003/11/25. doi: 10.1021/ac0341261. PubMed PMID: 14632076.
81. Benjamini Y, Hochberg Y. Controlling the false discovery rate: a practical and powerful approach to multiple testing. Journal of the Royal Statistical Society, Series B. 1995;57 (1):289–300. MR 1325392.
82. Bauer S, Grossmann S, Vingron M, Robinson PN. Ontologizer 2.0--a multifunctional tool for GO term enrichment analysis and data exploration. Bioinformatics. 2008;24(14):1650-1. Epub 2008/05/31. doi: 10.1093/bioinformatics/btn250. PubMed PMID: 18511468.
83. Bondy-Chorney E, Abramchuk I, Nasser R, Holinier C, Denoncourt A, Baijal K, et al. A Broad Response to Intracellular Long-Chain Polyphosphate in Human Cells. Cell Rep. 2020;33(4):108318. Epub 2020/10/29. doi: 10.1016/j.celrep.2020.108318. PubMed PMID: 33113373.

84. Karginov A, Agaphonov M. A simple enrichment procedure improves detection of membrane proteins by immunoblotting. Biotechniques. 2016;61(5):260-1. Epub 2016/11/15. doi: 10.2144/000114474. PubMed PMID: 27839511.
85. Hall BG, Acar H, Nandipati A, Barlow M. Growth rates made easy. Mol Biol Evol. 2014;31(1):232-8. Epub 2013/10/31. doi: 10.1093/molbev/mst187. PubMed PMID: 24170494.
86. McCarthy L, Abramchuk I, Wafy G, Denoncourt A, Lavallee-Adam M, Downey M. Ddp1 Cooperates with Ppx1 to Counter a Stress Response Initiated by Nonvacuolar Polyphosphate. mBio. 2022:e0039022. Epub 2022/07/22. doi: 10.1128/mbio.00390-22. PubMed PMID: 35862758.
87. Herrera CM, Voss BJ, Trent MS. Homeoviscous Adaptation of the Acinetobacter baumannii Outer Membrane: Alteration of Lipooligosaccharide Structure during Cold Stress. mBio. 2021;12(4):e0129521. Epub 2021/08/25. doi: 10.1128/mBio.01295-21. PubMed PMID: 34425709; PubMed Central PMCID: PMCPMC8406137.
88. Deutsch EW, Csordas A, Sun Z, Jarnuczak A, Perez-Riverol Y, Ternent T, et al. The ProteomeXchange consortium in 2017: supporting the cultural change in proteomics public data deposition. Nucleic Acids Res. 2017;45(D1):D1100-D6. Epub 2016/12/08. doi: 10.1093/nar/gkw936. PubMed PMID: 27924013; PubMed Central PMCID: PMCPMC5210636.
89. Perez-Riverol Y, Csordas A, Bai J, Bernal-Llinares M, Hewapathirana S, Kundu DJ, et al. The PRIDE database and related tools and resources in 2019: improving support for quantification data. Nucleic Acids Res. 2019;47(D1):D442-D50. Epub 2018/11/06. doi: 10.1093/nar/gky1106. PubMed PMID: 30395289; PubMed Central PMCID: PMCPMC6323896.

2.8. Supplemental Figures

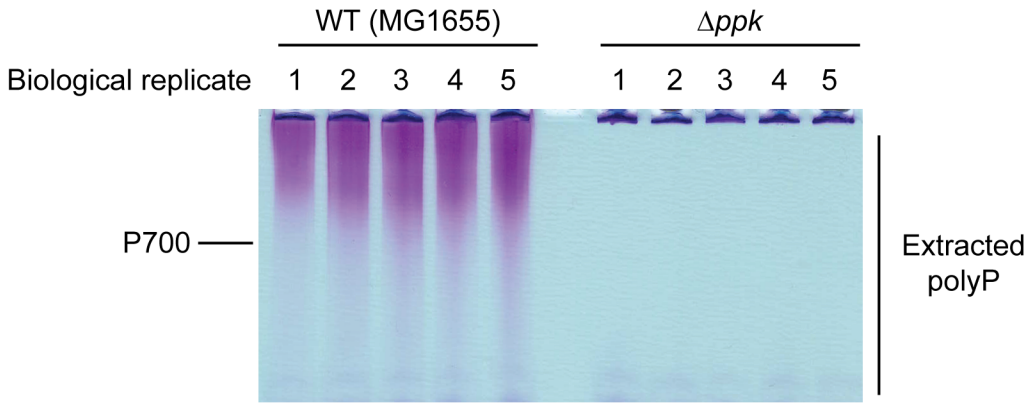

S1 Figure. Wild-type *E. coli* accumulate polyP in MOPS minimal media while Δ*ppk* mutants do not. PolyP extraction gel from wild-type and Δ*ppk* mutant cultures used for mass spectrometry sample preparation. Overnight cultures were grown in LB media to mid-exponential phase and then shifted into MOPS minimal media for 3 hours to induce starvation and polyP accumulation. PolyP extracts were run on a TBE-urea gel and stained with toluidine blue. The migration of a chain ~700 phosphate residues in length (p700) is indicated.

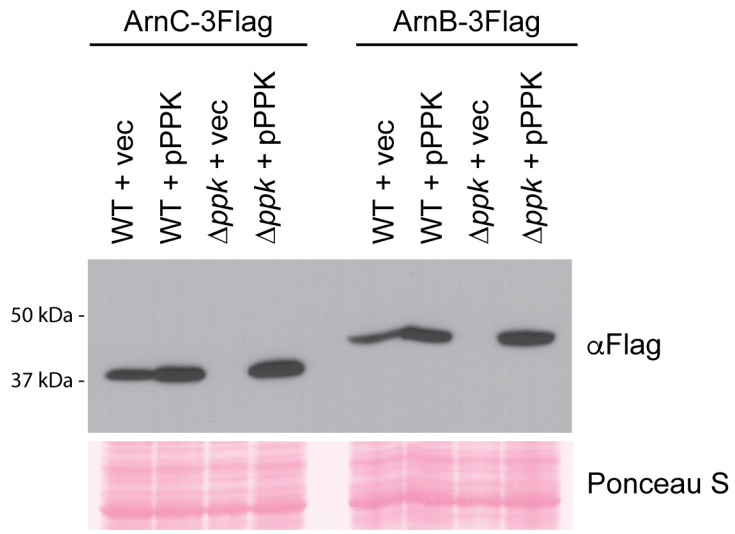

S2 Figure. Arn expression is PPK-dependent during MOPS starvation. A) Rescue of Arn expression following 3 hours in MOPS media. Extracted protein samples were resolved using SDS-PAGE, transferred to PVDF and detected using an anti-Flag antibody.

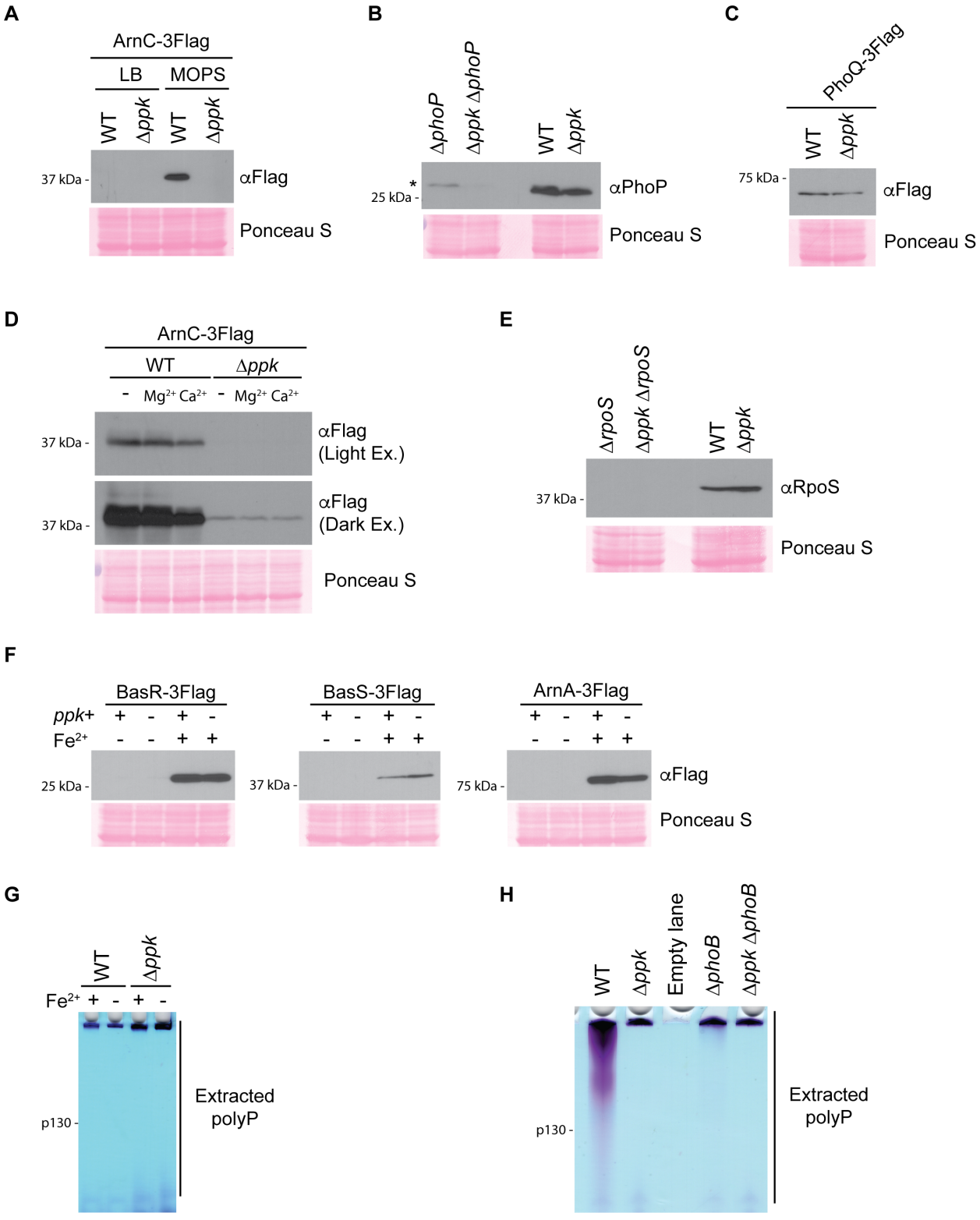

S3 Figure. Molecular control of Arn and EptA protein expression by PPK. A) Induction of ArnC-3Flag expression upon the switch from LB to MOPS media. The indicated strains were

grown in LB media to mid-log phase and shifted to MOPS media for 3 hours. Proteins were extracted and resolved via SDS-PAGE prior to transfer to a PVDF membrane. Tagged proteins were detected using an anti-Flag antibody. **B)** Expression of PhoP between wild-type cells and Δ*ppk* mutants. The indicated strains were starved in MOPS media for 3 hours prior to protein extraction, separation by SDS-PAGE and detection with an antibody against PhoP. A background band (*) in Δ*phoP* mutants (controls used to validate the antibody) is PPK-regulated, which makes evaluation of changes to PhoP protein expression difficult. Regardless, regulation of PhoP by PPK appears to be minimal. **C)** Expression of PhoQ-3Flag between wild-type cells and Δ*ppk* mutants. The indicated strains were starved in MOPS media for 3 hours and proteins were analyzed as described in (B) using an antibody towards Flag. **D)** Influence of magnesium (Mg^{2+}) on ArnC-3Flag expression in MOPS media. Cells were grown to mid-exponential phase in LB and then shifted to MOPS minimal media in the absence or presence of 1 mM magnesium chloride or calcium chloride (control) for 3 hours. Extracted protein samples were resolved using SDS-PAGE, transferred to PVDF, and detected using an anti-Flag antibody. Images shown are representative of results from ≥3 experiments. **E)** Expression of RpoS between wild-type cells and Δ*ppk* mutants. The indicated strains were starved in MOPS media for 3 hours prior to protein extraction, separation by SDS-PAGE, and detection with an antibody directed against RpoS. The Δ*rpoS* mutant strains serve to validate the antibody. **F)** Expression of BasS-3Flag, BasR-3Flag and ArnA-3Flag in LB supplemented with iron by wild-type and Δ*ppk* mutants. The indicated strains grown in LB or LB + iron (200 μM $FeSO_4$) for 1.5 hours prior to protein extraction, separation by SDS-PAGE, transfer to PVDF, and detection of tagged proteins with an anti-Flag antibody. **G-H)** Influence of iron (G) and *phoB* mutation (H) on polyP accumulation. PolyP was extracted from the indicated strains grown in LB or LB + iron (200 μM $FeSO_4$) for 1.5 hours or in MOPS for 3 hours following a shift from LB and analyzed on TBE-urea gels stained with toluidine blue. Note: the same BasR-tagged strains used for S2F were used for S2G polyP extraction, and the same ArnC-tagged strains used for 3I were used for the polyP extraction shown in S3H. Images shown are representative of results from ≥3 experiments, except for the polyP extractions in S3G and S3H, which are representative of 2 independent replicates.

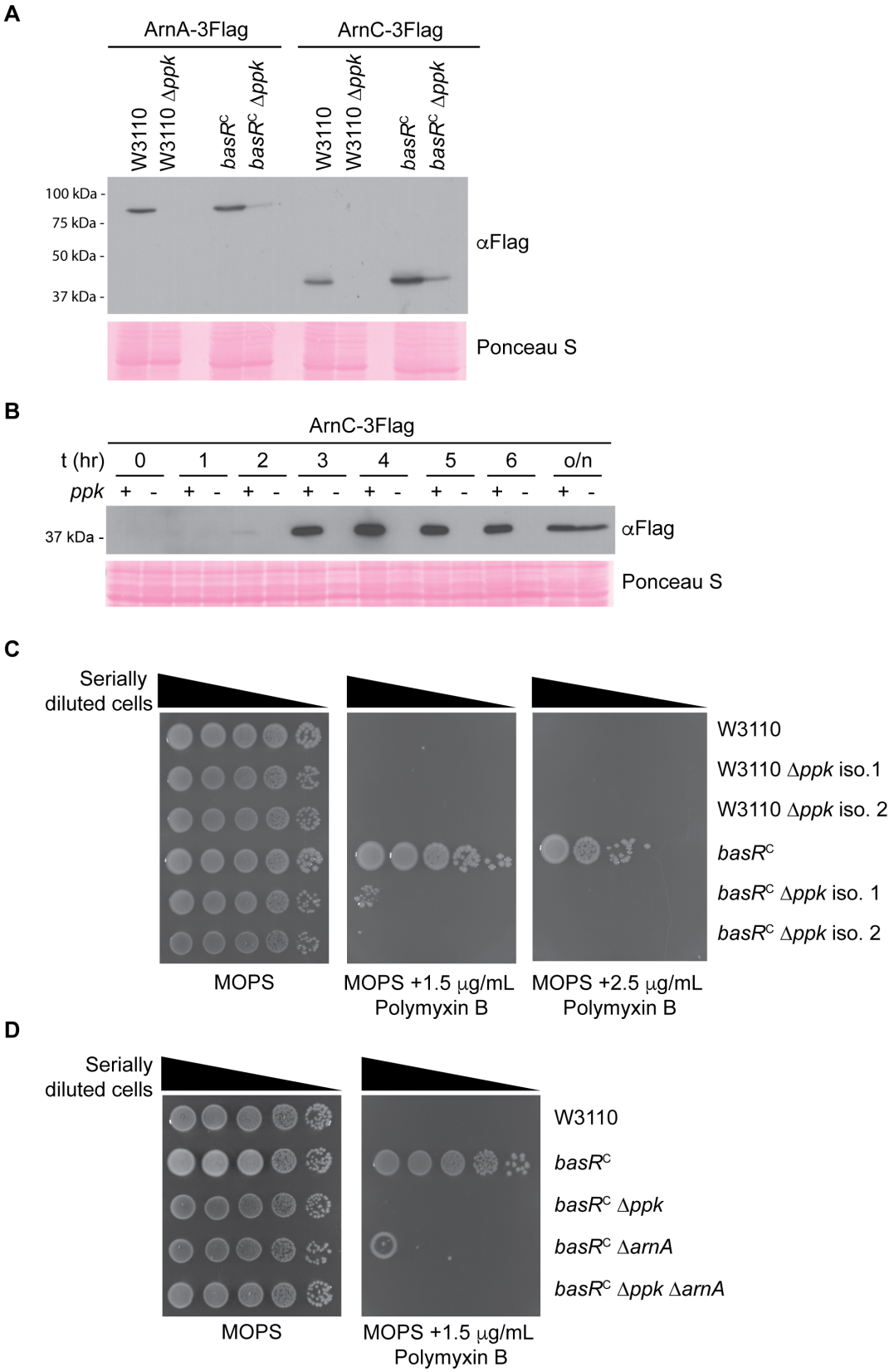

S4 – Figure legend on the next page.

S4 Figure. Regulation of Arn protein expression and polymyxin resistance by PPK in the W3110 and WD101 (*basR*^{C}) backgrounds. A) PPK-dependent Arn-3Flag expression in W3110 and WD101 (*basR*^{C}) strains. The indicated strains were grown in LB to mid log phase prior to shifting to MOPS for 3 hours. Proteins were extracted and separated via SDS-PAGE prior to transfer to PVDF membrane and detection with anti-Flag antibody. **B)** Time course of ArnC-3Flag expression following the shift from LB to MOPS media. Expression was analyzed for the indicated strains at the timepoints shown. Protein samples were resolved using a 12% SDS-PAGE gel, transferred to PVDF membrane, and proteins detected using an anti-Flag antibody. **C)** Role of *ppk* in polymyxin resistance. Impact of *ppk* on the innate polymyxin resistance of W3110 and *basR*^{C} strains. The indicated strains were spotted in 10-fold serial dilutions on the indicated media and incubated at 37 °C for 2 days prior to imaging. **D)** Arn-dependence of polymyxin resistance in *basR*^{C} strains. Strains were diluted and grown as described in C. Images shown are representative of results from ≥3 experiments.

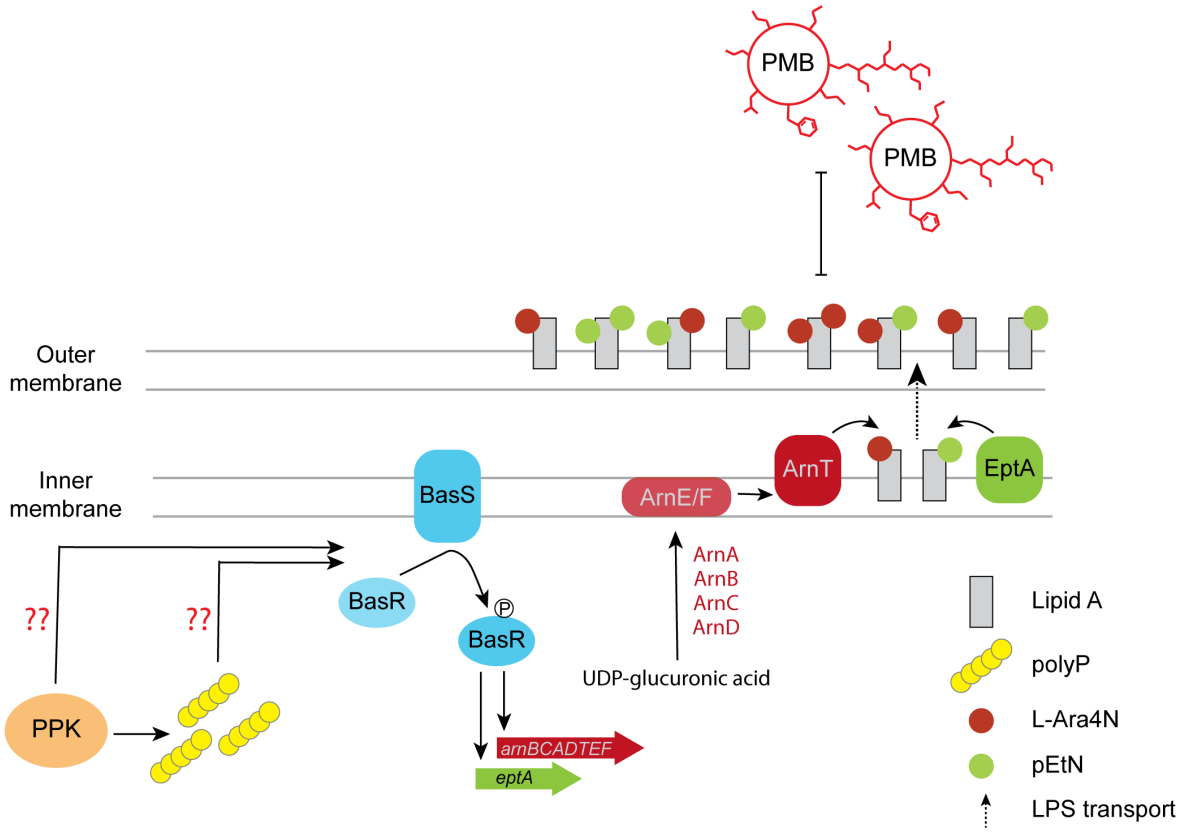

S5 Figure. The role of PPK in the regulation of lipid A modification and polymyxin resistance. PolyP synthesized by PPK upon a switch from LB to MOPS media triggers BasS activation by autophosphorylation. Activated BasS then transphosphorylases BasR to induces downstream transcription of the *arnBCADTEF* operon and *EptA* gene. This results in increased level of Arn and EptA proteins, and upregulation of the respective L-Ara4N and pEtN modifications. Dashed arrows indicate an additional step where the modified lipid A (a key structural component of the LPS) is transported to the outer membrane by the LPS transport system. This reduces the net negative charge of the outer membrane and results in polymyxin B (PMB) resistance. What is still unknown is whether polyP is acting directly in BasS activation and if PPK has a role independent of polyP synthesis.

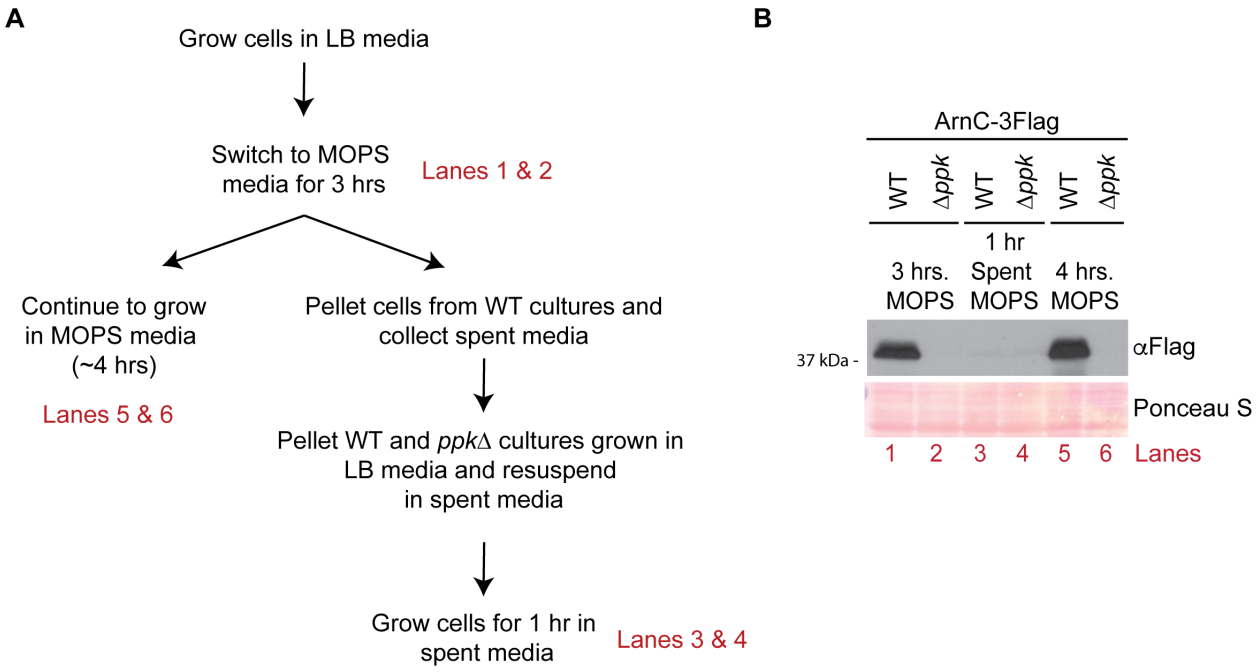

S6 Figure. Spent MOPS media from wild-type cultures does not induce Arn-3Flag expression of naïve cells. A-B) Schematic (A) and western blotting (B) of media switch experiment. Cells were grown in LB media to mid-exponential phase and then shifted to MOPS media for 3 hours to induce Arn expression (lanes 1 and 2). After 3 hours in MOPS, spent media from wild-type cultures was centrifuged to remove cells and used for the media switch. The remainder of the culture was left to grow for another hour (lanes 5 and 6). For the media switch, cells exponentially growing in LB were pelleted, washed, and resuspended in the spent MOPS media from wild-type cultures. These cultures were left to grow for 1 hour to test if the spent media contained the trigger needed to induce Arn expression (lanes 3 and 4). For western blotting extracted protein samples were resolved using SDS-PAGE, transferred to PVDF, and detected using an anti-Flag antibody. Images shown are representative of results from ≥2 experiments.

2.9. Supplemental Tables

Here, I have included tables that are relevant for the interpretation of the presented data. Please see '*Supporting information*' tab of online article for detailed view of Supplemental tables 1-4 (direct links provided below).

List of tables presented:

S1 Table. Mass spectrometry-identified proteins and differential expression analysis.

1. S1-Tab 1: List of significantly differentially expressed proteins and associated FDR-adjusted p-values.
2. S1-Tab 2: Spectral counts for proteins classified as all-or-none.

S2 Table. Comparison of overlap between Varas *et al.* and Baijal *et al.* mass spectrometry data sets.

1. S2-Tab 1: Direction of change of significantly differentially expressed proteins between our data set and the *Varas et al* data set.

S3 Table. Bacterial strains, plasmids and qPCR primers used for this work.

1. S3-Tab 1: Bacterial strains used in this study.
2. S3-Tab 2: Plasmids used in this study.

Online version of tables:

S1 Table. Mass spectrometry-identified proteins and differential expression analysis.
See online: https://doi.org/10.1371/journal.pbio.3002558.s007

S2 Table. Comparison of overlap between Varas *et al.* and Baijal *et al.* mass spectrometry data sets.
See online: https://doi.org/10.1371/journal.pbio.3002558.s008

S3 Table. Bacterial strains, plasmids and qPCR primers used for this work.
See online: https://doi.org/10.1371/journal.pbio.3002558.s009

S4 Table. Reagents and antibody conditions used for this work.
See online: https://doi.org/10.1371/journal.pbio.3002558.s010

S1 Table-Tab 1 – List of significantly differentially expressed proteins and associated FDR-adjusted p-values.

protein.uniprot	FDR-adjusted p-value
GLTB_ECOLI	0.000562762
AK1H_ECOLI	0.001077085
ILVA_ECOLI	0.001077085
UGPB_ECOLI	0.001077085
YEAG_ECOLI	0.001801541
GLTD_ECOLI	0.001869174
LIVJ_ECOLI	0.001869174
PHOB_ECOLI	0.001869174
PSTS_ECOLI	0.001869174
CYSI_ECOLI	0.001869174
GSIB_ECOLI	0.002309786
YJGR_ECOLI	0.004306924
ILVD_ECOLI	0.00549115
AROG_ECOLI	0.00549115
YNHG_ECOLI	0.00549115
CYSM_ECOLI	0.007772958
ILVH_ECOLI	0.008224227
MASY_ECOLI	0.008224227
TGT_ECOLI	0.008224227
CATE_ECOLI	0.008224227
MSCS_ECOLI	0.008685934
METE_ECOLI	0.008685934
OTSA_ECOLI	0.008685934
CYSK_ECOLI	0.009417238
BTUB_ECOLI	0.00972456
NQOR_ECOLI	0.009730928
YHJE_ECOLI	0.009730928
ALF1_ECOLI	0.009799845
ARTJ_ECOLI	0.009799845

ACSA_ECOLI	0.012498509
THRC_ECOLI	0.015611801
TRPA_ECOLI	0.015611801
LUXS_ECOLI	0.015611801
GLNQ_ECOLI	0.015624513
GLMM_ECOLI	0.019497014
DHE4_ECOLI	0.019570428
GALM_ECOLI	0.019570428
ILVE_ECOLI	0.019570428
HIS1_ECOLI	0.021652365
DHG_ECOLI	0.025867933
RS8_ECOLI	0.027184844
GUAA_ECOLI	0.027336362
ARGD_ECOLI	0.028901887
DHAS_ECOLI	0.030396426
YFIA_ECOLI	0.030396426
SLT_ECOLI	0.030396426
CYSD_ECOLI	0.030396426
SERC_ECOLI	0.030396426
ACUI_ECOLI	0.030396426
6PGL_ECOLI	0.030396426
YDCL_ECOLI	0.030396426
AAT_ECOLI	0.030852909
GLNH_ECOLI	0.030852909
LNT_ECOLI	0.030852909
ISPG_ECOLI	0.030852909
TRHP_ECOLI	0.030852909
CLPA_ECOLI	0.032090386
TRPC_ECOLI	0.032116101
APT_ECOLI	0.032116101
RS7_ECOLI	0.032814845
PPSA_ECOLI	0.033227748

GLTI_ECOLI	0.033839723
ILVC_ECOLI	0.034014668
OSMC_ECOLI	0.034119067
FABY_ECOLI	0.034425762
TYRB_ECOLI	0.035663618
CYSN_ECOLI	0.035663618
ASMA_ECOLI	0.041744129
HCXB_ECOLI	0.041744129
YAEH_ECOLI	0.041744129
GCH1_ECOLI	0.044496598
KBP_ECOLI	0.044496598
AHPF_ECOLI	0.044496598
RLUB_ECOLI	0.044496598
YEGP_ECOLI	0.044496598
PYRI_ECOLI	0.045361838
ENO_ECOLI	0.0496003
YCFP_ECOLI	0.0496003

S1 Table-Tab 2 – Spectral counts for proteins classified as all-or-none.

Spectral counts from mass spectrometry proteomics										
protein.uniprot	**WT_1**	**WT_2**	**WT_3**	**WT_4**	**WT_5**	**Δ*ppk*_1**	**Δ*ppk*_2**	**Δ*ppk*_3**	**Δ*ppk*_4**	**Δ*ppk*_5**
YBDL_ECOLI	3	3	3	3	3	0	0	0	0	0
ARNC_ECOLI	1	1	2	1	3	0	0	0	0	0
ARNB_ECOLI	15	13	8	1	4	0	0	0	0	0
SUPH_ECOLI	3	1	1	2	1	0	0	0	0	0
CSPB_ECOLI	2	4	5	2	1	0	0	0	0	0
EPTA_ECOLI	13	11	6	9	9	0	0	0	0	0
GGT_ECOLI	10	4	7	5	9	0	0	0	0	0
PHND_ECOLI	17	16	21	18	18	0	0	0	0	0
ISCR_ECOLI	0	0	0	0	0	5	5	10	3	6
YCGL_ECOLI	0	0	0	0	0	1	1	2	1	1
YAFK_ECOLI	1	1	1	1	2	0	0	0	0	0
ULAR_ECOLI	2	1	1	3	1	0	0	0	0	0
AROD_ECOLI	4	2	2	2	2	0	0	0	0	0
PHOE_ECOLI	11	14	12	13	8	0	0	0	0	0

S2 Table-Tab 1 – Direction of change of significantly differentially expressed proteins between our data set and the *Varas et al* data set. Total 7 proteins classified as significantly differentially expressed in both datasets overlapped.

Green = significantly differentially expressed proteins overlapping between both data sets + change in same direction; Orange = significantly differentially expressed proteins overlapping between both data sets + change in different directions.

Protein	**Significant in Baijal *et al.* ($p<0.05$)**	**Direction of change in Baijal *et al.***	**≥1 or ≤-1 log2 in Varas *et al.***	**Direction of change in Varas *et al.***
sp|P21179|CATE_ECOLI	Yes	Up in WT	≥1	Up in WT
sp|P0ADE6|YGAU_ECOLI (sp|P0ADE6|KBP_ECOLI)	Yes	Up in WT	≥1	Up in WT
sp|P0ACY3|YEAG_ECOLI	Yes	Up in WT	≥1	Up in WT
sp|P00561|AK1H_ECOLI	Yes	Up in WT	≤1	Up in Δ*ppk*
sp|P0AEQ3|GLNH_ECOLI	Yes	Up in WT	≤1	Up in Δ*ppk*
sp|P08997|MASY_ECOLI	Yes	Up in WT	≤1	Up in Δ*ppk*
sp|P27550|ACSA_ECOLI	Yes	Up in Δ*ppk*	≤1	Up in Δ*ppk*

S3 Table-Tab 1 – Bacterial strains used in this study. For simplicity the 'Background' column has been omitted from this version of the table. All strains made for this study are in the MG1655 background.

Reference number	Genotype	Marker	Source
BMD0058	F-, λ-, *rph-1 ilvG- rfb-50* (**MG1655**)	--	Gift from Michael Gray
BMD0059	Δ*ppk* (*kan*^{r} excised)	--	Gift from Michael Gray
BMD0128	*arnC-3xFlag-kan*^{r}	*kan*$^+$	This study
BMD0146	Δ*ppk* (*kan*^{r} excised) *arnC-3xFlag-kan*^{r}	*kan*$^+$	This study
BMD0324	*arnC-3xFlag* (*kan*^{r} excised)	--	This study
BMD0314	Δ*ppk* (*kan*^{r} excised) *arnC-3xFlag* (*kan*^{r} excised)	--	This study
BMD0363	*arnC-3xFlag* (*kan*^{r} excised) [pPWSK129, Kan^r]	*kan*$^+$	This study
BMD373	*arnC-3xFlag* (*kan*^{r} excised) [pPPK10, Kan^r]	*kan*$^+$	This study
BMD0353	Δ*ppk* (*kan*^{r} excised) *arnC-3xFlag* (*kan*^{r} excised) [pPWSK129, Kan^r]	*kan*$^+$	This study
BMD0342	Δ*ppk* (*kan*^{r} excised) *arnC-3xFlag* (*kan*^{r} excised) [pPPK10, Kan^r]	*kan*$^+$	This study
BMD0217	*arnB-3xFlag-kan*^{r}	*kan*$^+$	This study
BMD219	Δ*ppk* (*kan*^{r} excised) *arnB-3xFlag-kan*^{r}	*kan*$^+$	This study
BMD0326	*arnB-3xFlag* (*kan*^{r} excised)	--	This study
BMD0316	Δ*ppk* (*kan*^{r} excised) *arnB-3xFlag* (*kan*^{r} excised)	--	This study
BMD0365	*arnB-3xFlag* (*kan*^{r} excised) [pPWSK129, Kan^r]	*kan*$^+$	This study
BMD0375	*arnB-3xFlag* (*kan*^{r} excised) [pPPK10, Kan^r]	*kan*$^+$	This study
BMD0355	Δ*ppk* (*kan*^{r} excised) *arnB-3xFlag* (*kan*^{r} excised) [pPWSK129, Kan^r]	*kan*$^+$	This study
BMD0344	Δ*ppk* (*kan*^{r} excised) *arnB-3xFlag* (*kan*^{r} excised) [pPPK10, Kan^r]	*kan*$^+$	This study

BMD0221	*metE-3xFlag-kan*^{r}	*kan*$^+$	This study
BMD0223	Δ*ppk* (*kan*^{r} excised) *metE-3xFlag-kan*^{r}	*kan*$^+$	This study
BMD0225	*ybdL-3xFlag-kan*^{r}	*kan*$^+$	This study
BMD0227	Δ*ppk* (*kan*^{r} excised) *ybdL-3xFlag-kan*^{r}	*kan*$^+$	This study
BMD0251	*YeaG-3xFlag-kan*^{r}	*kan*$^+$	This study
BMD0253	Δ*ppk* (*kan*^{r} excised) *yeaG-3xFlag-kan*^{r}	*kan*$^+$	This study
BMD0229	*otsA-3xFlag-kan*^{r}	*kan*$^+$	This study
BMD0231	Δ*ppk* (*kan*^{r} excised) *otsA-3xFlag-kan*^{r}	*kan*$^+$	This study
BMD0275	*raiA-3xFlag-kan*^{r}	*kan*$^+$	This study
BMD0277	Δ*ppk* (*kan*^{r} excised) *raiA-3xFlag-kan*^{r}	*kan*$^+$	This study
BMD0486	*eptA-3xFlag-kan*^{r}	*kan*$^+$	This study
BMD0458	Δ*ppk* (*kan*^{r} excised) *eptA-3xFlag-kan*^{r}	*kan*$^+$	This study
BMD0265	*arnA-3xFlag-kan*^{r}	*kan*$^+$	This study
BMD0266	Δ*ppk* (*kan*^{r} excised) *ArnA-3xFlag-kan*^{r}	*kan*$^+$	This study
BMD0330	*arnA-3xFlag* (*kan*^{r} excised)	--	This study
BMD0322	Δ*ppk* (*kan*^{r} excised) *arnA-3xFlag* (*kan*^{r} excised)	--	This study
BMD0474	*ArnT-3xFlag-kan*^{r}	*kan*$^+$	This study
BMD0476	Δ*ppk* (*kan*^{r} excised) *arnT-3xFlag-kan*^{r}	*kan*$^+$	This study
BMD0463	*phoQ-3xFlag-kan*^{r}	*kan*$^+$	This study
BMD0465	Δ*ppk* (*kan*^{r} excised) *phoQ-3xFlag-kan*^{r}	*kan*$^+$	This study
BMD0466	*ΔrpoS::kan*^{r}	*kan*$^+$	This study
BMD0468	Δ*ppk* (*kan*^{r} excised) *ΔrpoS::kanr*	*kan*$^+$	This study
BMD0472	*phoP::kan*^{r}	*kan*$^+$	This study

BMD0470	Δ*ppk* (*kan*^{r} excised) *phoP::kanr*	*kan*$^+$	This study
BMD0261	*basS-3xFlag-kan*^{r}	*kan*$^+$	This study
BMD0263	Δ*ppk* (*kan*^{r} excised) *basS-3xFlag-kan*^{r}	*kan*$^+$	This study
BMD0320	*basS-3xFlag* (*kan*^{r} excised)	--	This study
BMD0332	Δ*ppk* (*kan*^{r} excised) *basS-3xFlag* (*kan*^{r} excised)	--	This study
BMD0257	*basR-3xFlag-kan*^{r}	*kan*$^+$	This study
BMD0259	Δ*ppk* (*kan*^{r} excised) *basR-3xFlag-kan*^{r}	*kan*$^+$	This study
BMD0328	*basR-3xFlag* (*kan*^{r} excised)	--	This study
BMD0318	Δ*ppk* (*kan*^{r} excised) *basR-3xFlag* (*kan*^{r} excised)	--	This study
BMD0399	*arnC-3xFlag* (*kan*^{r} excised) Δ*phoB*:: *kan*^{r}	*kan*$^+$	This study
BMD0401	Δ*ppk* (*kan*^{r} excised) *arnC-3xFlag* (*kan*^{r} excised) Δ*phoB*:: *kan*^{r}	*kan*$^+$	This study
BMD0387	*F-, λ- rph-1 INV(rrnD, rrnE)1 rph-1*	--	Trent Lab
BMD0395	W3110 Δ*ppk::kan*^{r}	*kan*$^+$	This study
BMD0407	W3110 Δ*ppk* (*kan*^{r} excised)	--	This study
BMD0388	W3110*, basR*^{C}	--	Trent Lab
BMD0397	*basR*^{C} Δ*ppk::kan*^{r}	*kan*$^+$	This study
BMD0437	*basR*^{C} Δ*ppk* (*kan*^{r} excised)	--	This study
BMD0413	*arnA-3xFlag-kan*^{r}	*kan*$^+$	This study
BMD0415	Δ*ppk* (*kan*^{r} excised) *arnA-3xFlag-kan*^{r}	*kan*$^+$	This study
BMD0417	*basR*^{C} *arnA-3xFlag-Kan*^{r}	*kan*$^+$	This study
BMD0419	*basR*^{C} Δ*ppk* (*kan*^{r} excised) *arnA-3xFlag-kan*^{r}	*kan*$^+$	This study
BMD0421	*arnC-3xFlag-kan*^{r}	*kan*$^+$	This study
BMD0423	Δ*ppk* (*kan*^{r} excised) *arnC-3xFlag-kan*^{r}	*kan*$^+$	This study

BMD0425	*basR*^{C} *arnC-3xFlag-kan*^{r}	*kan*$^{+}$	This study
BMD0427	*basR*^{C} Δ*ppk* (*kan*^{r} excised) *arnC-3xFlag-kan*^{r}	*kan*$^{+}$	This study
BMD0460	*basR*^{C} Δ*arnA::kan*^{r}	*kan*$^{+}$	This study
BMD0461	*basR*^{C} Δ*ppk* (*kan*^{r} excised) ΔarnA*::kan*^{r}	*kan*$^{+}$	This study
BMD0440	[pPWSK129, Kan^{r}]	*kan*$^{+}$	This study
BMD0444	Δ*ppk* (*kan*^{r} excised) [pPWSK129, Kanr]	*kan*$^{+}$	This study
BMD0446	Δ*ppk* (*kan*^{r} excised) [pPPK10, Kanr]	*kan*$^{+}$	This study
BMD0448	*basR*^{C} [pWSK129, Kan^{r}]	*kan*$^{+}$	This study
BMD0450	*basR*^{C} [pPPK10, Kan^{r}]	*kan*$^{+}$	This study
BMD0452	*basR*^{C} Δ*ppk* (*kan*^{r} excised) [pWSK129, Kan^{r}]	*kan*$^{+}$	This study
BMD0454	*basR*^{C} Δ*ppk* (*kan*^{r} excised) [pPPK10, Kan^{r}]	*kan*$^{+}$	This study
UPEC0001		--	Jakob Lab
UPEC0003	Δ*ppk::KanR*	*kan*$^{+}$	Jakob Lab
UPEC0006	Δ*ppk* (*kan*^{r} excised)	--	This study
UPEC0014	*arnA-3xFlag-kan*^{r}	*kan*$^{+}$	This study
UPEC0016	Δ*ppk* (*kan*^{r} excised) *arnA-3xFlag-kan*^{r}	*kan*$^{+}$	This study
UPEC0018	*arnB-3xFlag-kan*^{r}	*kan*$^{+}$	This study
UPEC0020	Δ*ppk* (*kan*^{r} excised) *arnB-3xFlag-kan*^{r}	*kan*$^{+}$	This study
UPEC0022	*arnC-3xFlag-kan*^{r}	*kan*$^{+}$	This study
UPEC0024	Δ*ppk* (*kan*^{r} excised) *arnC-3xFlag-kan*^{r}	*kan*$^{+}$	This study

S3 Table-Tab 2 – Plasmids used in this study. For each plasmid's source, Addgene catalog number and references see online version of the table.

Plasmid	Description	Marker	Temp. sensitivity
pPWSK129	Empty vector	*kan*$^+$	--
pPPK10	pWSK129 *with ppk* under endogenous promoter and terminator	*kan*$^+$	--
pKD46	RED recombineering plasmid for site directed mutagenesis – arabinose inducible	*amp*$^+$	30°C
pSIM6	RED recombineering plasmid for site directed mutagenesis – temperature inducible 42°C	*amp*$^+$	30°C
pSUB11	Template plasmid for creating c-terminal 3xFlag epitope tag using recombineering. Kanamycin selection marker is flanked by FRT recognition sites for excision.	*amp*$^+$, *kan*$^+$	--
pKD4	Template plasmid for using recombineering to delete genes with a FRT flanked kanamycin cassette	*amp*$^+$, *kan*$^+$	--
pCP20	Constitutively expressed FLP recombinase for excision of selection markers flanked by FRT sites	*amp*$^+$, *cam*$^+$	30°C

2.10. Supplemental Data

Please see '*Supporting information*' tab of online article for detailed view of all Supplemental Data files. Supplemental data includes data, statistical values and raw blots used to make figures. The following Supplemental Data files were included with this manuscript publication.

S1 Data. Raw data for volcano plot, all-or-none protein bubble plot and GO term analysis presented in Figs. 1B, 1C and 1E.
See online: https://doi.org/10.1371/journal.pbio.3002558.s011

S2 Data. Raw data for the growth curves and growth curve analysis presented in Figs. 2A-D.
See online: https://doi.org/10.1371/journal.pbio.3002558.s012

S3 Data. Raw data for qPCR analysis presented in Fig. 3G.
See online: https://doi.org/10.1371/journal.pbio.3002558.s013

S1 Raw Images. Uncropped and unadjusted western blot, ponceau S, polyP gel, lipid A profile and spot test images.
See online: https://doi.org/10.1371/journal.pbio.3002558.s014

CHAPTER 3 – MANUSCRIPT #2

Identification of polyphosphate-binding proteins in *E. coli* uncovers targets involved in translation control and ribosome biogenesis

Publication information:
Baijal, K., Kore, B., Abramchuk, I., Denoncourt, A., Han, S., Simms, A., Dagenais, A., Long, A.R., Rudner, A.D., Lavallée-Adam, M., Gray, M.J., and Downey, D. (2025) Identification of polyphosphate-binding proteins in *E. coli* uncovers targets involved in translation control and ribosome biogenesis. Submitted to *mBio*: Out for review.
https://www.biorxiv.org/content/10.1101/2025.02.12.637445v1

Author's contributions:
Conceptualization: K.B., M.D. Methodology: K.B., I.A., B.K. Investigation: K.B., I.A., D.A., S.H., A.S., A.D., A.L. Supervision: A.D.R., M.L.A., M.G.J., M.D. Writing – original draft: K.B., M.D. Writing – review and editing: All authors.

Contributions by figure: Fig 1 (K.B., I.A.,), Fig 2 (K.B., B.K., A.D.), Fig 3 (K.B., B.K., A.D., S., H.), Fig 4 (K.B.), Fig 5 (K.B., B.K.), Fig S1 (K.B., I.A.), Fig S2 (K.B), Fig S3 (K.B., B.K.), Fig S4 (K.B.), Fig S5 (K.B., B.K.).

Identification of polyphosphate-binding proteins in *E. coli* uncovers targets involved in translation control and ribosome biogenesis

Kanchi Baijal[1,2], Brianna Kore[1,2], Iryna Abramchuk[2,3], Alix Denoncourt[1,2], Shauna Han[1,2], Abby Simms[1,2], Amy Dagenais[1,2], Abagail R. Long[4], Adam D. Rudner[2,3], Mathieu Lavallée-Adam[2,3], Michael J. Gray[4], and Michael Downey[1,2*]

1. Department of Cellular and Molecular Medicine, University of Ottawa, Ottawa, Ontario, Canada

2. Ottawa Institute of Systems Biology, University of Ottawa, Ottawa, Ontario, Canada

3. Department of Biochemistry, Microbiology and Immunology, University of Ottawa, Ottawa, Ontario, Canada

4. Department of Microbiology, University of Alabama at Birmingham, Birmingham, Alabama, USA

* Correspondence: mdowne2@uottawa.ca

3.1. Abstract

In many bacteria, polyphosphate kinase (PPK) enzymes use ATP to synthesize polyphosphate (polyP) in response to cellular stress. These chains of inorganic phosphates are joined by high-energy bonds and can reach hundreds of residues in length. PolyP plays diverse functions in helping bacteria adjust to changing environmental conditions. However, the molecular mechanisms underlying these functions are poorly understood. In eukaryotic cells, polyacidic serine- and lysine-rich (PASK) motifs of proteins can mediate binding to polyP chains. Whereas PASK motifs are relatively common in yeast and human cells, we report that these sequences are rare in bacteria commonly used for polyP research. Thus, to identify novel polyP-binding proteins in *Escherichia coli,* we carried out an untargeted screen and identified 7 novel targets with links to translation control and ribosome biogenesis. For two targets, the GTPase activating protein YihI and the ribonuclease Rnr, we mapped the regions of polyP interaction to non-PASK sequences and identified lysine residues critical for binding. We found that deletion of *rnr* suppressed the slow growth phenotype of Δ*ppk* mutants grown on minimal media. Conversely, *ppk* deletion resulted in decreased Rnr protein expression. These phenotypes were dependent on the polyP binding region of Rnr but independent of polyP binding itself, suggesting a complex interplay between PPK and Rnr function in *E. coli.* Overall, our work provides new insights into the scope of polyP binding proteins and extends the connections between polyP and the regulation of protein translation in *E. coli.*

3.2. Introduction

Polyphosphate (polyP) chains are multifunctional polymers composed of three to hundreds of phosphate monomers linked by high-energy phosphoanhydride bonds (1). Although polyP molecules are found broadly across prokaryotic and eukaryotic cells, the mechanisms of polyP synthesis differ between species (2). In bacteria, polyP is synthesized by the polyphosphate kinase (PPK) enzymes, usually in response to cellular stresses such as starvation (3) or treatment with oxidizing agents (4). While some bacteria, such as the Gram negative *Escherichia coli,* have only one PPK enzyme, others express both PPK1 and PPK2 proteins (2). Compared to PPK2, PPK1 is the dominant polyP-synthesizing enzyme in bacteria and preferentially uses ATP as a substrate (5). PPK1 enzymes can also catalyze the reverse reaction to generate ATP from ADP and polyP (6). although the extent to which this activity regulates pools of polyP *in vivo* is uncertain. Alternatively, polyP molecules can be degraded into free inorganic phosphate (Pi) via the action of the exopolyphosphatase PPX, which cleaves phosphoanhydride bonds beginning at the ends of polyP chains (7). Bacterial cells mutated for *ppk* genes show defects in stress and antibiotic resistance (4, 8, 9), reduced biofilm formation (10), and decreased ability to infect host cells (11). These phenotypes underly efforts to develop PPK inhibitors as a new tool in the fight against antimicrobial resistance. PPK enzymes are also present in some lower eukaryotic organisms, including the slime mold *Dictyostelium discoideum*, having been acquired by horizontal gene transfer (12, 13).

In yeast, polyP is synthesized by the vacuole-bound vacuolar transporter chaperone (VTC) complex (14). VTC activity is coupled to polyP transport into the vacuole lumen and its sequestration therein (15). The VTC complex (and presumably polyP) has been linked to ion and phosphate homeostasis (16, 17), cell cycle control (18), microautophagy (19), and the regulation

of protein translation (20). There are no mammalian homologs of VTC or PPK proteins, and the mechanism of polyP synthesis remain poorly defined in higher eukaryotes such as humans (21, 22). There is one report that the mitochondrial F_oF1 ATPase can synthesize polyP (23), but it is unclear if this activity impacts total cellular levels of the polymer. The levels of polyP in human cells are generally thought to be lower than that measured in microorganisms (21), although this assertion has recently been challenged (24). Regardless, diverse roles for polyP have been suggested in mammalian cells including cell signaling (25-27), protein folding (28), energy metabolism (29), and blood clotting (30). While polyP could impact cell function through diverse mechanisms, there is particular interest in roles mediated by its interaction with protein targets (reviewed in (31)). Previous work in eukaryotes has collectively identified dozens of polyP-binding partners (20, 32-37). In bacteria, however, examples of polyP-interacting proteins are less common. In *E. coli*, during stress, polyP serves as a molecular adaptor for the Lon protease to promote the degradation of ribosomal proteins as well as the DnaA replication initiation protein (38, 39). PolyP binding to CsgA plays a role in the regulation of biofilm formation (28). Finally, polyP also binds to the chaperone Hfq to promote its tight interaction with DNA and regulate its phase separation (40). Beyond *E. coli*, the regulation of stress responses by polyP binding proteins is a common theme. For example, in *Helicobacter pylori*, polyP binding to sigma 80 is thought to directly regulate a transcriptional program to help bacteria adapt to starvation (41). Since the deletion of *ppk* homologs in many bacteria impacts diverse molecular pathways (10, 40, 42, 43), we speculated that additional polyP binding proteins remain to be found.

In this work, we report the use of an untargeted proteomic screen to identify 7 novel polyP-binding proteins in *E. coli.* Remarkably, all 7 of these targets are linked to ribosome biogenesis and protein translation. For two proteins, YihI and Rnr (RNase R), we mapped the region of polyP

binding to lysine-rich sequences of the proteins that are important for ribosome- and translation-related functions. Unexpectedly, while Rnr levels are downregulated in Δ*ppk* mutants relative to wild-type controls grown on minimal media, deletion of the *rnr* gene or truncation of the polyP-binding region suppresses the slow growth phenotype of Δ*ppk* mutants under these same conditions. However, mutational analysis revealed that these effects are likely independent of Rnr binding to polyP, suggesting the possibility that polyP impacts Rnr function through both direct and indirect mechanisms. Together, our work extends the scope of polyP-protein interactions in *E. coli* and identifies new avenues for exploration of the PPK-dependent regulation of ribosome biogenesis and protein translation *in vivo.*

3.3. Results

3.3.1. The landscape of PASK-containing proteins in bacteria

In eukaryotic cells, we have been particularly interested in the interaction of polyP with polyacidic-serine and lysine-rich (PASK) motifs of target proteins. In *Saccharomyces cerevisiae*, for example, there are 427 PASK-containing proteins, and work from our group and others have validated polyP binding to 27 of these (20, 36, 44). While interaction between polyP and PASK-containing proteins was originally proposed to be covalent (36), recent work challenges this assertion, suggesting instead a non-covalent interaction with positively charged PASK lysines (34). Regardless of the mechanism at play, we reasoned that PASK-containing proteins would be excellent candidates for novel polyP effectors in bacteria.

To investigate the occurrence of PASK motifs in bacteria, we searched the proteomes of both Gram negative and positive species commonly used in polyP research. We did so using a program we call PASKMotifFinder, which was also recently used to find PASK-containing

proteins in Trypanosomes (45). We defined a PASK motif as a protein subsequence of 20 amino acids containing at least 75% D/E/S/K residues and at least one lysine residue, consistent with the definition we used previously for eukaryotic cells (20). We found that compared to yeast and human cells, PASK-containing proteins are rare in both reviewed (**Figure 1A**) and unreviewed (**Figure S1A**) UniProt database entries (46) from proteomes of bacterial species commonly used for polyP research.

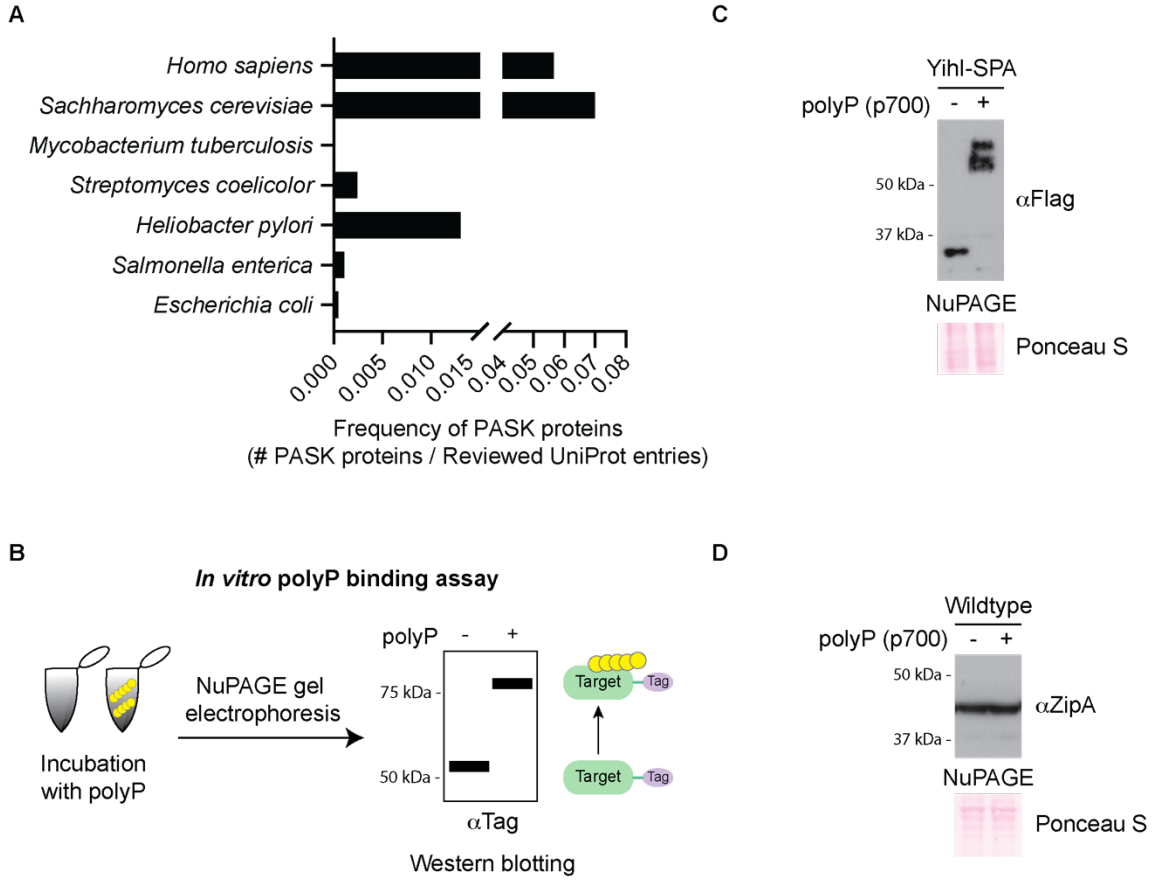

Figure 1. Characterization of PASK sequences in *E. coli.* (A) Frequency of PASK motifs in bacteria. The number of proteins containing 1 or more PASK motifs (75% D/E/S/K content with at least one lysine within a 20 amino acid window) from reviewed proteomes of the indicated species were normalized by the total number of reviewed UniProt entries of each species. **(B)** Schematic of the *in vitro* polyP binding assay. Whole cell extracts incubated in the absence or presence of synthetic polyP (p700) were resolved using a Bis-Tris gel (sold under the name NuPAGE) electrophoresis. Target proteins were visualized by western blotting using an antibody towards an epitope tag or the endogenous protein. Proteins that have slower migration in the presence of polyP compared to in its absence are thought to bind polyP. **(C-D)** *In vitro* polyP

binding to (C) YihI-SPA and (D) ZipA. Assays were conducted as described in B. In both cases, samples were resolved using NuPAGE and transferred to PVDF. YihI-SPA and ZipA were detected using anti-Flag or anti-ZipA antibodies, respectively. Ponceau S was used to show that samples migrated equally. Images are representative of results from ≥3 experiments.

3.3.2. *E. coli* YihI is a novel polyP-binding protein

We focused on the only two PASK-containing proteins in *E. coli*, ZipA and YihI, that were identified using PASKMotifFinder. ZipA is an essential protein required for cell division (47), and YihI is an activating protein for the essential GTPase Der (48). Together, these two proteins represent 0.05% of the total proteome – a stark contrast to the situation in *S. cerevisiae*, where the fraction of PASK-containing proteins is 7.3% (20). To determine if ZipA and YihI interact with polyP, we looked for polyP-induced electrophoretic shifts (hereafter 'polyP shift') on bis-tris polyacrylamide gels, which are sold commercially under the NuPAGE brand name (**Figure 1B**). This technique has previously been used to characterize polyP binding to PASK motifs (20, 34, 36, 49). To conduct these *in vitro* polyP binding assays, we incubated whole cell extracts from SPA-tagged and wild-type strains with polyP of 700 units in length (p700). The YihI-SPA fusion protein was detected using an anti-Flag antibody. In contrast, for ZipA detection we used a commercially available antibody that we first validated in **Figure S1B.** In this assay YihI-SPA, but not ZipA, demonstrated the characteristic polyP shift indicative of polyP binding (**Figure 1C and 1D**) and this effect was dependent on the concentration of polyP used (**Figure S1C**).

3.3.3. Characterization of the YihI PASK-like motif

Next, we aimed to further investigate how the YihI PASK was contributing to polyP binding. Previous work showed that mutation of lysine residues to arginine (K-R) abolished the polyP shift on NuPAGE gels for other PASK-containing proteins (20, 36, 50, 51). Therefore, we used GST-

YihI fusion proteins to test if this held true for YihI. Our bioinformatics analysis located the PASK motif to the C-terminus of the YihI protein (**Figure 2A**). Surprisingly, mutation of the two lysine residues in this region failed to prevent polyP interaction, suggesting that YihI does not bind to polyP via its defined PASK motif (**Figure 2B**). We noticed that the N-terminus of YihI is also lysine-rich (**Figure 2A**). Mutation of 7 N-terminal lysines to arginine severely abrogated the polyP shift (**Figure 2B**). Therefore, we conclude that YihI interacts with polyP primarily through this region. A YihI mutant where all lysines were replaced with arginine residues completely lost its ability to bind polyP as judged by NuPAGE analysis (**Figure 2B**), suggesting that other lysines may also contribute to polyP binding, at least in the absence of those in the N-terminus. While the N-terminus does not fit the formal definition of a PASK motif, it does contain a 3 serine and 5 acidic residues in addition to 7 lysine residues required for polyP interaction. Therefore, we refer to this region as 'PASK-like'. Notably, both the N- and C-termini of YihI are disordered (**Figure 2C**), which is fitting for the molecular chaperone and scaffold-like functions of polyP (4, 52). Additionally, the N-terminus of YihI may play regulatory functions. For example, truncation mutants lacking residues 1-45 show enhanced binding to Der and activation of Der's GTP hydrolysis activity (48), suggesting an overall inhibitory role for the N-terminus of YihI. We speculate that polyP binding may regulate these functions *in vivo*.

Previous mutagenesis work on yeast targets demonstrated that serine residues in PASK motifs are not required for polyP binding (36). In contrast, mutation of acidic residues (aspartic and glutamic acid) to alanine or leucine prevented polyP interaction (53). In both cases, analogous N-terminal mutations resulted in a similar impact on polyP binding to GST-YihI (**Figure 2D**). To test if polyP binding depends on the negative charge of these acidic residues, we also mutated aspartic and glutamic acids to asparagine and glutamine, respectively. With these changes, GST-

YihI was still able bind to polyP (**Figure 2D**), suggesting that negative charge *per se* is not required for polyP interaction, at least for this 'PASK-like' region of YihI (**See Discussion**).

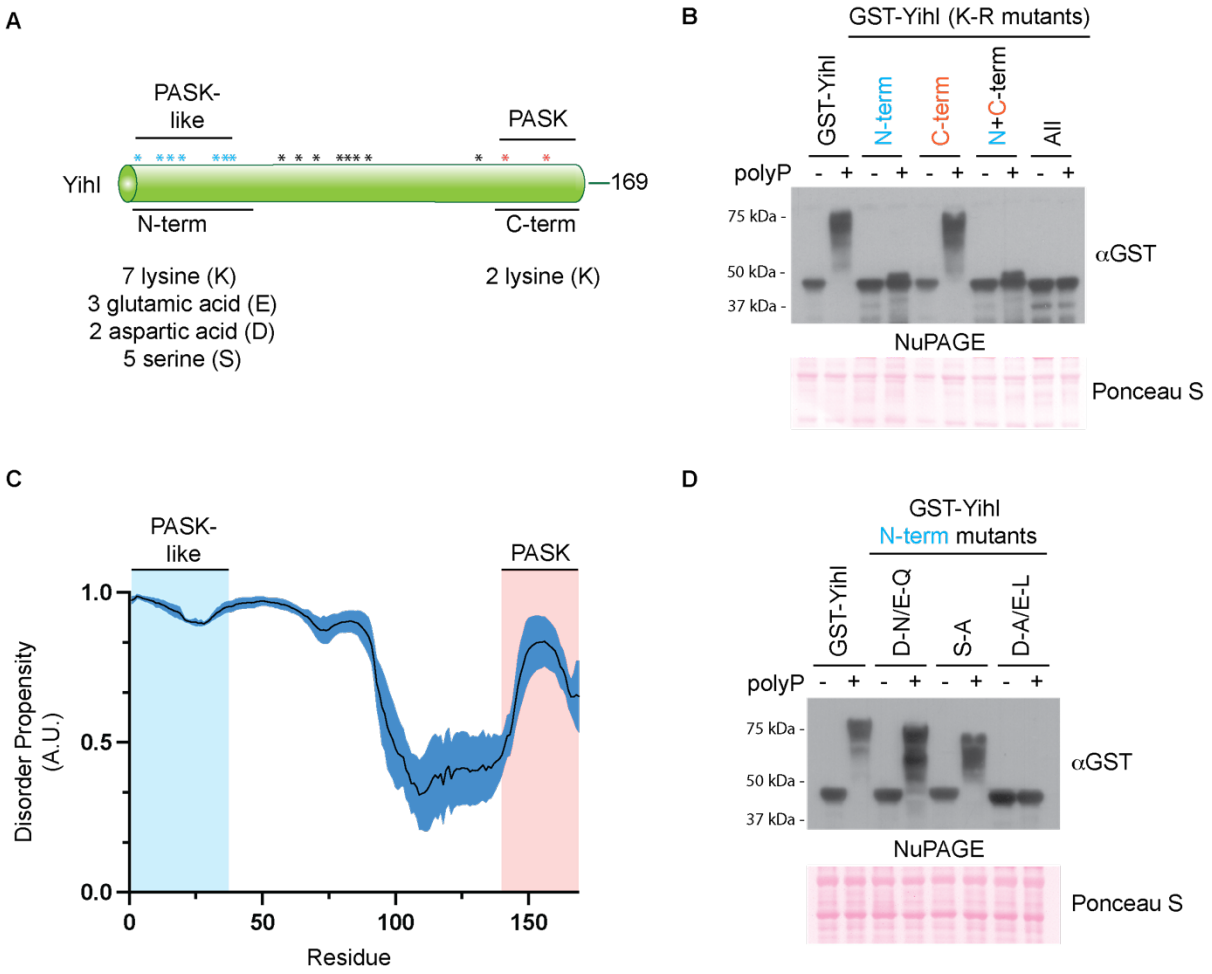

Figure 2. PolyP binds a disordered lysine-rich region of YihI. (A) Schematic and amino acid distribution of full-length YihI (169 residues total). YihI has a C-terminal PASK domain and a N-terminal PASK-like domain. The indicated amino acids distributed across the PASK or PASK-like domains were targeted for mutagenesis experiments. An asterisk (*) is used to display the distribution of PASK (orange), PASK-like (blue) and other lysine (black) residues within YihI. **(B)** PolyP binds primarily via the N-terminus of YihI. *In vitro* polyP binding assay was conducted (as described in Figure 1B) using whole cell extract expressing wild-type or lysine to arginine (K-R) mutated GST-YihI. **(C)** Disorder propensity of YihI shows that the N- and C-termini are highly unstructured (>0.5). Graph shows the average (±standard error) of computational prediction scores, represented as arbitrary units (A.U.), that were obtained using NetSurfP-3.0 (95), Metapredict (96) and IUPred3 (97). **(D)** The N-terminal PASK amino acids play a structural role in promoting polyP binding. Various GST-YihI mutants were grown and analyzed as described in (B). D-N/E-Q = aspartic acid to asparagine/glutamic acid to glutamine; S-A = serine to alanine;

D-A/E-L = aspartic acid to alanine/glutamic acid to leucine. For both (B) and (D), samples were resolved using NuPAGE, transferred to PVDF and probed using an anti-GST antibody. Ponceau S was used to show that samples migrated equally. Images are representative of results from ≥3 experiments.

3.3.4. Novel non-PASK polyP-binding proteins in *E. coli*

To extend our search for polyP binding proteins in bacteria, we took advantage of two sets of *E. coli* strains where individual open-reading frames are expressed as fusion proteins with C-terminal SPA (781 strains) or TAP (243 strains) epitope tags (**Supplemental Table 1**) (54). We generated protein extracts from these strains and carried out *in vitro* polyP binding assays, as described above (**Figure 1B**). The SPA tag (55) contains a 3Flag epitope and the TAP tag has a protein A moiety that is recognized by most mouse antibodies. Therefore, we used a mouse anti-Flag antibody to detect both SPA and TAP targets after NuPAGE gel electrophoresis and western blotting.

After accounting for redundancy between the two epitope-tagged sets and proteins that were not detected by western blotting, we evaluated polyP binding for a total of 589 unique proteins using this assay (**Figure 3A** and **Supplemental Table 1**). Seven of these (1.2% of total proteins screened) shifted on NuPAGE gels in the presence of polyP (**Figure 3B**). With 4288 predicted open reading frames in *E. coli*, we anticipate at least ~50 proteins from *E. coli* would undergo a polyP shift in this assay. This value is likely an underestimate, as work with human polyP interactors demonstrated that not all undergo polyP shifts on NuPAGE gels (32). Indeed, we observed that the Lon protease, a well-characterized polyP binding protein from *E. coli* (38, 39), does not shift on NuPAGE gels even in the presence of high concentrations of polyP (**Figure S2**).

Intriguingly, all 7 polyP binders identified have links to ribosome assembly or function (**Figure 3C**). This finding is consistent with the enrichment of this same category in our yeast polyP-PASK interaction study (20), as well as the remodelling of nucleoli, the site of ribosome

biogenesis, in human cells ectopically expressing bacterial PPK to produce high levels of polyP (56). Altogether, this suggests the possibility of evolutionarily conserved roles for polyP in the regulation of translation.

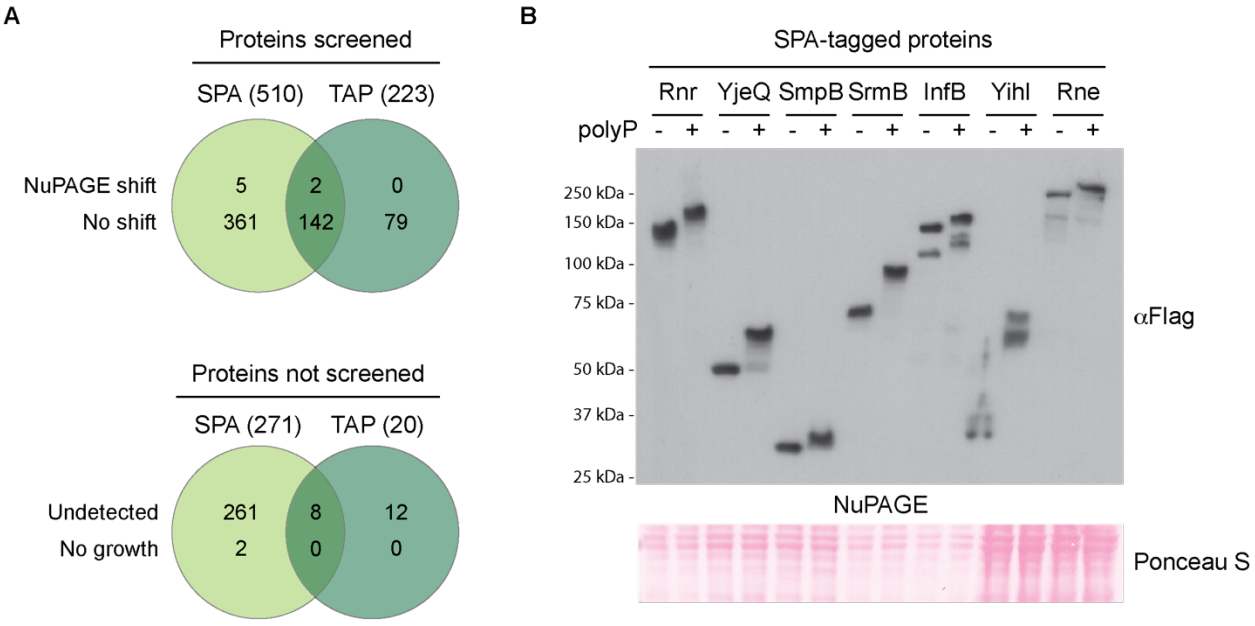

C

Protein	Function
Rnr	Exoribonuclease, maturation of structured RNAs and rescue of stalled ribosomes
YjeQ	GTPase involved in later stages of 30S ribosomal subunit maturation
SmpB	Marks proteins synthesized by stalled ribosomes for degradation, interacts with Rnr
SrmB	DEAD-box RNA helicase invovled in early stages of 50S ribosome subunit assembly
InfB	Translation initiation, and stabilization of 50S and 70S ribosomes on mRNA
YihI	GTPase activating protein, potentially involved in 50S ribosome biogenesis
Rne	Endoribonuclease involved in processing of rRNA, tRNA, and other RNAs

Figure 3. A screen for novel polyP-binding proteins in *E. coli.* (A) A total of 589 unique *E. coli* proteins were screened for polyP binding. Together, the SPA and TAP collection sets contain a total of 1024 strains with epitope tags encoded at the chromosomal loci of relevant open reading frames. Of these, 152 proteins are redundantly tagged between the SPA and TAP collection sets, and 291 (283 non-redundant) could not be screened for polyP binding. **(B)** Seven novel polyP binding proteins were identified by the screen. Proteins that shifted from the screen were reconfirmed using the *in vitro* polyP binding assay. Samples were resolved using NuPAGE, transferred to PVDF and probed using an anti-Flag antibody which detects the SPA tag. Ponceau S was used to show that samples migrated equally. Images are representative of results from ≥3 experiments. **(C)** The 7 polyP binding proteins are involved in ribosome biogenesis or translation processes. General descriptions of each protein's functions are provided.

3.3.5. Interaction of target proteins with endogenous polyP

To test if native polyP was also able to bind our newly identified targets, we switched SPA-tagged strains grown in LB media to MOPS minimal media to induce nutrient starvation and polyP accumulation prior to protein extraction and NuPAGE analysis. Out of the 7 targets, SrmB-SPA, and YihI-SPA consistently displayed an obvious MOPS-induced polyP shift while Rnr-SPA did so occasionally (**Figure S3A**). This result is perhaps surprising considering that the chain lengths of polyP that accumulate during MOPS appear to be larger than the p700 chains used in our *in vitro* assays (**Figure S3B**). We speculate that long-chain bacterial polyP is organized *in vivo* in a manner that in some instances hinders its interaction with protein targets. In support of this idea, we found that a large fraction of polyP that accumulates during MOPS treatment is resistant to ectopically expressed yeast Ppx1 (*Sc*Ppx1), a highly active exopolyphosphatase (**Figure S3C**). This finding is reminiscent of the situation in mammalian cell culture where *Sc*Ppx1 treatment results in a partial, but not complete, loss of the polyP signal in nuclear polyP foci detected using the PPBD-Xpress tag probe (57). In contrast, *Sc*Ppx1 overexpression in yeast appears to completely degrade the non-vacuolar pool of polyP synthesized by *E. coli* PPK expression (58).

3.3.6. Functional interaction between *rnr* and *ppk*

We reasoned that some genes encoding polyP-interacting proteins might display genetic interactions with Δ*ppk* under conditions where polyP is important for cell growth or viability (**Figure S4A**). As previously reported and consistent with work from other groups (3, 59), we found that Δ*ppk* mutants displayed a slow growth phenotype on MOPS minimal media relative to wild-type controls (**Figure 4A and Figure S4A**). This phenotype is likely attributable to an extended lag phase and decreased doubling time in Δ*ppk* mutant cells (42). We observed that

deletion of *rnr* does not impact polyP levels in wild-type cells (**Figure S4B**) but consistently improved the growth of Δ*ppk* mutant cells on MOPS media (**Figure 4A & S4A**). While the rescue was not complete, we conclude that in Δ*ppk* mutants, one or more activities of Rnr hinder cell growth during nutrient limitation.

Rnr (also referred to as VacB in literature) is a 3' to 5' exoribonuclease that plays a role in maintaining RNA homeostasis in cells (60, 61). It primarily targets rRNAs and structured RNAs, including RNA duplexes, but not DNA (60, 62-64). Rnr has a complex role *in vivo*. It is thought to play a role in RNA turnover and the recycling of excess rRNA during stress, such as starvation, cold shock, and stationary phase growth (65-67). It has also been proposed to participate in trans-translation through its role in the maturation of tmRNA (68), which binds SmpB (another polyP binding protein identified by our screen) (69) and is required for tagging abnormal peptides and releasing stalled ribosomes (70-72)**.** Additionally, in an SmpB-dependent manner (73), Rnr degrades 'non-stop' transcripts that result in ribosome stalling (72, 74).

These complex functions and interactions of Rnr are mediated by various domains that work together in a coordinated manner. For example, Rnr possesses two cold shock domains with helicase activity (75), cold shock specific functions (75), and a role in substrate binding (62), as well as a catalytic core termed the ribonuclease domain where reduction reactions take place (62, 76) (**Figure 4B**). It also possesses S1 and basic domains that are involved in protein stabilization (77), substrate positioning (62), and ribosome binding (78) (**Figure 4B**). Intriguingly, the basic domain is both disordered (**Figure 4C**) and lysine-rich, hinting at a possible role in polyP binding.

Figure 4 and Figure 4 – Figure legend on the next page.

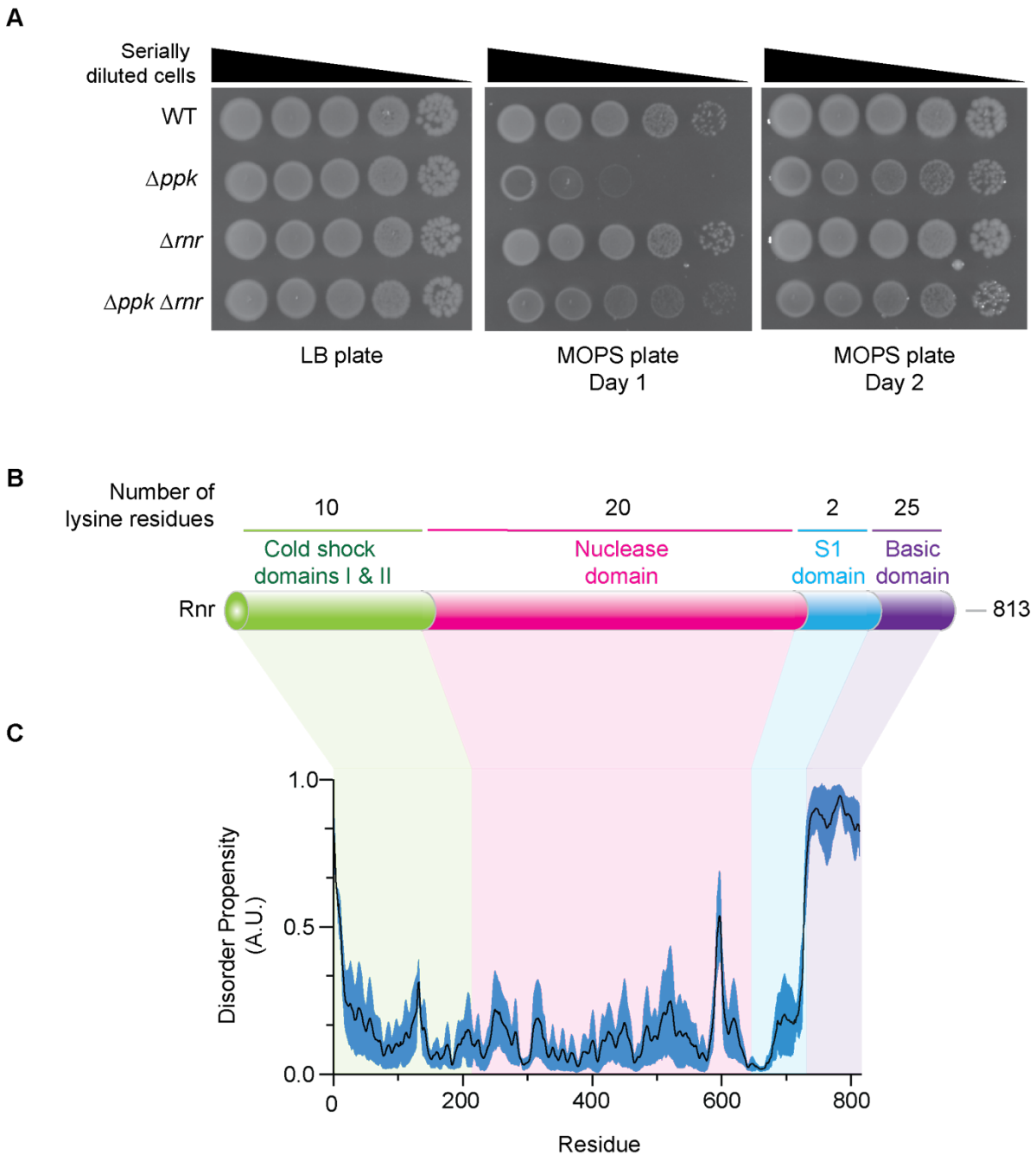

Figure 4. Rnr is functionally regulated by polyP. (A) Loss of *rnr* partially rescues the slow growth phenotype of *ppk* mutants. The indicated strains were serially diluted and spotted on LB or MOPS plates and incubated at 37°C as indicated. Images are representative of results from ≥3 experiments. **(B)** Schematic of the functional domains of full-length Rnr (813 residues total). Rnr has 2 cold shock domains (residues 1-216), a nuclease domain (residues 217-643), an S1 domain (residues 644-730) and a basic domain (residues 731-813). **(C)** The basic domain of Rnr has a high disorder propensity (>0.5). Graph shows the average (±standard error) of computational prediction scores, represented as arbitrary units (A.U.), that were obtained using NetSurfP-3.0 (95), Metapredict (96) and IUPred3 (97).

3.3.7. Complex regulation of Rnr by PPK and polyP

To map the region of Rnr required for interaction with polyP, we expressed its individual domains as GST-fusion proteins and carried out *in vitro* polyP binding assays as described for YihI. These experiments demonstrated that the C-terminus of the protein (S1+basic domain) was responsible for polyP binding (**Figure S5A**). Indeed, deletion of this region from chromosomally expressed Rnr (detected using an anti-Rnr antibody, validated in **Figure S5B**), resulted in a loss of the polyP shift (**Figure 5A**), as did mutation of 27 S1+basic lysine residues to arginine (K-R) (**Figure 5B**). Since NuPAGE assays determine protein-polyP interactions under largely denaturing conditions, we also tested if polyP interacts with Rnr in its folded state. To do this, Rnr-3Flag was immunoprecipitated under non-denaturing conditions and incubated with polyP prior to washing and elution with sample buffer. In this experiment, unbound polyP is expected to be removed prior to NuPAGE analysis (**Figure S5C**). Immunoprecipitated Rnr incubated with polyP shifted on NuPAGE gels after washing, suggesting that polyP can also bind to Rnr when folded (**Figure S5C**).

In growth assays, deletion of the Rnr S1+basic domain, but not the basic domain on its own, improved growth of Δ*ppk* mutants on MOPS (**Figure 5C** and **Figure S5D**), suggesting that together, these regions mediate toxicity in MOPS media in the absence of polyP. If polyP binding to the S1+basic domain functions to promote growth of wild-type cells on MOPS media, we predict that under these conditions, wild-type cells expressing the K-R mutant should display a slow growth phenotype, similar to Δ*ppk* mutants. However, the K-R mutant grew similarly to wild-type cells on MOPS media (**Figure 5C**).

Next, we investigated if polyP-binding could impact Rnr expression. In exponential phase Rnr is rapidly degraded as a result of acetylation at lysine544 (K544; within the S1 domain) (79).

This degradation is thought to be mediated through an interaction with SmpB via the Rnr C-terminus that results in recruitment of HslUV and Lon proteases (77, 80). In contrast, Rnr is stabilized during stationary phase and under stress conditions (81), and its activity increases upon carbon, nitrogen and phosphorus starvation (66). Therefore, since protein binding to polyP has been shown to modulate protein degradation (39), we evaluated Rnr expression in wild-type and Δ*ppk* mutants during nutrient starvation in MOPS, where polyP levels in wild-type cells are normally high. We found that Rnr levels were reproducibly decreased in Δ*ppk* mutants (**Figure 5D**). However, like the genetic interactions described above, this effect was not directly mediated by polyP binding to Rnr, because truncation and K-R mutants that failed to interact with polyP (**Figure 5A** and **5B**) still showed decreased expression in the Δ*ppk* mutant background (**Figure 5D**). Therefore, we conclude that PPK plays an indirect role in Rnr expression while the role of Rnr's polyP binding remains unclear (**Figure 5E**).

Figure 5 and Figure 5 – Figure legend on the next page.

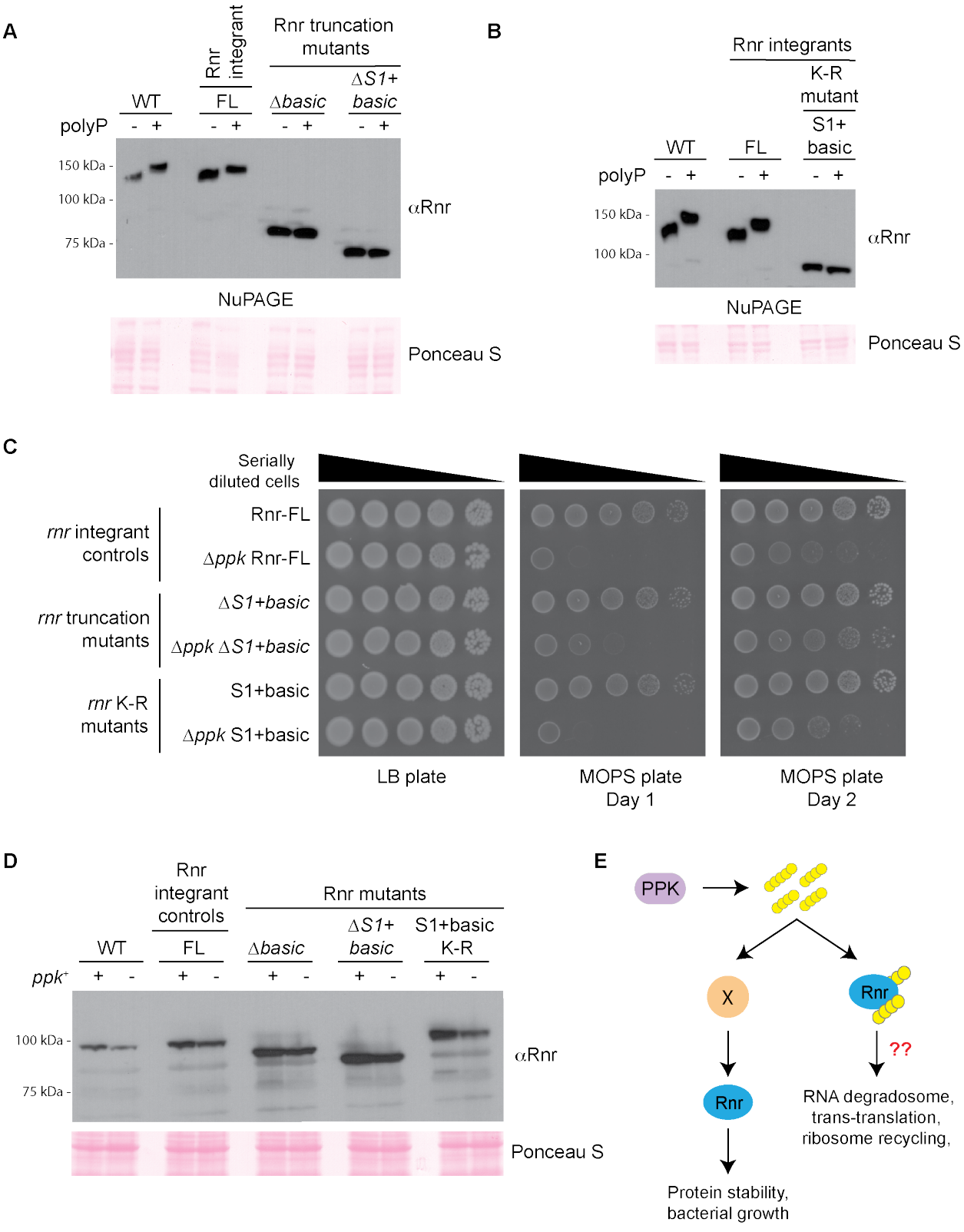

Figure 5. The Rnr S1 and basic domains are involved in polyP binding. (A-B) The characteristic NuPAGE shift is abrogated when the S1 and basic domains of Rnr are (A) truncated

or (B) mutated. An *in vitro* polyP binding assay was conducted using the indicated chromosomally truncated or lysine to arginine (K-R) mutated Rnr strains. FL represents the wild-type Rnr protein expressed in a background that is isogenic to the truncated and mutated strains (see methods *Bacterial strains* section for details on how these strains were constructed). Samples were resolved using NuPAGE, transferred to PVDF and probed using an anti-Rnr antibody. Ponceau S was used to show that samples migrated equally. Images are representative of results from ≥3 experiments. **(C)** Truncation but not K-R mutation of the S1+basic polyP-binding domain partially rescues the slow growth phenotype of *ppk* mutants. The indicated strains were serially diluted and spotted on LB or MOPS plates and incubated at 37°C as indicated. Images are representative of results from ≥3 experiments. **(D)** Expression of wild-type and mutant Rnr is downregulated in *ppk* mutants compared to wild-type cells during growth in MOPS. FL is as described for (A). Whole cell extract from wild-type and mutant Rnr strains that were grown in LB media then exposed to nutrient down shift for 3 hours were resolved using 10% SDS-PAGE, transferred to PVDF and probed using an anti-Rnr antibody. Ponceau S was used to show equal loading. Images are representative of results from ≥3 experiments. **(E)** Model of how polyP impacts Rnr function. PolyP synthesized by PPK can indirectly impact Rnr stability through an unknown pathway. PolyP may also bind Rnr directly to modulate a variety of functions related to translation control and mRNA metabolism.

3.4. Discussion

In this work, we have identified 7 novel polyP binding proteins in *E. coli* and provided additional evidence to support an evolutionarily conserved role for polyP in the regulation of protein translation.

Previous work in eukaryotic cells has demonstrated that PASK motifs, often found in predicted disordered regions, are a frequent site for polyP binding. To our surprise, PASK-containing proteins are rare in bacterial models commonly used for polyP research. Of the 7 proteins that we identified as polyP binders, only YihI has a PASK motif that fits our previous definitions of 75% D/E/S/K with at least one lysine in a 20 amino acid window. However, this motif makes at most a minor contribution to YihI's polyP binding activity. Instead, we mapped this function to the N-terminus of the protein which we refer to as PASK-like. Similar to what was described for PASK motifs, mutation of YihI's N-terminal lysine residues to arginines abolished polyP interaction as judged by the NuPAGE shift assay, whereas mutation of serines to alanines had no effect. Since arginine holds a greater positive charge than lysine, these experiments

demonstrate that concentration of positive charge is not the sole determinant of polyP binding. On the other hand, mutation of the acidic residues, glutamic and aspartic acid to leucine or alanine, abolished polyP interaction. However, mutation of these same residues to uncharged glutamine and asparagine had no effect. Our interpretation of these data is that the negative charge of the PASK-like region is dispensable for polyP interaction. One possibility is that the glutamic and aspartic acid residues instead provide a structural context for polyP binding with surrounding lysine residues and that this unique context is preserved with the glutamine and asparagine substitutions. We surmise that the impact of these substitutions will also hold true for canonical PASK motifs in proteins such as yeast Nsr1 and Top1 (36), but this remains to be tested. Indeed, it is currently unclear if there is a tangible difference between PASK and PASK-like motifs in the way that they interact with polyP molecules. In addition to PASK motifs, polyP has also been shown to bind other linear motifs namely polyHistidine (35) and polyLysine stretches (34). However, these motifs do not appear to be present in the targets that we identified. Certainly, we cannot discount the possibility that other linear polyP interacting motifs exist, and it will therefore be important to systematically map the binding region for each target.

A limitation of our work is that our detection of polyP-protein interactions relied on the previously described NuPAGE 'polyP shift' assay. Not all polyP binding proteins shift upon NuPAGE analysis in the presence of polyP, as demonstrated with our experiments using purified Lon protease. As such, we have no doubt that additional polyP-binding proteins in *E . coli* remain to be identified. In particular, polyP interactions that require folded protein structures would be missed in our assay, as these would likely be denatured during NuPAGE analysis. On the other hand, the ability of targets identified here to interact with polyP under denaturing conditions suggests polyP may play a role in their folding or re-folding after cellular stress. Indeed, this

chaperone-like activity for polyP has been described previously for the *E. coli* CsgA protein involved in biofilm production (28), and globally to stabilize proteins that become insoluble in response to oxidative stress (4).

Our work adds to a growing body of evidence for an evolutionarily conserved role for polyP in regulating protein translation. Previously, Δ*ppk* mutant strains were found to have disrupted polysome profiles (82). Further, polyP promotes translation fidelity *in vitro* and Δ*ppk* mutants have increased mistranslation *in vivo* (82). In this regard, it is noteworthy that all of our newly identified polyP-binding proteins are linked in some way to ribosome biogenesis or translational control. We speculate that polyP binding to these proteins may therefore play a role in reprogramming translation during stress. Alternatively, polyP may help to stabilize critical regulators of translation so that they are ready to act upon a return to favourable growth conditions. Most of our new targets are highly conserved across other bacterial species (**Supplemental Table 2**), and in some cases are expressed in pathogens (83-87). Therefore, it will be important to test whether polyP interacts with their homologs in these species.

In addition to identifying novel polyP-binding proteins linked to translation, we found evidence for a bidirectional regulation between PPK and Rnr. Namely, while PPK promotes Rnr expression during starvation, Rnr is also detrimental for growth in Δ*ppk* mutant cells grown on MOPS media. We propose a model where Rnr's various molecular functions must be carefully balanced during cellular stress, and that this balance is lost in the absence of PPK. Importantly, mutation of the S1+basic domain lysine residues of Rnr to prevent polyP binding did not impact Rnr protein levels or growth characteristics in an otherwise wild-type background. The simplest explanation for these observations is that the described bidirectional regulation is indirect in that

it does not depend on the Rnr-polyP interaction. Alternatively, the regulation may become relevant under situations where growth is already compromised, as is the case in Δ*ppk* mutant cells.

Since polyP binds to Rnr in both its denatured and folded states, it is possible that polyP impacts Rnr biology at multiple levels, and additional work will be required to tease out specific molecular functions. For example, based on the C-terminal binding of polyP, it may disrupt functions associated with the S1 and basic domains, which includes an intrinsically disordered segment. As observed for Nsr1 and Top1 in yeast (36), polyP binding may disrupt the interaction between tmRNA-SmpB and Rnr, which is mediated via the basic domain (77). This in turn could play a role in stabilizing Rnr in some contexts, potentially through cross regulation with a previously reported acetylation at K544 that is known to promote Rnr turnover (79). Additionally, polyP interaction with the S1 domain could alter Rnr substrate selectivity (64). Very likely, polyP binding to Rrn is part of a broader function for polyP in adapting to cellular stress. We note, for example, that Rnr also plays a role in the RNA degradosome in conjunction with Rne (88), another polyP-binding protein identified in our screen. As such, we do not discount the possibility that dramatic phenotypes would only be observed after mutating polyP binding motifs on multiple proteins involved in the processes of ribosome biogenesis or translation.

In vivo, local subcellular distribution of polyP may govern whether a protein interacts with it. Moreover, we demonstrate here that a large fraction of intracellular polyP is resistant to degradation via overexpression of the highly active yeast Ppx1. As such, *in vivo* some polyP may be inaccessible to potential protein interactors. It is tempting to speculate that this property is dictated by the ability of polyP to phase separate *in vivo* (40) and the investigation of this property and its relationship to protein-polyP interactions is deserving of further attention. Another important area for future investigation will be to determine how polyP-protein interactions are

reversed upon return to normal growth conditions. We speculate that bacterial PPX enzymes may play a critical role in this process. Indeed, this activity has been demonstrated previously for yeast Ppx1(36). Alternatively, in the presence of ADP, PPK itself may drive the conversion of protein-bound polyP to ATP. This would relieve polyP dependent modulation of translation, while providing ATP pools required for renewed efforts towards ribosome biogenesis and growth.

3.5. Experimental Procedures

General information about strains and plasmids

All bacterial strains and plasmids, as well as their sources, used in this work are listed in **Supplemental Table 3**. Plasmids were sequenced using Sanger sequencing (Genome Quebec) or Nanopore sequencing (Plasmidsaurus). All plasmids (**Supplemental Table 3**) generated for this work will be made available from Addgene (www.addgene.com) upon final publication. The sequences of oligonucleotides used for cloning or genetic manipulations are available upon request.

Bacterial strains

Unless otherwise indicated, the MG1655 strain background was used for all experiments. All lab-generated strains used in this study are listed in **Supplemental Table 3**. The Dharmacon Collection of SPA- and TAP-tagged *E. coli* strains (DY330 background) were obtained from Horizon Discovery and have been described previously (54). The strains list for both of these collection sets can be found online under the *Resources* tab (https://horizondiscovery.com/en/non-mammalian-research-tools/products/e-coli-tagged-orfs#description).

Chromosomally-tagged and deletion strains were generated using the lambda-red homologous recombination system using pKD46 (induced with 0.2% arabinose) (89) or pSIM6 (induced with a temperature shift to 42 °C for 12 minutes) (90). Respectively, the kanamycin deletion and 3Flag-kanamycin tagging cassettes were amplified from pKD4 (89) and pSUB11 (91) plasmids. Rnr truncations were made by using forward primers that introduced a premature stop codon and led to recombination that deleted the end of the gene, replacing the region with the KanR selection cassette. For the basic and S1+basic mutant, a stop codon was introduced after residue 2190 and 1929, respectively. An FRT scar was also introduced at the end of full-length Rnr to control for

polar effects (92). This strain is referred to as full-length (FL) and is isogenic to the *rnr* truncation mutants (ΔS1+basic and Δbasic). For genetic experiments, cells were made electrocompetent and plasmids or double-stranded DNA used for recombineering were transformed into cells via electroporation (93). Antibiotics were added when appropriate: kanamycin (50 μg/ml) and ampicillin (100 μg/ml). As needed, the resistance markers used for selection of positive transformants were removed using the pCP20 FLP-recombinase system[94]. Epitope tag insertions and deletions were confirmed by PCR, followed by western blotting.

Plasmids

(1) YihI plasmids

The GST-YihI wild-type and mutant sequence plasmids were purchased from GenScript. The respective YihI sequences were cloned between the EcoRI and NotI sites. These vectors are called: pYihI, pYihI-N-term K-R, pYihI-C-term K-R, pYihI-N+C-term K-R, pYihI-All K-R, pYihI-N-term D-N/E-Q, pYihI-N-term S-A, pYihI-N-term D-A/E-L.

(2) Rnr plasmids

The Rnr cold shock domains I and II (residues 1-216), nuclease domain (residues 217-643) and S1+basic domains (residues 644-813) were cloned into pGEX4T1 between the EcoRI and NotI restriction sites using Gibson Assembly Cloning. These vectors are called pRnr-CSD, pRnr-ND and pRnr-S1BD, respectively.

(3) ScPpx1 plasmid

The *ScPPX1* plasmid was constructed by amplifying the S. cerevisiae *PPX1* sequence from pET-15b-His-*PPX1* and cloning it between EcoRI and SalI sites of pBAD18. The empty and cloned vectors are called pBAD18 and p*ScPPX1*, respectively.

Bacterial growth conditions

(1) General growth conditions

SPA- and TAP-tagged strains[54] (DY330 background) were grown at 30°C while all other strains in the MG1655 background were grown at 37°C. Unless otherwise specified, strains were grown in LB media.

(2) Nutrient downshift

Starvation experiments were performed as previously described[42]. Briefly, overnight cultures grown in LB were diluted to 0.1 OD_{600} in LB media and grown to mid-exponential phase (~0.6 OD_{600}) before being switched to MOPS minimal media. Cells were pelleted and washed once with 1x PBS to remove trace LB before resuspension in freshly prepared MOPS media (1x MOPS – Teknova, 0.1 mM K_2HPO_4, 0.4% glucose). Cells were grown in MOPS media for the indicated amount of time. Typically, we see peak polyP accumulation after 3 hours in MOPS media. For western blotting and polyP extractions, 3 and 5 OD_{600} equivalent of cells were harvested by centrifugation, respectively.

PASKMotifFinder Software

The PASKMotifFinder software used to search for PASK motifs was implemented in Java and is platform independent. The code is open source and freely available at the following GitHub repository: https://github.com/LavalleeAdamLab/PASKMotifFinder/. The software uses a sliding window approach to scan subsequences of 20 amino acids throughout the proteome and identifies regions where D, E, S and/or K amino acids make up at least 75% of the window (i.e. 15 amino acids), and contain at least one K. The program was run on the *E. coli* (strain K12) proteome UP000000625, and other proteomes listed in **Supplemental Data 1**. All proteomes were downloaded on January 13, 2025 from UniProt release version 2024_06.

In vitro polyP binding assay

In vitro assays were conducted using whole cell extract or purified proteins.

Whole cell extract was prepared as described under *Western blotting – protein extraction* using 200 µL of overnight culture. For the polyP binding assay, 10 µL of whole cell extract was incubated at room temperature in the presence of 10 mM sodium phosphate pH 6.0 (control matching the pH of the polyP) or p700 (Kerafast) polyP for 20 minutes. For the concentration shift assay, control reactions contained sodium phosphate matching the highest concentration of polyP used. All control (minus polyP) and reaction samples were boiled for 10 minutes and loaded onto a NuPAGE Bis-Tris Mini Protein Gel, 4-12%, 1.5 mm. See methods on *Western blotting* for the subsequent steps used for visualizing proteins.

Purified Rts1 and Lon protease (purchased from SinoBio) were used for the *in vitro* polyP binding assay, as described previously (20**).** Briefly, the purified proteins (0.032 mg of each) were incubated at room temperature with increasing concentrations of p700 (5, 10, 15 and 20 mM) or 20 mM sodium phosphate pH 6.0 (negative control) for 20 minutes. All control (minus polyP) and reaction samples were boiled for 10 minutes and loaded onto a NuPAGE Bis-Tris Mini Protein Gel, 4-12%, 1.5 mm. The gel was stained using the Invitrogen Colloidal Blue Staining Kit.

Western blotting

(1) Protein extraction

As indicated, 200 µL of an overnight culture or 1.5-3 OD_{600} equivalents of cells were harvested by centrifugation for analysis by western blotting. Cells were resuspended in 100 µL of sample buffer (800 uL sample buffer stock (160 mM Tris-HCl pH 6.8, 30% glycerol, 6% SDS, 0.004% bromophenol blue) + 100 uL 1 M DTT, 100 1.5 M Tris-HCl pH 8.8), boiled for 10 minutes and then centrifuged at 13,000 rpm for 2 minutes to remove insoluble material. The supernatant was

transferred to a fresh tube. Typically, to normalize for equal loading 10 µL and 13 µL of extract from wild-type and Δ*ppk* mutant cells were loaded per blot, respectively.

(2) Gel electrophoresis and transfer

NuPAGE or SDS-PAGE gels were used to resolve protein extracts. SDS-PAGE was primarily used to visualize protein levels while NuPAGE gels were solely used to detect polyP dependent shifts of our candidate proteins. After electrophoretic separation, proteins were transferred onto PVDF membranes and visualized by western blotting using the indicated antibodies. SDS-PAGE and NuPAGE buffer recipes have been described previously[20].

(3) Western blotting

Membranes were blocked for 20 minutes with shaking using 5% milk in TBST and washed 3 times for 10 minutes after both primary and secondary antibody incubations. See **Supplemental Table 4** for incubation conditions for each antibody. Note: both SPA- and TAP-tags were detected using an anti-Flag antibody, which was then detected using a goat anti-mouse secondary coupled to HRP. After probing, target proteins were detected using Immobilon Western Chemiluminescent HRP Substrate and exposure to autoradiography film from Thomas Scientific. Scanned images were opened in Photoshop, and linear brightness and contrast adjustments were made to lighten the image background. Adjustments were applied evenly across the entire image prior to cropping and labelling. For all western blots, staining with Ponceau S was used to verify equal loading, protein migration, and even transfer across the PVDF membrane.

Mapping polyP binding domains

YihI (wild-type and mutated sequences) and Rnr domains were cloned into pGEX4T1 and transformed into BL21 for expression. Overnight cultures harboring the plasmids were diluted 1/100 in LB + ampicillin and grown to mid-exponential phase (~2 hours). Cells were induced with

0.1 mM IPTG for 2 hours and 1.5 OD_{600} equivalent of cells were harvested. Whole cell extract was prepared by resuspending pellets in 100 µL of sample buffer and was used to conduct *in vitro* polyP binding assays (described above).

YihI and Rnr disorder predictions

The amino acid sequences for YihI (UniProt accession: B1XAM2) and Rnr (UniProt accession: P21499) were entered into the following disorder prediction programs: NetSurfP-3.0 (https://services.healthtech.dtu.dk/services/NetSurfP-3.0/) (95**),** Metapredict online (v3.0) (https://metapredict.net/) (96) and IUPred3 (https://iupred3.elte.hu/) (97). These programs were selected to account for variations between prediction algorithms and prevent bias (98, 99). Disorder scores from the three programs were averaged and graphed with the standard error envelope using GraphPad Prism as described by Pastic *et al.*[100]. See Supplemental Data 2 for individual prediction scores.

Screen for polyP binding proteins

(1) Bacterial growth

SPA and TAP collection sets (54) were pinned on LB + kanamycin plates and grown overnight at 30°C. The next day, grown colonies were inoculated into 3 mL LB + kanamycin and grown at 30°C overnight.

(2) Protein extraction

From the overnight cultures, 200 µL of cells were pelleted and used to prepare whole cell extract as described in the *Western blotting* section of the methods.

(3) *In vitro* polyP binding assay

The extracts were screened as described above. In brief, whole cell extract of the tagged strains was incubated in the absence or presence of polyP (modal size p700) and resolved using NuPAGE

(as described in the *Western blotting* section of the methods).

(4) Confirming positive hits

Positive candidates were streaked for single colonies and the correct position of the tag was confirmed via PCR analyses. Primers used in these confirmation assays are available upon request. These proteins were re-screened using sodium phosphate pH 6.0 (matching the pH of p700) as a control. With the exception of the screen, sodium phosphate pH 6.0 was used as a control for all *in vitro* polyP binding assays. The screened strains are listed in **Supplemental Table 1.**

Ppx1 overexpression assay

Strains harboring the pBAD18 (empty vector) and *ScPPX1* plasmids were grown in the presence of ampicillin at all stages. Overnight cultures were diluted into LB media and induced with 0.5% arabinose, grown to mid-exponential phase and then nutrient downshifted into MOPS media (as described above under *Growth conditions* for 3 hours. The only variation is that for the MOPS media, 0.5% arabinose was included, and glucose (0.4%) was replaced with glycerol (0.5%) as the carbon source. For western blotting and polyP extraction, 3 and 5 OD_{600} equivalent of cells were harvested, respectively.

PolyP extraction

(1) Extraction

PolyP extractions were performed as described previously (42) and have been briefly summarized with similar wording here. Five OD_{600} equivalents of cells were used for polyP extractions. Cell pellets were resuspended in LETS buffer (100 mM LiCl, 10 mM EDTA, 10 mM Tris-HCl pH 7.4 and 0.2% SDS). PolyP was extracted using the phenol/chloroform method and precipitated overnight at -20°C in 100% ethanol containing 120 mM sodium acetate. Precipitated polyP was pelleted by centrifugation, resuspended in 30 μL sterile water and stored at -80°C.

(2) Gel analysis

Extracted polyP, mixed 1:1 with loading dye (10 mM Tris-HCl (pH 7), 1 mM EDTA, 30% glycerol, and bromophenol blue) was resolved using a 15.8% TBE-urea gel (5.25 g urea, 7.9 ml 30% acrylamide, 3 ml 5xTBE, 150 µl 10% APS, and 15 µl TEMED) run at 100 V for 1 hour and 45 mins in 1x TBE. The gel was then stained in fixing solution (25% methanol, 5% glycerol) containing 0.05% toluidine blue and then de-stained in fixing solution without toluidine blue. For the polyP standards, 6 µL of each chain length at the specified concentration, p130 (1.25 mM) and p700 (1 mM), was mixed 1:1 with loading dye and 10 µL was loaded into the gel.

Growth assays

Spot tests were conducted as described previously, with the details reiterated here (42). The indicated strains were streaked on LB plates and incubated overnight at 37°C. The next day, single colonies were resuspended in 100 µL of sterile water and serially diluted 10-fold 5 times in sterile water. Next, 5 µL of each dilution was spotted onto LB or MOPS (1x MOPS, 0.4% glucose, 0.1 mM K_2HPO_4) and incubated at 37°C. To prepare MOPS plates, 10x MOPS, glucose and K_2HPO_4 were added after autoclaving water + agar. LB plates were imaged after 1 overnight while MOPS plates were imaged post-day 1 and -day 2. Spot tests were imaged using ImageQuant LAS 4000 and edited across the entire image by making minor linear brightness and contrast adjustments in Photoshop to lighten the background.

Immunoprecipitation and *in vitro* polyP-binding assay

Overnight culture of the Rnr-3Flag tagged strain was diluted to 0.1 OD_{600} in 300 mL of LB and grown to mid-exponential phase. Fifty OD_{600} equivalent of cells were harvested on ice and stored at -80°C until used for immunoprecipitation. Cells were resuspended in 700 µL buffer A (50 mM HEPES pH 7.9, 150 mM NaCl, 1 mM EDTA, 0.5% Triton X-100, 5% glycerol, 1 mM PMSF,

Roche cOmplete protease inhibitor cocktail tablet) and sonicated (Misonix 3000) on ice for 3 cycles of 10 seconds at power level 3 with 30 second rest in between. The lysate was cleared by centrifugation for 15 minutes at 15,000 rpm at 4°C and then incubated with 5 µL of the 50% anti-FLAG M2 magnetic bead slurry (Sigma Aldrich M8823-1ML) for 1 hour at 4°C. Next, the beads and bound proteins were washed 3 times with 1 mL of buffer A using cut pipette tips. Beads were then resuspended in 10 mM sodium phosphate (pH 6.0) or p700 in a final volume of 250 uL of buffer B (same as buffer A, but with 0.05% Triton X-100 and no protease inhibitor tablet) and incubated at room temperature with end-to-end rotation for 20 minutes. Excess polyP was then washed away using three 1 mL washes with buffer B. Finally, proteins were eluted in 60 µL 2X sample buffer containing no DTT by incubating at 65°C for 10 minutes. Finally, the sample was transferred to a new tube, DTT was added to a final concentration of 100 mM and the sample was boiled at 100°C for 10 minutes prior to resolving (20 µL per sample) on NuPAGE gels.

Chromosomal Rnr lysine to arginine mutants

Gene fragments encoding lysine to arginine mutants for the S1+basic domain were purchased from Twist Bioscience. Towards the 5' and 3' ends, the fragments had homology needed for the recombineering transformation and homology towards the beginning of the pKD4 cassette, respectively. In a separate PCR reaction, the KanR cassette was amplified from pKD4. This reaction used forward and reverse primers introducing homology towards the K-R fragments and homology needed for the recombineering transformation, respectively. Next, in a two-step PCR the two fragments (K-R gene fragments + KanR cassette) were combined at a 1:1 molar ratio and amplified. The final products were gel extracted and transformed into *rnr*-Δbasic mutants by electroporation. Correct integration of the K-R mutations was confirmed by Premium PCR sequencing from Plasmidsaurus.

Anti-GST antibody purification:

The anti-GST antibody was purified from sera collected from rabbits injected with a GST-Cdc26 fusion protein (101). Prior to anti-Cdc26 antibody purification on a Cdc26 affinity column, the sera was cleared of anti-GST antibodies on a 50 mL GST affinity column, as described (101). Anti-GST antibodies were eluted with 100 mM glycine, pH 2.1, neutralized in 2 M tris-base and dialyzed in antibody storage buffer (1x PBS, 500 mM NaCl, 50% glycerol).

Anti-Rnr antibody

An antibody towards Rnr was raised by immunizing New Zealand NZW female rabbits with purified GST-Rnr nuclease domain (amino acids 649-1929). This domain was chosen for immunization as it does not bind polyP and therefore, would not impact detection of truncated or mutant Rnr. The pGEX4T1 vector was cloned with sequence encoding the Rnr nuclease domain (amino acids 649-1929) using standard Gibson assembly. The oligonucleotides used for this strategy are available upon request. The vector was transformed into BL21 DE3 pLysS *E. coli* and plated on LB + ampicillin + chloramphenicol. Overnight cultures of cells harboring the vector were diluted to 0.1 OD_{600} and grown at 30°C until they reached OD_{600} of 0.4-0.6. Cells were then induced with 0.25 mM IPTG for 4 hours prior to harvesting and freezing at -80°C in 40 mL of freezing buffer (1x PBS).

(1) GST-fusion purification

Frozen cell lysates were thawed in a water bath, then immediately transferred onto ice to prevent degradation. Next, 40 mL of 1x PBS containing 2 mM EDTA, 2 mM EGTA, 2 mM PMSF, 30 mM DTT, 1 M NaCl was added to bring the final volume of the cell slurry to 80 mL. Lysozyme was added at a final concentration of 200 μg/mL and the lysate was incubated on ice for 30 minutes before disruption using the Misonix sonicator (3 cycles of 1 min at power level 7, with 2 minutes

rest on ice in between). Triton X-100 was added after sonication to a final concentration of 0.5%. The lysate was centrifuged at 40,000 x g for 30 minutes, then cleared through a 0.45 micron filter and then batch bound for 2 hour to glutathione agarose beads that had been equilibrated in wash buffer with detergent (1x PBS, 0.1% NP-40, 0.5 M NaCl, 1 mM DTT, 1 mM EDTA, 1 mM EGTA and 1 mM PMSF). The GST-bound beads were washed with 15 column volumes of wash buffer with detergent and 5 column volumes with wash buffer without detergent (no NP-40). The column was eluted with 20 mL elution buffer (50 mM Tris-HCl pH 8.0, 0.5 M NaCl, 10 mM glutathione, 1 mM DTT and 1 mM PMSF) and dialyzed into the storage buffer (1x PBS, 100 mM NaCl, 15% glycerol). The dialysis buffer was changed 3 times. The GST-purified protein was concentrated using an Amicon Ultra-15 centrifugal filter and quantified against serially diluted BSA standards using gel electrophoresis and Coomassie staining and quantification. The final protein was aliquoted at stored at -80°C.

(2) Injection preparation

For the first immunization, 675 µL of purified protein, at a final concentration of 2 mg/mL, was combined with 75 µL penicillin (10 U/mL) / streptomycin (10 µg/mL) and 750 µL Freund's Complete Adjuvant. In contrast, Freund's Incomplete Adjuvant was used to prepare subsequent booster injections.

(3) Injections

For both primary and booster immunizations, four 100 µL subcutaneous and two 250 µL intramuscular injections were administered. The booster was administered 4 weeks after the initial immunization and the rabbits were terminally bled 4 weeks later. All antigen injections and blood collections were administered under general anesthesia to minimize pain and suffering. Rabbits

were first sedated with injectable sedatives butorphanol and midazolam and induced into general anesthesia with inhaled isoflurane from a precision vaporizer.

(4) Antibody validation

Sera was validated in the lab by western blotting, using wild-type and Δ*rnr* (negative control) *E. coli* whole cell extracts (**Figure S5B**).

Sequence similarity comparison analyses

Protein sequences of the 7 hits were individually blasted against the *Salmonella enterica* (taxid: 28901), *Helicobacter pylori* (taxid: 210), *Streptomyces coelicolor* (taxid: 1902) and *Mycobacterium tuberculosis* (taxid: 1773) proteomes using NCBI Blast (https://blast.ncbi.nlm.nih.gov/Blast.cgi?PAGE=Proteins). Search settings were as follow: standard databases, non-redundant protein sequences (nr) and blastp (protein-protein BLAST). For each comparison, a single result with the greatest query coverage and, secondly, lowest E-value is presented in **Supplemental Table 2**.

3.6. Acknowledgements

This work was funded by a Canadian Institutes of Health Research (CIHR) Project Grant to MD and MLA (PJT-148722). KB was supported in part by an Ontario Graduate Scholarship. IA was supported in part by a Canada Graduate Scholarship from the Natural Sciences and Engineering Research Council of Canada (NSERC). We thank members of the Downey lab for helpful suggestions and critical reading of the manuscript.

3.7. Ethics Statement

This study was performed in strict accordance with standards for animal care and use outlined in the Canadian Council on Animal Care (CCAC) policies and guidelines. The University of Ottawa holds a certificate of Good Animal Practice with the CCAC and is a registered research facility under the Province of Ontario's Animals for Research Act. The animal use protocol (BMIe-3469) was approved by the University of Ottawa Animal Care Committee.

3.8. References

1. Kornberg, A., Rao, N.N. & Ault-Riche, D. Inorganic polyphosphate: a molecule of many functions. *Annu Rev Biochem* **68**, 89-125 (1999).
2. Denoncourt, A. & Downey, M. Model systems for studying polyphosphate biology: a focus on microorganisms. *Curr Genet* (2021).
3. Kuroda, A. *et al.* Inorganic polyphosphate kinase is required to stimulate protein degradation and for adaptation to amino acid starvation in Escherichia coli. *Proc Natl Acad Sci U S A* **96**, 14264-14269 (1999).
4. Gray, M.J. *et al.* Polyphosphate is a primordial chaperone. *Mol Cell* **53**, 689-699 (2014).
5. Ahn, K. & Kornberg, A. Polyphosphate kinase from Escherichia coli. Purification and demonstration of a phosphoenzyme intermediate. *J Biol Chem* **265**, 11734-11739 (1990).
6. Tzeng, C.M. & Kornberg, A. The multiple activities of polyphosphate kinase of Escherichia coli and their subunit structure determined by radiation target analysis. *J Biol Chem* **275**, 3977-3983 (2000).
7. Akiyama, M., Crooke, E. & Kornberg, A. An exopolyphosphatase of Escherichia coli. The enzyme and its ppx gene in a polyphosphate operon. *J Biol Chem* **268**, 633-639 (1993).
8. Chen, J. *et al.* Polyphosphate Kinase Mediates Antibiotic Tolerance in Extraintestinal Pathogenic Escherichia coli PCN033. *Front Microbiol* **7**, 724 (2016).
9. Lv, H. *et al.* Polyphosphate Kinase Is Required for the Processes of Virulence and Persistence in Acinetobacter baumannii. *Microbiol Spectr* **10**, e0123022 (2022).
10. Rashid, M.H. *et al.* Polyphosphate kinase is essential for biofilm development, quorum sensing, and virulence of Pseudomonas aeruginosa. *Proc Natl Acad Sci U S A* **97**, 9636-9641 (2000).
11. Roewe, J. *et al.* Bacterial polyphosphates interfere with the innate host defense to infection. *Nat Commun* **11**, 4035 (2020).
12. Zhang, H., Gomez-Garcia, M.R., Shi, X., Rao, N.N. & Kornberg, A. Polyphosphate kinase 1, a conserved bacterial enzyme, in a eukaryote, Dictyostelium discoideum, with a role in cytokinesis. *Proc Natl Acad Sci U S A* **104**, 16486-16491 (2007).
13. Yagisawa, F. *et al.* A fusion protein of polyphosphate kinase 1 (PPK1) and a Nudix hydrolase is involved in inorganic polyphosphate accumulation in the unicellular red alga Cyanidioschyzon merolae. *Plant Mol Biol* **115**, 9 (2024).
14. Hothorn, M. *et al.* Catalytic core of a membrane-associated eukaryotic polyphosphate polymerase. *Science* **324**, 513-516 (2009).
15. Gerasimaite, R., Sharma, S., Desfougeres, Y., Schmidt, A. & Mayer, A. Coupled synthesis and translocation restrains polyphosphate to acidocalcisome-like vacuoles and prevents its toxicity. *J Cell Sci* **127**, 5093-5104 (2014).
16. Klompmaker, S.H., Kohl, K., Fasel, N. & Mayer, A. Magnesium uptake by connecting fluid-phase endocytosis to an intracellular inorganic cation filter. *Nat Commun* **8**, 1879 (2017).
17. Austin, S. & Mayer, A. Phosphate Homeostasis - A Vital Metabolic Equilibrium Maintained Through the INPHORS Signaling Pathway. *Front Microbiol* **11**, 1367 (2020).
18. Bru, S. *et al.* Polyphosphate is involved in cell cycle progression and genomic stability in Saccharomyces cerevisiae. *Mol Microbiol* **101**, 367-380 (2016).

19. Uttenweiler, A., Schwarz, H., Neumann, H. & Mayer, A. The vacuolar transporter chaperone (VTC) complex is required for microautophagy. *Mol Biol Cell* **18**, 166-175 (2007).
20. Bentley-DeSousa, A. *et al.* A Screen for Candidate Targets of Lysine Polyphosphorylation Uncovers a Conserved Network Implicated in Ribosome Biogenesis. *Cell Rep* **22**, 3427-3439 (2018).
21. Baijal, K. & Downey, M. The promises of lysine polyphosphorylation as a regulatory modification in mammals are tempered by conceptual and technical challenges. *Bioessays*, e2100058 (2021).
22. Desfougeres, Y., Saiardi, A. & Azevedo, C. Inorganic polyphosphate in mammals: where's Wally? *Biochem Soc Trans* **48**, 95-101 (2020).
23. Baev, A.Y., Angelova, P.R. & Abramov, A.Y. Inorganic polyphosphate is produced and hydrolyzed in F0F1-ATP synthase of mammalian mitochondria. *Biochem J* **477**, 1515-1524 (2020).
24. Lazaro, B. *et al.* Optimized biochemical method for human Polyphosphate quantification. *Methods* (2025).
25. Holmstrom, K.M. *et al.* Signalling properties of inorganic polyphosphate in the mammalian brain. *Nat Commun* **4**, 1362 (2013).
26. Bae, J.S., Lee, W. & Rezaie, A.R. Polyphosphate elicits pro-inflammatory responses that are counteracted by activated protein C in both cellular and animal models. *J Thromb Haemost* **10**, 1145-1151 (2012).
27. Hassanian, S.M., Dinarvand, P., Smith, S.A. & Rezaie, A.R. Inorganic polyphosphate elicits pro-inflammatory responses through activation of the mammalian target of rapamycin complexes 1 and 2 in vascular endothelial cells. *J Thromb Haemost* **13**, 860-871 (2015).
28. Cremers, C.M. *et al.* Polyphosphate: A Conserved Modifier of Amyloidogenic Processes. *Mol Cell* **63**, 768-780 (2016).
29. Da Costa, R.T., Riggs, L.M. & Solesio, M.E. Inorganic polyphosphate and the regulation of mitochondrial physiology. *Biochem Soc Trans* **51**, 2153-2161 (2023).
30. Muller, F. *et al.* Platelet polyphosphates are proinflammatory and procoagulant mediators in vivo. *Cell* **139**, 1143-1156 (2009).
31. McCarthy, L., Baijal, K. & Downey, M. A framework for understanding and investigating polyphosphate-protein interactions. *Biochem Soc Trans* (2025).
32. Azevedo, C. *et al.* Screening a Protein Array with Synthetic Biotinylated Inorganic Polyphosphate To Define the Human PolyP-ome. *ACS Chem Biol* **13**, 1958-1963 (2018).
33. Krenzlin, V. *et al.* Bacterial-Type Long-Chain Polyphosphates Bind Human Proteins in the Phosphatidylinositol Signaling Pathway. *Thromb Haemost* **122**, 1943-1947 (2022).
34. Neville, N., Lehotsky, K., Klupt, K.A., Downey, M. & Jia, Z. Polyphosphate attachment to lysine repeats is a non-covalent protein modification. *Mol Cell* **84**, 1802-1810 e1804 (2024).
35. Neville, N. *et al.* Modification of histidine repeat proteins by inorganic polyphosphate. *Cell Rep* **42**, 113082 (2023).
36. Azevedo, C., Livermore, T. & Saiardi, A. Protein polyphosphorylation of lysine residues by inorganic polyphosphate. *Mol Cell* **58**, 71-82 (2015).
37. Negreiros, R.S. *et al.* Inorganic polyphosphate interacts with nucleolar and glycosomal proteins in trypanosomatids. *Mol Microbiol* **110**, 973-994 (2018).

38. Kuroda, A. *et al.* Role of inorganic polyphosphate in promoting ribosomal protein degradation by the Lon protease in E. coli. *Science* **293**, 705-708 (2001).
39. Gross, M.H. & Konieczny, I. Polyphosphate induces the proteolysis of ADP-bound fraction of initiator to inhibit DNA replication initiation upon stress in Escherichia coli. *Nucleic Acids Res* **48**, 5457-5466 (2020).
40. Beaufay, F. *et al.* Polyphosphate drives bacterial heterochromatin formation. *Sci Adv* **7**, eabk0233 (2021).
41. Yang, Z.X., Zhou, Y.N., Yang, Y. & Jin, D.J. Polyphosphate binds to the principal sigma factor of RNA polymerase during starvation response in Helicobacter pylori. *Mol Microbiol* **77**, 618-627 (2010).
42. Baijal, K. *et al.* Polyphosphate kinase regulates LPS structure and polymyxin resistance during starvation in E. coli. *PLoS Biol* **22**, e3002558 (2024).
43. Racki, L.R. *et al.* Polyphosphate granule biogenesis is temporally and functionally tied to cell cycle exit during starvation in Pseudomonas aeruginosa. *Proc Natl Acad Sci U S A* **114**, E2440-E2449 (2017).
44. McCarthy, L. *et al.* Proteins required for vacuolar function are targets of lysine polyphosphorylation in yeast. *FEBS Lett* **594**, 21-30 (2020).
45. Crowe, L.P., Gioseffi, A., Bertolini, M.S. & Docampo, R. Inorganic Polyphosphate Is in the Surface of Trypanosoma cruzi but Is Not Significantly Secreted. *Pathogens* **13** (2024).
46. UniProt, C. UniProt: the Universal Protein Knowledgebase in 2025. *Nucleic Acids Res* **53**, D609-D617 (2025).
47. Hale, C.A. & de Boer, P.A. Direct binding of FtsZ to ZipA, an essential component of the septal ring structure that mediates cell division in E. coli. *Cell* **88**, 175-185 (1997).
48. Hwang, J. & Inouye, M. A bacterial GAP-like protein, YihI, regulating the GTPase of Der, an essential GTP-binding protein in Escherichia coli. *J Mol Biol* **399**, 759-772 (2010).
49. Azevedo, C. *et al.* Development of a yeast model to study the contribution of vacuolar polyphosphate metabolism to lysine polyphosphorylation. *J Biol Chem* (2019).
50. Bentley-DeSousa, A. & Downey, M. Vtc5 Is Localized to the Vacuole Membrane by the Conserved AP-3 Complex to Regulate Polyphosphate Synthesis in Budding Yeast. *mBio* **12**, e0099421 (2021).
51. Gauthier, C.M. *et al.* Intrinsic disorder of a nucleoplasmin-like histone chaperone specifies its discrete nuclear and nucleolar functions. *FEBS Lett* **598**, 187-198 (2024).
52. Guan, J. & Jakob, U. The Protein Scaffolding Functions of Polyphosphate. *J Mol Biol* **436**, 168504 (2024).
53. Azevedo, C. *et al.* Development of a yeast model to study the contribution of vacuolar polyphosphate metabolism to lysine polyphosphorylation. *J Biol Chem* **295**, 1439-1451 (2020).
54. Butland, G. *et al.* Interaction network containing conserved and essential protein complexes in Escherichia coli. *Nature* **433**, 531-537 (2005).
55. Zeghouf, M. *et al.* Sequential Peptide Affinity (SPA) system for the identification of mammalian and bacterial protein complexes. *J Proteome Res* **3**, 463-468 (2004).
56. Borghi, F., Azevedo, C., Johnson, E., Burden, J.J. & Saiardi, A. A mammalian model reveals inorganic polyphosphate channeling into the nucleolus and induction of a hyper-condensate state. *Cell Rep Methods* **4**, 100814 (2024).
57. Samper-Martin, B. *et al.* Polyphosphate degradation by Nudt3-Zn(2+) mediates oxidative stress response. *Cell Rep* **37**, 110004 (2021).

58. McCarthy, L. *et al.* Ddp1 Cooperates with Ppx1 to Counter a Stress Response Initiated by Nonvacuolar Polyphosphate. *mBio*, e0039022 (2022).
59. Hamm, C.W. & Gray, M.J. Inorganic polyphosphate and the stringent response coordinately control cell division and cell morphology in Escherichia coli. *mBio*, e0351124 (2024).
60. Cheng, Z.F. & Deutscher, M.P. An important role for RNase R in mRNA decay. *Mol Cell* **17**, 313-318 (2005).
61. Andrade, J.M., Hajnsdorf, E., Regnier, P. & Arraiano, C.M. The poly(A)-dependent degradation pathway of rpsO mRNA is primarily mediated by RNase R. *RNA* **15**, 316-326 (2009).
62. Vincent, H.A. & Deutscher, M.P. The roles of individual domains of RNase R in substrate binding and exoribonuclease activity. The nuclease domain is sufficient for digestion of structured RNA. *J Biol Chem* **284**, 486-494 (2009).
63. Cheng, Z.F. & Deutscher, M.P. Purification and characterization of the Escherichia coli exoribonuclease RNase R. Comparison with RNase II. *J Biol Chem* **277**, 21624-21629 (2002).
64. Matos, R.G., Barbas, A. & Arraiano, C.M. RNase R mutants elucidate the catalysis of structured RNA: RNA-binding domains select the RNAs targeted for degradation. *Biochem J* **423**, 291-301 (2009).
65. Basturea, G.N., Zundel, M.A. & Deutscher, M.P. Degradation of ribosomal RNA during starvation: comparison to quality control during steady-state growth and a role for RNase PH. *RNA* **17**, 338-345 (2011).
66. Chen, C. & Deutscher, M.P. Elevation of RNase R in response to multiple stress conditions. *J Biol Chem* **280**, 34393-34396 (2005).
67. Andrade, J.M., Cairrao, F. & Arraiano, C.M. RNase R affects gene expression in stationary phase: regulation of ompA. *Mol Microbiol* **60**, 219-228 (2006).
68. Cairrao, F., Cruz, A., Mori, H. & Arraiano, C.M. Cold shock induction of RNase R and its role in the maturation of the quality control mediator SsrA/tmRNA. *Mol Microbiol* **50**, 1349-1360 (2003).
69. Gutmann, S. *et al.* Crystal structure of the transfer-RNA domain of transfer-messenger RNA in complex with SmpB. *Nature* **424**, 699-703 (2003).
70. Karzai, A.W., Susskind, M.M. & Sauer, R.T. SmpB, a unique RNA-binding protein essential for the peptide-tagging activity of SsrA (tmRNA). *EMBO J* **18**, 3793-3799 (1999).
71. Roche, E.D. & Sauer, R.T. SsrA-mediated peptide tagging caused by rare codons and tRNA scarcity. *EMBO J* **18**, 4579-4589 (1999).
72. Dulebohn, D., Choy, J., Sundermeier, T., Okan, N. & Karzai, A.W. Trans-translation: the tmRNA-mediated surveillance mechanism for ribosome rescue, directed protein degradation, and nonstop mRNA decay. *Biochemistry* **46**, 4681-4693 (2007).
73. Richards, J., Mehta, P. & Karzai, A.W. RNase R degrades non-stop mRNAs selectively in an SmpB-tmRNA-dependent manner. *Mol Microbiol* **62**, 1700-1712 (2006).
74. Ge, Z., Mehta, P., Richards, J. & Karzai, A.W. Non-stop mRNA decay initiates at the ribosome. *Mol Microbiol* **78**, 1159-1170 (2010).
75. Awano, N. *et al.* Escherichia coli RNase R has dual activities, helicase and RNase. *J Bacteriol* **192**, 1344-1352 (2010).
76. Vincent, H.A. & Deutscher, M.P. Insights into how RNase R degrades structured RNA: analysis of the nuclease domain. *J Mol Biol* **387**, 570-583 (2009).

77. Liang, W. & Deutscher, M.P. A novel mechanism for ribonuclease regulation: transfer-messenger RNA (tmRNA) and its associated protein SmpB regulate the stability of RNase R. *J Biol Chem* **285**, 29054-29058 (2010).
78. Liang, W. & Deutscher, M.P. Ribosomes regulate the stability and action of the exoribonuclease RNase R. *J Biol Chem* **288**, 34791-34798 (2013).
79. Liang, W., Malhotra, A. & Deutscher, M.P. Acetylation regulates the stability of a bacterial protein: growth stage-dependent modification of RNase R. *Mol Cell* **44**, 160-166 (2011).
80. Liang, W. & Deutscher, M.P. Transfer-messenger RNA-SmpB protein regulates ribonuclease R turnover by promoting binding of HslUV and Lon proteases. *J Biol Chem* **287**, 33472-33479 (2012).
81. Chen, C. & Deutscher, M.P. RNase R is a highly unstable protein regulated by growth phase and stress. *RNA* **16**, 667-672 (2010).
82. McInerney, P., Mizutani, T. & Shiba, T. Inorganic polyphosphate interacts with ribosomes and promotes translation fidelity in vitro and in vivo. *Mol Microbiol* **60**, 438-447 (2006).
83. Thepaut, M. *et al.* Safe and easy in vitro evaluation of tmRNA-SmpB-mediated trans-translation from ESKAPE pathogenic bacteria. *RNA* **27**, 1390-1399 (2021).
84. Cheng, Z.F., Zuo, Y., Li, Z., Rudd, K.E. & Deutscher, M.P. The vacB gene required for virulence in Shigella flexneri and Escherichia coli encodes the exoribonuclease RNase R. *J Biol Chem* **273**, 14077-14080 (1998).
85. Miyoshi, A. *et al.* The role of the vacB gene in the pathogenesis of Brucella abortus. *Microbes Infect* **9**, 375-381 (2007).
86. Steffensen, S.A., Poulsen, A.B., Mortensen, K.K. & Sperling-Petersen, H.U. E. coli translation initiation factor IF2--an extremely conserved protein. Comparative sequence analysis of the infB gene in clinical isolates of E. coli. *FEBS Lett* **419**, 281-284 (1997).
87. Yang, J., Jain, C. & Schesser, K. RNase E regulates the Yersinia type 3 secretion system. *J Bacteriol* **190**, 3774-3778 (2008).
88. Blum, E., Py, B., Carpousis, A.J. & Higgins, C.F. Polyphosphate kinase is a component of the Escherichia coli RNA degradosome. *Mol Microbiol* **26**, 387-398 (1997).
89. Datsenko, K.A. & Wanner, B.L. One-step inactivation of chromosomal genes in Escherichia coli K-12 using PCR products. *Proc Natl Acad Sci U S A* **97**, 6640-6645 (2000).
90. Datta, S., Costantino, N. & Court, D.L. A set of recombineering plasmids for gram-negative bacteria. *Gene* **379**, 109-115 (2006).
91. Uzzau, S., Figueroa-Bossi, N., Rubino, S. & Bossi, L. Epitope tagging of chromosomal genes in Salmonella. *Proc Natl Acad Sci U S A* **98**, 15264-15269 (2001).
92. Mateus, A. *et al.* Transcriptional and Post-Transcriptional Polar Effects in Bacterial Gene Deletion Libraries. *mSystems* **6**, e0081321 (2021).
93. Sharan, S.K., Thomason, L.C., Kuznetsov, S.G. & Court, D.L. Recombineering: a homologous recombination-based method of genetic engineering. *Nat Protoc* **4**, 206-223 (2009).
94. Cherepanov, P.P. & Wackernagel, W. Gene disruption in Escherichia coli: TcR and KmR cassettes with the option of Flp-catalyzed excision of the antibiotic-resistance determinant. *Gene* **158**, 9-14 (1995).
95. Hoie, M.H. *et al.* NetSurfP-3.0: accurate and fast prediction of protein structural features by protein language models and deep learning. *Nucleic Acids Res* **50**, W510-W515 (2022).

96. Emenecker, R.J., Griffith, D. & Holehouse, A.S. Metapredict: a fast, accurate, and easy-to-use predictor of consensus disorder and structure. *Biophys J* **120**, 4312-4319 (2021).
97. Erdos, G., Pajkos, M. & Dosztanyi, Z. IUPred3: prediction of protein disorder enhanced with unambiguous experimental annotation and visualization of evolutionary conservation. *Nucleic Acids Res* **49**, W297-W303 (2021).
98. Nielsen, J.T. & Mulder, F.A.A. Quality and bias of protein disorder predictors. *Sci Rep* **9**, 5137 (2019).
99. Necci, M., Piovesan, D., Predictors, C., DisProt, C. & Tosatto, S.C.E. Critical assessment of protein intrinsic disorder prediction. *Nat Methods* **18**, 472-481 (2021).
100. Pastic, A. *et al.* Chromosome compaction is triggered by an autonomous DNA-binding module within condensin. *Cell Rep* **43**, 114419 (2024).
101. Hwang, L.H. & Murray, A.W. A novel yeast screen for mitotic arrest mutants identifies DOC1, a new gene involved in cyclin proteolysis. *Mol Biol Cell* **8**, 1877-1887 (1997).

3.9. Supplemental Figures

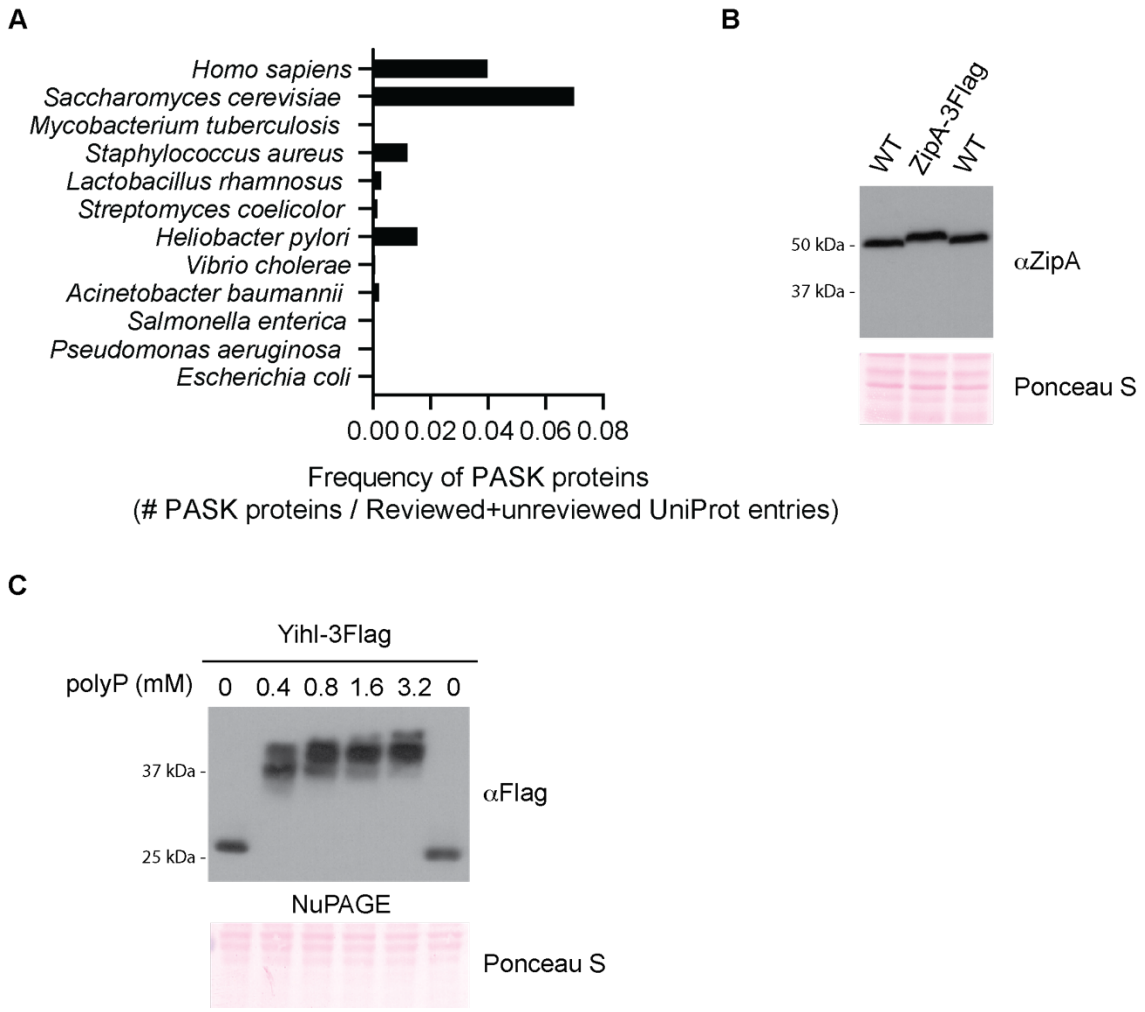

S1 Figure. The PASK is not a good indicator of polyP-protein binding in bacteria. **(A)** PASK frequency using reviewed+unreviewed proteomes. The number of proteins containing 1 or more PASK motifs (75% D/E/S/K content with at least one lysine within a 20 amino acid window) from reviewed and unreviewed proteomes of the indicated species were normalized by the total number of reviewed+unreviewed UniProt entries for each species. **(B)** Anti-ZipA antibody validation blot. Whole cell extracts from wild-type and ZipA-3Flag tagged strains were resolved on 12% SDS-PAGE, transferred to PVDF and probed using an anti-ZipA antibody. Ponceau S was used to show equal protein loading and that samples migrated equally. A deletion mutation of Δ*zipA* could not be used because *zipA* is essential. ZipA-3Flag displayed a shift in migration as expected, confirming the antibody recognizes ZipA. **(C)** YihI-polyP binding shifts on NuPAGE are polyP concentration dependent. Whole cell extract from a YihI-3Flag tagged strain was used for an *in vitro* polyP binding assay in the presence of increasing concentrations of polyP. Samples were resolved using NuPAGE, transferred to PVDF and probed using an anti-Flag antibody. Ponceau S was used to show that samples migrated equally. Images are representative of results from ≥3 experiments.

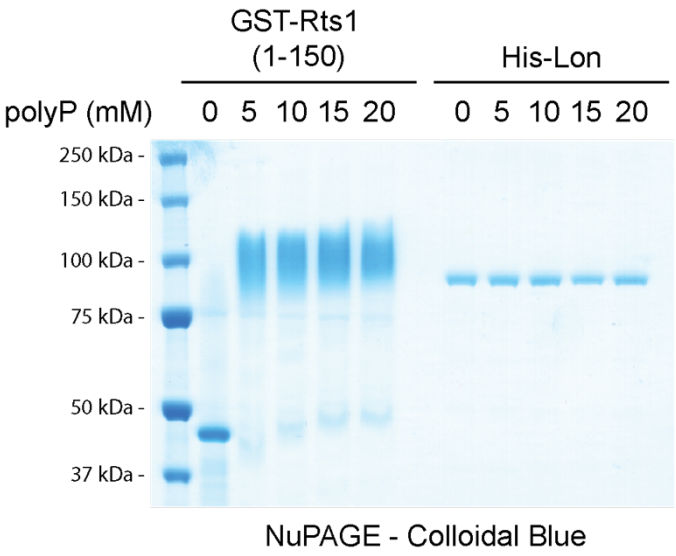

S2 Figure. NuPAGE electrophoresis is not effective for detecting polyP binding to Lon. Lon does not display the characteristic polyP binding shift on NuPAGE gels. Increasing concentrations of polyP (p700) were incubated with 0.032 mg of purified Rts1 (positive control)[20] or Lon protease. Samples were resolved using NuPAGE and the gel was stained using Colloidal Blue to visualize the proteins. Image is representative of results from ≥3 experiments.

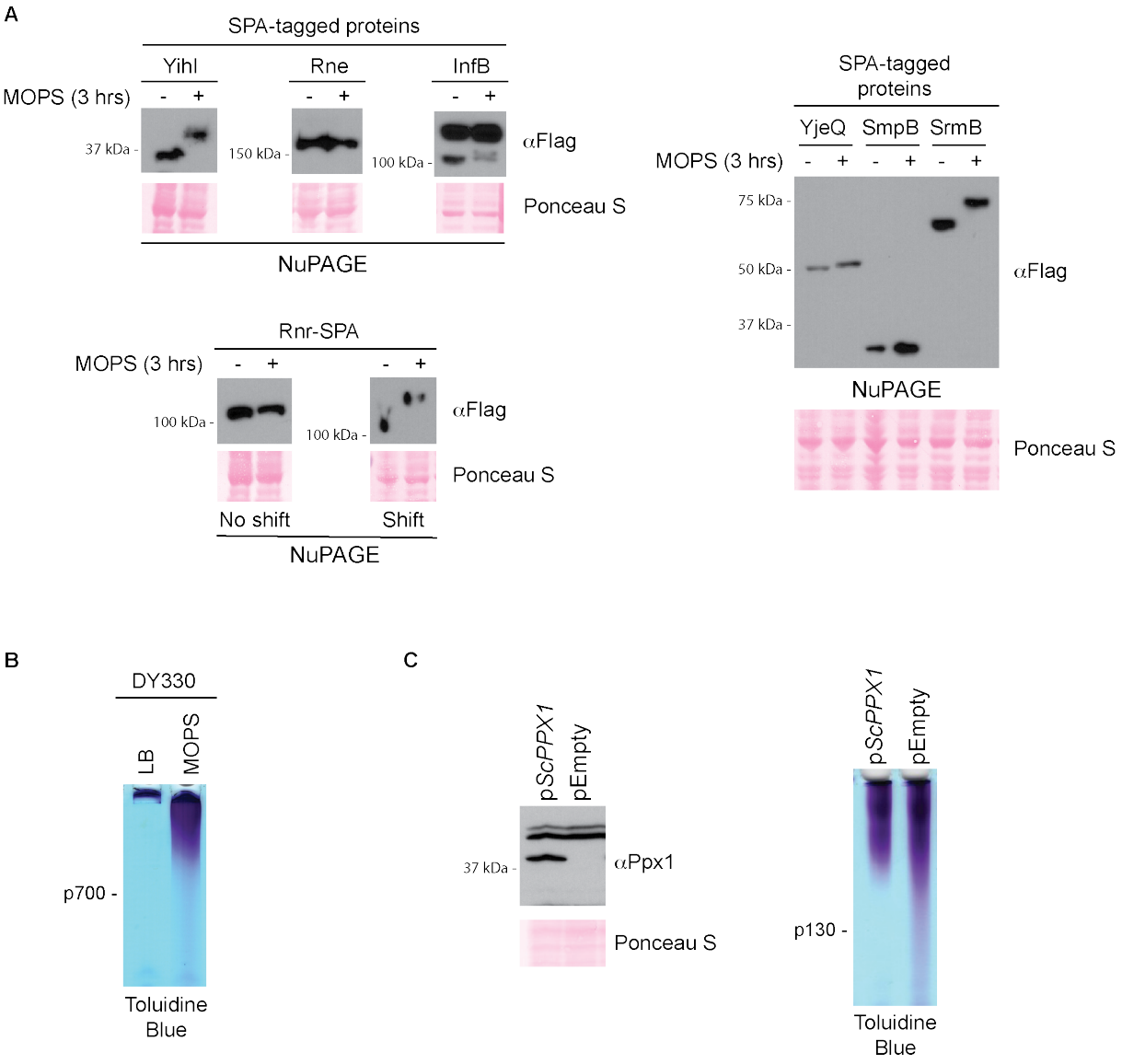

S3 Figure. PolyP-binding proteins may have limited access to endogenous polyP that accumulates in response to stress. (A) YihI, SmpB and Rnr display NuPAGE shifts in the presence of endogenous polyP. Whole cell extract from SPA-tagged strains that were grown in LB media (- MOPS) or exposed to nutrient downshift (+ MOPS) for 3 hours was resolved using NuPAGE, transferred to PVDF and probed using an anti-Flag antibody which detects the SPA tag. Ponceau S was used to show that samples migrated equally. Images are representative of results from ≥3 experiments. **(B)** *E. coli* makes long chain polyP after 3 hours in MOPS media. PolyP was extracted from cells grown in LB media or MOPS for 3 hours (as described for S3A) was resolved using a TBE-urea acrylamide gel and stained using toluidine blue. The gel shows that endogenous polyP is longer than the p700 standard. Images are representative of results from ≥3 experiments. **(C)** Endogenous polyP is not fully degraded by ectopic expression of *S. cerevisiae* exopolyphosphatase Ppx1 (*Sc*Ppx1). Western blotting (left) and polyP extractions (right) of *E. coli* with p*ScPPX1* or the empty vector. Cells were grown in LB media in the presence of 0.5% arabinose (the inducer) before undergoing a nutrient downshift to MOPS media for 3 hours. PolyP

and whole cell extracts were resolved using a TBE-urea acrylamide gel or 12% SDS-PAGE, respectively. The polyP gel was stained using toluidine blue and Ppx1 expression was detected using an anti-Ppx1 antibody. Images are representative of ≥3 results.

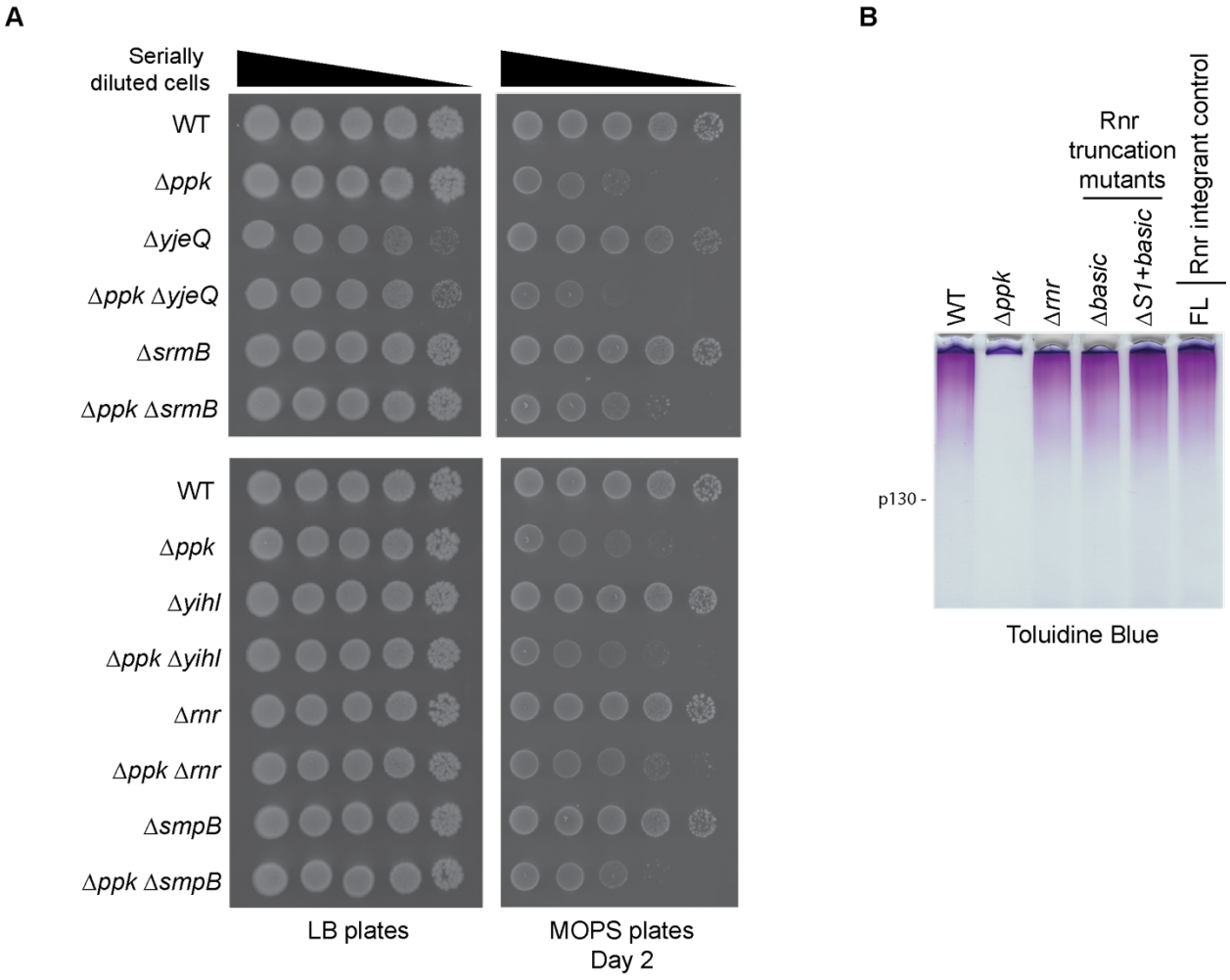

S4 Figure. Loss of polyP binding proteins SrmB and Rnr rescues *ppk* mutant growth phenotypes. (A) Spot test of *E. coli* mutated for genes encoding the polyP binding proteins. The indicated strains were serially diluted and spotted on LB or MOPS plates and incubated at 37°C as indicated. Images are representative of results from ≥3 experiments. **(B)** Mutation of *rnr* does not impact polyP accumulation in an otherwise wild-type background. PolyP extracted from cells grown in LB media and exposed to nutrient down shift for 3 hours was resolved using a TBE-urea acrylamide gel and stained using toluidine blue. The migration of a standard of modal length p130 is indicated. FL represents the wild-type Rnr protein expressed in a background that is isogenic to the truncated and mutated strains (see methods *Bacterial strains* section for details on how these strains were made). Images are representative of results from ≥3 experiments.

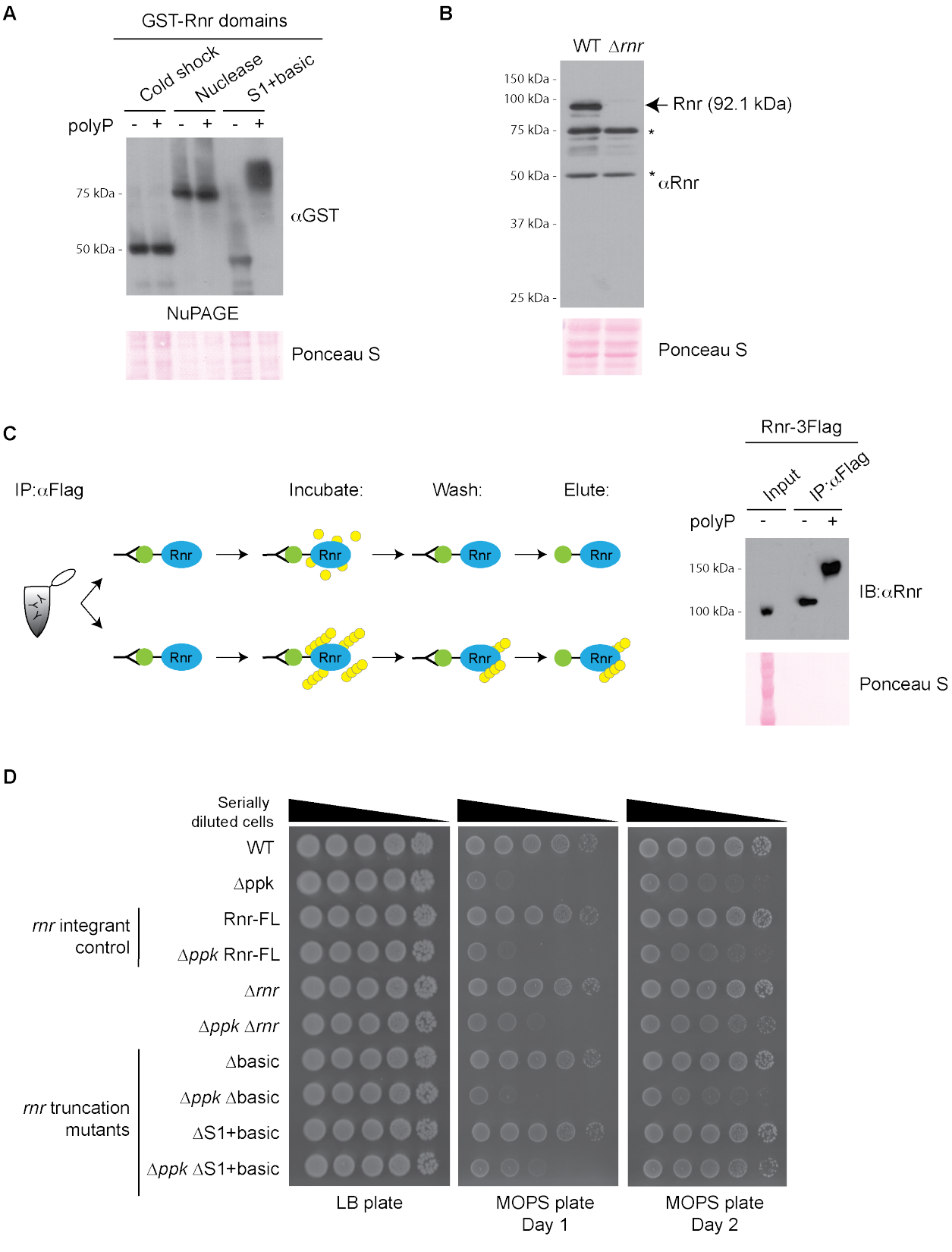

S5 – Figure legend on the next page.

S5 Figure. A complex interplay between PPK and the Rnr polyP binding domain. (A) PolyP binds to the S1 and basic domain of Rnr. Whole cell extract from cells expressing GST-tagged Rnr domains were used to conduct *in vitro* polyP binding assays, resolved using NuPAGE, transferred to PVDF and probed using an anti-GST antibody. Ponceau S was used to show that samples migrated equally. Images are representative of results from ≥3 experiments. **(B)** Anti-Rnr antibody validation blot. An arrow is used to show the band corresponding to Rnr while asterisks (*) indicate background bands. Whole cell extract from WT and Δ*rnr* strains was resolved on 12% SDS-PAGE, transferred to PVDF and probed using the anti-Rnr antibody. Ponceau S was used to show equal protein loading. **(C)** PolyP binds the native form of Rnr. Schematic (left): Rnr-3Flag was immunoprecipitated (IP) from whole cell extract under non-denaturing conditions using anti-Flag beads and then incubated with polyP (p700). Excess polyP was then washed away before eluting the protein. IP'ed proteins were resolved using NuPAGE, transferred to PVDF and probed using an anti-Rnr antibody. Images are representative of results from ≥3 experiments. **(D)** Loss of the Rnr S1 and basic domains rescues *ppk* mutant growth phenotypes comparable to Δ*ppk* Δ*rnr* double mutants. FL represents the wild-type Rnr protein expressed in a background that is isogenic to the truncated and mutated strains (see methods *Bacterial strains* section for details on how these strains were made). The indicated strains were serially diluted and spotted on LB or MOPS plates and incubated at 37°C as indicated. Images are representative of results from ≥3 experiments.

3.10. Supplemental Tables

Here, I have included tables that are relevant for the interpretation of the presented data. Please see '*Supporting information*' tab of online article for detailed view of Supplemental tables 1-4 (direct links provided below).

List of tables presented:

S1 Table. Screened and unscreened strains from the SPA- and TAP-collection sets.

1. S1-Tab 4: Summary of the SPA- and TAP-tag screen.

S2 Table. Conservation analysis of polyP-binding proteins across species commonly used for polyP research.

1. S2-Tab 1: Conservation analysis for each of the 7 polyP-binding hits identified in this work.

S3 Table. Bacterial strains and plasmids used in this study.

1. S3-Tab 1: Bacterial strains used in this study.
2. S3-Tab 2: Plasmids used in this study.

Online version of tables:

S1 Table. Screened and unscreened strains from the SPA- and TAP-collection sets.
See online: [supplements/637445_file03.xlsx]

S2 Table. Conservation analysis of polyP-binding proteins across species commonly used for polyP research.
See online: [supplements/637445_file04.xlsx]

S3 Table. Bacterial strains and plasmids used in this study.
See online: [supplements/637445_file05.xlsx]

S4 Table. Antibodies used in this study.
See online: [supplements/637445_file06.xlsx]

S1 Table-Tab 1 – Summary of the SPA- and TAP-tag screen.

		TAP	SPA	Redundant proteins	Total
Not screened	Undetected	20	269	8	281
	No growth	0	2	0	2
Screened	Shift	2	7	2	7
	No shift	221	503	142	582

S2 Table-Tab 1 – Conservation analysis for each of the 7 polyP-binding hits identified in this work.

YihI (Accession: B1XAM2)							
Species	**Accession of conserved protein**	**Max score**	**Total score**	**Query cover**	**E-value**	**Percent identity**	**Accession length**
Salmonella enterica	EHV4870114.1	256	256	99%	4E-86	82.56%	174
Helicobacter pylori	No significant similarlity found						
Streptomyces coelicolor	No significant similarlity found						
Mycobacterium tuberculosis	SGD51214.1	122	122	94%	2E-34	49.70%	167

YjeQ (Accession: Q1R396)							
Species	**Accession of conserved protein**	**Max score**	**Total score**	**Query cover**	**E-value**	**Percent identity**	**Accession length**
Salmonella enterica	EBQ8794825.1	705	705	99%	0	95.52%	358
Helicobacter pylori	GAA6941635.1	416	416	96%	3E-143	55.04%	372
Streptomyces coelicolor	WP_011030687.1	140	140	78%	1E-38	32.07%	366
Mycobacterium tuberculosis	SGC95647.1	531	531	97%	0	73.43%	349

SrmB (Accession: P21507)							
Species	**Accession of conserved protein**	**Max score**	**Total score**	**Query cover**	**E-value**	**Percent identity**	**Accession length**
Salmonella enterica	HED5891532.1	885	885	100%	0	96.85%	444
Helicobacter pylori	GAA7511757.1	583	583	98%	0	65.75%	441
Streptomyces coelicolor	WP_187438399.1	233	233	73%	1E-69	38.62%	735
Mycobacterium tuberculosis	SGC78406.1	691	691	98%	0	77.42%	448

Table continues onto the next page.

SmpB (Accession: P0A832)							
Species	**Accession of conserved protein**	**Max score**	**Total score**	**Query cover**	**E-value**	**Percent identity**	**Accession length**
Salmonella enterica	EAA2219722.1	318	318	100%	5E-111	95%	160
Helicobacter pylori	GAA6942736.1	259	259	100%	7E-88	75.00%	162
Streptomyces coelicolor	NUV54154.1	116	116	88%	3E-34	43.97%	159
Mycobacterium tuberculosis	SGC78749.1	298	298	100%	5E+104	86.25%	160

Rnr (Accession: P21499)							
Species	**Accession of conserved protein**	**Max score**	**Total score**	**Query cover**	**E-value**	**Percent identity**	**Accession length**
Salmonella enterica	WP_079809962.1	1625	1625	100%	0	96.06%	812
Helicobacter pylori	GAA6940550.1	1038	1038	91%	0	66.71%	793
Streptomyces coelicolor	NUV55590.1	45.4	45.4	11%	0.00006	33.33%	497
Mycobacterium tuberculosis	SGC96063.1	1233	1233	98%	0	74.13%	815

Rne (Accession: A0A024L3B3)							
Species	**Accession of conserved protein**	**Max score**	**Total score**	**Query cover**	**E-value**	**Percent identity**	**Accession length**
Salmonella enterica	EAA4711280.1	1558	1558	100%	0	82.01%	1067
Helicobacter pylori	GAA6942612.1	951	951	100%	0	53.98%	952
Streptomyces coelicolor	WP_375336291.1	282	282	35%	6E-82	39.58%	774
Mycobacterium tuberculosis	SGC84990.1	1102	1102	100%	0	59.64%	1057

InfB (Accession: A7ZS65)							
Species	**Accession of conserved protein**	**Max score**	**Total score**	**Query cover**	**E-value**	**Percent identity**	**Accession length**
Salmonella enterica	MFE8205114.1	1795	1795	100%	0	100%	890
Helicobacter pylori	GAA6941223.1	1041	1041	81%	0	74.35%	840
Streptomyces coelicolor	NUV57353.1	550	550	65%	0	48.91%	1021
Mycobacterium tuberculosis	SGC97055.1	1326	1326	100%	0	76.42%	910

S3 Table-Tab 1 – Bacterial strains. For simplicity the 'Background' column has been omitted from this version of the table. Unless specified to be in the DY330 background, all strains made for this study are in the MG1655 background.

Bacterial Strains (BMD)			
Reference number	**Genotype**	**Marker**	**Source [PMID]**
BMD0011	*ΔlacU169 gal490 λcI857 Δ(cro-bioA)* (**DY330**)	--	[10811905]
BMD0058	F-, λ-, *rph-1 ilvG- rfb-50* (**MG1655**)	--	Gift from Michael Gray
BMD0059	M1655, Δ*ppk* (*kan*^{r} excised)	--	Gift from Michael Gray
BMD0093	YihI-3Flag-KanR	*kan*$^+$	This study
BMD0244	VacB-3Flag-KanR	*kan*$^+$	This study
BMD498	ZipA-3Flag-KanR	*kan*$^+$	This study
BMD503	Δ*vacB*::KanR	*kan*$^+$	This study
BMD505	Δ*ppk* (KanR excised) Δ*vacB*::KanR	*kan*$^+$	This study
BMD507	Δ*smpB*::KanR	*kan*$^+$	This study
BMD509	Δ*ppk* (KanR excised) Δ*smpB*::KanR	*kan*$^+$	This study
BMD552	VacB-SPA-Kan (DY330)	*kan*$^+$	[15253427]
BMD553	Rne-SPA-Kan (DY330)	*kan*$^+$	[15253427]
BMD554	InfB-SPA-Kan (DY330)	*kan*$^+$	[15253427]
BMD555	YihI-SPA-Kan (DY330)	*kan*$^+$	[15253427]
BMD556	YjeQ-SPA-Kan (DY330)	*kan*$^+$	[15253427]
BMD557	SmpB-SPA-Kan (DY330)	*kan*$^+$	[15253427]
BMD558	SrmB-SPA-Kan (DY330)	*kan*$^+$	[15253427]
BMD559	Δ*vacB* (KanR excised)	--	This study
BMD592	VacB-Δ*basic* (KanR excised)	--	This study
BMD596	VacB-Δ*S1+basic* (KanR excised)	--	This study
BMD600	VacB-full length (KanR inserted and excised after stop codon)	--	This study

BMD604	Δ*ppk* (KanR excised) VacB-Δ*basic* (KanR excised)	--	This study
BMD608	Δ*ppk* (KanR excised) VacB-Δ*S1+basic* (KanR excised)	--	This study
BMD612	Δ*ppk* (KanR excised) VacB-full length (KanR inserted and excised after stop codon)	--	This study
BMD616	Δ*vacB* (KanR excised)	--	This study
BMD669	VacB-S1+basic K-R (kanR excised)	--	This study
BMD671	VacB-basic K-R (KanR excised) Δppk1 (KanR excised)	--	This study
BMD709	Δ*yjeQ*::KanR	*kan*$^+$	This study
BMD711	Δ*ppk* (KanR excised) Δ*yjeQ*::KanR	*kan*$^+$	This study
BMD713	Δ*srmB*::KanR	*kan*$^+$	This study
BMD715	Δ*ppk* (KanR excised) Δ*srmB*::KanR	*kan*$^+$	This study
BMD724	Δ*yihI*::KanR	*kan*$^+$	This study
BMD726	Δ*yihI*::KanR Δ*ppk* (KanR excised)	*kan*$^+$	This study
BMD581	*ScPPX1*-pBAD18 (AmpR)	*amp*$^+$	This study
BMD585	pBAD18 EV (AmpR)	*amp*$^+$	This study

S3 Table-Tab 2 – Plasmids used in this study. For each plasmid's source, Addgene catalog number and references see online version of the table.

Plasmid	Description	Marker	Temp. sensitivity
pKD46	RED recombineering plasmid for site directed mutagenesis – arabinose inducible	*amp*$^+$	30°C
pSIM6	RED recombineering plasmid for site directed mutagenesis – temperature inducible 42°C	*amp*$^+$	30°C
pSUB11	Template plasmid for creating c-terminal 3xFlag epitope tag using recombineering. Kanamycin selection marker is flanked by FRT recognition sites for excision.	*amp*$^+$, *kan*$^+$	--
pKD4	Template plasmid for using recombineering to delete genes with a FRT flanked kanamycin cassette	*amp*$^+$, *kan*$^+$	--
pCP20	Constitutively expressed FLP recombinase for excision of selection markers flanked by FRT sites	*amp*$^+$, *cam*$^+$	30°C
pYihI	pGEX4T1 expressing GST-YihI	*amp*$^+$	37°C
pYihI-N-term K-R	pGEX4T1 expressing GST-YihI with N-term lysines (K) mutated to arginine (R)	*amp*$^+$	37°C
pYihI-C-term K-R	pGEX4T1 expressing GST-YihI with C-term lysines (K) mutated to arginine (R)	*amp*$^+$	37°C
pYihI-N+C-term K-R	pGEX4T1 expressing GST-YihI with N+C-term lysines (K) mutated to arginine (R)	*amp*$^+$	37°C
pYihI-All K-R	pGEX4T1 expressing GST-YihI with all lysines (K) mutated to arginine (R)	*amp*$^+$	37°C
pYihI-N-term D-N/E-Q	pGEX4T1 expressing GST-YihI with N-term aspartic acids (D) mutated to asparagine (N) and glutamic acids (E) mutated to glutamine (Q)	*amp*$^+$	37°C
pYihI-N-term S-A	pGEX4T1 expressing GST-YihI with N-term serines (S) mutated to alanine (A)	*amp*$^+$	37°C
pYihI-N-term D-A/E-L	pGEX4T1 expressing GST-YihI with N-term aspartic acids (D) mutated to alanine (A) and glutamic acids (E) mutated to leucine (L)	*amp*$^+$	37°C
pRnr-CSD	pGEX4T1 expressing the GST-VacB cold shock domains (CSD) I and II (amino acids 1 to 648)	*amp*$^+$	37°C
pRnr-ND	pGEX4T1 expressing the GST-VacB nuclease domain (amino acids 649 to 1929)	*amp*$^+$	37°C
pRnr-S1BD	pGEX4T1 expressing the GST-VacB S1 domain and basic domain (amino acids 1930 to 2442)	*amp*$^+$	37°C
pBAD18	pBAD18 empty vector	*amp*$^+$	37°C
pScPPX1	pBAD18 expressing *Saccharomyces cerevisiae* Ppx1	*amp*$^+$	37°C

3.11. Supplemental Data

S1 Data. Raw data used to determine frequence of proteins with a PASK motif in bacteria in (Figures 1A and S1A)
See online: [supplements/637445_file07.xlsx]

S2 Data. Raw data used to graph YihI (Figure 2C) and Rnr (Figure 4C) disorder propensity graphs.
See online: [supplements/637445_file08.xlsx]

CHAPTER 4 – DISCUSSION

Statement of rights and permissions

(1) *McCarthy, L., ***Baijal, K.**, & Downey, M. (2024) A framework for understanding and investigating polyphosphate-protein interactions. *Biochemical Society Transactions*, 21:BST20240678. https://doi.org/10.1042/BST20240678.
*Co-first authors

The following sections of this chapter were reproduced from the review article listed above (2024), of which I am a first co-author. Some sections were further adapted to fit the discussion with new ideas.

Sections: 4.6. to 4.9.

Note, apart from section 4.7., that was strictly reproduced, new ideas have been incorporated into the other sections to tailor the discussion to the manuscripts presented in my thesis.

(2) **Baijal, K.**, & Downey, M. (2021). Targeting polyphosphate kinases in the fight against *Pseudomonas aeruginosa*. *mBio*, 12(4), e0147721. https://doi.org/10.1128/mBio.01477-21.

The last section in this chapter was reproduced and adapted from the commentary listed above (2021), of which I am a first author.

Section: 4.11.

This section has been adapted to discuss ideas specific to the manuscripts presented in my thesis.

4.1. Polyphosphate plays an adaptive role during starvation in *E. coli*

The collection of work presented in this thesis underscores the role of polyphosphate (polyP) in helping *Escherichia coli* adapt to stress. Our mass spectrometry analysis revealed significant proteomic differences between wild-type *E. coli* and Δ*ppk* mutants, that are unable to produce polyP. While wild-type cells upregulated pathways necessary for adapting to nutrient starvation, Δ*ppk* mutants failed to do so. Additionally, Δ*ppk* mutants exhibited slow growth phenotypes, which could only be partially rescued by add back of amino acids.

Looking forward, it would be valuable to explore how the role of PPK and polyP extends to other polyP-inducing stress conditions. *In E. coli*, and some other bacterial species, this is in part complicated by the fact that the exact trigger for polyP accumulation is not known. For instance, in our studies, polyP accumulation was induced by switching cultures from nutrient rich LB media to MOPS minimal media for 3 hours, eliciting a response specific to nutrient adaptation. Other researchers have utilized stressors such as hypochlorous acid (or bleach) and cisplatin (an antimicrobial that elicits iron toxicity) treatment to promote oxidative stress-induced polyP accumulation in *E. coli* (1,2). Additionally, polyP accumulation has been observed in response to nitrogen starvation and osmotic stress (3).

Given the growing list of stressors associated with polyP accumulation, a critical question arises: what exactly triggers polyP accumulation under these various conditions? Further, how do differences in the trigger between these conditions affect the translatability of our findings? These questions also highlight the need to investigate how variations in polyP regulation among bacteria may influence its role in stress adaptation.

Recent gene expression analysis suggests that the response to cisplatin, for example, involves the upregulation of pathways (e.g. SOS response, Fur regulon, iron uptake and iron-sulfur

cluster assembly) that differ from those activated in response to nutrient starvation in our study (2). However, some overlap was observed in the PPK-dependent expression of genes related to amino acid transport, translation, ion homeostasis and amino acid synthesis (2). This underscores the complexity of polyP's role across different stressors. Perhaps, the PPK* allele, which produces polyP in the absence of a stressor (4), can be used to identify functions of polyP that are independent of stress.

4.2. PPK regulates ribosome biogenesis and translation related processes

Our mass spectrometry data revealed that during the first 3 hours of nutrient starvation, wild-type *E. coli* upregulated proteins involved in restoring the availability of amino acids and small molecules. In contrast, Δ*ppk* mutants primarily upregulated proteins associated with ribosome biogenesis and translation. We interpret this as reflecting processes that were already active in Δ*ppk* mutants growing in nutrient rich media, which suggests their failure to effectively recognize and adapt to the stressor. However, a more direct comparison of Δ*ppk* mutants before and after nutrient downshift is needed to definitively confirm this interpretation.

Growth analysis further indicated that, although Δ*ppk* mutants did not match the growth rate of wild-type cells, they were still able to achieve a phase of exponential growth. Similarly, the expression of ArnC-3Flag, which is upregulated in wild-type cells compared to Δ*ppk* mutants after 3 hours in MOPS, becomes comparable between the two strains in overnight cultures. These findings suggest that even in the absence of PPK, mutant cells can regulate the expression of certain pathways identified in our mass spectrometry data as to be PPK-dependent. However, the question remains: to how many of the differentially expressed proteins in our dataset does this apply to, and what mechanisms are involved in compensating for the loss of PPK? Additionally,

do ribosome biogenesis and translation related proteins become downregulated in Δ*ppk* mutants before they enter exponential growth after the extended lag phase?

A time-course proteomic analysis would be valuable in answering these questions, helping to identify other proteins that could compensate for the role of PPK during nutrient starvation. Such an analysis would provide a deeper understanding of how *E. coli* balances PPK-dependent and -independent pathways to adapt to nutrient stress.

4.3. It is unclear how PPK or polyP activate the BasRS two-component system

In this work we established that PPK-dependent misregulation of the BasRS two-component system is responsible for differential expression of the Arn proteins between wild-type and Δ*ppk* mutants. Since two-component systems regulate their own expression, we hypothesize that PPK is somehow responsible for activating BasRS, either directly via polyP, or indirectly through other pathways impacted by the loss of *ppk*. One potential indirect mechanism of regulation involves BasS, which detects and becomes activated by high iron levels. Although, MOPS media contains low iron (0.01 mM) compared to >0.2 mM that is needed to activate BasS in nutrient rich media, our data with the iron chelator BPS suggests that iron is playing a role in this activation.

Furthermore, because BasS is located within the inner membrane with its sensor domain facing the periplasmic space (5), iron accumulation within the periplasmic space could mimic high iron concentrations. This could result from differences in iron transport or membrane permeability between wild-type and Δ*ppk* mutants, though this remains speculative and requires further testing. One possible approach is to examine the expression of genes involved in iron uptake and utilization, as Δ*ppk* mutants have shown reduced expression of these genes when exposed to

cisplatin treatment (an iron stressor), compared to wild-type *E. coli* (2). Membrane permeability can be assessed using an envelope integrity assay (6). Alternatively, polyP could directly act as a substrate for BasRS activation which can be tested using an *in vitro* phosphorylation assay (7).

4.4. Further investigation into the mass-spectrometry dataset

Overall, our mass spectrometry dataset serves as a valuable resource to identify proteins, and pathways, that function in a PPK- or polyP-dependent manner. It can be utilized by researchers to uncover proteins within various pathways that may not have been previously known to be regulated by PPK. Moreover, the dataset includes several intriguing proteins that have yet to be validated and investigated. For example, the AsmA protein, which is significantly upregulated in wild-type cells compared to Δ*ppk* mutants, remains poorly understood. However, AsmA and AsmA-like proteins are thought to play roles in membrane assembly and in the transport of newly synthesize lipopolysaccharide molecules between the inner and outer membranes (8,9). Once validated, the potential interaction between PPK or polyP and AsmA could offer new insight into AsmA function and how bacteria maintain membrane homeostasis under stress conditions.

Gene ontology (GO) and gene set enrichment analysis (GSEA) of our dataset suggests that polyP plays a role in the regulation of ribosome biogenesis and translation processes. Previous work by McInerney *et al.* (10) demonstrated that polyP binds to the 70S ribosome, and its subunits (50S and 30S), from *E. coli in vitro*. The loss of polyP binding may contribute to increased amino acid misincorporation and higher frequency of stop-codon read-through by ribosomes from Δ*ppk* mutants (10). Additionally, they observed a reduction in polysome-associated ribosomes in Δ*ppk* mutants compared to wild-type cells (10). These findings align with disrupted polysome profiles observed in *vtc4*Δ mutant yeast (11). However, the analysis by McInerney *et al.* (10) was conducted

in nutrient rich media, where there is no detectable polyP accumulation, leaving the effects of polyP on ribosome function unaddressed.

To further investigate how polyP regulates ribosome function, we can perform a series of complementary experiments. Ribosome profiling, for example, could capture a 'snapshot' of transcripts that are actively being translated by ribosomes, providing insight into the abundance of translated transcripts, protein synthesis rates and translation efficiency of ribosomes that are assembled in the absence and presence of polyP (12). Additionally, ribosome assembly defects between wild-type and Δ*ppk* mutants exposed to polyP-inducing conditions can be assessed using sucrose density gradient to separate and quantify different ribosomal subunits and polysomes (11,13,14).

Furthermore, RNA sequencing (RNA-Seq) could be employed to explore how polyP influences mRNA stability, potentially revealing new pathways by which polyP modulates gene expression (15). Together, these techniques will provide a comprehensive view of how polyP regulates ribosome function and translation processes in bacteria.

4.5. PolyP binds bacterial proteins involved in ribosome biogenesis and translation control

To further investigate how polyP mechanistically regulates stress adaptation, we identified 7 bacterial proteins that can bind polyP. All 7 of these proteins (YihI, RsgA or YjeQ, SrmB, SmpB, Rnr, Rne and InfB) were also detected in our mass spectrometry dataset (**Chapter 2 – S1 Table-Tab 1**) but were not found to be significantly differentially expressed between wild-type and Δ*ppk* mutants. Therefore, in contrast to the adaptor-like role of polyP in mediating Lon-dependent degradation of proteins, this suggests an exciting alternative role for polyP binding to our ribosome- and translation-related targets.

For example, stress induced polyP was previously shown to drive the formation of HP-bodies (bacterial inclusion bodies that form by phase separation) that sequester and protect poly-adenylated mRNA and play a role in heterochromatin formation (3,16). Recently, polyP-dependent localization of proteins involved in ribonucleoprotein complex assembly and ribosome biogenesis to HP-bodies was investigated (3). Of these HP-body localizing proteins were polyP-binding proteins identified by our screen (InfB, SmpB) and Der which is the GTPase activated by YihI, another polyP-binding protein. Additionally, Lon was found within these condensates, as well as PPK itself. However, included in the dataset are additional proteins whose polyP binding affinities are unknown. Therefore, it would be interesting to further investigate how polyP-protein binding events are coordinated and contribute to HP-body formation.

Additionally, proteins affected by PPK expression, including those identified by our mass spectrometry analysis, may be potential targets of polyP-binding. For instance, BasS and BasR were not included in the SPA- and TAP-collection sets, meaning that they were not screened for polyP-binding. As such, we do not rule out the possibility that their regulation may be directly influenced by polyP-binding.

4.6. PolyP can only bind targets upon contact

Overall, bacteria serve as an excellent model organism to study the *in vivo* functions of polyP-protein binding. One key advantage is the ability to regulate polyP accumulation in response to environmental changes, such as shifting from nutrient-rich to minimal media, providing precise temporal control over polyP levels (17). Additionally, the enzymes responsible for polyP synthesis and degradation in bacteria are well understood, and bacterial cells exhibit relatively simple subcellular organization compared to eukaryotes, like budding yeast, where polyP is mainly stored

in the vacuole (18). Despite these advantages, not all our polyP-binding targets show shifts in the presence of endogenous polyP, prompting further investigation to determine subcellular localization of polyP-binding proteins with respect to polyP and PPK. For instance, in *Pseudomonas aeruginosa* and *E. coli*, polyP may be organized into granules which facilitate interactions with target proteins (3,19). Evidence for this is seen with the RNA-binding protein Hfq in *E. coli,* which forms phase separated condensates (or HP-bodies) potentially involved in heterochromatin formation (3,16).

Furthermore, the 7 polyP-binding proteins identified by our screen do not contain known polyP binding elements such as PASK, polyLys, and polyHis motifs. Instead, these proteins may reveal novel polyP-binding motifs. Unlike eukaryotes, where PASK motifs are common, bacteria may not rely on such motifs due to differences in polyP localization. Notably, when polyP is forcibly synthesized by expression of the *E. coli* PPK in different environments, such as outside of the vacuole in yeast or at high concentrations in human cells, it is toxic. These factors could be indicative of different modes of regulating polyP-binding events that are dependent on cellular polyP-organization. This may be especially important given the non-enzymatic mode of attachment of polyP to proteins. Additionally, length of polyP chains may influence how polyP interacts with binding proteins, affecting both the binding mechanism and the resulting functional outcomes. This is similar to how different chain lengths impact the immune response, where shorter and longer chains can elicit distinct signalling effects (20–22).

4.7. Regulation of polyP-protein binding in bacteria

In addition to regulation by localization, another important consideration that has not been explored in detail is the potential interplay between post-translational modifications and polyP

binding. Direct modification of lysine residues, by acetylation or methylation for example (23,24), could alter the net charge of amino acids and prevent polyP from interacting with them. The ability of the polyphosphatases enzymes to degrade polyP chains makes them candidate regulators that could turn off or dampen signaling cascades initiated by polyP-protein interactions. *In vitro* work has shown that recombinant yeast Ppx1 can cleave protein-bound polyP (25), and many studies have used exogenous Ppx1 expression to study the effects of polyP in mammalian cells (26,27). Polyphosphatases were initially proposed to remove the covalently interacting polyP chains from proteins (25,28,29), although there is no reason to assume that the mode of interaction would have any bearing on the ability of these enzymes to act on polyP bound to protein targets. Understanding how these polyphosphatases are regulated could shed light on pathways mediated by polyP-protein interactions. Since most polyphosphatase enzymes are dependent on cations for their function (30), we speculate that local concentrations of these cofactors are important determinants for the reversal of polyP-protein interactions *in vivo*.

4.8. Bridging the gap from *in vitro* binding to *in vivo* function of polyP-protein interactions

Despite the growing list of polyP-binding proteins identified, there is still limited evidence supporting functions for polyP binding *in vivo*. So, how can we begin to test if the observed effects are due to the loss of polyP interaction? We think genetic experiments offer the most compelling approach. In bacteria, this is somewhat simplified because polyP exists within the same compartment as the target proteins, and the polyP synthetase, PPK, is well-characterized. Additionally, a switch from nutrient rich to minimal media can be used to stress cells and trigger a polyP-dependent response. However, regardless of the model organism, we expect that cells expressing mutant versions of the target proteins, which cannot bind to polyP, will exhibit similar

phenotypes to cells mutated for polyP synthetase enzymes (Δ*ppk* mutants, for example). Critically, the mutants should behave epistatically, meaning that the phenotype of the double mutant should not be more dramatic than that of the stronger single mutant. Of course, this ideal scenario could be complicated by complex genetic interactions, especially if polyP affects multiple proteins (directly or indirectly) feeding into the same biological readout.

In our epitasis analysis of Rnr-polyP binding, we observed a complex genetic interaction. Loss of *rnr* in a Δ*ppk* mutant background rescued the growth defects of Δ*ppk* single mutants, making them comparable to wild-type cells. This rescue depended on the polyP binding region of Rnr (C-terminal S1 + basic domain), but it was independent of polyP binding itself. To assess phenotypic changes linked to polyP-binding, we used lysine to arginine mutations. However, these mutations had no noticeable impact on wild-type growth. The double mutant (Δ*ppk rnr*$^{\text{S1+Basic K-R}}$) exhibited a more sever slow-growth phenotype than the single (*rnr*$^{\text{S1+Basic K-R}}$) mutant. This finding disproved our initial hypothesis that polyP-binding to the Rnr S1+basic domain was required during stress and in its absence, Rnr retained activity that was toxic to the cell.

However, an important consideration is the type of mutation made. Lysine to arginine mutations seem to prevent interaction of PASK (and polyHis or polyLys) proteins with polyP as judged by NuPAGE analysis (11,25,31,32), but it is unclear whether they fully prevent interaction *in vivo*. More substantial mutations, lysine to alanine substitutions, may more effectively disrupt polyP binding *in vivo,* but they could also be more likely to impact target stability and function, independent of polyP-binding. Furthermore, since polyP-binding proteins in *E. coli* are involved in related functions, we wonder if lysine to arginine mutation of several of these proteins' binding regions might be required to observe phenotypic changes resulting from the loss of polyP-binding.

4.9. Teasing apart the direct versus indirect effects of polyP

An important consideration in understanding how polyP is acting mechanistically is to distinguish between its direct versus indirect roles.

Delineating between direct and indirect effects of polyP-protein binding is complicated by its highly anionic nature and ability to form electrostatic interactions with molecules other than proteins (33–35). For example, it is not surprising that enzymes requiring cationic cofactors might be inhibited by polyP that sequesters these in solution. Also, polyP, in the presence of cations, can induce liquid-liquid phase separation (36–38), which may promote polyP-protein interactions. Evidence suggests that polyP can interact with the Hfq protein from *E. coli*, forming phase-separated condensates *in vitro* that may be functionally relevant for heterochromatin formation *in vivo* (16). Similarly, the positively charged green fluorescent protein (+36GFP) colocalizes with polyP granules during nutrient starvation when expressed in *Citrobacter freundii* and forms phase separated condensates in the presence of polyP *in vitro,* although direct polyP binding has not been demonstrated (38). Whether direct polyP-protein interactions in these condensates are required for the observed effects remains an open question. An important control would be to test whether phase separation in the absence of polyP yields similar outcomes.

In contrast, indirect effects of polyP can arise from its influence on cellular processes. In both our work and others' studies in the bacterial-polyP field, conclusions about polyP's role are often drawn by comparing wild-type cells to Δ*ppk* mutants. GO term and GSEA analysis of our mass spectrometry data revealed significant differences in the biological processes occurring between wild-type and Δ*ppk* mutant cells. Therefore, it is plausible that what might be interpreted as a direct effect of polyP, in fact, could stem from metabolic or regulatory shifts resulting from the loss of PPK. This complicates epistatic analysis of polyP-protein binding as the broader

changes in cellular processes can obscure the direct effects of polyP-binding to specific targets. Therefore, care must be taken to avoid attributing Δ*ppk* mutant phenotypes solely to changes in polyP metabolism.

To overcome this, we propose creating polyP-deficient strains that lack the slow growth phenotype of Δ*ppk* mutants to reassess polyP's role in the bacterial stress response. Identifying growth suppressors or expressing an exopolyphosphatase (like the highly active *Saccharomyces cerevisiae* Ppx1) to degrade polyP in wild-type cells upon the MOPS switch may help. Alternatively, an inducible bacterial degron system could be used to temporally control PPK degradation and prevent polyP accumulation (39,40). This type of system could also enable a deeper understanding of the *in vivo* kinetics of polyP degradation, by the exopolyphosphatase PPX, which degrades polyP chains from the molecule's end (18). In contrast, PPK inhibitors may not be as effective for this purpose due to their stochastic effect. Finally, identifying the exact trigger for PPK activation could further provide a solution to this issue.

4.10. Exploiting PPK and polyP biology for antimicrobial therapy

With the rise in multidrug resistant (MDR) bacterial infections, there is an increasing push for alternative antimicrobial strategies. Our work validates PPK as a target to sensitize bacteria to last-resort antimicrobials such as polymyxin B. Polymyxins are cationic antimicrobial peptides that have off target effects due to the lack of specificity between human and microbial membranes (41,42). This challenge is compounded when bacteria modify their membranes with positively charged lipid A modifications, which reduce polymyxin efficacy (43). Consequently, PPK inhibitors could be useful tools to lower the minimum inhibitory concentration (MIC) of polymyxins required for effective treatment.

In the case of polymyxin resistance, the WD101 strain acquires resistance through two amino acid substitutions (A42T and G53E) in the BasR allele (44). However, polymyxin resistance can also arise from other mutations in BasRS, and within other two-component systems, which extend beyond *E. coli* to other species of bacteria (summarized in this review (45) by Olaitan *et al.*). These two-component systems include PhoPQ, ParRS, ColRS and CprRS (45,46). Additionally, resistance can be mediated through changes in efflux pump activity and capsule formation (47,48). Testing the role of PPK and polyP in mediating resistance via these alternative mechanisms could provide valuable insight.

Furthermore, bacteriophage therapy is gaining traction as a promising strategy to fight MDR bacteria, and it would be intriguing to explore whether bacterial polyP contributes to phage defense mechanisms. This area of research could open new avenues for understanding polyP's broader protective roles in bacterial survival.

Moreover, polyP's role may be physiologically relevant under harsh conditions, such as in the gut, where pH fluctuations and oxidative stress are common, or at infection sites, where there is competition for nutrients. Biofilms—where persister cells that are resistant to antimicrobials are present—are also thought to have nutrient gradients which could mimic nutrient starvation (49). In these environments, polyP may play a critical role in bacterial survival.

Finally, as a step towards clinical applications, testing the effects of known PPK inhibitors, such as mesalamine and gallein, on Bas-Arn expression, lipid A modifications, and PPK-dependent polymyxin resistance would be valuable. Additionally, this research could explore their synergistic effect with polymyxins in treating resistant infections. Together, this could drive forward the motivation to explore novel PPK inhibitors as therapeutic options.

4.11. Application of PPK inhibitors beyond the clinic

Beyond their potential clinical applications for treating bacterial infections, PPK inhibitors like mesalamine and gallein can serve as powerful tools for studying the fundamental aspects of PPK biology in bacteria. For example, if a significant loss of polyP can be achieved by PPK inhibition, this approach may help researchers identify new roles for PPK and phenotypes for PPK-deficient cells while avoiding genetic manipulations of the *ppk* gene.

Notably, researchers could streamline the screening of available mutant collection sets in the presence and absence of PPK inhibitors, for example, to define synthetic lethal relationships and thereby map the landscape of PPK and polyP biology. In our lab we are interested in testing if two-component systems are involved in regulating polyP accumulation. As opposed to mutating *ppk* in each strain background, PPK inhibitors can be utilized for screening. Additionally, the polymyxin resistant variants listed above can be rapidly screened in the absence and presence of PPK inhibitors, such as gallein and mesalamine, to test the involvement of PPK. This method not only moves us closer to the clinic but also offers a versatile tool for advancing our understanding of polyP's diverse biological functions.

4.12. References

1. Gray MJ, Wholey WY, Wagner NO, Cremers CM, Mueller-Schickert A, Hock NT, et al. Polyphosphate Is a Primordial Chaperone. Mol Cell. 2014;53(5):689–99.
2. Beaufay F, Quarles E, Franz A, Katamanin O, Wholey WY, Jakob U. Polyphosphate functions in vivo as an iron chelator and fenton reaction inhibitor. mBio. 2020;11(4):1–14.
3. Guan,J., Hurto,RL., Rai,A., Azaldegui,CA., Ortiz-Rodríguez, LA., Biteen,JS., Freddolino,L., Jakob U. HP-Bodies – Ancestral Condensates that Regulate RNA Turnover and Protein Translation in Bacteria. BioRxiv. 2025;
4. Rudat AK, Pokhrel A, Green TJ, Gray MJ. Mutations in Escherichia coli polyphosphate kinase that lead to dramatically increased in vivo polyphosphate levels. J Bacteriol. 2018;200(6).
5. Perez JC GEA. Acid pH activation of the PmrA/PmrB two-component regulatory system of Salmonella enterica. Mol Microbiol. 2007;63(1):283–93.
6. Baker KR, Jana B, Franzyk H GL. A High-Throughput Approach To Identify Compounds That Impair Envelope Integrity in Escherichia coli. Antimicrob Agents Chemother. 2016;60(10):5995–6002.
7. Yamamoto K, Hirao K, Oshima T, Aiba H, Utsumi R IA. Functional characterization in vitro of all two-component signal transduction systems from Escherichia coli. J Biol Chem. 2005;280(2):1448–56.
8. Deng M MR. Examination of AsmA and its effect on the assembly of Escherichia coli outer membrane proteins. Mol Microbiol. 1996;21(3):605–12.
9. Kumar S RN. Bacterial AsmA-Like Proteins: Bridging the Gap in Intermembrane Phospholipid Transport. Sage Journals. 6:1–9.
10. McInerney P, Mizutani T, Shiba T. Inorganic polyphosphate interacts with ribosomes and promotes translation fidelity in vitro and in vivo. Mol Microbiol. 2006;60(2):438–47.
11. Bentley-DeSousa A, Holinier C, Moteshareie H, Tseng YC, Kajjo S, Nwosu C, et al. A Screen for Candidate Targets of Lysine Polyphosphorylation Uncovers a Conserved Network Implicated in Ribosome Biogenesis. Cell Rep. 2018;22(13):3427–39.
12. Brar, GA., Weissman JS. Ribosome profiling reveals the what, when, where and how of protein synthesis. Mol Cell Biol. 2015;16(11):651–64.
13. Chassé H, Boulben S, Costache V, Cormier P MJ. Analysis of translation using polysome profiling. Nucleic Acids Res. 2017;45(3):e15.
14. Dos Santos RF, Bárria C, Arraiano CM AJM. Isolation and Analysis of Bacterial Ribosomes Through Sucrose Gradient Ultracentrifugation. Methods Mol Biol. 2020;2106:299–310.
15. Croucher NJ TNR. Studying bacterial transcriptomes using RNA-seq. Curr Opin Microbiol. 2010;13(5):619–24.
16. Beaufay F, Amemiya HM, Guan J, Basalla J, Meinen BA, Chen Z, et al. Polyphosphate drives bacterial heterochromatin formation. Sci Adv. 2021;7(52).
17. Kuroda A, Tanaka S, Ikeda T, Kato J, Takiguchi N, Ohtake H. Inorganic polyphosphate kinase is required to stimulate protein degradation and for adaptation to amino acid starvation in Escherichia coli. Proc Natl Acad Sci U S A. 1999;96(25):14264–9.
18. Denoncourt A, Downey M. Model systems for studying polyphosphate biology: a focus on microorganisms. Vol. 67, Current Genetics. 2021. p. 331–46.

19. Racki LR, Tocheva EI, Dieterle MG, Sullivan MC, Jensen GJ, Newman DK. Polyphosphate granule biogenesis is temporally and functionally tied to cell cycle exit during starvation in Pseudomonas aeruginosa. Proc Natl Acad Sci U S A. 2017;114(12):E2440–9.
20. Roewe J, Stavrides G, Strueve M, Sharma A, Marini F, Mann A, et al. Bacterial polyphosphates interfere with the innate host defense to infection. Nat Commun [Internet]. 2020;11(1):1–12. Available from: http://dx.doi.org/10.1038/s41467-020-17639-x
21. Rijal R, Cadena LA, Smith MR, Carr JF, Gomer RH. Polyphosphate is an extracellular signal that can facilitate bacterial survival in eukaryotic cells. Proc Natl Acad Sci U S A. 2020;117(50):31923–34.
22. Brandt S, Krauel K, Jaax M, Renné T, Helm CA, Hammerschmidt S, et al. Polyphosphates form antigenic complexes with platelet factor 4 (PF4) and enhance PF4-binding to bacteria. Thromb Haemost. 2015;114(6):1189–98.
23. Azevedo C, Saiardi A. Why always lysine? The ongoing tale of one of the most modified amino acids. Adv Biol Regul. 2016;60:144–50.
24. Wang ZA, Cole PA. The Chemical Biology of Reversible Lysine Post-translational Modifications. Cell Chem Biol. 2020;27(8):953–69.
25. Azevedo C, Livermore T, Saiardi A. Protein polyphosphorylation of lysine residues by inorganic polyphosphate. Mol Cell. 2015;58(1):71–82.
26. Abramov AY, Fraley C, Diao CT, Winkfein R, Colicos MA, Duchen MR, et al. Targeted polyphosphatase expression alters mitochondrial metabolism and inhibits calcium-dependent cell death. Proc Natl Acad Sci U S A. 2007;104(46):18091–6.
27. Wang L, Fraley CD, Faridi J, Kornberg A, Roth RA. Inorganic polyphosphate stimulates mammalian TOR, a kinase involved in the proliferation of mammary cancer cells. Proc Natl Acad Sci U S A. 2003;100(20):11249–54.
28. Bentley-DeSousa A, Downey M. From underlying chemistry to therapeutic potential: open questions in the new field of lysine polyphosphorylation. Vol. 65, Current Genetics. 2019. p. 57–64.
29. Azevedo C, Saiardi A. The new world of inorganic polyphosphates. Biochem Soc Trans. 2016;44:13–7.
30. McCarthy L, Downey M. The emerging landscape of eukaryotic polyphosphatases. FEBS Lett. 2023;597(11):1447–61.
31. Neville N, Lehotsky K, Yang Z, Klupt KA, Denoncourt A, Downey M, et al. Modification of histidine repeat proteins by inorganic polyphosphate. Cell Rep. 2023;42(9).
32. Neville N, Lehotsky K, Klupt KA, Downey M, Neville N, Lehotsky K, et al. Polyphosphate attachment to lysine repeats is a non-covalent protein modification. Mol Cell. 2024;84(9):1802–10.
33. Cramer CL DRH. Polyphosphate-cation interaction in the amino acid-containing vacuole of Neurospora crassa. J Biol Chem. 1984;259(8):5152–7.
34. Toso DB, Henstra AM, Gunsalus RP ZZH. Structural, mass and elemental analyses of storage granules in methanogenic archaeal cells. Environ Microbiol. 2011;13(9):2587–99.
35. Onaka, T., Miyajima, T., Ohashi S. On the binding of magnesium to long-chain polyphosphate ions. J Inorg Nucl Chem. 1981;43(12):3323–7.
36. Borghi, F., Azevedo, C., Johnson, E., Burden, J.J. and Saiardi A. A mammalian model reveals inorganic polyphosphate channeling into the nucleolus and induction of a hyper-condensate state. Cell Rep Methods. 2024;4(7):100814.

37. Furuki T, Togo A, Usuda H, Nobeyama T, Hirano A SK. Monovalent Ion Effect on Liquid-Liquid Phase Separation of Aqueous Polyphosphate-Salt Mixtures. J Phys Chem B. 2024;128(26):11435–40.
38. Wang X, Shi C, Mo J, Xu Y, Wei W ZJ. An Inorganic Biopolymer Polyphosphate Controls Positively Charged Protein Phase Transitions. Angew Chem Int Ed Engl. 2020;59(7):2679–83.
39. Izert MA, Klimecka MM GMW. Applications of Bacterial Degrons and Degraders - Toward Targeted Protein Degradation in Bacteria. Front Mol Biosci. 2021;8:669762.
40. Jadhav P, Chen Y, Butzin N, Buceta J UA. Bacterial degrons in synthetic circuits. Open Biol. 2022;12(8):220180.
41. Mohapatra SS, Dwibedy SK PI. Polymyxins, the last-resort antibiotics: Mode of action, resistance emergence, and potential solutions. J Biosci. 2021;46(3):85.
42. Nang SC, Azad MAK, Velkov T, Zhou QT LJ. Rescuing the Last-Line Polymyxins: Achievements and Challenges. Pharmacol Rev. 2021;73(2):679–728.
43. Moffatt JH, Harper M, Boyce JD. Mechanisms of Polymyxin Resistance. Adv Exp Med Biol. 2019;1145:55–71.
44. Trent MS, Ribeiro AA, Doerrler WT, Lin S, Cotter RJ, Raetz CRH. Accumulation of a polyisoprene-linked amino sugar in polymyxin-resistant Salmonella typhimurium and Escherichia coli: Structural characterization and transfer to lipid A in the periplasm. Journal of Biological Chemistry [Internet]. 2001;276(46):43132–44. Available from: http://dx.doi.org/10.1074/jbc.M106962200
45. Olaitan AO, Morand S, Rolain JM. Mechanisms of polymyxin resistance: Acquired and intrinsic resistance in bacteria. Front Microbiol. 2014;5(NOV):1–18.
46. Iredell J, Brown J, Tagg K. Antibiotic resistance in Enterobacteriaceae: Mechanisms and clinical implications. BMJ (Online). 2016;352.
47. Padilla E, Llobet E, Doménech-Sánchez A, Martínez-Martínez L, Bengoechea JA, Albertí S. Klebsiella pneumoniae AcrAB efflux pump contributes to antimicrobial resistance and virulence. Antimicrob Agents Chemother. 2010;54(1):177–83.
48. Campos MA, Vargas MA, Regueiro V, Llompart CM, Albertí S, Bengoechea JA. Capsule polysaccharide mediates bacterial resistance to antimicrobial peptides. Infect Immun. 2004;72(12):7107–14.
49. Beitelshees M, Hill A, Jones CH, Pfeifer BA. Phenotypic variation during biofilm formation: Implications for anti-biofilm therapeutic design. Materials. 2018;11(7):1–18.

Chapter 5 – APPENDIX A

The promises of lysine polyphosphorylation as a regulatory modification in mammals are tempered by conceptual and technical challenges

Review: Problems and Paradigms

Publication information:
Baijal, K., & Downey, M. (2021). The promises of lysine polyphosphorylation as a regulatory modification in mammals are tempered by conceptual and technical challenges. *BioEssays : news and reviews in molecular, cellular and developmental biology*, *43*(7), e2100058. https://doi.org/10.1002/bies.202100058

Author's contributions:
Conceptualization: K.B., M.D. Supervision: M.D. Writing – original draft: K.B., M.D. Writing – review and editing: K.B., M.D.

The promises of lysine polyphosphorylation as a regulatory modification in mammals are tempered by conceptual and technical challenges

Kanchi Baijal[1,2] & Michael Downey[1,2*]

[1]Department of Cellular & Molecular Medicine, University of Ottawa, Ottawa, Ontario, Canada

[2]Ottawa Institute of Systems Biology, University of Ottawa, Ottawa, Ontario, Canada

* Corresponding author: mdowne2@uottawa.ca

5.1. Abstract

Polyphosphate (polyP) is a ubiquitous biomolecule thought to be present in all cells on earth. PolyP is deceivingly simple, consisting of repeated units of inorganic phosphates polymerized in long energy-rich chains. PolyP is involved in diverse functions in mammalian systems – from cell signaling to blood clotting. One exciting avenue of research is a new non-enzymatic post-translational modification, termed lysine polyphosphorylation, wherein polyP chains are covalently attached to lysine residues of target proteins. While the modification was first characterized in budding yeast, recent work has now identified the first human targets. There is significant promise in this area of biomedical research, but a number of technical issues and knowledge gaps present challenges to rapid progress. In this review, we summarize the current state of the field and introduce existing roadblocks related to the study of lysine polyphosphorylation in higher eukaryotes. We discuss how limited methods to identify targets of polyphosphorylation are further impacted by low concentration, unknown regulatory enzymes and sequestration of polyP into compartments in mammalian systems. Furthermore, we present suggestions on how these obstacles could be addressed or what their physiological relevance may be within mammalian cells.

5.2. Introduction

5.2.1 Polyphosphate – A ubiquitous 'Jack of all trades'

Individual phosphate molecules can be joined together via high-energy phosphoanhydride bonds to form chains called polyphosphates (hereafter referred to as polyP). These simple chains are universally conserved across biological kingdoms. While chains of 3 inorganic phosphate units (Pi) or greater are classified as polyP, longer chains of many hundreds or even thousands of residues are found in both prokaryotic and eukaryotic cells. In bacteria, polyP is synthesized by conserved polyphosphate kinases (PPK1 and/or PPK2), which use ATP or GTP molecules as substrates (1,2). In many bacteria, polyP is not constitutively present but accumulates rapidly in response to stresses (1). On the other hand, polyP accumulation is countered by the action of polyphosphatases (1). For example, *Escherichia coli* PPX is an exopolyphosphatase that degrades long polyP chains starting at the end of the chain (3). In the budding yeast *Saccharomyces cerevisiae*, polyP is synthesized by the vacuolar transporter chaperone (VTC) complex at the vacuolar membrane (4), prior to being stored at high levels (200 mM total cellular concentration, in terms of individual Pi units) in the vacuole lumen (5,6). Yeast polyP can be degraded by a suite of enzymes that include exopolyphosphatases and/or endopolyphosphatases, which cleave the chains internally to give two chains of smaller sizes (7-11). In stark contrast to bacterial and fungal species, the mechanisms for polyP synthesis and turnover in higher eukaryotes remain poorly understood. Neither PPK nor VTC enzymes appear to be conserved in mammals (12). Despite this roadblock, polyP research in humans has pushed ahead. A variety of creative approaches have been used to link polyP to a seemingly eclectic group of functions that include protein quality control (13), diverse aspects of cell signaling (14-17), and blood clotting (18,19). While the molecular mechanisms by which polyP exerts these effects is not completely understood, it is

thought to bind directly to a number of protein targets, and may serve as a hub for cell signaling and protein-protein interactions. Recent work, discussed below, suggests an exciting alternative for how polyP impacts diverse processes at the molecular level.

5.2.2. A new mechanism of action – Polyphosphorylation

In 2015, Azevedo *et al.* made the surprising discovery that polyphosphates can be attached to the lysine residues of yeast proteins Nsr1 (functional homolog of mammalian RNA binding protein Nucleolin) and Top1 (DNA topoisomerase I) as a covalent post-translational modification (PTM) (20). These proteins are modified in regions consisting of polyacidic, serine and lysine amino acids (referred to as PASK clusters) (20).Treatment with chemicals that attack the nitrogen-phosphorus bond formed by polyP attachment to lysine side chains removes polyphosphorylation. Moreover, polyphosphorylation is prevented altogether when PASK lysines are mutated to arginine. While synthesis of polyP itself requires enzymes (in this case the budding yeast VTC complex), the subsequent attachment to lysines does not (20). Thus, lysine polyphosphorylation joins a growing list of non-enzymatic protein modifications that include oxidation, glycation, nitrosylation, and at least under some circumstances, lysine acetylation (21). Mechanistically, polyphosphorylation may regulate the physical interaction of Nsr1 and Top1, as well as their subcellular localization (20). *In vitro* assays also suggest that polyphosphorylation inhibits the DNA topoisomerase activity of Top1 (20), although this effect has yet to be confirmed *in vivo.* Subsequent work by our group screened PASK-containing proteins in budding yeast to identify 23 additional targets of lysine polyphosphorylation in budding yeast, including a conserved network of proteins involved in ribosome biogenesis (22,23). This work suggests that polyphosphorylation may impact many processes, rather than simply being a quirk of Nsr1 and Top1 biology. We

suggest that polyphosphorylation may be a global PTM, although testing this assertion will require further study.

The workflow for studying polyphosphorylation is similar to that proposed for other PTMs (**Figure 1**). The function of polyphosphorylation on additional targets discovered in yeast is unknown, but we suggest that polyP chains may be particularly well suited to disrupt protein-protein or protein-nucleic acid interactions involving polyphosphorylated stretches of amino acids. Indeed, polyP has been shown to disrupt a physical interaction between polyphosphorylated yeast proteins Nsr1 and Top1 (20). Polyphosphorylation could also directly block other lysine based PTMs such as acetylation or ubiquitylation (12). The consequences of polyphosphorylation may depend on the number of lysine residues modified, the length of polyP chains attached, and whether those chains are bound to specific proteins, counter-ions, or other small molecules (**Figure 2**). We and others have discussed these and other intriguing possibilities elsewhere (12,24). The promise of polyphosphorylation as a regulatory modification lies in the possibility that any phenotypes associated with polyP deficiency (both previously described and those yet to be discovered), may ultimately stem from defects in lysine polyphosphorylation. Deciphering these mechanisms will require careful biochemical and genetic analysis of mutant proteins wherein lysines are mutated to prevent polyphosphorylation (**Figure 1**). Importantly, we caution that covalent polyphosphorylation is only one of many ways that polyP could impact cellular functions.

While budding yeast remains fertile ground for probing the function and regulation of lysine polyphosphorylation, work from both our group and a collaborative effort between the Saiardi and Jessen labs demonstrates that human proteins can also be covalently modified by polyP, with 14 confirmed targets to date (22,25) (**Table 1**). The potential for conservation of polyphosphorylation in higher eukaryotes brings new opportunities. But, it also raises unique

questions and caveats that further complicate the proposed workflow outlined in **Figure 1**. This review is dedicated to defining the promises and challenges associated with studying lysine polyphosphorylation in human cells and tissues, as well as recent work and new ideas that begin to address those challenges.

Table 1. Polyphosphorylation targets in human cells. Presence or absence of a PASK cluster is based on the definition put forth by Bentley-DeSousa *et al.* (2018). Herein a PASK cluster is defined as 75% D, E, S, or K amino acids, with a least 1 K, all within a 20 amino acid sliding window.

Target	Function	PASK Motif?	How First Identified?
AP3B1	Protein trafficking[83]	Yes	NuPAGE gel shift[25]
DEK	Chromatin organization[84]	Yes	NuPAGE gel shift[22]
eIF2B5	Translational control[85]	Yes	Protein microarray[25]
eIF5B	Translational control[86]	Yes	NuPAGE gel shift[22]
EYA1	Phosphatase/transcriptional activator[87]	No	Protein microarray[25]
Gelsolin	Actin dynamics[88]	No	Protein microarray[25]
GTF2I	Transcription[89]	No	Protein microarray[25]
HSP90□□□	Protein folding[90]	Yes	NuPAGE gel shift[25]
HSP90B1	Protein folding[91]	Yes	Protein microarray[25]
MESD	Protein chaperone[92]	Yes	NuPAGE gel shift[22]
NOP56	Ribosome biogenesis[93]	Yes	NuPAGE gel shift[22]
Nucleolin	Ribosome biogenesis[94]	Yes	NuPAGE gel shift[22,25]
TTC27	Unknown	No	Protein microarray[25]
UPF3B	Splicing[95]	Yes	NuPAGE gel shift[22]

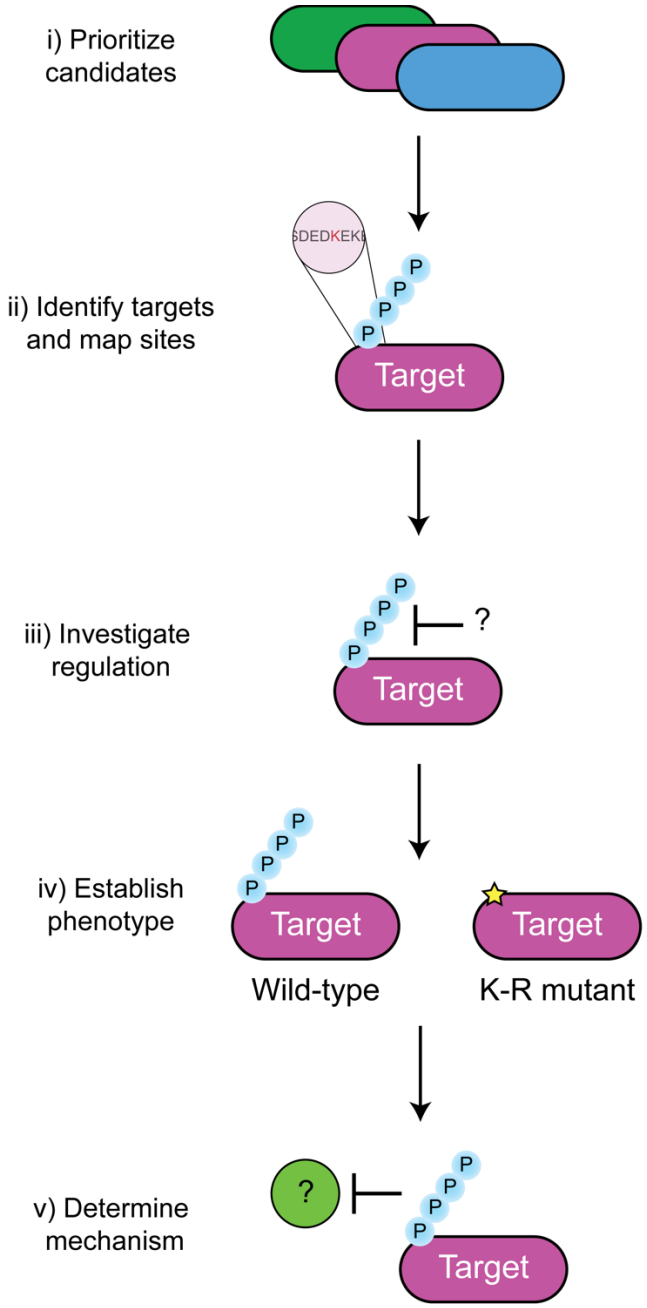

Figure 1. Proposed workflow for characterization of polyphosphorylation targets. Targets can be identified on a candidate basis or as part of large-scale screens. Determining the sites of modification allows for generation of mutant alleles (issuing lysine-arginine mutations) that cannot be polyphosphorylated. Polyphosphorylation regulation is heavily influenced by the synthesis and turnover of polyP itself, and possibly by polyphosphatases acting directly on targets. Phenotypic effects may be best studied at the cell or organism level and are target specific. Mechanisms at play are target specific and could involve changes to protein–protein interactions, subcellular localization, or enzymatic activity

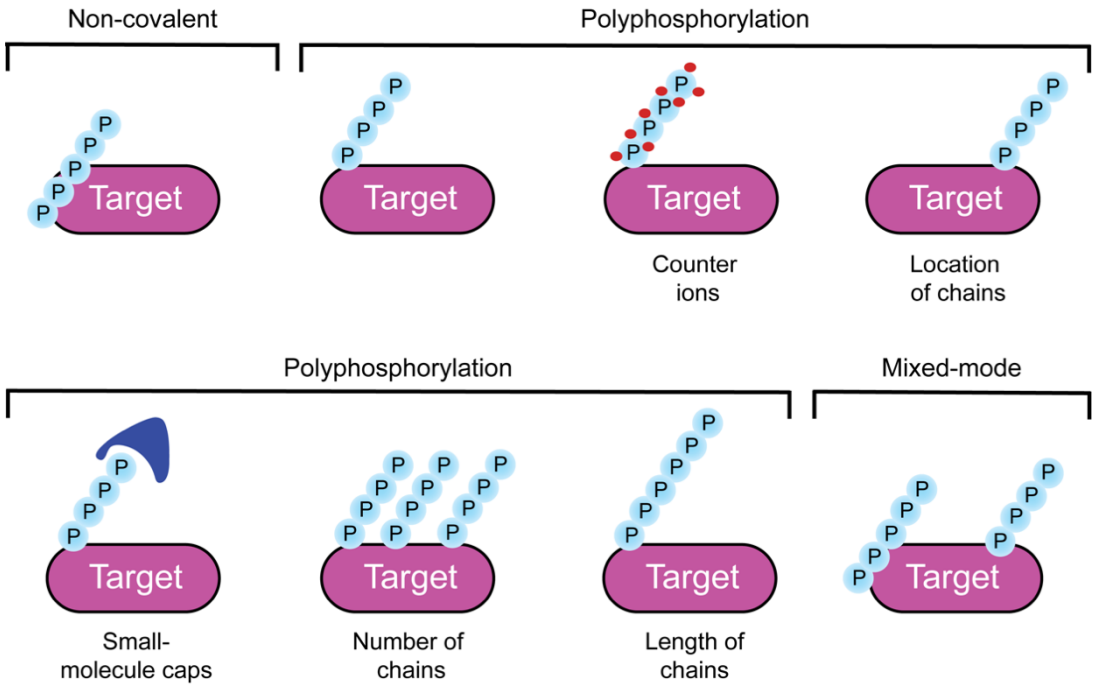

Figure 2. Diversity of polyP chains could impact target function. Interactions can be noncovalent or covalent by polyphosphorylation. Polyphosphorylated chains could exist in a variety of forms that confer different functions. Mixed chain types, including both noncovalent and covalent interactions, may also be possible for some targets

5.3. Problems and Challenges

5.3.1. Broadening the scope of polyphosphorylation in higher eukaryotes

Methods (or lack thereof) that exist to detect polyphosphorylation have challenges that have undoubtedly shaped our current understanding of the modification (**Table 2**). Polyphosphorylation causes an electrophoretic shift of target proteins analyzed on denaturing Bis-Tris gels (sold commercially under the NuPAGE brand name), causing them to migrate slower relative to their unmodified counterparts (20,22) (**Figure 3**). Electrophoretic shifts induced by polyphosphorylation can be extreme, in some cases adding 100 kDa or more to the apparent

molecular weight (20,22). The degree of shift also seems to be correlated with the length of polyP chains and number of lysine residues that are modified, with longer chains and more polyphosphorylated lysines resulting in a larger shift (22). In contrast to NuPAGE, traditional SDS-PAGE page does not resolve polyphosphorylation. While the reason for this is unclear, it may stem from the inclusion of tetramethylethylenediamine (TEMED) as a catalyst in SDS-PAGE gel polymerization (22). TEMED is not usually used in Bis-Tris PAGE polymerization, but its inclusion in the recipe collapses shifts for polyphosphorylated proteins (22). The reason for this effect is currently unknown, although we speculate that TEMED may strip polyP chains from modified lysines (12).

Table 2. Conceptual challenges of current and proposed methods to identify polyphosphorylation targets. The challenges associated with each technique and how it applies to identifying polyphosphorylation targets is listed below. These challenges extend beyond identifying targets in mammalian cells.

.

Proposed Method	Conceptual Challenges
NuPAGE analysis (gel shift)	• Resolving polyP-induced shift requires high polyP concentration and/or longer chain lengths • Requires tagged constructs or validated antibodies against candidate targets • Low throughput • Proteins with only a few modified lysine residues may go undetected
Protein microarray	• Identifies proteins that bind polyP non-covalently as well as covalently • Requires additional confirmation by NuPAGE • Limited to proteins and isoforms included on the arrays
Mass spectrometry	• Theoretical approach – requires development • Enrichment scheme likely required • PolyP chains may be lost during sample preparation for analysis • Complex spectra from fragmentation of polyphosphorylated peptides may be difficult to predict

To date, "NuPAGE analysis" is the only method that has been used to detect polyphosphorylation. In yeast, it is straightforward to compare the migration of proteins isolated from wild-type cells versus cells lacking Vtc4, the catalytic subunit of the polyP synthetase (**Figure 3**) (20,22,23,26). However, in mammalian cells, polyP levels are normally very low and the enzymes that make polyP are unknown (see below for a full discussion of these issues). We previously circumvented this problem in HEK293T cells by ectopically expressing the *E. coli* PPK enzyme (*Ec*PPK) (15,22) (**Figure 3**).

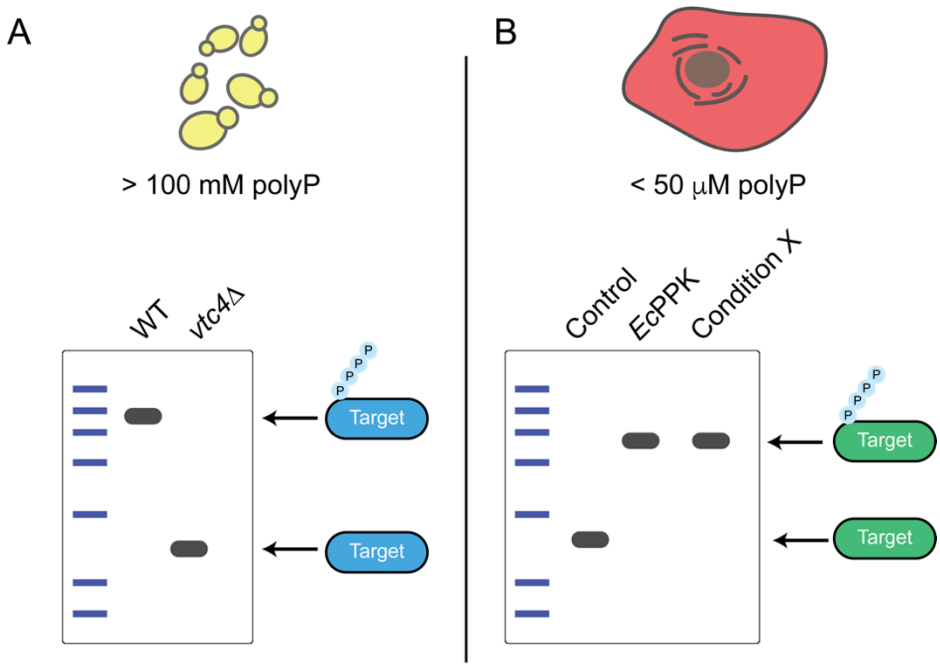

Figure 3. Detection of polyphosphorylation by NuPAGE analysis. Polyphosphorylation confers an electrophoretic shift to protein targets. **A)** Yeast cells normally have high levels of polyP. As such polyphosphorylation targets from wild-type cells will show decreased electrophoretic mobility relative to those isolated from *vtc4*Δ cells, which lack polyP. **B)** In mammalian cells, polyP levels are normally too low to cause a detectable electrophoretic shift for proteins analysed on NuPAGE gels. We have used ectopically expressed *E. coli* polyP synthetase (*Ec*PPK) to artificially increase polyP concentration in HEK293T cells. This allows detectable polyphosphorylation of selected targets. Growth conditions, stress treatments, or disease states (e.g., condition X) that stimulate polyP accumulation to high levels will facilitate the study of polyphosphorylation in higher eukaryotes and identify scenarios where it is most likely to be physiologically relevant.

This allows hyperaccumulation of long chain polyP throughout the cell to levels approximating 1 mM (15), which is sufficient to trigger polyphosphorylation, prior to NuPAGE analysis (**Figure 3**). We first used the *Ec*PPK expression system to confirm polyphosphorylation of 6 proteins that were prioritized based on the presence of PASK clusters (22). These targets are functionally diverse and include Nucleolin (a possible functional homolog of yeast Nsr1), translation factor eIF5B, splicing regulator UPF3B, ribosomal biogenesis factor NOP56, protein chaperone MESD, and chromatin protein DEK (**Table 1**) (22). Since polyphosphorylation occurs non-enzymatically, targets can also be identified by comparing electrophoretic mobilities of proteins incubated with or without synthetic polyP chains of various lengths *in vitro* (20,22). Certainly, there is tremendous value in continuing to pursue hypothesis-driven and candidate-based searches for polyphosphorylation substrates. Pathways at the heart of processes impacted by polyP (e.g. blood clotting (27,28) , osteoblast differentiation (29), neurobiology (14,30), protein folding (31-33)) represent ideal starting points for the search.

While we can expect to see candidate-based analysis continue to identify small numbers of polyphosphorylation targets, a global understanding of polyphosphorylation will require the development of techniques allowing researchers to search their favourite proteomes in an unbiased fashion. To this end, the Saiardi and Jessen labs screened commercially available mammalian protein microarrays to identify candidate targets (25). Glass slides spotted with 1000s of recombinant proteins were probed with short-chain biotinylated polyP. Following washing to remove unbound polyP, biotinylated polyP interacting with proteins on the array were detected with fluorophore-conjugated streptavidin, which binds tightly to biotin. This approach identified 75 candidate polyP-interacting proteins in common between two replicates of the screen (25). Not all candidates that emerge from this type of analysis will turn out to be polyphosphorylated; some

proteins on the microarray may interact with polyP non-covalently. The authors distinguished between these possibilities for selected candidates using NuPAGE analysis. They confirmed 6 new polyphosphorylation targets (eIF2B5, EYA1, Gelsolin, GTF2I, HSP90B1 and TTC27), with 2 additional targets (HSP90α/β, AP3B1) emerging from directed follow-up work (**Table 1**) (25). Like those we previously identified, these newly confirmed targets include both nuclear and cytoplasmic proteins and fall into diverse functional categories (25). Interestingly, only 4/8 (50 %) of these targets have PASK clusters based on previously defined criteria (**Table 1**) (22). It is intriguing to speculate that the PASK is only the tip of the iceberg when it comes to polyphosphorylation motifs, and that other sequences (or even other amino acids) permitting non-enzymatic addition of polyP remain to be discovered.

Many large-scale analyses of other lysine-based modifications (e.g., ubiquitylation (34), acetylation (35), succinylation (36)) have employed mass spectrometry. A mass spectrometry approach to identifying lysine polyphosphorylations would go a long way to speed the discovery of new targets. Moreover, in contrast to protein analysis on NuPAGE gels, which simply tells us if a protein is polyphosphorylated, mass spectrometry could be used to map the location of lysine polyphosphorylation sites. This knowledge would facilitate downstream mutational and phenotypic analyses (**Figure 1**). However, Azevedo *et al.* were unable to identify polyphosphorylation of Nsr1 and Top1 by mass spectrometry (20), and no further progress in this area has been reported. It is possible that long polyP chains are too unstable to be detected via current methods. Moreover, even if these chains can be maintained throughout the processes of sample preparation and peptide fragmentation within the mass spectrometer, the heterogenous nature of polyP chains *in vivo* may present a computational problem. This is because the identification of peptides requires prior knowledge of their expected masses. As a starting point,

we suggest prioritizing proof-of-concept experiments employing protein targets (or peptides) with a limited number of lysine residues polyphosphorylated using polyP of very short length, which should reduce the complexity of mass spectra. Alternatively, the Eyers lab has recently described methods to characterize lysine monophosphorylation (37). It may be possible to map sites of polyphosphorylation on purified targets by removing all but the first phosphate residue in a reaction with purified exopolyphosphatase, such as *S. cerevisiae* Ppx1 (20). It is also tempting to speculate that some of the lysine monophosphorylations already mapped in work from the Eyers lab could have started out as longer polyP chains that were degraded during sample preparation. While development of a mass spectrometry method to identify lysine polyphosphorylations is anything but straightforward, it is an endeavour that is likely to pay significant dividends.

Finally, the non-enzymatic nature of polyphosphorylation raises an additional caveat that is likely to impact all methods of finding new targets. Namely, the polyphosphorylation reaction occurs within minutes *in vitro,* even in harsh conditions (20,22). As such, polyphosphorylation can occur after cell lysis, including on proteins that are never in contact with polyP within intact cells (12,26). Genetic analysis of point mutants that cannot be polyphosphorylated (**Figure 1**) is a critical step to make sure that the polyphosphorylations are important *in vivo.*

5.3.2. Missing in action – Mammalian enzymes that make and degrade polyP

In contrast to prokaryotes and lower eukaryotes, we know almost nothing about enzymes that make or degrade polyP in human cells (2). From a polyphosphorylation perspective, finding these enzymes is important for three reasons. First, the synthesis and turnover of the relevant metabolite is one of the ways by which non-enzymatic modifications are regulated. Second, polyphosphatases could directly remove polyP chains from protein targets, as is proposed for the

polyphosphatases Ppx1 and Ddp1 in yeast (20). Third, the spectrum of phenotypes associated with mutation or overexpression of enzymes involved in polyP metabolism will define the possible functions of polyphosphorylation. For example, it would be difficult to argue that polyphosphorylation of proteins in the blood clotting cascade is important if the enzymes that make polyP itself are not required for that same process. Alternatively, if it turns out that the polyP biosynthetic machinery is needed for ribosome biogenesis, then it would make sense to prioritize related polyP targets (e.g., NOP56, Nucleolin) for follow-up mutational and phenotypic analyses. So, what *do* we know about mammalian polyP metabolism?

Candidate polyP synthetases: As described above, there are no obvious homologs of bacterial or yeast enzymes involved in polyP synthesis encoded in mammalian genomes. As such, the identity of the mammalian polyP synthesis enzymes is a prized goal in the field (2). Recent work from the Abramov lab suggests that polyP can be synthesized by mitochondrial F_0F_1-ATPase (38) (**Figure 4**). Whether this enzyme represents a significant source of polyP for the cell (or even the main source of polyP for the mitochondria in wild-type cells) remains to be tested. However, the synthesis of polyP at the site where it is used or stored makes intuitive sense, and suggests that other polyP synthetases may concentrate in areas of polyP accumulation such as the nucleolus (39), and platelet dense granules (40) (see discussion on polyP compartmentalization, below).We recommend prioritizing candidate enzymes from these compartments for directed analyses.

Candidate polyphosphatases: While mammalian polyphosphatase activities are also poorly characterized, a number of intriguing candidates have been proposed (**Figure 4**). H-Prune is a member of the DHH superfamily of phosphodiesterases, with activity towards cAMP and cGMP (41). In 2008, it was reported that H-Prune also has exopolyphosphatase activity (42). H-Prune is a multifunctional adaptor protein that cooperates with GSK-3 to regulate cell migration (43). It is

important for brain development and has been discussed as a potential target for cancer therapies (44-46). The possibility that H-Prune's polyphosphatase activity is involved in regulating these functions is exciting. Notably, in addition to regulating the length of free polyP chains, H-Prune could act to reverse polyphosphorylations *in vivo* (**Figure 4**) (20). Indeed, H-Prune physically interacts with the actin-binding protein Gelsolin (47), a known polyphosphorylated target (**Table 1**) (25). However, it is important to note that H-Prune is most active against very short polyP chains of 3-4 residues, with almost no activity against polyP chains of 25-65 residues similar to those used in polyphosphorylation reactions (42,48). Therefore, it is difficult to imagine that H-Prune functions as an all-purpose exopolyphosphatase. More importantly, to our knowledge, the polyphosphatase activity of H-Prune has not been tested *in vivo*. Besides H-Prune, the Nudix hydrolases DIPP1, DIPP2 and DIPP3 possess endopolyphosphatase activity *in vitro* (7). Here again, their activities have yet to be tested *in vivo* and this should be a priority of future work. Finally, alkaline phosphatase (ALP) has robust exopolyphosphatase activity *in vitro* against polyP of various sizes (49). In contrast to other candidates, ALP is thought to act at the outer cell surface to degrade polyP at the surface of bone precursors, and this activity may be important for skeletal mineralization and for generation of ATP at the cell surface (29,50).

A number of groups have ectopically expressed the potent yeast exopolyphosphatase Ppx1 in human cell lines, with the downstream effects attributed to degradation of cellular polyP (51,52). While this has the potential to be a powerful tool given our current lack of knowledge, there are a number of caveats of this approach that should be considered. First, it is unclear if Ppx1 has additional activities *in vivo* beyond its exopolyphosphatase activity that could confound results. Second, as suggested previously (52), some polyP pools may be inaccessible to Ppx1 activity.

Careful interpretation of conclusions drawn from ectopic expression of yeast Ppx1 in mammalian cells is warranted.

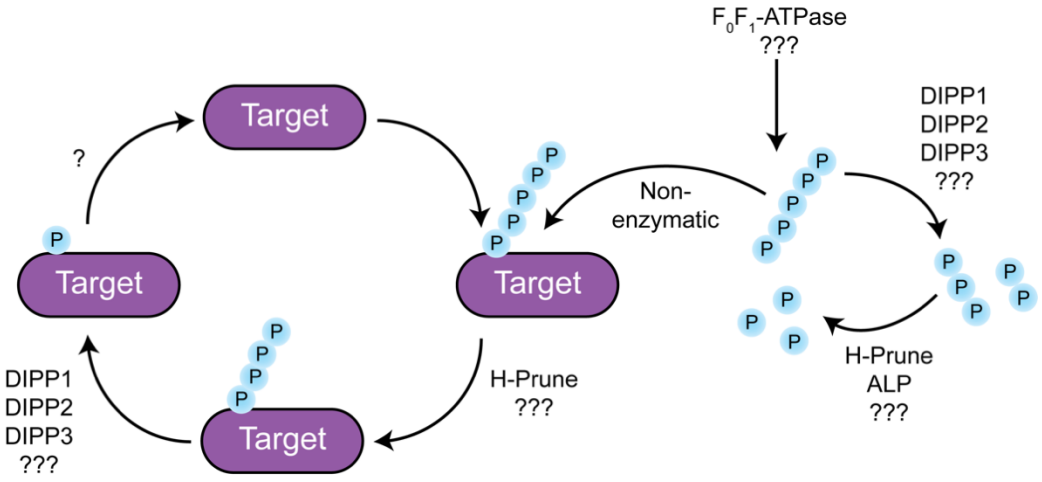

Figure 4. Candidate enzymes involved in polyP metabolism in humans. Mechanisms of polyP synthesis are mostly unknown, although the F_0F_1-ATPase in mitochondria has been proposed. Alkaline phosphatase (ALP) is suggested to degrade polyP on the cell surface, whereas other polyphosphatases shown have *in vitro* activities that have not been investigated *in vivo*. Polyphosphatases may degrade or remove polyP chains attached to lysine residues of protein targets. Cleavage of the terminal phosphate, joined to lysine residues by a P-N bond, may require a distinct enzymatic activity.

5.3.3. The highs and the lows – Linking polyP concentration to lysine polyphosphorylation

PolyP functions are likely defined by concentration and chain length. Concentration is best measured via quantification of free Pi released from chemical or enzymatic digestion of polyP chains (53). Chain length is commonly determined by polyP separation using polyacrylamide gel electrophoresis followed by staining with toluidine blue or DAPI (54,55). Notably, DAPI and toluidine may not properly detect polyP shorter than 15 residues in length (56,57). Nevertheless, these assays are readily applied to microorganisms such as *E. coli* and yeast because these species accumulate polyP chains to very high cellular concentrations (20 mM and >200 mM, respectively, customarily expressed in terms of phosphate monomers) (1). In contrast, polyP concentrations are

lower in mammalian cells, and in some cases may be very close to the threshold of detection, at least for commonly applied assays. In some studies, this may be compounded by degradation of polyP in response to cell death or during extraction (2). Concentrations of polyP in mammalian cells are usually measured at levels between 25-120 μM (58). Platelets represent an interesting exception, with concentrations estimated at ~1 mM (40). PolyP chains from mammalian cells and tissues are most often reported to be of the short type (5–100 Pi units) (19,40,58). Here again, there are exceptions. For example, in the brain polyP chains are ~800 Pi units (58), similar in length to those produced by many bacteria (1).

Low concentrations of polyP present an issue for the detection of polyphosphorylation, understanding of its mechanism of action, and interpretation of its biological significance in mammalian cells. First, while it is unknown if a minimum polyP concentration is needed for *in vivo* polyphosphorylation to occur, it is certainly required for detection of the modification by NuPAGE gels. Mammalian targets of polyphosphorylation do not show an electrophoretic shift on NuPAGE gels without expression of *Ec*PPK in cells (**Figure 3**), or the addition of at least 1 mM synthetic polyP to protein extracts (22,25). However, just because a protein does not shift by NuPAGE analysis does not mean it is not polyphosphorylated. Limited polyphosphorylation impacting only a few lysine residues, the addition of short chains, or modification of only a fraction of the total protein population may go undetected by NuPAGE analysis. The development of sensitive methods to detect polyphosphorylation (e.g. mass spectrometry, discussed above) will permit more rigorous investigation of polyphosphorylation occurring *in vivo*.

It is also important to consider the consequences of polyphosphorylation stemming from low levels of polyP. Indeed, we cannot be certain that low levels of polyphosphorylation – particularly on any one specific target, confer any meaningful function. Still, the possibilities are

exciting. Under physiological conditions, low levels of polyphosphorylation may limit the saturation of available lysine residues by polyP, leaving neighbouring lysines accessible for cross-regulation by other PTMs. Decreased availably of polyP may also increase the specificity of polyphosphorylation, restricting modification to amino acid sequences that are more predictive than the PASK cluster. Low concentrations could also impact the mechanism of polyphosphorylation itself. Instead of being strictly non-enzymatic as suggested by the current prevailing model (12,20), it is not impossible that *in vivo* polyphosphorylation could be facilitated by an enzyme (beyond those required to make polyP itself) when polyP levels are at their lowest. This dual mode of PTM addition has been described previously for lysine acetylation. Nuclear acetylation is widely studied as a PTM catalyzed by enzymes (called KATs) (59). In contrast, lysine acetylation in the mitochondria, where acetyl-CoA levels are very high, is thought to occur largely non-enzymatically both in yeast and in higher eukaryotes (60,61). Finally, it is possible that polyP levels in mammalian cells are purposefully kept low to avoid constitutive polyphosphorylation, which may be toxic.

Assuming there is a connection between polyP levels and polyphosphorylation, cells with naturally high polyP concentration may point to areas of functional relevance for this PTM. For example, polyP levels are high in platelets and work from several groups has demonstrated interaction of polyP with proteins in the blood clotting cascade (62,63). While most of these interactions are proposed to be non-covalent in nature, it is intriguing to speculate that polyphosphorylation also has an important role in this process. Efforts to understand the functions of polyphosphorylation will also benefit from the exploration of conditions that result in polyP accumulation. Several of these conditions have already been identified. For example, plasma cells (a type of white blood cell) contain little to no polyP under normal conditions, compared to

malignant plasma cells, referred to as myeloma cells, that accumulate high concentrations of polyP within the nucleolus (39). This accumulation of polyP is thought to modulate RNA polymerase I activity (39). A similar effect is observed when other cancer cell lines are treated with cisplatin, a commonly used chemotherapeutic drug that induces DNA damage (52). These cells respond to cisplatin treatment by accumulating polyP in the nucleolus (52). This increase in polyP is suggested to trigger apoptosis (52). The mechanism by which polyP exerts these functions is unclear, but polyphosphorylation is an exciting possibility. Notably, our work showed upregulation of DNA binding and transcription factor proteins in cells accumulating polyP via *Ec*PPK expression (15). Perhaps these proteins and those involved in the DNA damage and apoptotic response can be considered new candidate targets for polyphosphorylation. Finally, recent work by Roewe *et al*. presents data suggesting that macrophages can internalize bacterial long-chain polyP and that this inhibits the immune response (64). Here again, it would be interesting to test if this results in polyphosphorylation of mammalian proteins involved in infection control. It is also tempting to speculate that such polyphosphorylations might be prevented by treatment with mesalamine, a drug used to treat inflammatory bowel disease that serves as an inhibitor of bacterial PPK enzymes (65).

5.3.4. PolyP hot spots – Compartmentalization in mammalian cells

In yeast, polyP is not uniformly distributed throughout the cell. In fact, the majority of polyP is sequestered within the vacuole, which may prevent polyP from interacting with cytoplasmic proteins (5,22). In mammalian cells there are also polyP 'hot-spots', but no uniform pattern of localization across cell types. For instance, the Kornberg lab showed that rat liver cells have higher polyP concentrations in the nuclei and plasma membrane compared to the cytosol,

mitochondria and microsome fractions (58). In contrast, cultured astrocytes compartmentalize 40% of the polyP in mitochondria, some in putative ATP containing vesicles and varying amounts in lysosomes (66). In platelets, polyP levels are concentrated in small dense granules (40). Overall, polyP compartmentalization may have an evolutionary advantage in eukaryotes, making it readily available to serve various functions. It is likely that sequestration of polyP also protects it from polyphosphatases. Notably, compartmentalization may also provide a way to increase local concentration of polyP and drive polyphosphorylation of select targets, while avoiding unwanted polyphosphorylation of other targets. In platelet dense granules, polyP concentrations are estimated to be upwards of 130 mM (40), more than enough to drive quantitative polyphosphorylation that is detectable via NuPAGE. Strategically, subcellular localization of polyP can help us prioritize follow-up of select targets. For example, it would make sense to focus on targets related to energy metabolism in astrocytes, where much of the polyP is localized to the mitochondria (66,67).

How does polyP localize to distinct areas of the cell? We envision two possibilities: polyP could be synthesized locally or transported to specific locations. The mitochondrial F_0F_1-ATPase could be responsible for polyP accumulation in the mitochondria (38). The identification of other enzymes that make polyP will tell us whether local synthesis is a common theme. In terms of transport, it is intriguing to speculate that one or more of the polyP binding proteins identified by Azevedo using proteome microarrays (25) could be involved in polyP transport and/or its protection from polyphosphatases within specific compartments. Some polyP binding receptors (CD4 (68), RAGE (16,17), and P2Y1 (17)) have been identified. However, it is not clear if these actually promote internalization of exogenous polyP, and this is an important area for future research. Currently there are several methods available for visualization of polyP within cells.

First, DAPI, customarily used to visualize DNA, undergoes a long-wave excitation and emission spectral shift when bound to polyP (69). Similarly, polyP-specific fluorescent probes (such as JC-D7/D8) have successfully been applied to visualize polyP in live mammalian tissues (66,70). Alternatively, the purified recombinant polyP binding domain (PPBD) of PPX linked to an epitope tag can be used to target polyP for visualization (71). These probes offer high sensitivity and specificity, making them a valuable detection tool for cells with low polyP levels (39,72,73). However, PPBD probes have only been applied to fixed cells (52,71). Additionally, work with these reagents must be interpreted with care. It is likely that polyP-detecting probes can recognize molecules or structures other than polyP and convincing controls are not used in all studies. Notably, the ectopic expression of yeast Ppx1 to degrade polyP can be used as a control to establish background signal (74). On the other hand, it is important to note that polyP participating in polyphosphorylation or non-covalent interactions with proteins or small molecules may go undetected by these methods. Probes used within live cells could also bind to or sequester polyP, which could disrupt downstream functions.

As an alternative to microscopy, we recently used cell fractionation to demonstrate that polyP made by ectopically expressed *Ec*PPK in HEK293T cells results in accumulation of polyP in varying amounts in the cytoplasm, membrane and organelle, and nuclear/cytoskeleton fractions (15). This was accompanied by changes in the subcellular localization of polyphosphorylated targets eIF5b, GTF2I and DEK (15). For example, in *Ec*PPK-expressing cells, DEK was redistributed from the nucleus/cytoskeleton to other fractions (15). One possibility is that polyphosphorylation of newly synthesized DEK in the cytoplasm prevents its nuclear import. On the other hand, we postulate that polyphosphorylation of protein targets may play an active role in the distribution of polyP throughout the cell. For example, perhaps nucleolar localization of polyP

in myeloma cells is a by-product of polyphosphorylation of targets that normally localize to this compartment.

5.3.5. Into the clinic – Polyphosphorylation in polyP-directed therapies

Manipulation of polyP levels has been proposed as a therapeutic for ulcerative colitis (75), bacterial (64) and viral infection (68,76), and wound healing (77). Given the breadth of processes impacted by polyP, we are likely to see additional clinical applications in the near future. Various mechanisms are being explored for polyP delivery including nanoparticle delivery (78), local application to sites of infection (79), oral administration (75), or injection (19,80). If, as we have suggested, polyphosphorylation plays an important role in the mechanism of polyP action across diverse processes, then investigation of this modification and resolution of the challenges raised in this review will provide insights facilitating its use in the clinic. Notably, strategies that aim to increase local concentrations of polyP in cells or tissues may reprogram cell signaling via polyphosphorylation of targets whose regulation by polyP is not a part of normal cellular physiology. As a starting point, it will be interesting to evaluate if known targets become polyphosphorylated via the polyP delivery mechanisms proposed so far. If relevant targets are polyphosphorylated, it will also be important to determine how long that modification persists after the source of polyphosphate is removed. To this end, the identification of enzymes that metabolize polyP will allow for a better understanding of which cell types, and even which patients, may be most susceptible to polyP therapies. For example, cells expressing high levels of candidate polyphosphatases (81,82) may be more resistant to these types of therapies. On the other hand, treatment with inhibitors of those polyphosphatases may enhance the impact of polyP delivery.

5.4. Conclusion

Lysine polyphosphorylation represents an exciting new area of polyP research. Indeed, we suggest that many of the functions attributed to polyP over the last 20 years could be mediated at least in part by this new PTM, including those related to human health. However, the non-enzymatic nature of polyphosphorylation and limited means of detection make its investigation difficult. This is particularly true when it comes to connecting *in vitro* observations to biological consequences. While these issues are common across multiple experimental systems, the study of polyP in mammals is hindered by additional challenges including a poor understanding of polyP metabolism accompanied by low polyP concentrations *in vivo*. Where possible, we have made practical suggestions on how to begin to address these issues throughout this review. Our hope is that this will play an important role in moving the field forward. Notably, advances required for studying polyphosphorylation (e.g. identification of enzymes that make polyP), will necessarily have a positive impact on other areas of the polyP field. Finally, we note that the identification of lysine polyphosphorylation as a new lysine-based PTM has the capacity to bring new scientists with fresh perspectives and skillsets into the general area of polyP research. It may be these individuals who are best equipped to solve the critical open questions in the field.

5.5. Acknowledgements

The authors thank members of the Downey lab for critical reading of the manuscript. Funding for polyphosphate research in the Downey lab is provided by a Canadian Institutes of Health Research Project Grant PJT-148722. Trainees in the Downey lab are supported in part by an Early Research Award from the Ontario Ministry of Innovation and Research.

5.6. References

1. Denoncourt, A., & Downey, M. (2021). Model systems for studying polyphosphate biology: a focus on microorganisms. *Curr Genet*. doi: 10.1007/s00294-020-01148-x
2. Desfougeres, Y., Saiardi, A., & Azevedo, C. (2020). Inorganic polyphosphate in mammals: where's Wally? *Biochem Soc Trans, 48*(1), 95-101. doi: 10.1042/BST20190328
3. Akiyama, M., Crooke, E., & Kornberg, A. (1993). An exopolyphosphatase of Escherichia coli. The enzyme and its ppx gene in a polyphosphate operon. *J Biol Chem, 268*(1), 633-639.
4. Hothorn, M., Neumann, H., Lenherr, E. D., Wehner, M., Rybin, V., Hassa, P. O., . . . Mayer, A. (2009). Catalytic core of a membrane-associated eukaryotic polyphosphate polymerase. *Science, 324*(5926), 513-516. doi: 10.1126/science.1168120
5. Gerasimaite, R., Sharma, S., Desfougeres, Y., Schmidt, A., & Mayer, A. (2014). Coupled synthesis and translocation restrains polyphosphate to acidocalcisome-like vacuoles and prevents its toxicity. *J Cell Sci, 127*(Pt 23), 5093-5104. doi: 10.1242/jcs.159772
6. Auesukaree, C., Homma, T., Tochio, H., Shirakawa, M., Kaneko, Y., & Harashima, S. (2004). Intracellular phosphate serves as a signal for the regulation of the PHO pathway in Saccharomyces cerevisiae. *J Biol Chem, 279*(17), 17289-17294. doi: 10.1074/jbc.M312202200
7. Lonetti, A., Szijgyarto, Z., Bosch, D., Loss, O., Azevedo, C., & Saiardi, A. (2011). Identification of an evolutionarily conserved family of inorganic polyphosphate endopolyphosphatases. *J Biol Chem, 286*(37), 31966-31974. doi: 10.1074/jbc.M111.266320
8. Gerasimaite, R., & Mayer, A. (2017). Ppn2, a novel Zn(2+)-dependent polyphosphatase in the acidocalcisome-like yeast vacuole. *J Cell Sci, 130*(9), 1625-1636. doi: 10.1242/jcs.201061
9. Shi, X., & Kornberg, A. (2005). Endopolyphosphatase in Saccharomyces cerevisiae undergoes post-translational activations to produce short-chain polyphosphates. *FEBS Lett, 579*(9), 2014-2018. doi: 10.1016/j.febslet.2005.02.032
10. Sethuraman, A., Rao, N. N., & Kornberg, A. (2001). The endopolyphosphatase gene: essential in Saccharomyces cerevisiae. *Proc Natl Acad Sci U S A, 98*(15), 8542-8547. doi: 10.1073/pnas.151269398
11. Wurst, H., Shiba, T., & Kornberg, A. (1995). The gene for a major exopolyphosphatase of Saccharomyces cerevisiae. *J Bacteriol, 177*(4), 898-906. doi: 10.1128/jb.177.4.898-906.1995
12. Bentley-DeSousa, A., & Downey, M. (2019). From underlying chemistry to therapeutic potential: open questions in the new field of lysine polyphosphorylation. *Curr Genet, 65*(1), 57-64. doi: 10.1007/s00294-018-0854-4
13. Cremers, C. M., Knoefler, D., Gates, S., Martin, N., Dahl, J. U., Lempart, J., . . . Jakob, U. (2016). Polyphosphate: A Conserved Modifier of Amyloidogenic Processes. *Mol Cell, 63*(5), 768-780. doi: 10.1016/j.molcel.2016.07.016
14. Stotz, S. C., Scott, L. O., Drummond-Main, C., Avchalumov, Y., Girotto, F., Davidsen, J., . . . Colicos, M. A. (2014). Inorganic polyphosphate regulates neuronal excitability through modulation of voltage-gated channels. *Mol Brain, 7*, 42. doi: 10.1186/1756-6606-7-42
15. Bondy-Chorney, E., Abramchuk, I., Nasser, R., Holinier, C., Denoncourt, A., Baijal, K., . . . Downey, M. (2020). A Broad Response to Intracellular Long-Chain Polyphosphate in Human Cells. *Cell Rep, 33*(4), 108318. doi: 10.1016/j.celrep.2020.108318
16. Hassanian, S. M., Ardeshirylajimi, A., Dinarvand, P., & Rezaie, A. R. (2016). Inorganic polyphosphate promotes cyclin D1 synthesis through activation of mTOR/Wnt/beta-catenin signaling in endothelial cells. *J Thromb Haemost, 14*(11), 2261-2273. doi: 10.1111/jth.13477

17. Hassanian, S. M., Dinarvand, P., Smith, S. A., & Rezaie, A. R. (2015). Inorganic polyphosphate elicits pro-inflammatory responses through activation of the mammalian target of rapamycin complexes 1 and 2 in vascular endothelial cells. *J Thromb Haemost, 13*(5), 860-871. doi: 10.1111/jth.12899
18. Smith, S. A., Mutch, N. J., Baskar, D., Rohloff, P., Docampo, R., & Morrissey, J. H. (2006). Polyphosphate modulates blood coagulation and fibrinolysis. *Proc Natl Acad Sci U S A, 103*(4), 903-908. doi: 10.1073/pnas.0507195103
19. Muller, F., Mutch, N. J., Schenk, W. A., Smith, S. A., Esterl, L., Spronk, H. M., . . . Renne, T. (2009). Platelet polyphosphates are proinflammatory and procoagulant mediators in vivo. *Cell, 139*(6), 1143-1156. doi: 10.1016/j.cell.2009.11.001
20. Azevedo, C., Livermore, T., & Saiardi, A. (2015). Protein polyphosphorylation of lysine residues by inorganic polyphosphate. *Mol Cell, 58*(1), 71-82. doi: 10.1016/j.molcel.2015.02.010
21. Harmel, R., & Fiedler, D. (2018). Features and regulation of non-enzymatic post-translational modifications. *Nat Chem Biol, 14*(3), 244-252. doi: 10.1038/nchembio.2575
22. Bentley-DeSousa, A., Holinier, C., Moteshareie, H., Tseng, Y. C., Kajjo, S., Nwosu, C., . . . Downey, M. (2018). A Screen for Candidate Targets of Lysine Polyphosphorylation Uncovers a Conserved Network Implicated in Ribosome Biogenesis. *Cell Rep, 22*(13), 3427-3439. doi: 10.1016/j.celrep.2018.02.104
23. McCarthy, L., Bentley-DeSousa, A., Denoncourt, A., Tseng, Y. C., Gabriel, M., & Downey, M. (2020). Proteins required for vacuolar function are targets of lysine polyphosphorylation in yeast. *FEBS Lett, 594*(1), 21-30. doi: 10.1002/1873-3468.13588
24. Azevedo, C., & Saiardi, A. (2016). The new world of inorganic polyphosphates. *Biochem Soc Trans, 44*(1), 13-17. doi: 10.1042/bst20150210
25. Azevedo, C., Singh, J., Steck, N., Hofer, A., Ruiz, F. A., Singh, T., . . . Saiardi, A. (2018). Screening a Protein Array with Synthetic Biotinylated Inorganic Polyphosphate To Define the Human PolyP-ome. *ACS Chem Biol, 13*(8), 1958-1963. doi: 10.1021/acschembio.8b00357
26. Azevedo, C., Desfougeres, Y., Jiramongkol, Y., Partington, H., Trakansuebkul, S., Singh, J., . . . Saiardi, A. (2020). Development of a yeast model to study the contribution of vacuolar polyphosphate metabolism to lysine polyphosphorylation. *J Biol Chem, 295*(6), 1439-1451. doi: 10.1074/jbc.RA119.011680
27. Smith, S. A., & Morrissey, J. H. (2014). Polyphosphate: a new player in the field of hemostasis. *Curr Opin Hematol, 21*(5), 388-394. doi: 10.1097/MOH.0000000000000069
28. Morrissey, J. H., & Smith, S. A. (2015). Polyphosphate as modulator of hemostasis, thrombosis, and inflammation. *J Thromb Haemost, 13 Suppl 1*, S92-97. doi: 10.1111/jth.12896
29. Phelipe Hatt, L., Thompson, K., Muller, W. E. G., Stoddart, M. J., & Armiento, A. R. (2019). Calcium Polyphosphate Nanoparticles Act as an Effective Inorganic Phosphate Source during Osteogenic Differentiation of Human Mesenchymal Stem Cells. *Int J Mol Sci, 20*(22). doi: 10.3390/ijms20225801
30. Holmstrom, K. M., Marina, N., Baev, A. Y., Wood, N. W., Gourine, A. V., & Abramov, A. Y. (2013). Signalling properties of inorganic polyphosphate in the mammalian brain. *Nat Commun, 4*, 1362. doi: 10.1038/ncomms2364
31. Gray, M. J., & Jakob, U. (2015). Oxidative stress protection by polyphosphate--new roles for an old player. *Curr Opin Microbiol, 24*, 1-6. doi: 10.1016/j.mib.2014.12.004

32. Gray, M. J., Wholey, W. Y., Wagner, N. O., Cremers, C. M., Mueller-Schickert, A., Hock, N. T., . . . Jakob, U. (2014). Polyphosphate is a primordial chaperone. *Mol Cell, 53*(5), 689-699. doi: 10.1016/j.molcel.2014.01.012
33. Xie, L., & Jakob, U. (2019). Inorganic polyphosphate, a multifunctional polyanionic protein scaffold. *J Biol Chem, 294*(6), 2180-2190. doi: 10.1074/jbc.REV118.002808
34. Goodman, C. A., Davey, J. R., Hagg, A., Parker, B. L., & Gregorevic, P. (2021). Dynamic Changes to the Skeletal Muscle Proteome and Ubiquitinome Induced by the E3 Ligase, ASB2beta. *Mol Cell Proteomics*, 100050. doi: 10.1016/j.mcpro.2021.100050
35. Hansen, B. K., Gupta, R., Baldus, L., Lyon, D., Narita, T., Lammers, M., . . . Weinert, B. T. (2019). Analysis of human acetylation stoichiometry defines mechanistic constraints on protein regulation. *Nat Commun, 10*(1), 1055. doi: 10.1038/s41467-019-09024-0
36. Gut, P., Matilainen, S., Meyer, J. G., Pallijeff, P., Richard, J., Carroll, C. J., . . . Verdin, E. (2020). SUCLA2 mutations cause global protein succinylation contributing to the pathomechanism of a hereditary mitochondrial disease. *Nat Commun, 11*(1), 5927. doi: 10.1038/s41467-020-19743-4
37. Hardman, G., Perkins, S., Brownridge, P. J., Clarke, C. J., Byrne, D. P., Campbell, A. E., . . . Eyers, C. E. (2019). Strong anion exchange-mediated phosphoproteomics reveals extensive human non-canonical phosphorylation. *EMBO J, 38*(21), e100847. doi: 10.15252/embj.2018100847
38. Baev, A. Y., Angelova, P. R., & Abramov, A. Y. (2020). Inorganic polyphosphate is produced and hydrolyzed in F0F1-ATP synthase of mammalian mitochondria. *Biochem J, 477*(8), 1515-1524. doi: 10.1042/BCJ20200042
39. Jimenez-Nunez, M. D., Moreno-Sanchez, D., Hernandez-Ruiz, L., Benitez-Rondan, A., Ramos-Amaya, A., Rodriguez-Bayona, B., . . . Ruiz, F. A. (2012). Myeloma cells contain high levels of inorganic polyphosphate which is associated with nucleolar transcription. *Haematologica, 97*(8), 1264-1271. doi: 10.3324/haematol.2011.051409
40. Ruiz, F. A., Lea, C. R., Oldfield, E., & Docampo, R. (2004). Human platelet dense granules contain polyphosphate and are similar to acidocalcisomes of bacteria and unicellular eukaryotes. *J Biol Chem, 279*(43), 44250-44257. doi: 10.1074/jbc.M406261200
41. D'Angelo, A., Garzia, L., Andre, A., Carotenuto, P., Aglio, V., Guardiola, O., . . . Zollo, M. (2004). Prune cAMP phosphodiesterase binds nm23-H1 and promotes cancer metastasis. *Cancer Cell, 5*(2), 137-149. doi: 10.1016/s1535-6108(04)00021-2
42. Tammenkoski, M., Koivula, K., Cusanelli, E., Zollo, M., Steegborn, C., Baykov, A. A., & Lahti, R. (2008). Human metastasis regulator protein H-prune is a short-chain exopolyphosphatase. *Biochemistry, 47*(36), 9707-9713. doi: 10.1021/bi8010847
43. Kobayashi, T., Hino, S., Oue, N., Asahara, T., Zollo, M., Yasui, W., & Kikuchi, A. (2006). Glycogen synthase kinase 3 and h-prune regulate cell migration by modulating focal adhesions. *Mol Cell Biol, 26*(3), 898-911. doi: 10.1128/MCB.26.3.898-911.2006
44. Carotenuto, M., De Antonellis, P., Liguori, L., Benvenuto, G., Magliulo, D., Alonzi, A., . . . Zollo, M. (2014). H-Prune through GSK-3beta interaction sustains canonical WNT/beta-catenin signaling enhancing cancer progression in NSCLC. *Oncotarget, 5*(14), 5736-5749. doi: 10.18632/oncotarget.2169
45. Zollo, M., Ahmed, M., Ferrucci, V., Salpietro, V., Asadzadeh, F., Carotenuto, M., . . . Baple, E. L. (2017). PRUNE is crucial for normal brain development and mutated in microcephaly with neurodevelopmental impairment. *Brain, 140*(4), 940-952. doi: 10.1093/brain/awx014

46. Zollo, M., Andre, A., Cossu, A., Sini, M. C., D'Angelo, A., Marino, N., . . . Palmieri, G. (2005). Overexpression of h-prune in breast cancer is correlated with advanced disease status. *Clin Cancer Res, 11*(1), 199-205.
47. Garzia, L., Roma, C., Tata, N., Pagnozzi, D., Pucci, P., & Zollo, M. (2006). H-prune-nm23-H1 protein complex and correlation to pathways in cancer metastasis. *J Bioenerg Biomembr, 38*(3-4), 205-213. doi: 10.1007/s10863-006-9036-z
48. Nistala, H., Dronzek, J., Gonzaga-Jauregui, C., Chim, S. M., Rajamani, S., Nuwayhid, S., . . . Economides, A. N. (2021). NMIHBA results from hypomorphic PRUNE1 variants that lack short-chain exopolyphosphatase activity. *Hum Mol Genet, 29*(21), 3516-3531. doi: 10.1093/hmg/ddaa237
49. Lorenz, B., & Schroder, H. C. (2001). Mammalian intestinal alkaline phosphatase acts as highly active exopolyphosphatase. *Biochim Biophys Acta, 1547*(2), 254-261. doi: 10.1016/s0167-4838(01)00193-5
50. Muller, W. E. G., Ackermann, M., Tolba, E., Neufurth, M., Ivetac, I., Kokkinopoulou, M., . . . Wang, X. (2018). Role of ATP during the initiation of microvascularization: acceleration of an autocrine sensing mechanism facilitating chemotaxis by inorganic polyphosphate. *Biochem J, 475*(20), 3255-3273. doi: 10.1042/BCJ20180535
51. Wang, L., Fraley, C. D., Faridi, J., Kornberg, A., & Roth, R. A. (2003). Inorganic polyphosphate stimulates mammalian TOR, a kinase involved in the proliferation of mammary cancer cells. *Proc Natl Acad Sci U S A, 100*(20), 11249-11254. doi: 10.1073/pnas.1534805100
52. Xie, L., Rajpurkar, A., Quarles, E., Taube, N., Rai, A. S., Erba, J., . . . Knoefler, D. (2019). Accumulation of Nucleolar Inorganic Polyphosphate Is a Cellular Response to Cisplatin-Induced Apoptosis. *Front Oncol, 9*, 1410. doi: 10.3389/fonc.2019.01410
53. Bru, S., Jimenez, J., Canadell, D., Arino, J., & Clotet, J. (2016). Improvement of biochemical methods of polyP quantification. *Microb Cell, 4*(1), 6-15. doi: 10.15698/mic2017.01.551
54. Clark, J. E., & Wood, H. G. (1987). Preparation of standards and determination of sizes of long-chain polyphosphates by gel electrophoresis. *Anal Biochem, 161*(2), 280-290. doi: 10.1016/0003-2697(87)90452-0
55. Smith, S. A., & Morrissey, J. H. (2007). Sensitive fluorescence detection of polyphosphate in polyacrylamide gels using 4',6-diamidino-2-phenylindol. *Electrophoresis, 28*(19), 3461-3465. doi: 10.1002/elps.200700041
56. [56] Ohtomo, R., Sekiguchi, Y., Kojima, T., & Saito, M. (2008). Different chain length specificity among three polyphosphate quantification methods. *Anal Biochem, 383*(2), 210-216. doi: 10.1016/j.ab.2008.08.002
57. Christ, J. J., Willbold, S., & Blank, L. M. (2020). Methods for the Analysis of Polyphosphate in the Life Sciences. *Anal Chem, 92*(6), 4167-4176. doi: 10.1021/acs.analchem.9b05144
58. Kumble, K. D., & Kornberg, A. (1995). Inorganic polyphosphate in mammalian cells and tissues. *J Biol Chem, 270*(11), 5818-5822. doi: 10.1074/jbc.270.11.5818
59. Drazic, A., Myklebust, L. M., Ree, R., & Arnesen, T. (2016). The world of protein acetylation. *Biochim Biophys Acta, 1864*(10), 1372-1401. doi: 10.1016/j.bbapap.2016.06.007
60. Weinert, B. T., Moustafa, T., Iesmantavicius, V., Zechner, R., & Choudhary, C. (2015). Analysis of acetylation stoichiometry suggests that SIRT3 repairs nonenzymatic acetylation lesions. *EMBO J, 34*(21), 2620-2632. doi: 10.15252/embj.201591271
61. Weinert, B. T., Iesmantavicius, V., Moustafa, T., Scholz, C., Wagner, S. A., Magnes, C., . . . Choudhary, C. (2014). Acetylation dynamics and stoichiometry in Saccharomyces cerevisiae. *Mol Syst Biol, 10*, 716. doi: 10.1002/msb.134766

62. Travers, R. J., Smith, S. A., & Morrissey, J. H. (2015). Polyphosphate, platelets, and coagulation. *Int J Lab Hematol, 37 Suppl 1*, 31-35. doi: 10.1111/ijlh.12349
63. Mailer, R. K. W., Hanel, L., Allende, M., & Renne, T. (2019). Polyphosphate as a Target for Interference With Inflammation and Thrombosis. *Front Med (Lausanne), 6*, 76. doi: 10.3389/fmed.2019.00076
64. Roewe, J., Stavrides, G., Strueve, M., Sharma, A., Marini, F., Mann, A., . . . Bosmann, M. (2020). Bacterial polyphosphates interfere with the innate host defense to infection. *Nat Commun, 11*(1), 4035. doi: 10.1038/s41467-020-17639-x
65. Dahl, J. U., Gray, M. J., Bazopoulou, D., Beaufay, F., Lempart, J., Koenigsknecht, M. J., . . . Jakob, U. (2017). The anti-inflammatory drug mesalamine targets bacterial polyphosphate accumulation. *Nat Microbiol, 2*, 16267. doi: 10.1038/nmicrobiol.2016.267
66. Angelova, P. R., Iversen, K. Z., Teschemacher, A. G., Kasparov, S., Gourine, A. V., & Abramov, A. Y. (2018). Signal transduction in astrocytes: Localization and release of inorganic polyphosphate. *Glia, 66*(10), 2126-2136. doi: 10.1002/glia.23466
67. Angelova, P. R., Baev, A. Y., Berezhnov, A. V., & Abramov, A. Y. (2016). Role of inorganic polyphosphate in mammalian cells: from signal transduction and mitochondrial metabolism to cell death. *Biochem Soc Trans, 44*(1), 40-45. doi: 10.1042/BST20150223
68. Lorenz, B., Leuck, J., Kohl, D., Muller, W. E., & Schroder, H. C. (1997). Anti-HIV-1 activity of inorganic polyphosphates. *J Acquir Immune Defic Syndr Hum Retrovirol, 14*(2), 110-118. doi: 10.1097/00042560-199702010-00003
69. Aschar-Sobbi, R., Abramov, A. Y., Diao, C., Kargacin, M. E., Kargacin, G. J., French, R. J., & Pavlov, E. (2008). High sensitivity, quantitative measurements of polyphosphate using a new DAPI-based approach. *J Fluoresc, 18*(5), 859-866. doi: 10.1007/s10895-008-0315-4
70. Angelova, P. R., Agrawalla, B. K., Elustondo, P. A., Gordon, J., Shiba, T., Abramov, A. Y., . . . Pavlov, E. V. (2014). In situ investigation of mammalian inorganic polyphosphate localization using novel selective fluorescent probes JC-D7 and JC-D8. *ACS Chem Biol, 9*(9), 2101-2110. doi: 10.1021/cb5000696
71. Saito, K., Ohtomo, R., Kuga-Uetake, Y., Aono, T., & Saito, M. (2005). Direct labeling of polyphosphate at the ultrastructural level in Saccharomyces cerevisiae by using the affinity of the polyphosphate binding domain of Escherichia coli exopolyphosphatase. *Appl Environ Microbiol, 71*(10), 5692-5701. doi: 10.1128/AEM.71.10.5692-5701.2005
72. Moreno-Sanchez, D., Hernandez-Ruiz, L., Ruiz, F. A., & Docampo, R. (2012). Polyphosphate is a novel pro-inflammatory regulator of mast cells and is located in acidocalcisomes. *J Biol Chem, 287*(34), 28435-28444. doi: 10.1074/jbc.M112.385823
73. Solesio, M. E., Demirkhanyan, L., Zakharian, E., & Pavlov, E. V. (2016). Contribution of inorganic polyphosphate towards regulation of mitochondrial free calcium. *Biochim Biophys Acta, 1860*(6), 1317-1325. doi: 10.1016/j.bbagen.2016.03.020
74. Seidlmayer, L. K., Gomez-Garcia, M. R., Blatter, L. A., Pavlov, E., & Dedkova, E. N. (2012). Inorganic polyphosphate is a potent activator of the mitochondrial permeability transition pore in cardiac myocytes. *J Gen Physiol, 139*(5), 321-331. doi: 10.1085/jgp.201210788
75. Fujiya, M., Ueno, N., Kashima, S., Tanaka, K., Sakatani, A., Ando, K., . . . Okumura, T. (2020). Long-Chain Polyphosphate Is a Potential Agent for Inducing Mucosal Healing of the Colon in Ulcerative Colitis. *Clin Pharmacol Ther, 107*(2), 452-461. doi: 10.1002/cpt.1628
76. Muller, W. E. G., Neufurth, M., Schepler, H., Wang, S., Tolba, E., Schroder, H. C., & Wang, X. (2020). The biomaterial polyphosphate blocks stoichiometric binding of the SARS-CoV-2

S-protein to the cellular ACE2 receptor. *Biomater Sci, 8*(23), 6603-6610. doi: 10.1039/d0bm01244k
77. Carney, B. C., Simbulan-Rosenthal, C. M., Gaur, A., Browne, B. J., Moghe, M., Crooke, E., . . . Rosenthal, D. S. (2020). Inorganic polyphosphate in platelet rich plasma accelerates re-epithelialization in vitro and in vivo. *Regen Ther, 15*, 138-148. doi: 10.1016/j.reth.2020.07.004
78. Fernandes-Cunha, G. M., McKinlay, C. J., Vargas, J. R., Jessen, H. J., Waymouth, R. M., & Wender, P. A. (2018). Delivery of Inorganic Polyphosphate into Cells Using Amphipathic Oligocarbonate Transporters. *ACS Cent Sci, 4*(10), 1394-1402. doi: 10.1021/acscentsci.8b00470
79. Yamaoka, M., Uematsu, T., Shiba, T., Matsuura, T., Ono, Y., Ishizuka, M., . . . Furusawa, K. (2008). Effect of inorganic polyphosphate in periodontitis in the elderly. *Gerodontology, 25*(1), 10-17. doi: 10.1111/j.1741-2358.2007.00185.x
80. Bae, J. S., Lee, W., & Rezaie, A. R. (2012). Polyphosphate elicits pro-inflammatory responses that are counteracted by activated protein C in both cellular and animal models. *J Thromb Haemost, 10*(6), 1145-1151. doi: 10.1111/j.1538-7836.2012.04671.x
81. Sarko, J. (2005). Bone and mineral metabolism. *Emerg Med Clin North Am, 23*(3), 703-721, viii. doi: 10.1016/j.emc.2005.03.017
82. Price, C. P., & Sammons, H. G. (1974). The nature of the serum alkaline phosphatases in liver diseases. *J Clin Pathol, 27*(5), 392-398. doi: 10.1136/jcp.27.5.392
83. Huizing, M., Malicdan, M. C. V., Wang, J. A., Pri-Chen, H., Hess, R. A., Fischer, R., . . . Gochuico, B. R. (2020). Hermansky-Pudlak syndrome: Mutation update. *Hum Mutat, 41*(3), 543-580. doi: 10.1002/humu.23968
84. Teng, Y., Lang, L., & Jauregui, C. E. (2018). The Complexity of DEK Signaling in Cancer Progression. *Curr Cancer Drug Targets, 18*(3), 256-265. doi: 10.2174/1568009617666170522094730
85. Pavitt, G. D. (2018). Regulation of translation initiation factor eIF2B at the hub of the integrated stress response. *Wiley Interdiscip Rev RNA, 9*(6), e1491. doi: 10.1002/wrna.1491
86. Wang, J., Wang, J., Shin, B. S., Kim, J. R., Dever, T. E., Puglisi, J. D., & Fernandez, I. S. (2020). Structural basis for the transition from translation initiation to elongation by an 80S-eIF5B complex. *Nat Commun, 11*(1), 5003. doi: 10.1038/s41467-020-18829-3
87. Zhang, H., Wang, L., Wong, E. Y. M., Tsang, S. L., Xu, P. X., Lendahl, U., & Sham, M. H. (2017). An Eya1-Notch axis specifies bipotential epibranchial differentiation in mammalian craniofacial morphogenesis. *Elife, 6*. doi: 10.7554/eLife.30126
88. Nag, S., Larsson, M., Robinson, R. C., & Burtnick, L. D. (2013). Gelsolin: the tail of a molecular gymnast. *Cytoskeleton (Hoboken), 70*(7), 360-384. doi: 10.1002/cm.21117
89. Rossl, A., Bentley-DeSousa, A., Tseng, Y. C., Nwosu, C., & Downey, M. (2016). Nicotinamide Suppresses the DNA Damage Sensitivity of Saccharomyces cerevisiae Independently of Sirtuin Deacetylases. *Genetics, 204*(2), 569-579. doi: 10.1534/genetics.116.193524
90. Biebl, M. M., & Buchner, J. (2019). Structure, Function, and Regulation of the Hsp90 Machinery. *Cold Spring Harb Perspect Biol, 11*(9). doi: 10.1101/cshperspect.a034017
91. Ansa-Addo, E. A., Thaxton, J., Hong, F., Wu, B. X., Zhang, Y., Fugle, C. W., . . . Li, Z. (2016). Clients and Oncogenic Roles of Molecular Chaperone gp96/grp94. *Curr Top Med Chem, 16*(25), 2765-2778. doi: 10.2174/1568026616666160413141613

92. Hsieh, J. C., Lee, L., Zhang, L., Wefer, S., Brown, K., DeRossi, C., . . . Holdener, B. C. (2003). Mesd encodes an LRP5/6 chaperone essential for specification of mouse embryonic polarity. *Cell, 112*(3), 355-367. doi: 10.1016/s0092-8674(03)00045-x
93. Bohnsack, K. E., & Bohnsack, M. T. (2019). Uncovering the assembly pathway of human ribosomes and its emerging links to disease. *EMBO J, 38*(13), e100278. doi: 10.15252/embj.2018100278
94. Abdelmohsen, K., & Gorospe, M. (2012). RNA-binding protein nucleolin in disease. *RNA Biol, 9*(6), 799-808. doi: 10.4161/rna.19718
95. Raimondeau, E., Bufton, J. C., & Schaffitzel, C. (2018). New insights into the interplay between the translation machinery and nonsense-mediated mRNA decay factors. *Biochem Soc Trans, 46*(3), 503-512. doi: 10.1042/BST20170427